

UNIVERSITY OF LJUBLJANA
BIOTECHNICAL FACULTY

Vito KOVAČ

**OCCURRENCE AND EFFECTS OF OXIDATIVE
STRESS INDUCED BY METAL MATERIALS
FROM FIXED ORTHODONTIC APPLIANCES**

DOCTORAL DISSERTATION

Ljubljana, 2022

UNIVERSITY OF LJUBLJANA
BIOTECHNICAL FACULTY

Vito KOVAČ

**OCCURRENCE AND EFFECTS OF OXIDATIVE
STRESS INDUCED BY METAL MATERIALS
FROM FIXED ORTHODONTIC APPLIANCES**

DOCTORAL DISSERTATION

**NASTANEK IN UČINKI OKSIDATIVNEGA STRESA,
POVZROČENEGA S KOVINSKIMI MATERIALI
NESNEMNIH ORTODONTSKIH APARATOV**

DOKTORSKA DISERTACIJA

Ljubljana, 2022

Based on the Statute of the University of Ljubljana and the decision of the Biotechnical Faculty senate, as well as the decision of the Commission for Doctoral Studies of the University of Ljubljana adopted on 28th September 2020, it has been confirmed that the candidate meets the requirements for pursuing a PhD in the interdisciplinary doctoral programme in Biosciences, scientific field Biotechnology. The research work was performed in the laboratories of the Chair of Biotechnology, Microbiology and Food Safety Department of Food Science and Technology, Biotechnical Faculty, University of Ljubljana and in the laboratories of the Chair of Genetics, Animal biotechnology and Immunology, Biotechnical Faculty, University of Ljubljana. The work was funded by the Slovenian Research Agency. Senate of the University of Ljubljana has named assoc. prof. dr. Borut Poljšak as the supervisor and prof. dr. Polona Jamnik as the co-advisor of the doctoral thesis.

Na podlagi Statuta Univerze v Ljubljani in po sklepu senata Biotehniške fakultete ter sklepu Komisije za doktorski študij Bioznanosti Univerze v Ljubljani z dne 28.9.2020 je bilo potrjeno, da kandidat izpolnjuje pogoje za opravljanje doktorata znanosti na interdisciplinarnem doktorskem študijskem programu Bioznanosti, znanstveno področje biotehnologija. Za mentorja je bil imenovan izr. prof. dr. Borut Poljšak in za somentorico prof. dr. Polona Jamnik. Doktorsko delo je bilo opravljeno v Laboratoriju za proteomiko in Laboratoriju za industrijske mikroorganizme, Katedre za biotehnologijo, mikrobiologijo in varnost živil, Oddelka za živilstvo na Biotehniški fakulteti Univerze v Ljubljani, in v Laboratoriju za celične kulture, Katedre za genetiko, animalno biotehnologijo in imunologijo, Oddelka za zootehniko na Biotehniški fakulteti univerze v Ljubljani.

Supervisor (Mentor): assoc. prof. dr. Borut POLJŠAK
Univ. of Ljubljana, Faculty of Health Sciences, Department of Sanitary
Engineering

Co-advisor (Somentrica): prof. dr. Polona JAMNIK
Univ. of Ljubljana, Biotechnical Faculty, Department of Food Science
and Technology

Committee for the evaluation and the defense (Komisija za oceno in zagovor):

Chair (Predsednica): prof. dr. Mojca NARAT
Univ. of Ljubljana, Biotechnical Faculty, Department of Animal
Science

Member (Član): assoc. prof. dr. Iztok PRISLAN
Univ. of Ljubljana, Biotechnical Faculty, Department of Food Science
and Technology

Member (Član): prof. dr. Stjepan ŠPALJ
Univ. of Rijeka, Faculty of Dental Medicine, Department of
Orthodontics

Date of the defense (datum zagovora):

PhD student:
Vito Kovač

KEY WORDS DOCUMENTATION

DN Dd
DC UDC 606:616-089.23(043.3)
CX Oxidative stress, ROS, metal ions, nanoparticle, orthodontic appliance, *Saccharomyces cerevisiae*, HGF
AU KOVAČ, Vito, M.Sc.
AA POLJŠAK, Borut (supervisor), JAMNIK, Polona (co-advisor)
PP SI-1000 Ljubljana, Jamnikarjeva 101
PB University of Ljubljana, Biotechnical Faculty, Interdisciplinary Doctoral Programme of Biosciences, Scientific Field Biotechnology
PY 2022
TI OCCURRENCE AND EFFECTS OF OXIDATIVE STRESS INDUCED BY METAL MATERIALS FROM FIXED ORTHODONTIC APPLIANCES
DT Doctoral Dissertation
NO XV, 128, [67] p., 7 tab., 22 fig., 14 ann., 405 ref.
LA en
AL en/sl
AB Misaligned teeth are often corrected with fixed orthodontic appliances. Prolonged stay of the orthodontic appliance in the oral cavity leads to corrosion and wear of the material, from which metal ions and nanoparticles can be released that catalyze reactive oxygen species-generating reactions, which in turn lead to oxidative stress. The objective of this work was to investigate the level of selected systemic oxidative stress parameters during orthodontic treatment, the composition of selected orthodontic alloys, the release of metal ions, and the oxidative consequences that the metal ions may have on the model organism *Saccharomyces cerevisiae* (*S. cerevisiae*). The work also aimed to investigate the effects of nanoparticles on the human gingival cell line (HGF). An increase in systemic oxidative stress levels was detected in the capillary blood of orthodontic patients only after 24 hours, after which oxidative stress parameters normalized. The release of metal ions from orthodontic appliances into artificial saliva is constant, but the metal concentrations released are still below the maximum tolerated daily dose. Only high metal ion concentrations were able to generate large amounts of reactive oxygen species in the yeast *S. cerevisiae*, which the antioxidant system was unable to regulate adequately, resulting in oxidative stress and its damage to biological molecules. The toxicity of nanoparticles and the ability to generate reactive oxygen species in HGF mainly depend on the type, concentration and properties of nanoparticles. We have shown that metal ions from orthodontic appliances are released at such low concentrations that they cannot induce oxidative stress in the yeast *S. cerevisiae*, although some change in the antioxidant activity of the enzyme was observed. Of the selected nanoparticles, the WS₂ nanoparticle was the least toxic to HGF.

KLJUČNA DOKUMENTACIJSKA INFORMACIJA

ŠD	Dd
DK	UDK 606:616-089.23(043.3)
KG	Oksidativni stres, ROS, kovinski ioni, nanodelci, ortodonski aparati, <i>Saccharomyces cerevisiae</i> , HGF
AV	KOVAČ, Vito, mag. biotehnol.
SA	POLJŠAK, Borut (mentor) / JAMNIK, Polona (somentor)
KZ	SI-1000 Ljubljana, Jamnikarjeva 101
ZA	Univerza v Ljubljani, Biotehniška fakulteta, Interdisciplinarni doktorski študijski program Bioznanosti, znanstveno področje Biotehnologija
LI	2022
IN	NASTANEK IN UČINKI OKSIDATIVNEGA STRESA, POVZROČENEGA S KOVINSKIMI MATERIALI NESNEMNIH ORTODONTSKIH APARATOV
TD	Doktorska disertacija
OP	XV, 128 [67] str., 7 pregl., 22 sl., 14 pril., 405 vir.
IJ	en
JI	en/sl
AI	Malokluzija se pogosto odpravi s nesnemnimi ortodontskimi aparati. Dolgotrajna izpostavljenost ortodontskega aparata v ustnem okolju vodi do korozije in obrabe materiala, iz katerega se lahko sprostijo kovinski ioni in nanodelci, ki katalizirajo reakcije nastanka reaktivnih kisikovih zvrst in posledično povzročijo oksidativni stres. Namen disertacije je bil raziskati sistemske spremembe parametrov oksidativnega stresa med ortodontskim zdravljenjem, sestavo izbranih ortodontskih zlitin, sproščanje kovinskih ionov in oksidativne posledice, ki jih lahko imajo kovinski ioni na modelni organizem <i>Saccharomyces cerevisiae</i> (<i>S. cerevisiae</i>). Namen disertacije je bil tudi raziskati učinke nanodelcev na celično linijo fibroblastov človeške dlesni (HGF). Povečanje ravni sistemskega oksidativnega stresa je bilo mogoče opaziti v kapilarni krvi ortodontskih pacientov šele po 24 urah, nato pa se parametri oksidativnega stresa normalizirajo. Sproščanje kovinskih ionov iz ortodontskih aparatov v umetno slino je konstantno, vendar so koncentracije sproščenih kovin še vedno pod maksimalno dovoljeno dnevno dozo. Le visoke koncentracije kovinskih ionov so sposobne ustvariti velike količine reaktivnih kisikovih zvrst v kvasovki <i>S. cerevisiae</i> , katerih antioksidativni sistem ni zmožen uravnati, in zato prihaja do oksidativnega stresa in oksidativnih poškodb molekul. Toksičnost nanodelcev in sposobnost ustvarjanja reaktivnih kisikovih zvrst v celični liniji HGF je odvisna od vrste, koncentracije in lastnosti nanodelcev. Dokazali smo, da se iz nesnemnih zobnih aparatov sproščajo kovinski ioni, čigar koncentracije so prenzke, da bi lahko povečale nivo ROS in inducirale oksidativni stres v kvasovki <i>S. cerevisiae</i> , čeprav so bile opažene nekatere spremembe v aktivnosti antioksidativnih encimov. Izmed izbranih nanodelcev so se nanodelci WS ₂ izkazali kot najmanj toksični v celični liniji HGF.

TABLE OF CONTENTS

	KEY WORDS DOCUMENTATION.....	III
	KLJUČNA DOKUMENTACIJSKA INFORMACIJA	IV
	LIST OF TABLES	IX
	LIST OF FIGURES	X
	LIST OF ANNEXES	XI
	ABBREVIATIONS AND SYMBOLS.....	XII
1	INRODUCTION	1
1.1	PROBLEM DESCRIPTION.....	1
1.2	RESEARCH GOALS	3
2	LITERATURE REVIEW	4
2.1	FIXED ORTHODONTIC APPLIANCES.....	4
2.1.1	Biocompatibility	4
2.1.2	Orthodontic alloys	5
2.1.3	Nanotechnology in orthodontics	6
2.1.3.1	Antibacterial activity	6
2.1.3.2	Reduction of friction	7
2.1.3.3	Increase in strength	8
2.2	OXIDATIVE STRESS	9
2.2.1	Reactive oxygen species	9
2.2.2	Metal ions and ROS	12
2.2.3	Nanomaterials and ROS	14
2.2.4	Molecular targets of ROS	15
2.2.4.1	Lipid oxidation.....	16
2.2.4.2	Nucleic acid oxidation	16
2.2.4.3	Protein oxidation	17
2.2.5	Cellular Antioxidative defense system	18
2.2.5.1	Enzymatic defense	18
2.2.5.1.1	Superoxide dismutase	19
2.2.5.1.2	Catalase	20

2.2.5.1.3	Glutathione peroxidase	20
2.2.5.1.4	Glutathione reductase.....	20
2.2.5.1.5	Peroxiredoxin	21
2.2.5.1.6	Thioredoxin reductase.....	21
2.2.5.2	Non-enzymatic defense.....	22
2.2.5.2.1	Glutathione.....	22
2.3	MODEL ORGANISM AND CELL LINE	22
2.3.1	Yeast <i>Saccharomyces cerevisiae</i>	22
2.3.2	Human gingiva fibroblast cell line	23
3	MATERIALS AND METHODS	24
3.1	RESEARCH WORK FLOW	24
3.2	SYSTEMIC OXIDATIVE STRESS PARAMETERS IN PATIENTS DURING ORTHODONTIC TREATMENT WITH FIXED APPLIANCES.....	24
3.2.1	Ethical approval	24
3.2.2	Subjects and cohort design	24
3.2.3	Insertion of the orthodontic appliance	25
3.2.4	Capillary blood collection	25
3.2.5	Free oxygen radical test	26
3.2.6	Free oxygen radical defense	26
3.3	TYPE AND AMOUNT OF OF METAL IONS RELEASED FROM ORTHODONTIC ALLOYS.....	26
3.3.1	Orthodontic materials	26
3.3.2	<i>In vitro</i> conditions	26
3.3.3	Inductively coupled plasma mass spectrometry analysis	27
3.3.3.1	Released metal ions in saliva	27
3.3.3.2	Metal alloy composition.....	27
3.3.3.3	Metal ion concentration measurement	27
3.4	OXIDATIVE STRESS IN YEAST CELL MODEL	28
3.4.1	Yeast cultures	28
3.4.2	Metal ion mixtures and yeast treatment	29

3.4.3	Cell viability	29
3.4.3.1	Cell culturability	29
3.4.3.2	Metabolic activity of the cells.....	30
3.4.4	ROS level determination	30
3.4.4.1	Determination of ROS content.....	30
3.4.4.1.1	Modification of the protocol	31
3.4.5	Enzymatic antioxidant defense	31
3.4.5.1	Cell lysate preparation	31
3.4.5.2	Superoxide dismutase activity	32
3.4.5.3	Catalase activity	32
3.4.5.4	Glutathione peroxidase activity	33
3.4.5.5	Glutathione reductase activity.....	33
3.4.5.6	TrxR activity	34
3.4.5.7	Peroxiredoxine activity	34
3.4.5.8	In-gel enzyme activity of SOD and CAT.....	35
3.4.5.8.1	Electrophoresis gels	35
3.4.5.8.2	Electrophoresis buffers	36
3.4.5.8.3	Loading of samples and electrophoresis	36
3.4.5.9	SOD in-gel activity staining.....	36
3.4.5.9.1	CAT in-gel activity staining.....	37
3.4.6	Oxidative damages	37
3.4.6.1	Oxidative lipid damages.....	37
3.4.6.2	Oxidative protein damages.....	38
3.5	OXIDATIVE STRESS IN HGF	38
3.5.1	HGF cell line	38
3.5.2	Nanoparticle characterisation and preparation for treatment	38
3.5.3	HGF cell viability	39
3.5.3.1	Resazurin assay	40
3.5.3.2	Neutral red uptake assay	40
3.5.3.3	Coomassie Blue Assay	41

3.5.3.4	The trypan blue cellular debris assay	41
3.5.4	ROS level determination	42
3.6	STATISTICAL ANALYSIS.....	42
4	RESULTS WITH DISCUSSION.....	44
4.1	CHANGES IN OXIDATIVE STRESS PARAMETERS IN THE CAPILLARY BLOOD.....	44
4.2	METAL ION RELEASE FROM DIFFERENT ORTHODONTIC ALLOYS..	46
4.3	CAUSATION OF OXIDATIVE STRESS BY METAL IONS IN <i>S. CEREVISIAE</i>	53
4.3.1	Culturability	53
4.3.2	Metabolic activity	56
4.3.3	Intracellular ROS level.....	57
4.3.4	Lipid oxidation	62
4.3.5	Antioxidative defense.....	63
4.3.6	Protein oxidation	67
4.4	THE EFFECT OF METAL MIXTURES ON HGF CELL LINE	68
4.5	EFFECT OF NANOPARTICLE EXPOSURE TO HGF CELL LINE	75
4.5.1	Nanoparticle characteristics.....	75
4.5.2	Cytotoxicity of NPs.....	77
4.6	STUDY LIMITATIONS AND FUTURE PERSPECTIVES	87
5	CONCLUSIONS	89
6	SUMMARY (POVZETEK)	90
6.1	SUMMARY.....	90
6.2	POVZETEK.....	91
7	REFERENCES.....	101
	ACKNOWLEDGEMENTS	
	ANNEXES	

LIST OF TABLES

Table 1: Orthodontic alloys and their metal composition (Dentaurum, 2020).....	6
Table 2: Main ROS molecules (Arjunan et al., 2015).....	10
Table 3: <i>Saccharomyces cerevisiae</i> strains used in the study.	28
Table 4: Metal ion w/v ratios for simulating orthodontic alloys.	29
Table 5: Nanoparticles used in the study.....	39
Table 6: Components of orthodontic appliances used in the study with their corresponding metal composition in weight percentages (%) (Kovač et al., 2022).....	48
Table 7: Size and surface charge of used nanoparticles	77

LIST OF FIGURES

Figure 1: Lipid oxidation (Barrera et al., 2018).	16
Figure 2: Enzymatical antioxidant defense system (Kovač et al., 2021).	19
Figure 3: The Trx system and Prx mechanism (Lu and Holmgren, 2014).	21
Figure 4: Research work flow.	24
Figure 5: Changes in FORT/FORD oxidative stress parameter during the one week orthodontic treatment.	45
Figure 6: The release of metal ions from different parts of fixed orthodontic appliances. .	51
Figure 7: Cell culturability of Wt, Δ Sod1 and Δ Ctt1 yeast after 24-hour metal treatment.	55
Figure 8: Metabolic activity of Wt, Δ Sod1 and Δ Ctt1 yeast treated with different metal mixtures.	57
Figure 9: Intracellular ROS level of Wt, Δ Sod1 and Δ Ctt1 yeast was performed with two different methods, each with a different time point of H ₂ DCFDA dye addition. .	59
Figure 10: Intracellular ROS level in culturable Wt, Δ Sod1 and Δ Ctt1 yeast cells after the 24-hour metal treatment.	61
Figure 11: Influence of 24-h metal treatment on the formation of oxidative lipid damage in yeast cells.	63
Figure 12: In-gel antioxidative activity of SOD (A) and CAT (B) enzyme after metal ion mixture treatment.	64
Figure 13: Yeast antioxidant enzyme activity after 24-hour metal mixture treatment.	65
Figure 14: Protein carbonyl content as a result of oxidative protein damage in <i>S. cerevisiae</i> after 24-hour metal mixture treatment.	68
Figure 15: HGF cell viability after 24-hour treatment with metal mixtures	70
Figure 16: Relative cell death of HGF cells after 24-hour metal mixture treatment.	71
Figure 17: HFG cell intracellular oxidation level after metal mixture treatment.	73
Figure 18: Cell viability of HFG after treatment with three types of TiO ₂ -NPs.	78
Figure 19: Cell viability of HFG after treatment with WS ₂ -NPs.	80
Figure 20: Cell viability of HFG after treatment with two different ZnO-NPs.	81
Figure 21: Cell viability of HFG after treatment with different concentrations of Ag-NPs.	82
Figure 22: Intracellular ROS generation of HGF cells, treated with different types and concentrations of NPs.	84

LIST OF ANNEXES

ANNEX A Ethical approval (0120-523/2018/8).....	129
ANNEX B Patients consent.....	130
ANNEX C Questionnaire	131
ANNEX D ICP-MS operating parameters	140
ANNEX E Release of metal ions from SS, Ni-Ti, β -Ti and Co-Cr alloys.....	141
ANNEX F TEM pictures of TiO ₂ NP.....	144
ANNEX G TEM pictures of AgNP	145
ANNEX H TEM pictures of ZnONP	146
ANNEX I TEM pictures of WS ₂ NP	147
ANNEX J Consent from publisher Hindawi for the re-publication of article in the print and electronic versions of the doctoral dissertation	148
ANNEX K Published article Kovač et al., 2019	149
ANNEX L Consent from publisher MDPI for the re-publication of article in the print and electronic versions of the doctoral dissertation	155
ANNEX M Published article Kovač et al., 2020.....	156
ANNEX N Published article Kovač et al., 2021	171

ABBREVIATIONS AND SYMBOLS

$O_2^{\bullet -}$ - superoxide anion
 $\bullet OH$ - hydroxyl radical
 1O_2 - singlet oxygen
3R - Replacement, Reduction, and Refinement
8-OH-dG - 8-hydroxy-2'-deoxyguanosine
AD - antioxidant defense
Ag - silver
Ag-NPs - silver nanoparticles
Al - aluminum
APS - ammonium persulfate
ATP- adenosine-5-triphosphate
CAT - catalase
CFU - colony forming units
CG - control group
Co - cobalt
Co-Cr - cobalt-chromium
Cr - chromium
Cu - copper
DCF - dichlorofluorescein
DLS - dynamic light scattering
DNA - deoxyribonucleic acid
DNPH - 2,4-dinitrophenylhydrazine
DTNB - 5,5'-dithiobis(2-nitrobenzoic acid)
DTT - 1,4-dithio- DL -threitol
ELG - elgiloy
ETC - electron transport chain
F - fluorescence
Fe - iron
FORD - Free oxygen radical defense
FORT - Free oxygen radical test
FOX - ferrous xylenol orange
GPx -glutathione peroxidase
GR - glutathione reductase
GSH - glutathione
GSSG - generating oxidized glutathione
H₂DCF- DA - 2', 7'-dichlorofluorescein diacetate
H₂O₂ - hydrogen peroxide
HGF - human gingiva fibroblast
HNE - 4-hydroxy-2-nonenal

HNO₂ - nitrous acid
HOCl - hypochlorous acid
HOO[•] - hydroperoxyl
hTERT - human telomerase reverse transcriptase
ICP-MS - inductively coupled plasma mass spectrometry
IF-MoS₂ - inorganic fullerene-like molybdenum disulfide
IF-WS₂ - inorganic fullerene-like tungsten disulfide
L[•] - lipid radical
LIP - liable iron pool
LO[•] - lipid alkoxy radical
LOO[•] - lipid peroxy radical
LOOH - lipid hydroperoxide
MDA - malondialdehyde
Mo - molybdenum
MPs - micro particles
mRNA - messenger ribonucleic acid
NADH - nicotinamide adenine dinucleotide
NADPH - reduced nicotinamide adenine dinucleotide phosphate
NBT - nitroblue tetrazolium
Ni - nickel
NiTi - nickel-titanium
NO[•] - nitric oxide
NO₂[•] - nitrogen dioxide
NPs - nanoparticles
O₂^{•-} - superoxide
O₃ - ozone
OD - optical density
OH[•] - hydroxyl
ONOO⁻ - peroxy nitrite
ONOOH - peroxy nitrous acid
PBS - phosphate-buffered saline
PI - propidium iodide
PPB - potassium phosphate buffer
Prx - peroxiredoxin
PUFA - Polyunsaturated fatty acid
REM - remaloy
RNS - reactive nitrogen species
RO[•] - alkoxy radical
RO[•] - alkoxy radical
RO₂ONO - peroxy nitrate
ROO[•] - peroxy radical

ROO[•] - peroxy radical
ROOH - organic peroxide
ROONO - peroxy nitrite
ROS - reactive oxygen species
S. cerevisiae - *Saccharomyces cerevisiae*
SOD - superoxide dismutase
SS - stainless steel
TBA - thiobarbituric acid
TBARS - thiobarbituric acid reactivity assay
TEM - transmission electron microscope
TEMED - tetramethylethylenediamine
TG - treatment group
Ti - titanium
TiO₂ - titanium dioxide
TiO₂-NP - titanium dioxide nanoparticles
TNB - 5-thio(2-nitrobenzoic) acid
Trx - thioredoxin
TrxR - thioredoxin reductase
UV - ultra violet
WS₂ - tungsten
WS₂-NPs – tungsten nanoparticles
WSL – white spot lesions
Wt – wild type
YPD - yeast extract-peptone-glucose
Zn – zinc
ZnO – zinc oxide
ZnO-NPs – zinc oxide nanoparticles
ZP - zeta potencial
β-Ti – beta-titanium

1 INTRODUCTION

1.1 PROBLEM DESCRIPTION

Tooth misalignment, also known as malocclusion, has a tremendous impact on oral and dental health. From a psychological perspective, malocclusions also contribute to a person's sense of well-being and self-esteem (Nguee et al., 2020). The most efficient method to correct the problem is orthodontic treatment. Orthodontic treatment uses the elastic force of arches to move teeth into the desired position. The arches are placed in brackets, which are attached to the dentin of the tooth in various ways using a plastic material. Depending on the severity of the condition, orthodontic treatment lasts an average of 15 to 24 months (Fleming et al., 2010). However, during this time, inflammation-related side effects may occur, including tooth resorption, pulp changes, periodontal tissue inflammation, hypersensitivity reactions due to the release of metal ions from the appliances, and enlarged gums (either due to poor oral hygiene or hypersensitivity reactions) (Talic, 2011).

Fixed orthodontic appliances consist of wire archwires, brackets, and bands. These are usually made of orthodontic metal alloys such as stainless steel, nickel-titanium alloys, or cobalt-chromium alloys. All of the above orthodontic parts are exposed in some way to the ever-changing oral environment. The harsh conditions such as changing pH, temperature, biological and enzymatic composition leave their mark on the orthodontic appliance. Electrochemical reactions, mechanical forces and general wear of the material (Sutow et al., 2004) in the oral cavity lead to corrosion, a deterioration process of orthodontic metals (von Fraunhofer, 1997). Microbial communities are also present on the surface of orthodontic appliances and cause the so-called biocorrosion, which further alters the protective surface layers, topography and mechanical properties of the appliance (Kameda et al., 2014).

With the structural weakening of the apparatus, the release of metal ions or metal particles may occur. Most of the released metals belong to the transition metal group, i.e., they have unpaired electrons in their outer shell and therefore can actively participate in the so-called Fenton- and Haber-Weiss-like reactions to generate reactive oxygen species (ROS) (Moriwaki et al., 2008). ROS molecules such as superoxide anion ($O_2^{\cdot-}$), hydroxyl radical ($\cdot OH$), hydroperoxyl radical ($HOO\cdot$), alkoxyl radical ($RO\cdot$), peroxy radical ($ROO\cdot$), hydrogen peroxide (H_2O_2) and singlet oxygen (1O_2) are also products of normal cell metabolism, cell signaling, the consequence of exposure to some external factors (e.g. environmental pollutants) or use of medicinal drugs (Murphy, 2008). When the amount of ROS exceeds the system's ability to protect itself from them, oxidative stress occurs (Kohen and Nyska, 2002), resulting in oxidative damage at the DNA, lipid, and protein levels (Pham-Huy et al., 2008). To ward off the harmful effects of excessive formation of ROS, organisms

employ a diverse antioxidant defense system consisting of enzymes and low molecular weight molecules.

The modern approach to minimizing appliance wear and improving its surface properties is to use nanoparticles (Batra, 2018). They are primarily used as coatings to increase material strength, reduce friction, and have antimicrobial properties, but are also included in orthodontic resins to reduce enamel demineralization (Zakrzewski et al., 2021). Nanoparticles have a size of less than 100 nm in diameter and a large surface-to-mass ratio, making them highly reactive (Boverhof et al., 2015). Due to their size, they can easily pass through membranes and due to their high chemical reactivity, they could pose a toxic hazard (Saafan et al., 2018). Metallic nanoparticles, such as TiO₂ in ZnO (Ghiciuc et al., 2017), exhibit a broad antibacterial spectrum and are considered to be a better bactericidal agent than drugs, mainly because some of them tend to release metal ions and with it, promoting the formation of ROS (Metin-Gürsoy et al., 2017; Morán-Martínez et al., 2018). While antibacterial effect is desirable, the harmful effect to other cells in the oral cavity, gastrointestinal tract or systemic effect are not desirable.

The aim of this dissertation was to investigate whether the occurrence of oxidative stress and consequently oxidative damage to molecules could be a consequence of released metal ions or metal nanoparticles from fixed orthodontic appliances. First, we wanted to observe whether the oxidative stress parameters in the capillary blood of volunteers change during orthodontic treatment, and then plan the in vitro metal release experiment to fully understand which and how many metal ions are released from orthodontic alloys. With the obtained results, cell exposures to metal ion combinations were performed on the model organism *Saccharomyces cerevisiae* and the occurrence of oxidative stress was evaluated. Since the use of nanoparticles in orthodontics is not well defined, we had to define a toxicity range for the selected metal nanoparticles and evaluate their ability to generate ROS in human gingival fibroblast cell line.

1.2 RESEARCH GOALS

The dissertation research objectives were established as follows:

- Investigate and observe the changes in selected parameters of oxidative stress in capillary blood of volunteers during treatment with fixed orthodontic appliances.
- Determine the type and amount of released metal ions from fixed orthodontic appliance in artificial saliva.
- Examine the effect of selected metal ion combinations (Fe, Ni, Cr, Co, Mo and Ti) of orthodontic alloys on the *Saccharomyces cerevisiae* model organism, either at the cellular or molecular level.
- Evaluate possible toxicity of certain metal nanoparticles (TiO₂, ZnO, Ag and IF-WS₂) on the human gingival fibroblast (HGF) cell line.
- Based on the obtained results, we can confirm/debunk that selected combinations of metal ions from orthodontic alloys and selected metal nanoparticles used in orthodontics generate oxidative stress and cause oxidative damage in cells.
- According to the toxicity results and changes in oxidative stress parameters we will recommend the least risky nanoparticle for orthodontic use.

2 LITERATURE REVIEW

2.1 FIXED ORTHODONTIC APPLIANCES

Fixed orthodontic appliances are used for various movements of teeth along the alveolar bone. The effectiveness of orthodontic treatment is dependent on the susceptibility of the periodontal tissues to the treatment and the characteristic of the fixed orthodontic appliance parts (Proffit et al., 2007). Brackets, archwire, bands and ligatures make up an orthodontic appliance. Different materials, like metal ceramics, polymers and composites, are used to make the parts, each with their own pros and cons (Chen and Thouas, 2015). The usage of ceramic or polymer is more visually appealing, they are quite fragile and tend to deform over a certain amount of time (Oh et al., 2005). Of them, metal alloys are the most employed material, due to good mechanical properties, strength and heat and electric conductivity (Park and Lakes, 2007). Their mayor flaw lies in the tendency to corrosion in the presence of biological liquids.

2.1.1 Biocompatibility

Orthodontic treatment with biocompatible appliances is crucial for the treatment efficiency and patient's safety. Biocompatible materials are considered to be the ones that do not inflict any negative effect on their environment, meaning that they are not toxic, carcinogenic and not capable of inducing allergic reactions (Widu et al., 1999). Another important property of biocompatible materials is that their physiological and mechanical properties do not change under *in vivo* conditions. In reality, no material suffices all the requirements.

When choosing the right material, the emphasis is pointed to the natural occurring elements in the human body. Carefulness is advised, because high concentrations of micronutrients like chromium, cobalt, copper, iron, iodine, manganese, molybdenum, selenium and zinc are toxic and cause mayor medical problems (Chen and Thouas, 2015). The decision on what material to use is also based on the mechanical properties, corrosion resistance, bending and melting properties, esthetics and finally the price (Upadhyay et al., 2006).

Biomaterials are in close contact with body liquids which can affect the material surface. In the presence of saliva or other fluids, orthodontic alloys tend to corrode over time, resulting in metal release from the alloy surface and basic weakening of the alloys properties (Mathew and Wimmer, 2011). In the process called corrosion, where there is a physicochemical (electrochemical) interaction between the metal and its environment, changes in the metal properties could happen. The body fluid, that the orthodontic alloys are exposed to, is saliva and it is a very heterogenic media, containing different microorganisms and having a vast array of physiological properties (House et al., 2008).

2.1.2 Orthodontic alloys

Stainless steel alloy (SS) and its variants are used for all parts of fixed orthodontic appliance, from brackets, wires, ligatures and bands. The composition of alloy SS is mainly Fe with smaller amounts of Ni, Cr and other elements (Sfondrini et al., 2009) Depending on the structure and chemical composition, five groups of SS alloys can be distinguished, of which the austenitic SS alloy is the most preferred for the production of orthodontic appliance parts (Arango Santander and Luna Ossa, 2015). The reason for the widespread use of alloy SS is its good corrosion resistance, which is due to the contained Cr and the ability to form a passive chromium oxide layer (Cr_2O_3) on the surface (Chaturvedi and Upadhayay, 2010). The SS alloy also has an excellent formability, strength and elasticity.

The cobalt-chromium alloys (Co-Cr) consist of about 40% Co, 20% Cr, and 14% Ni, with Fe and Mo in the lower 5% range. The mechanical properties such as elasticity and strength of Co-Cr alloy are very similar to SS alloy and they are also good against corrosion due to Cr_2O_3 passivation on the surface (Harini and Kannan, 2020).

According to the shape of Ti material, it can be distinguished between α -Ti and β -Ti. The hexagonal α -Ti is often stabilized with aluminum to obtain an alloy with high strength and low weight, while the β -Ti is stabilized with molybdenum (Mo) and vanadium (V) (Park and Kim, 2000). The most common Ti alloys are Ti6Al4V for brackets and NiTi or CuNiTi alloys for arches (Nakajima and Okabe, 1996). The NiTi alloys consist of about 55% Ni and 45% Ti, depending on the manufacturer. The 5% - 6% Cu is sometimes added to increase strength. NiTi alloys have greater flexibility compared to other alloys, such as SS, Co-Cr and β -Ti (Ferreira et al., 2012). The major advantage of NiTi alloy is its "shape memory", which means that the material retains its original shape even after bending.

Most brackets are made of SS alloy. In addition to iron (Fe), this steel consists of chromium (Cr), nickel (Ni) and sometimes molybdenum (Mo). The proportion of Cr and Ni varies depending on the specific SS alloy (Oh et al., 2004). Less common are titanium brackets, which are made of pure titanium or a titanium alloy (Gioka et al., 2004). In terms of material, orthodontic alloys for arches are extremely diverse. The first arches were made of the alloy SS, but were then replaced by a nickel-titanium alloy (NiTi) due to its better elasticity and easier bending manipulations. Other available options include beta-titanium (β -Ti) and cobalt-chromium (Co-Cr) alloy (Małkiewicz et al., 2018). The metal composition of orthodontic alloys is shown in Table 1.

Table 1: Orthodontic alloys and their metal composition (Dentaurum, 2020).

Alloy	Fe (%)	Ni (%)	Cr (%)	Co (%)	Mo (%)	Ti (%)	Other
SS (dentaflex®)	Residue	8 - 10	17 - 19	/	/	/	Si = 2 - 3 Mn ≤ 2
SS (remanium®)	Residue	8 - 10.5	17 - 9	/	/	/	Si ≤ 1 Mn ≤ 2
SS (AISI 1.4460)	Residue	4.5 - 6.5	25 - 28	/	1.3 - 2	/	Si ≤ 1 Mn ≤ 2
Co-Cr (Elgiloy®)	4-6	19 - 23	18 - 22	Residue	3 - 5	/	Mn = 1-3
Co-Cr (remaloy®)	Residue	14 - 16	19 - 21	38 - 42	6 - 8	/	Si ≤ 0.5 Mn ≤ 1 W = 3-5
Ni-Ti (rematitan® LITE)	/	50 - 60	/	/	/	Residue	Fe ≤ 0.5
β-Ti (rematitan® Special)	/	/	/	/	11.5	78	Zr ≤ 6 Sn ≤ 4.5

2.1.3 Nanotechnology in orthodontics

Nanotechnology represents a great opportunity for further improvements in the field of medicine and dentistry, either as a protective layer or as an improvement in the properties of materials, such as strength and durability. Nanoparticles possess advantageous properties such as high surface-to-volume ratio for better interaction with the environment, zeta potential, particle size and shape, surface chemistry, agglomeration, dissolution, and ion release. (Fernando et al., 2018) Due to their unique properties, such as catalytic, optical, and electromagnetic properties, metal nanoparticles (NPs) and nanomaterials are widely used in biological and medical applications (Mamunya et al., 2004), including orthodontics. NPs, especially metal NPs with their physicochemical, mechanical, and antibacterial properties, could have a great impact on the duration of orthodontic treatment, address certain associated problems, and improve oral health (Sharan et al., 2017). One way to apply NPs to orthodontic appliances is through coatings, where the biological properties of the surface layer and the mechanical properties of the alloy could be improved.

2.1.3.1 Antibacterial activity

Orthodontic appliances are a good site for bacterial plaque formation. Their configuration promotes food retention and impedes the self-cleaning of oral muscles and saliva and the maintenance of oral hygiene, allowing the formation of plaque (Lundström and Krasse, 1987), a common undesirable side effect of orthodontic treatment. Persistent plaque accumulation leads to a shift in the imbalance between demineralization and remineralization, which in turn leads to white spot lesions (WSL) (Sudjalim et al., 2006).

Antibiotics could be used in this manner, but fear of resistance development outweighs their potential. Resistance to NPs is less likely because their mode of action is based on direct contact with the cell wall of bacteria (Fernando et al., 2018). Ag-NPs have been shown to be a potentially useful substance for biomedical applications because of their high antimicrobial activity and low toxicity to the environment. Their mode of action is not yet well described, but many mechanisms have been proposed (Rizzello and Pompa, 2014).

The ability of Ag-NPs to inhibit yeasts, Gram-positive and - due to the thick cell wall - especially Gram-negative bacteria makes them widely applicable in antimicrobial research (Peiris et al., 2017). The mode of action is that they first make membranes permeable to allow more Ag-NPs to enter and release Ag ions (Marambio-Jones and Hoek, 2010), interacting with thiol-containing intracellular proteins (Chen and Schluesener, 2008), generate reactive oxygen species, interact with sulfur in DNA, and thus interfere with replication and cell division (Prabhu and Poulouse, 2012). It has also been suggested that the released silver ions inhibit respiratory enzymes at the membrane and eventually cause cell lysis (Bragg and Rainnie, 1974).

TiO₂-NP are readily available, low toxic, biocompatible, chemically stable and robust nanoparticles. Due to their photocatalytic activity and antibacterial properties, TiO₂-NPs are the most studied NPs. The main antibacterial mechanism of TiO₂-NP is based on the photocatalytic formation of ROS under UV light (Wu et al., 2009). Toxicity against bacteria has been demonstrated without UV illumination of TiO₂-NPs, indicating a mechanism of action other than the production of ROS (Sohm et al., 2015). However, the mode of action is still controversial. It is believed that the cause of bacterial death is membrane depolarization and eventually membrane permeability (Sohm et al., 2015).

Similar to TiO₂, ZnO is highly photocatalytic, meaning that under UV light, loosely bound oxygen is degraded in the form of reactive oxygen species (ROS) such as hydrogen peroxide (H₂O₂) and superoxide ions (O₂^{•-}) (Bao et al., 2011). These molecules have been shown to damage proteins and DNA, eventually leading to their death (Kirkinezos and Moraes, 2001). Another antibacterial effect is the release of Zn ions into the media, which disrupts transport, amino acid metabolism, and enzyme systems (Li et al., 2011). Changes in membrane permeability, and thus loss of proton motive force and other biological molecules, also occur when ZnNPs adhere to or are integrated into the membrane (Amro et al., 2000). Because of their antimicrobial activity, ZnNPs can reduce adhesion, proliferation, and biofilm inhibition.

2.1.3.2 Reduction of friction

Friction is defined as a force that opposes the opposing force of motion (Rossouw et al., 2003) and occurs as resistance to sliding along the orthodontic archwire when the archwire

is in contact with the brackets, reducing tooth movement and consequently reducing the efficiency of the orthodontic appliance (Prashant et al., 2015). Friction causes material wear in the form of loss of mass, loss of volume, or loss of coating surface (Zheng and Zhou, 2007). During orthodontic movement of the teeth, static and kinetic friction occur alternately as the teeth slide and flex along the orthodontic wire (Kachoei et al., 2016). The main focus in the manufacture of novel orthodontic appliances is to reduce the friction that occurs during orthodontic treatment. Low friction provides better transmission of force to the teeth and thus more effective tooth movement, while high friction results in a less effective mechanism and less tooth movement, may even lead to prolonged treatment and root resorption at the base (Wei et al., 2011).

Orthodontic friction is determined by the size, shape, and material (Muguruma et al., 2013) of the brackets, bands, and wires, the ligature (Thorstenson and Kusy, 2002) and angulation (Articolo and Kusy, 1999), and the dynamic interactions between them. For example, a wire with a round cross-section has a smaller contact area with the bracket and therefore generates less friction than a wire with a rectangular cross-section, which generates high friction forces because it is fully seated in the bracket space. In addition to the mechanical properties of the wire, the biological aspect must also be taken into account. For example, saliva, which contains mucin and other peptides such as statherine (Yakubov et al., 2015), is a natural lubricant that reduces friction but also causes debris to accumulate and bacteria to contribute to the formation of biofilms that increase friction (Marques et al., 2010). With the discovery of the dry lubrication properties of inorganic fullerenes of tungsten disulfide nanoparticles (IF-WS₂) (Tenne et al., 1992) and molybdenum disulfide nanoparticles (IF-MoS₂) (Feldman et al., 1995) came the inspiration to somehow incorporate them into orthodontic appliances. It appears that when the wire and bracket are aligned in parallel, IF nanoparticles on coated wires act as spacers, resulting in lower friction being observed. With increasing angular pressure, some IF nanoparticles delaminate and transform from tubes to sheets, allowing rolling and sliding in the contact area (Joly-Pottuz et al., 2005). The thin layer of nanosheets allows sliding movements between two bodies, the archwire and the bracket (Samorodnitzky-Naveh et al., 2009).

2.1.3.3 Increase in strength

From a mechanical point of view, orthodontic treatment is based on the movement of teeth to the desired position by the elastic strength of the archwires placed in the position of the brackets. Coating orthodontic appliances is one of the ways to mechanically and biologically modify and improve the metallic properties of the orthodontic material used. Reduction of surface roughness, thickness, mechanical and friction properties, corrosion resistance, antibacterial properties and stability are the desired properties that an ideal coating should provide (Arango et al., 2012).

2.2 OXIDATIVE STRESS

The term oxidative stress was first introduced by Helmut Sies as an imbalance between prooxidants and antioxidants in favor of the former, which disrupts redox signaling and causes molecular damage (Sies, 2020). The so-called reduction-oxidation (redox) balance can be disturbed either by an overproduction of prooxidants, by a deficiency of antioxidants, or even by both together. Minor fluctuations in the redox balance do not cause major problems because the organism has the ability to adapt to the reaction, while major disturbances lead to irreparable biological damage to the cell and even cell death (Burton and Jauniaux, 2011). Under physiological conditions, the levels of oxidative stress are considered low and the redox balance is only slightly shifted in favor of prooxidants because they are necessary for the normal functioning of the organism. However, when the balance tilts more and more in favor of the prooxidants, organelle damage and deteriorating processes can be observed (Auten and Davis, 2009).

2.2.1 Reactive oxygen species

Free radicals, amongst which are also some reactive oxygen species (ROS), have an incomplete outer electron layer and thus possess one or more unpaired electrons, making them highly reactive. They may be covalently bonded to another molecule with an unpaired electron or they may result from bonding with a nonradical molecule by donating an unpaired electron (reduction radical) or by accepting electrons (oxidation radical). The ensuing reaction can trigger a chain event, producing large amounts of ROS (Halliwell, 1991). The term ROS also includes some non-radical molecules, such as hydrogen peroxide (H_2O_2) and ozone (O_3), which are readily converted to radicals (Irani, 2007). The main ROS molecules found in the biological system are presented in Table 2. In biological systems, ROS can be formed from both endogenous and exogenous sources. In normally functioning cells, the mitochondria, peroxisomes, endoplasmic reticulum, and immune cells are the primary endogenous source of ROS (Burton and Jauniaux, 2011). ROS are constantly generated under normal physiological conditions and their homeostasis is constantly monitored and maintained. The theory of free radicals and oxidative stress was established more than half a century ago and initially ROS were considered harmful by-products of aerobic metabolism, but now ROS are considered to play an essential role in various biological processes (Finkel, 2011) from phagocytosis to cellular signal transduction.

Table 2: Main ROS molecules (Arjunan et al., 2015).

ROS (Reactive oxygen species)	
Free radical species	Non-radical species
$O_2^{\cdot-}$ (superoxide)	H_2O_2 (hydrogen peroxide)
OH^{\cdot} (hydroxyl)	O_3 (ozone)
HOO^{\cdot} (hydroperoxyl)	1O_2 (singlet)
RO^{\cdot} (alkoxyl)	ROOH (organic peroxide)
ROO^{\cdot} (peroxyl)	HOCl (hypochlorous acid)

The sources of ROS can be exogenous or endogenous. Exogenous triggers of ROS include UV radiation, heavy metal ions, O_3 , toxins, pollutants, pesticides, and insecticides (dos Santos et al., 2018; Mahajan et al., 2018). The major endogenous sites of ROS generation are the mitochondrial electron transport chain (ETC), the endoplasmic reticulum, peroxisomes, membrane NADPH oxidases, and nitric oxide synthase (Rodriguez and Redman, 2005).

The most important reaction in aerobic organisms is respiration, in which H_2O is formed by the reduction of O_2 with four electrons and oxidation of organic molecules occurs. Through a series of enzymatically catalyzed reactions, an energy source in the form of adenosine-5-triphosphate (ATP) is generated by the process of oxidative phosphorylation (Bertini et al., 1994). Electron loss can occur along the enzymes of the mitochondrial electron transfer chain, especially at mitochondrial complex I (NADH-ubiquinone oxidoreductase) and complex III (ubiquinol cytochrome c oxidoreductase) (Cadenas and Davies, 2000). Approximately 1-3% of circulating electrons from ETC are thought to be lost during ATP production (Hamanaka et al., 2013). Cellular components such as the endoplasmic reticulum, cytoplasmic enzymes, and the plasma membrane surface can also be a source of ROS (Sumimoto 2008; Tu and Weissman 2004), as can some enzyme systems: the cytochrome P₄₅₀ system, the xanthine oxidoreductase system, nitric oxide synthases, and the inflammatory process system.

The primary ROS is formed during the four-step reduction process of O_2 to H_2O (Halliwell and Gutteridge, 2015). The oxygen molecule has two unpaired electrons with parallel spin, called triplet oxygen (3O_2), which is harmless unless it is energetically activated. Activation can occur when enough energy is provided to reverse the spin of an unpaired electron, producing singlet oxygen (1O_2) or when a single electron has been added to the oxygen molecule, producing a superoxide radical ($O_2^{\cdot-}$), hydrogen peroxide (H_2O_2), and hydroxyl radical ($^{\cdot}OH$) (Apel and Hirt, 2004).

The electrons attack the molecular oxygen and produce a superoxide anion ($O_2^{\bullet-}$) as shown in the Equation 1. $O_2^{\bullet-}$ is considered a moderately reactive molecule, unable to penetrate the cell membrane due to its negative charge. However, $O_2^{\bullet-}$ is an important precursor for other ROS generation (Turrens, 2003). Although the redox potential of $O_2^{\bullet-}$ is considered high, it is not considered a good reducing agent nor a good oxidizing agent, with some molecules such as cytochrome c, ascorbate, and the enzyme superoxide dismutase being exceptions (Collin, 2019).



Further reduction of $O_2^{\bullet-}$ with an electron produces H_2O_2 , a moderately reactive, nonradical molecule with a fairly long half-life compared to other ROS (Equation 2). The reaction is plausible only in the presence of the antioxidant enzyme superoxide dismutase (SOD) (Fukai and Ushio-Fukai, 2011). Unlike other ROS, H_2O_2 is membrane permeable and therefore can act outside its site of generation (Van Breusegem et al., 2001). In this regard, H_2O_2 is considered an important signaling molecule (Covarrubias et al., 2008). $O_2^{\bullet-}$ also catalyzes reduction of nitric oxide (NO^{\bullet}) to peroxynitrite ($ONOO^-$) (Galaris and Pantopoulos, 2008).



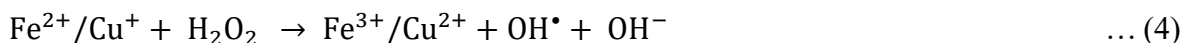
The reduction of H_2O_2 generates the most powerful and toxic oxygen radical, the hydroxyl radical ($\bullet OH$). It is capable of reacting with surrounding molecules and depriving them of their hydrogen atom, turning biological molecules into new radicals. $\bullet OH$ reacts instantly and is not selective towards its targets. The fact that there is no defense mechanism against $\bullet OH$ known to us indicates its harmful properties (Bhattacharjee, 2019).



One of the mechanisms for the generation of $\bullet OH$ is the Fenton reaction, first presented in 1894 (Fenton, 1894) and later corrected and completed to the reaction known today (Haber et al., 1934). The Fenton reaction involves ferrous iron (Fe^{2+}) and H_2O_2 which produce ferric iron (Fe^{3+}) and $\bullet OH$ (Equation 4). Many other elements with high valence such as copper (Cu), zinc (Zn), and aluminum (Al) have the property of transferring electrons and therefore can also participate in the Fenton reaction. When the reaction involves metals other than Fe or Cu, ligands, or peroxides, it is called a Fenton-like reaction (Meyerstein, 2021).

In the Haber-Weiss reaction, an addition to the original Fenton reaction, it is assumed that $O_2^{\bullet-}$ reacts again with H_2O_2 to form $\bullet OH$ and hydroxyl anion (OH^-) (Equation 5). It is important to note that the Haber-Weiss reaction is thermodynamically favored, but not kinetically, so it must be catalyzed by a transition metal. However, from a kinetic standpoint,

the $O_2^{\bullet -}$ reduction of Fe^{3+} to O_2 and Fe^{2+} is more likely to occur than the reduction of H_2O_2 by $O_2^{\bullet -}$ (Equation 6) (Das et al., 2015).



2.2.2 Metal ions and ROS

Metal ions play an important role in a variety of cellular functions such as electron transfer in respiration, synthesis and repair of DNA, and cellular metabolism. Elements with a partially filled *d* subshell and the ability to form cations are called transition elements or transition metals (McNaught and Wilkinson, 1997). Transition metals are found in Group 4-11 of the periodic table and have a large number of complex ions in many positively charged oxidation states with different catalytic properties. Some transition metals are essential elements and key components for many metalloproteins involved in the process of oxygen formation and hypoxia detection. Metal ions occur in various oxidation states and as such can undergo a redox reaction, associate with phospholipids to alter membrane stability, and promote lipid peroxidation. In contrast, the non-redox active metals (cadmium, arsenic, and lead) are maintained at physiological concentrations. Since the formation of ROS is closely related to the involvement of redox-active metals, their concentrations are kept strictly at physiological concentrations (Valko et al., 2005).

In the human body, iron (Fe) is the most abundant transition metal stored and transported in specific proteins (Ferrali et al., 1992) so Fe homeostasis is under strict control. Fe exists in ferrous (Fe^{2+}) and ferric (Fe^{3+}) ion configuration, and its ability to readily donate or accept electrons makes it an important catalyst in redox reactions (Galaris et al., 2019). Fe regulation prevents free intracellular Fe formation, but under stress conditions regulation fails and Fe can be released from iron-containing molecules into a so-called labile iron pool (LIP). Excess Fe from LIP can then be subjected to Fenton chemistry, forming extremely reactive OH^\bullet and since OH^\bullet reacts near its formation, Fe consequently functions in a site-specific manner (Chevion, 1988). Copper (Cu) is also an essential nutrient and a co-factor for enzymes (Uriu-Adams and Keen, 2005). It is capable of catalyzing the Fenton reaction even more effectively than Fe, but its abundance in the organism is less than that of Fe (Barbouti et al., 2001). When OH^\bullet is formed, it can have devastating consequences for biological molecules.

Nickel (Ni) compounds and salts are a hazard to humans and animals. Ni compounds are reported to cause DNA single-strand breaks, chromosome aberrations, and DNA-protein crosslinks (Chen et al., 2010). The mechanism of Ni damage is thought to be indirect, catalyzing the Haber-Weiss reaction to form OH^\bullet . Ni ions, $\text{Ni}^{2+}/\text{Ni}^{3+}$, do not efficiently generate ROS from reactive oxygen derivatives because the redox reactions are chemically unfavorable (Datta et al., 1992), but when bound to certain ligands, Ni^{2+} bound to the ligand can be oxidized to Ni^{3+} , generating ROS (Kasprzak et al., 2003).

Chromium (Cr), a naturally occurring metal, occurs in a variety of oxidation states but is most commonly found in trivalent (Cr^{3+}) and hexavalent (Cr^{6+}) forms, with the trivalent form used in dietary supplements and the hexavalent in industrial applications (Bagchi et al., 2002). The Cr^{6+} is considered more toxic because it can easily pass through cell membranes where it is reduced by ascorbic acid and low molecular weight thiol compounds to Cr^{5+} , Cr^{4+} and eventually to Cr^{3+} . Internalization of Cr^{3+} into cells is thought to occur actively by phagocytosis, in contrast to Cr^{6+} , which is taken up passively by nonspecific anion carriers (Fleury et al., 2006). The Cr^{5+} intermediate of the Cr^{6+} reduction generates a significant amount of OH^\bullet through Fenton-like reactions (Shi and Dalal, 1990). Although Cr^{3+} is 1000-fold less toxic than the hexavalent form, it can still cause damage at high concentrations when bound to a ligand.

Cobalt (Co) occurs in divalent (Co^{2+}) and trivalent (Co^{3+}) states, the former being rapidly reduced to a divalent state in aqueous media. Co is required in small amounts for the normal biological activity of some proteins. In addition, Co^{3+} occupies the catalytic site of vitamin B12 (Scharf et al., 2014) and elevated Co^{2+} concentrations are thought to have a negative effect on mitochondrial respiration. As shown by Foster et al. (2014), Co^{2+} competes with Fe^{2+} for iron binding sites in mitochondrial ETC complexes I, II and III iron (Fe-S) clusters. Since Co^{2+} forms more stable complexes than Fe^{2+} , mismetallization can occur, leading to disruption of oxidative phosphorylation and release of Fe (Salloum et al., 2018). The intracellular environment, filled with free (unbound) Fe, is now confronted with overproduction of ROS by the Fe-catalyzed Fenton reaction. In addition to Fe, Co is another Fenton-inducing metal with a favorable redox potential (Uzunboy et al., 2019).

Molybdenum (Mo) is another essential micronutrient and an important cofactor for some metalloenzymes. It occurs in many oxidation states, of which Mo^{4+} and Mo^{6+} are the most abundant. The possible involvement of Mo in the formation of ROS is still debated, but many researchers suspect the following two mechanisms: direct involvement in Fenton chemistry or the possibility that Mo is incorporated into specific ROS generating enzymes such as xanthine oxidase (Perkhulyn et al., 2017). Xanthine oxidase catalyzes the oxidation of hypoxanthine to xanthine, producing $\text{O}_2^{\bullet-}$, and also converts nitrite into nitric oxide, producing ONOO^- (Collin, 2019).

2.2.3 Nanomaterials and ROS

Nanotechnology is a multidisciplinary science that deals with objects, nanoparticles (NPs), at the nanoscale (from 1 to 100 nm) and seeks to understand the biological processes that occur at this level (Whitesides, 2003). In 2011, the European Commission defined nanomaterial as a natural or manufactured substance that exists in an unbound state, as an aggregate or as an agglomerate (Rauscher et al., 2013). NPs possess advantageous properties such as high surface area to volume ratio for greater interaction with the environment, zeta potential, particle size and shape, surface chemistry, agglomeration, dissolution, and ion release (Fernando et al., 2018). Due to their unique properties, such as catalytic, optical, and electromagnetic properties, metal NPs and nanomaterials are widely introduced into biological and medical applications (Mamunya et al., 2004), one of which is orthodontics. NPs, especially metal NPs with their physicochemical, mechanical, and antibacterial properties, could have a great impact on the duration of orthodontic treatment, remedy certain related problems, and improve oral health (Sharan et al., 2017). As beneficial as the unique properties of NPs may be, they are also considered potentially toxic. The high surface area to volume ratio makes them highly reactive or catalytic (Drasler et al., 2017) and their small size allows easy penetration into the cell membrane (Yin et al., 2012).

The presence and nature of metallic NPs and their metal ions can lead to the formation of ROS, a major cause of NP induced cytotoxicity (Yu et al., 2013). Three mechanisms have been proposed for the NPs formation of ROS: the first mechanism is the interaction between NPs and the cell, the second is the dissolution and release of metal ions from the NPs surface, and the third is the formation of prooxidant functional groups on the NPs surface (Wang et al., 2017a). The mechanism of ROS generation is NPs specific and not yet fully understood. Titanium dioxide nanoparticles (TiO₂-NPs) are the most common nanomaterial used in industry, mainly for whitening, whether in cosmetics, plastics, paints, personal care products, or food additives (Ray et al., 2009). TiO₂-NPs act as absorbers and deflectors for ultraviolet (UV) radiation. UVA Radiation provides enough energy to the valence electrons to cause them to jump into the conduction orbital, leaving electron holes in the valence band. Since it is necessary to fill the valence band, electrons must be removed from the water, resulting in ROS, [•]OH especially (Yin et al., 2012). On the other hand, Daimon and Nosaka (Daimon and Nosaka, 2007) postulate that the energy from irradiated TiO₂-NPs transfers to molecular oxygen to produce ¹O₂. Under nonirradiated conditions, the ability of TiO₂-NPs to generate ROS is still controversial.

Like TiO₂-NPs, zinc oxide nanoparticles (ZnO-NPs) are also used in various applications due to their semiconducting property and white appearance (Wang, 2008). The ROS generation mechanism of ZnO-NPs and TiO₂-NPs is the same as they are both semiconductors and thus have a gap between the valence band and conduction band. In aqueous media, the electrons of water molecules are hindered and generate [•]OH. ROS can

also be spontaneously generated on the ZnO-NPs (Saliani et al., 2016). Another mechanism for the generation of ROS by ZnO-NPs involves interaction with mitochondria, whose dysfunction leads to the generation of ROS (Sharma et al., 2012), and another proposed mechanism emphasizes the dissolution of Zn^{2+} ions, which causes the production of ROS (Lanone and Boczkowski, 2006).

Silver (Ag) has long been known to be a bactericidal agent, mainly due to the interactions between silver ions and molecular thiol groups, which affect DNA replication and cell wall structure (Morones et al., 2005). Silver nanoparticles (Ag-NPs) are found in numerous biomedical and industrial applications. Their bactericidal mechanism is based either on interactions between Ag-NPs and cell structures or on the release of Ag^+ and generation of ROS. Rohde et al. (2021) showed that not only Ag^+ released from NP can induce ROS in a Fenton-like reaction, but that the surface of Ag-NPs also catalyzes the reduction of H_2O_2 to $\cdot OH$ (He et al., 2012).

Tungsten disulfide (WS_2) belongs to transition metal dichalcogenides (TMDCs), a family of layered materials with the general formula MX_2 , where M stands for a transition metal and X for a chalcogen (Appel et al., 2016a). Tungsten disulfide nanoparticles (WS_2 -NPs) are gaining their reputation as inert, nontoxic, nonmagnetic, and highly resistant to oxidation and thermal degradation (Chang et al., 2006). Currently, their properties are mainly used as dry lubricants due to their effective friction reduction. The two structures of WS_2 -NPs are mainly in use: 2H- WS_2 and IF- WS_2 (inorganic fullerene-like). The underlying mechanism by which WS_2 -NPs induce oxidative stress is direct, in that the NPs generate ROS, or indirect, in that the NPs affect cellular components and cellular processes, which in turn generate ROS (Yang et al., 2014). Yuan et al. (2018) have shown that WS_2 -NPs, like other semiconductors, can generate ROS under irradiation conditions, and tungstate (W^{6+}) has also been shown to dissociate from the nanoparticles, but it did not generate ROS.

2.2.4 Molecular targets of ROS

ROS can have either a positive or a harmful effect on the biological system. In excess, ROS are considered to deteriorate biological molecules and cellular structures. The organism has the ability to reduce ROS and its damage, but oxidative damage accumulates over time and further damages DNA, proteins, or lipids (Valko et al., 2006). When the scales tip in favor of ROS, oxidative stress occurs and cells take countermeasures in the form of activated/silenced antioxidant defense genes, transcription factors, and structural proteins (Birben et al., 2012).

2.2.4.1 Lipid oxidation

Cellular components containing polyunsaturated fatty acids (PUFA) such as cell membranes and organelle membranes are very sensitive to oxidation. The PUFA backbone has two or more double bonds with which ROS can react. The more double bonds a PUFA has, the more likely it is to oxidize in the presence of ROS (Su et al., 2019). In addition to lipid peroxidation, ROS can disrupt the lipid bilayer and inactivate certain membrane-bound proteins and generally increase membrane permeability (Birben et al., 2012).

The three-step process of lipid oxidation has been described (Halliwell et al., 1993). In the first step, initiation, ROS ($\cdot\text{OH}$, $\text{RO}\cdot$ and $\text{ROO}\cdot$, but not H_2O_2 and $\text{O}_2^{\cdot-}$) subtracts hydrogen from the PUFA methyl group and generates a lipid radical ($\text{L}\cdot$). In the second step, propagation, the $\text{L}\cdot$ reacts with either O_2 to form a highly reactive lipid peroxy radical ($\text{LOO}\cdot$) or with transition metals (Fe^{2+}) to form lipid alkoxy radical ($\text{LO}\cdot$). Both radicals are able to subtract hydrogen from a new PUFA, generating lipid hydroperoxide (LOOH) and a new $\text{L}\cdot$, resulting in a chain reaction of lipid radical formation (Ayala et al., 2014). In the final step, termination, LOOH decomposes into aldehydes and ketones, such as malondialdehyde (MDA) and 4-hydroxy-2-nonenal (HNE) (Pisoschi and Pop, 2015).

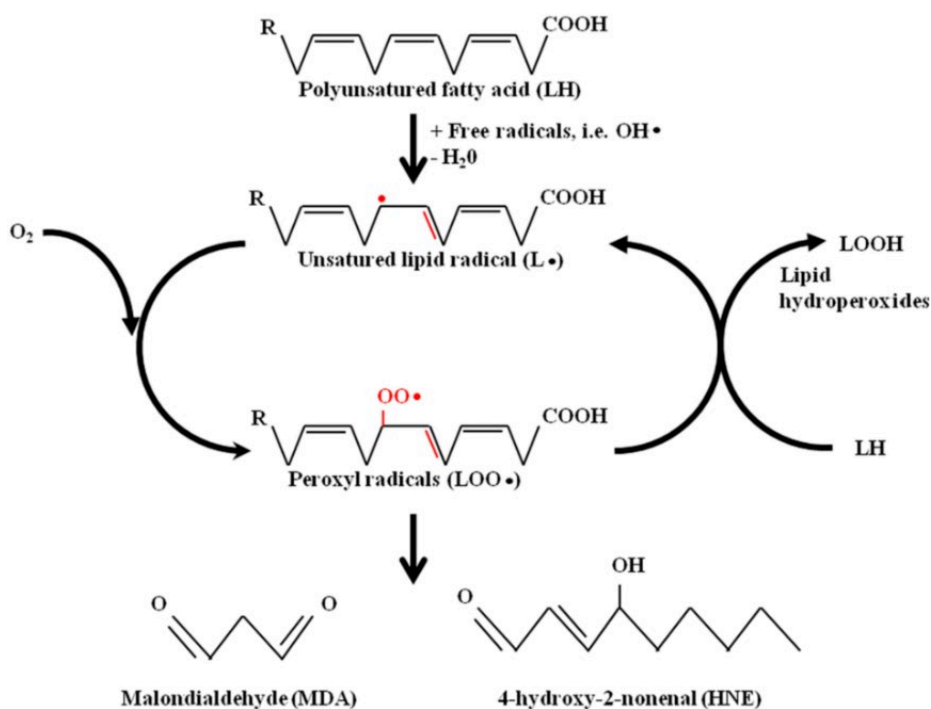


Figure 1: Lipid oxidation (Barrera et al., 2018).

2.2.4.2 Nucleic acid oxidation

DNA damage caused by free radicals is a source of mutagenesis, carcinogenesis, and aging in cells. The genetic material of biological systems is constantly threatened by ROS damage,

namely $\cdot\text{OH}$ is considered the main threat because it reacts with the purine, pyrimidine, or deoxyribose in the DNA backbone (Dizdaroglu et al., 2002). Other ROS such as H_2O_2 and $\text{O}_2^{\cdot-}$ are not directly involved in the generation of oxidative DNA damage. ROS induced damage is also considered as single or double strand DNA breaks and DNA crosslinks. These DNA changes can be observed in transcriptional fluctuations, signal transduction, genomic instability, and error-prone replication (Cooke et al., 2003).

The best known DNA oxidation product is the base modification 8-hydroxy-2'-deoxyguanosine (8-OH-dG), which is considered a reliable marker of oxidative damage. It is formed when $\cdot\text{OH}$ attacks guanine at the C-8 position. Due to the base pairing of adenine and cytosine, 8-OH-dG can cause transversion mutations from A:T to C:C or G:C to T:A (Kohen and Nyska, 2002). Other carbon positions of pyrimidines are also susceptible to ROS attack.

Not only nuclear DNA, but also mitochondrial DNA is susceptible to oxidative damage. The fact that mitochondria are the main source of ROS and their ROS oxidative activity is highly localized places them at higher risk for free radical-induced DNA damage. Because mitochondrial DNA lacks the nucleotide excision repair mechanism and is not protected by histones like nuclear DNA, it is extremely vulnerable to oxidative damage (Inoue et al., 2003).

2.2.4.3 Protein oxidation

Oxidation of proteins is a covalently modified process in which ROS or secondary byproducts of oxidative stress react with the protein molecule (Shacter, 2000). Amino acids, simple peptides, and proteins are all susceptible to ROS mediated damage. The consequences of protein oxidation are manifested by a loss of protein activity (receptor, enzyme, transport, or structure) and a tendency toward proteolysis or protein denaturation. The basic constituents of proteins, amino acids, are the primary target of ROS, particularly cysteine, methionine, and the aromatic amino acids (tyrosine, phenylalanine, and tryptophan) (Kehm et al., 2021).

One of the ROS induced protein damage is protein carbonylation, which occurs either by direct oxidation of protein amino acids, cleavage of the protein backbone, or incorporation of carbonyls into the protein backbone (Dalle-Donne et al., 2003a). Cleavage of the backbone is $\cdot\text{OH}$ dependent and generates a carbon-centered radical. In the presence of transition metals and hydroperoxyl radicals ($\text{HOO}\cdot$), further oxidative reactions of a carbon-centered radical occur. Peptide cleavage leads to the formation of alkyl, alkylperoxyl, and alkoxy radical intermediates, as well as the formation of carbonyl groups, a marker for protein oxidation (Sitte, 2003). It is also possible for carbon-centered radicals to react with each other to form protein-protein crosslinks.

So-called "primary protein carbonylation" occurs on proline, arginine, lysine, and threonine side chains when the redox reaction is catalyzed by transition metals. The oxidized side chains are stable and represent an effective protein oxidation marker (Dalle-Donne et al., 2003b). Secondary protein carbonylation can also occur when the oxidatively modified lipids or carbohydrates react with the amino acid side chains (Suzuki et al., 2010).

2.2.5 Cellular Antioxidative defense system

Because they are constantly exposed to ROS, aerobic organisms have developed an efficient defense system during evolution consisting of defense, neutralization, and repair mechanisms. The overproduction of ROS and its effects are mediated by antioxidants, either enzymatic antioxidants or non-enzymatic antioxidants. Cellular defenses use enzymatic and nonenzymatic antioxidants to regulate the production of free radicals and their metabolites. Depending on the function of the antioxidant defense, the agents can be classified as follows: those that inhibit the formation of ROS, those that bind metals to prevent the formation of ROS, the ROS deteriorating endogenous enzymes, and the radical and nonradical scavengers (Niki, 2014).

2.2.5.1 Enzymatic defense

There are four major defense enzymes responsible for maintaining ROS at appropriate levels: Superoxide dismutase (SOD), catalase (CAT), glutathione peroxidase (GPx), and the thioredoxin reductase system (Trx).

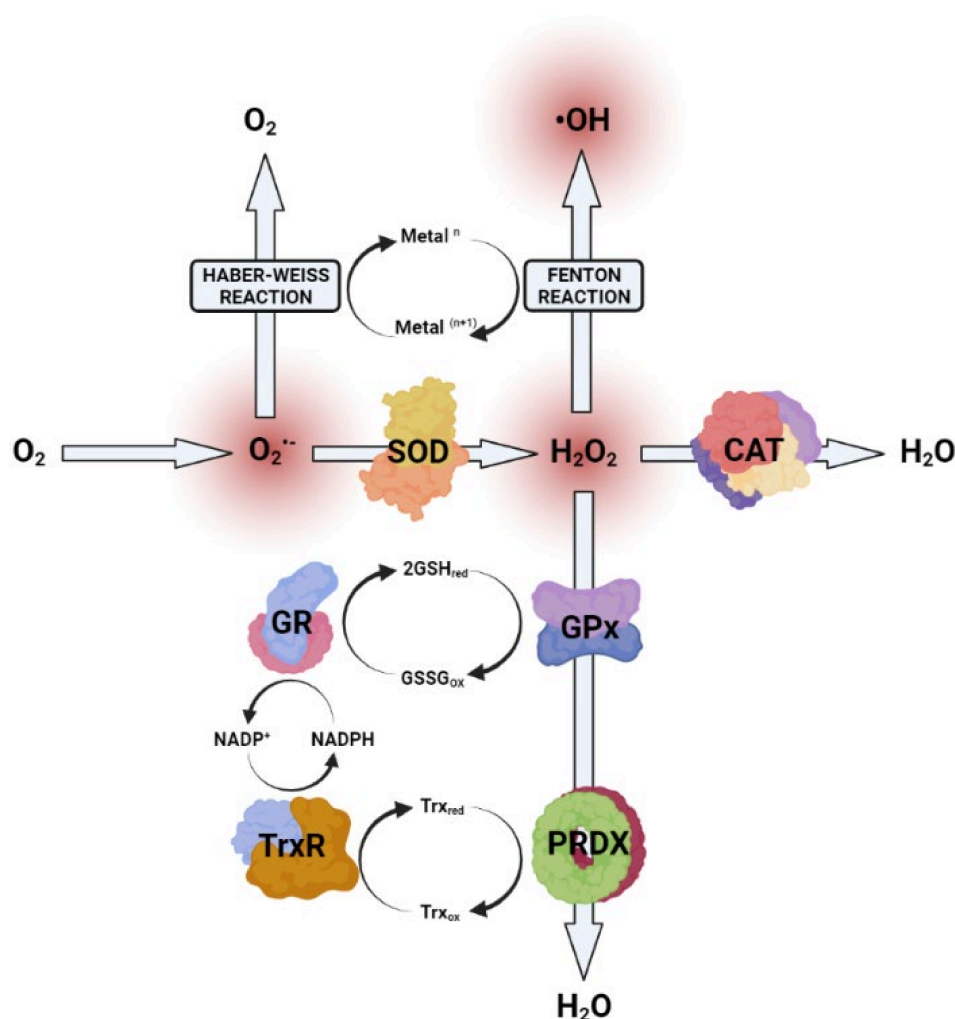


Figure 2: Enzymatical antioxidant defense system (Kovač et al., 2021).

2.2.5.1.1 Superoxide dismutase

SOD is a metalloenzyme that catalyzes the conversion of $O_2^{\bullet-}$ to O_2 and H_2O_2 . Since $O_2^{\bullet-}$ is the primary ROS, the SOD dismutation is of paramount importance in the cell. Depending on their metal cofactor and site of activity, SOD are classified into four groups; ferrous SOD (Fe-SOD) is found in bacteria and eukaryotic chloroplasts, manganese SOD (Mn-SOD) is present in mitochondria and in peroxisomes; copper-zinc SOD (Cu/Zn-SOD) is most abundant and is found in both the cytosol and extracellular matrix, and the last group is nickel SOD (Ni-SOD), which is mainly present in bacteria (Abreu and Cabelli, 2010).

For eukaryotes, Cu/Zn-SOD and Mn-SOD are two basic enzymes for $O_2^{\bullet-}$ scavenging. The Cu/Zn-SOD can be located in the cytosol, lysosomes, nucleus, and mitochondrial intermembrane space. The antioxidant activity of the enzyme is based on the redox activity of copper, which is reduced from Cu^{2+} to Cu^{1+} in the presence of $O_2^{\bullet-}$, thus generating O_2 . Another molecule of $O_2^{\bullet-}$ and two H^+ are scavenged to oxidize $Cu^{1+}/Zn-SOD$ to

Cu²⁺/ZnSOD producing H₂O as a byproduct. The Zn ion in SOD contributes to the stability of the protein structure (Patlevič et al., 2016). The same mechanism of dismutation of O₂⁻ is also postulated for Mn-SOD, where conversion of redox active Mn²⁺ to Mn³⁺ occurs, but only in the mitochondria where the Mn-SOD is found (Abreu and Cabelli, 2010).

2.2.5.1.2 Catalase

CAT is responsible for intracellular conversion of H₂O₂ to H₂O and O₂. There are many types of CAT enzymes in organisms, but the most common type consists of four subunits, each of which has an Fe³⁺ heme group in the active sites and each tetramer is bound to NADPH to protect against possible H₂O₂ inactivation (Kirkman et al., 1999). The two-step catalytic reduction of H₂O₂ occurs in peroxisomes, where in the first step the heme-Fe³⁺ reduces H₂O₂ to H₂O, and in the second step the generated heme compound from the first reaction step oxidizes the second H₂O₂ molecule to H₂O and O₂ (Putnam et al., 2000).

2.2.5.1.3 Glutathione peroxidase

Another enzyme responsible for the degradation of H₂O₂ is a tetramer with a selenium atom in the active site, glutathione peroxidase (GPx) (Arthur, 2000). GPx exert antioxidant functions in various cellular compartments. GPx1 is present in the cytosol and mitochondria, GPx2 is present in the cytosol and nucleus, Gpx3 is located in the plasma, and Gpx4 is a membrane-bound protein. (He et al., 2017) This selenoprotein uses glutathione (GSH) as a reducing substrate for the degradation of hydrogen peroxides and organic peroxides to water or the corresponding alcohol. The active form of the selenocysteine residue reduces peroxides, and the oxidized selenic acid uses two molecules of GSH to regenerate, generating oxidized glutathione (GSSG) (Deponte, 2013). Both GPx and CAT simultaneously eliminate H₂O₂, peroxisomal H₂O₂ is eliminated by CAT, while mitochondrial and cytosolic Cu/Zn-SOD generated H₂O₂ is eliminated by GPx (Arthur, 2000; Deponte, 2013).

2.2.5.1.4 Glutathione reductase

Although not directly involved in ROS defense, glutathione reductase (GR) plays an important role in GSH metabolism and as such is closely related to the glutathione redox system. GR is a homodimeric flavoprotein that is essentially an oxidoreductase, thus requiring NADPH, H⁺ and GSSG or its function and producing two molecules of GSH and NADP⁺ (Berkholz et al., 2008). GSH is not only considered a non-enzymatic antioxidant, but is also a necessary substrate for GPx activity. To maintain redox homeostasis, GR must reduce GSSG to GSH via an NADPH-dependent mechanism, thus maintaining the reduced GSH at high concentration (Jozefczak et al., 2012). Recycling of GSH by GR is essential for the GSH-dependent antioxidant system (Rogers et al., 2004).

2.2.5.1.5 Peroxiredoxin

Peroxiredoxin (Prx) is a member of the thiol peroxidase family and is closely associated with the Trx system, providing electrons necessary for its function. Because Prx have two Cys residues in their active site, they are often referred to as 2-Cys Prx. The antioxidant mechanism of Prx involves the deprotonated form of Prx reacting with H_2O_2 , ROOH, to release water or ROH. The newly formed molecule forms a disulfide bond with another Prx molecule. Using the Trx system, the two bound Prx molecules are reduced back to their active form (Lu and Holmgren 2014). The scavenging and catalytic ability of Prx is very efficient and comparable to that of CAT and GPx (Manta et al., 2009).

2.2.5.1.6 Thioredoxin reductase

When we talk about the redox defense of thioredoxin reductase (TrxR), the whole thioredoxin system should be mentioned, which also consists of NADPH and thioredoxin (Trx) (He et al., 2017). The system provides necessary electrons to a variety of enzymes responsible for DNA synthesis and protection from oxidative stress. The enzyme consists of the prosthetic group FAD, the NADPH-binding site, and a redox-active disulfide site (Du et al., 2012). Electron transfer from NADPH to the redox-active site allows TrxR to catalyze the reduction of Trx via disulfide reductase activity, thereby regulating the dithiol/disulfide balance of the protein (Balsera and Buchanan, 2019). Depending on their location in the cell, we can distinguish between the TrxR1 in the cytosol and the TrxR2 in the mitochondrion, although their function does not differ. The Trx system provides electrons for the enzyme peroxiredoxin (Prx) to degrade H_2O_2 , ROOH and $ONOO^-$ (Figure 3)(Lu and Holmgren, 2014).

The Trx system and the other thiol-dependent system, the GHS system, are functionally intertwined and appear to compete with each other, but the two systems are thought to work in parallel to reduce ROS accumulation in the cel (Du et al., 2012).

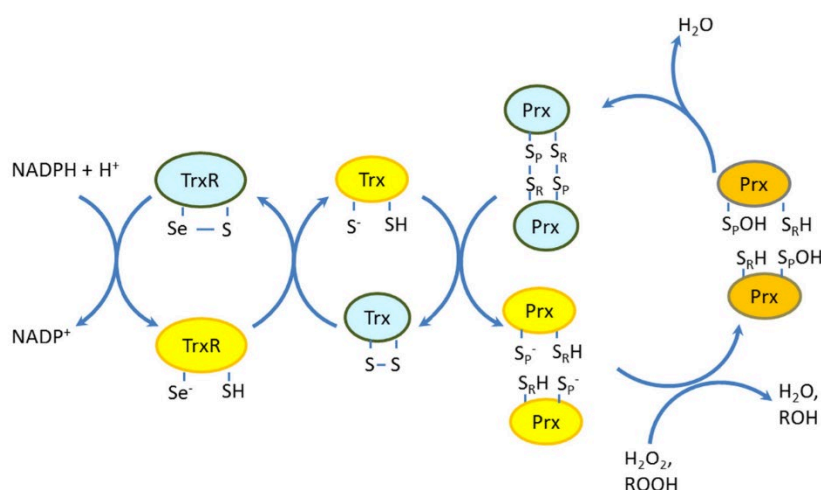


Figure 3: The Trx system and Prx mechanism (Lu and Holmgren, 2014).

2.2.5.2 Non-enzymatic defense

Non-enzymatic antioxidants are mainly low-molecular-weight substances, polypeptides, and proteins that are produced by the organism or ingested in the daily diet. They include vitamin A and vitamin C, β -carotene, uric acid, melatonin, and the most important of all, GSH.

2.2.5.2.1 Glutathione

The three amino acids glutamine, cysteine, and glycine form the most important molecule for non-enzymatic redox defense, glutathione (GSH) (Townsend et al., 2003). Its reduced form acts as an $O_2^{\cdot-}$ scavenger, an electron donor for H_2O_2 degradation by GPx, it modulates glutathionylation of proteins, and acts as a carrier and store of cysteine (Deponter 2013; Dickinson and Forman, 2002). In view of its multifunctional role in the organism, high levels of GSH and lower levels of GSSG are good indicators of normal or abnormal physiological conditions (Ballatori et al., 2009). Under normal physiological conditions, GSH is present in the reduced form and is found throughout the cell.

2.3 MODEL ORGANISM AND CELL LINE

2.3.1 Yeast *Saccharomyces cerevisiae*

Model organisms are irreplaceable tools in basic biology research and clinical trials research (Hunter, 2008). Initially, model organisms such as bacteria and bacteriophages focused on the study of key molecular mechanisms (replication, transcription, protein synthesis, and gene activity), but the field of research soon expanded to include more complex organisms (*Drosophila*, *Arabidopsis*, zebrafish and rodents). Once the biology of model organisms is well understood, they become not less, but even more important for the study of cellular processes because numerous genes and signaling pathways are conserved across species (Hunter, 2008). Model organisms are often chosen because they overcome ethical and experimental constraints, provide a model for developing, optimizing, and standardizing certain analyzes, and are a clear representative of a larger community of species with the same or similar biological processes (Karathia et al., 2011). It should be stressed however that data obtained on model organisms cannot be directly extrapolated on humans due to intra-species differences.

Saccharomyces cerevisiae (*S. cerevisiae*) is the best known, studied, and characterized eukaryotic model organism. Its cellular function and basic organization resembles that of mammalian cells, making it an ideal model for the study of biological processes or pathologies (Karathia et al., 2011). The complete sequence of the yeast genome reveals a well-conserved amino acid sequence and protein function between eukaryotic species (Botstein and Fink, 2011). Because of its high homology with the human genome,

comparable homology of protein functions, wide range of inexpensive genetic manipulations, ease and cheapness of cultivation and growth, study of multiple processes at once, and nearly complete database, *S. cerevisiae* is one of the ideal models for the study of oxidative stress response (de la Torre-Ruiz et al., 2015). The formation of ROS on the website ETC and the mechanism of oxidative stress response or defense is similar in yeast as in mammals (Herrero et al., 2008).

2.3.2 Human gingiva fibroblast cell line

To comply with the 3Rs (Replacement, Reduction, and Refinement) principle, alternatives to *in vivo* animal experiments should be considered by using either primary cells or cell lines (Krewski et al., 2010b). A focus should always be on the cell source, passage number, and cultivation method to allow comparison between laboratories. This includes the laboratory plastic used for culturing and assays, as well as growth conditions, morphology, and cell differentiation. Cell lines are generally preferred over primary cells because they are more stable, homogeneous, and generally available, resulting in better replication and comparison of scientific data. However, the advantages of using cell lines come at a price, as they do not differentiate and thus do not fully represent the *in vivo* situation (Gstraunthaler and Hartung, 2002).

Human gingival fibroblasts (HGF) are the most abundant representatives of the oral mucosa and are therefore frequently used in experiments to evaluate toxicity (Mah et al., 2014). Since they are in close proximity to the orthodontic alloys, they are a clinically relevant model. With each cell division, telomeres shorten and so does the lifespan of the cell. By expressing human telomerase reverse transcriptase (hTERT) in gingival fibroblasts, which prevents telomere shortening, a long-lived cell line can be obtained without altering physiology or phenotypic characteristics (Reijnders et al., 2015).

3 MATERIALS AND METHODS

3.1 RESEARCH WORK FLOW

The research was divided into four research sections, which are shown schematically in Figure 4.

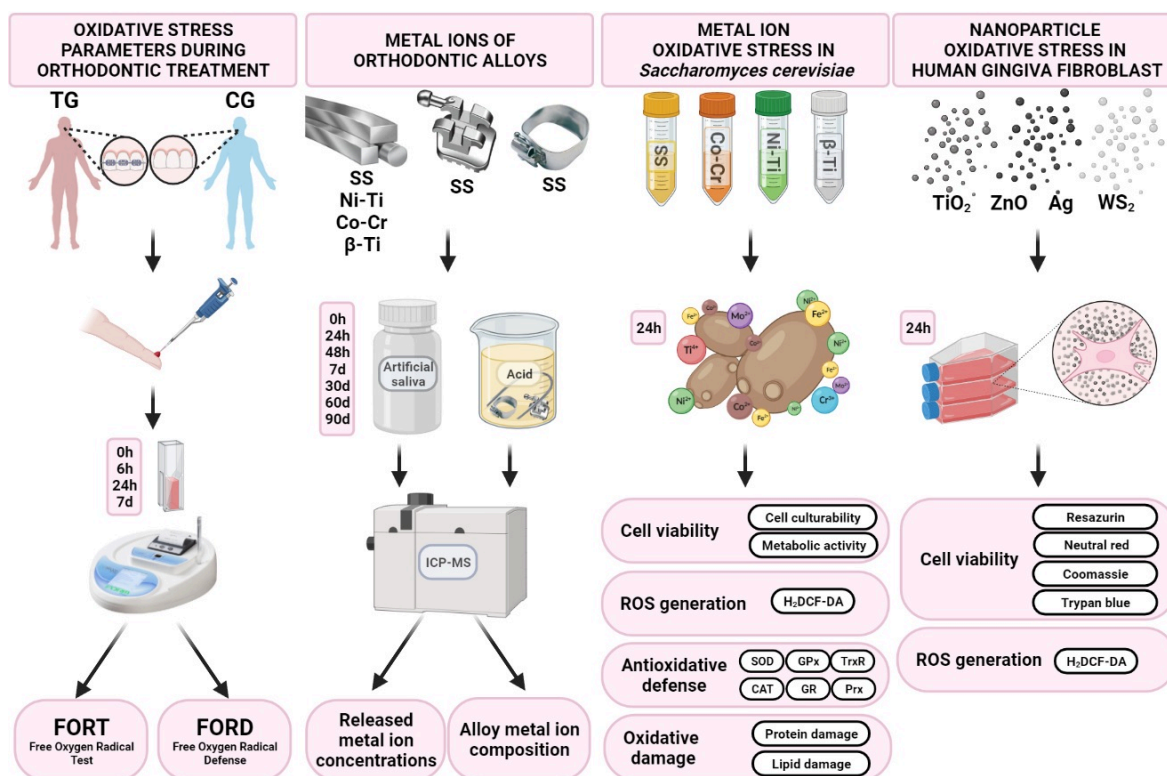


Figure 4: Research work flow.

3.2 SYSTEMIC OXIDATIVE STRESS PARAMETERS IN PATIENTS DURING ORTHODONTIC TREATMENT WITH FIXED APPLIANCES

3.2.1 Ethical approval

Ethical approval was obtained from the National Medical Ethics Committee (Annex A) prior to the start of the study, as well as informed consent from all patients prior to inclusion (Annex B). The study protocol was designed and conducted in accordance with the Declaration of Helsinki for Medical Research Involving Human Subjects (WHO, 2001).

3.2.2 Subjects and cohort design

Fifty-four healthy male patients between the ages of 19 and 28 who were diagnosed with dental anomalies (mild crowding and malocclusion) and were undergoing orthodontic

treatment at the Department of Orthodontics, College Medical Center of Ljubljana, Slovenia, participated in the study. Participation in the study was anonymous and voluntary. Before the start of the study, patients were informed about the purpose and procedure of the study. Withdrawal from the study was possible at any time. The research and sampling did not affect the course of orthodontic treatment. In addition, informed consent was obtained from each person to participate, and personal data were collected and stored in the archive of Assoc. prof. dr. Jasmine Primožič, Ph.D. dent. med, to which only she has access.

Before male subjects were enrolled in the study, a questionnaire about their lifestyle habits had to be completed to meet the inclusion/exclusion criteria (Annex C). Subjects with oral pathology (including periodontitis), poor oral hygiene, and known allergies, as well as smokers or subjects undergoing pharmaceutical therapy, including the use of food supplements with antioxidant properties, were excluded. The exclusive criteria were that subjects should not have prosthetic or other metallic materials in their body (implants, pricing, ...) and should not be exposed to metals in their daily life and should not consume synthetic antioxidants. Females were not included because of possible false results due to hormonal fluctuations.

The healthy male patients were randomly divided into two groups, the treatment group (TG), which underwent the orthodontic treatment, and the control group (CG), in which the orthodontic appliance was not placed in the oral cavity. The TG consisted of 27 male patients with a mean age of 24.6 ± 1.7 years, while the control group (CG) had the same number of patients with a mean age of 24.7 ± 1.7 years. During the study, patients adhered to a similar diet program and tried to avoid taking antioxidant supplements and alcohol. Extreme exercise and nocturnal living were discouraged. To exclude a possible influence of periodontal inflammation on the measurements of oxidative stress parameters, all participants were instructed on oral hygiene two weeks before the start of the study.

3.2.3 Insertion of the orthodontic appliance

The orthodontic appliance used to treat the malocclusion of the TG consisted of SS brackets (Gemini Brackets, 3M Unitek; USA) and two NiTi archwires (3M Unitek; USA). The appliance was inserted by a certified orthodontist.

3.2.4 Capillary blood collection

Capillary blood was collected from both TG and CG at four different time points: before orthodontic appliance insertion (time 0), after 6 hours, 24 hours, and after 7 days. The blood collection site was first disinfected with 70% ethanol and lightly massaged for better blood flow. A sterile needle is used to lightly prick the fingertip. The first drop of blood is discarded and the remainder, approximately 100 μ l, is collected in a heparinized tube.

3.2.5 Free oxygen radical test

Free oxygen radical test (FORT) is a colorimetric method using the Fenton reaction of transition metals to catalyze the degradation of hydroperoxides (ROOH) (Pavlatou et al., 2009). Capillary blood samples (50 μ l) were dissolved in an acidic medium where the ROOH reacts with transition metals to produce RO \cdot and ROO \cdot radicals. In the presence of phenylenediamine derivative (2CrNH $_2$), the RO \cdot and ROO \cdot radicals reacted with the additive. A color change, the intensity of which correlates with the ROOH concentration, can be measured spectrophotometrically at 505 nm using a special instrument FORM PLUS 3000 (Callegari 1930, Italy).

3.2.6 Free oxygen radical defense

Free oxygen radical defense (FORD) is based on the antioxidant ability of the sample to quench the chromogen signal (4-amino-N,N-diethylaniline sulfate). The samples are placed in an acidic buffer containing FeCl $_3$ and, depending on the concentration of the antioxidant, the chromogen loses its color proportionally (Pavlatou et al., 2009). The change is visible at 505 nm on the special instrument FORM PLUS 3000 (Callegari 1930, Italy). The values obtained are compared with the standard curve of Trolox, a non-enzymatic antioxidant.

3.3 TYPE AND AMOUNT OF OF METAL IONS RELEASED FROM ORTHODONTIC ALLOYS

3.3.1 Orthodontic materials

Both the upper and lower parts of SS, Ni-Ti, Co-Cr and β -Ti archwires were included in the study. Brackets and bands were all made of SS alloy. The surface area of each part (wire, bracket, and band) was measured using a digital caliper CD-AX /APX (Mitutoyo, Japan) and a rough estimate of the surface area was obtained. The detailed description of each orthodontic part used in the study is described in Table 6.

3.3.2 *In vitro* conditions

Artificial saliva was prepared internally to simulate oral conditions. It consisted of 400 mg/mL NaCl, 400 mg/mL KCl, 960 mg/L CaCl $_2$ ·2H $_2$ O, 690 mg/L NaH $_2$ PO $_4$ ·2H $_2$ O, 5 mg/L Na $_2$ S·9H $_2$ O, and 1000 mg/L urea, respectively (Kovač et al., 2021). All of the above chemicals were purchased from Merck (Darmstadt, Germany). Ultrapure water (Milli-Q, 18.2 M Ω cm) from a Direct-Q 5 Ultrapure (Millipore, Watertown, MA, USA) water system was used to dissolve the chemicals, and the pH of the saliva was adjusted to 6.7-6.8 with WTW 330 pH (Weilheim, Germany) to better match oral conditions.

250 mL of artificial saliva was placed in Teflon bottles (Merck, Germany) and the corresponding orthodontic parts, either two sets of wires, 24 brackets, or 4 molar bands, were immersed in it. A blind test with artificial saliva served as a control. Teflon bottles were used to minimize voids and prevent absorption of metals on the walls of the containers during the experiment. Samples were stored in a dust-free incubator (Kambič, Semič, Slovenia) at 37 °C for 90 days.

3.3.3 Inductively coupled plasma mass spectrometry analysis

3.3.3.1 Released metal ions in saliva

Prior to sampling, the Teflon bottles were carefully turned upside down to ensure an even distribution of elements in the sample volume. Saliva samples were collected at baseline, 2 hours, 24 hours, 48 hours, 7 days, 30 days, 60 days, and 90 days. Three samples of 3 mL were taken from each bottle, acidified with 6 µL Suprapur[®] nitric acid (Merc, Germany) and stored at -20 °C until analysis.

3.3.3.2 Metal alloy composition

Approximately 10 mg of each appliance part was dissolved in 5 mL of acid at 90 °C. The SS alloy parts were dissolved in aqua regia (HNO₃ + 3HCl), all titanium-based alloys (Ni-Ti and β-Ti) were dissolved in a mixture of HNO₃, HF, and HCl (volume ratio 4:2:1), and Co-Cr alloys in pure HCl. All acids were purchased from Merck (Germany).

3.3.3.3 Metal ion concentration measurement

The concentrations of metal ions, both of the digested orthodontic appliances and of the released metal ions in the artificial saliva, were determined by inductively coupled plasma mass spectrometry (ICP-MS) on an Agilent 7700x ICP-MS instrument (Tokyo, Japan), using matrix-matched standards for calibration. ICP-MS Measurement parameters are listed in (Appendix D) of the supplemental material.

Since there are no certified reference materials for the determination of trace elements in orthodontic appliances, the accuracy of the determination of metal ions in the analyzed samples was evaluated by the spike recovery test. For this purpose, known amounts of the analyzed elements were added to the bracket samples before digestion and the analytical procedure was applied. To verify the accuracy of the determination of the concentrations of metal ions released into the artificial saliva, the samples collected 90 days after incubation were spiked with known amounts of metals and the concentrations were determined using ICP-MS. Good agreement was obtained between the theoretically calculated and measured concentrations (differences did not exceed ±5%), confirming the accurate determination of

total metal concentrations and concentrations released into the artificial saliva by ICP-MS. In addition to the samples analyzed throughout the experiment, blank samples of the artificial saliva were also analyzed.

3.4 OXIDATIVE STRESS IN YEAST CELL MODEL

3.4.1 Yeast cultures

Wild type *S. cerevisiae* (BY4742) and two yeast mutants lacking certain antioxidative stress defense, Δ Sod1 *S. cerevisiae* (Y06913) and Δ Ctt1 *S. cerevisiae* (Y04718), were all purchased from EUROSCARF (Oberursel, Germany). The genotype of each yeast is listed in Table 3.

Table 3: *Saccharomyces cerevisiae* strains used in the study.

Strain	Genotype	Source
Y10000 (Wt)	BY4742; MATa; his3 Δ 1; leu2 Δ 0; lys2 Δ 0; ura3D Δ 0	EUROSCARF, Oberursel, Germany
Y06913 (Δ Sod1)	BY4741; MATa; ura3 Δ 0; leu2 Δ 0; his3 Δ 1; met15 Δ 0; YJR104c::kanMX4	EUROSCARF, Oberursel, Germany
Y04718 (Δ Ctt1)	BY4741; MATa; ura3 Δ 0; leu2 Δ 0; his3 Δ 1; met15 Δ 0; YGR088w::kanMX4	EUROSCARF, Oberursel, Germany

Yeast cell cultures were inoculated and maintained in Petri dishes containing solid yeast extract-peptone-glucose (YPD) medium (2% (w/v) glucose, 2% peptone, 1% (w/v) yeast extract, and 2% (w/v) agar (Merck, Darmstadt, Germany)). To facilitate growth of yeast cells, they were inoculated into 50 mL of liquid YPD medium (without agar). To achieve repeatable inoculation, the optical density of YPD with yeast cells (OD) at 650 nm had to be between 0.50 and 0.55. Once this was achieved, 20 mL of the cell suspension was transferred to an Erlenmeyer flask containing 180 mL of YPD. Submerged propagation of the yeast biomass occurred at 28 °C with constant shaking (220 RPM, InforsHT, Bottmingen, Switzerland) until it reached early stationary phase.

To obtain the yeast at the desired density, the yeast culture had to be transferred to PBS (phosphate buffer salt solution) (Merck, Darmstadt, Germany). Fifty mL of the yeast culture was centrifuged and the pellet containing yeast cells was washed three times with PBS. After the last washing step, 50 mL of the yeast cells suspension in PBS were transferred to a sterile Erlenmeyer flask containing 150 mL of PBS. The final concentration of cells was approximately 1×10^7 cells/mL. The yeast cells were kept in PBS (28 °C, 220 RPM) until treatment with the metal mixture, but not longer than 48 hours.

On the day of treatment, 10 mL of the yeast culture was aliquoted into an appropriate volume of sterile 50 mL Falcon tubes and sealed with foam plugs.

3.4.2 Metal ion mixtures and yeast treatment

The 0.2 M metal ion stock solutions were prepared in accordance with the safety data sheets of Dentaurum (Germany) (Dentaurum, 2020). The aim was to obtain a solution with a similar composition of metal ions as the orthodontic alloys. The selected metal alloys and their metal compositions are listed in Table 4. High-purity salts of $\text{FeCl}_3 \times 6\text{H}_2\text{O}$, $\text{CrCl}_3 \times 6\text{H}_2\text{O}$, $\text{NiCl}_2 \times 6\text{H}_2\text{O}$ and $\text{CoCl}_2 \times 6\text{H}_2\text{O}$ as well as TraceCERT® titanium and molybdenum standards for AAS were dissolved in sterile ddH₂O and their pH was adjusted to 7. All chemicals were purchased from Merck (Darmstadt, Germany). Each 0.2 M metal stock solution was used in an appropriate amount to obtain a metal mixture that corresponded to the orthodontic alloy composition, whether SS, Ni-Ti, Co-Cr, or β -Ti alloy. Before treatment, the metal stock solutions were briefly sonicated in an ultrasonic bath (Sonis 3 GT, Iskra Pio, Šentjernej, Slovenia).

Table 4: Metal ion w/v ratios for simulating orthodontic alloys.

Orthodontic alloy	Metal composition (w/v)					
	Fe	Ni	Cr	Co	Ti	Mo
Stainless steel (SS)	72%	10%	18%	/	/	/
Cobalt-chromium (Elgiloy - ELG)	18%	15%	20%	40%	/	7%
Cobalt-chromium (Remaloy - REM)	5%	21%	20%	50%	/	4%
Nickel-titanium (NiTi)	/	55%	/	/	45%	/
β -titanium (TiMo)	/	/	/	/	78%	12%

Falcon tubes containing 10 mL of yeast culture were used for the treatment with metal mixtures. Final concentrations of 1, 10, 100, and 1000 μM in yeast broth were performed for each of the five different metal ion mixtures. Yeast culture, which was not treated served as a control. The treatment lasted 24 h at 28 °C and 220 RPM.

3.4.3 Cell viability

3.4.3.1 Cell culturability

After metal treatment, serial dilutions of the treated cell samples were prepared (Koch, 2014) and then twenty 10- μl drops of the sample were placed on a fresh solid YPD plate with some

spacing and transferred to an incubator at 28°C for 48 hours. After incubation, the colony forming units (CFU) were counted. For each droplet, the number of colonies formed should be between 3 and 30 to be considered countable. The results were expressed as either CFU/mL or as percentages of cell culturability after each metal mixture treatment compared to the control sample.

3.4.3.2 Metabolic activity of the cells

For the assessment of cell metabolic activity, BacTiter-Glo™ Microbial Cell Viability Assay (Promega, San Luis Obispo, CA, USA) was used and performed according to the manufacturer's instructions. The kit is capable of determining the number of viable cells in the culture by quantitatively measuring ATP. The reagent provided lyses the cells and the thermostable luciferase reacts with the ATP from the lysed cells to produce a light signal. Hundred µL of the treated cells were added to a well of a white 96-well plate to which the same volume of BacTiter-Glo™ reagent was added. The microplate was immediately placed in a Tecan Spark® Cytro (Maennedorf, Switzerland) microplate reader, mixed for 30 seconds, and after 5 minutes of incubation, the intensity of emitted luminescence and OD were measured at 650 nm. The results were expressed as ratio of luminescence/optical density (L/OD) relative to the untreated control sample

3.4.4 ROS level determination

3.4.4.1 Determination of ROS content

The fluorescent dye 2,7-dichlorofluorescein diacetate (H₂DCF-DA) (Merck, Germany) was used to measure intracellular ROS (Jakubowski and Bartosz, 1997). The compound is added to cells in the form of diacetate ester, which can cross the cell membrane due to its nonpolarity. Inside the cells, it is deacetylated by nonspecific esterase to 2,7-dichlorodihydrofluorescein (H₂DCF). The polarity of the newly formed molecule prevents it from crossing the membrane, so it remains trapped inside the cells. Inside the cell, it becomes the target of ROS and in their presence it is oxidized to dichlorofluorescein (DCF), a fluorescent product whose fluorescence intensity can be measured at an excitation wavelength of 488 nm and an emission wavelength of 520 nm (Tetz et al., 2013).

We took 2 mL of the metal-treated cell sample, centrifuged and washed the cell sample three times with 50 mM PBS (pH 7.8). After the third wash, the pellet was resuspended in 500 µL PBS. Hundred µL of this cell suspension was transferred to a tube containing 890 µL PBS and 10 µL of a freshly prepared 1 mM H₂DCF-DA solution was added. The dye-containing samples were incubated in the dark at 28 °C and 220 RPM for 30 minutes. After incubation, the cells were washed again, plated on a black 96-well plate in 200 µL volume, and then the

fluorescence signal (488/520) and OD650 were measured in a designated plate reader. The results were expressed as F/OD relative to the control sample.

3.4.4.1.1 Modification of the protocol

In the first approach (protocol I), H₂DCF-DA solution was added to the yeast suspension at a final concentration of 10 µM immediately after the addition of the metal ion mixtures. After 24 hours of metal treatment, the yeast cells were washed only once with PBB. Then, the suspension was aliquoted into the appropriate microplate wells and the fluorescence signal and OD (650 nm) were measured using a microplate reader. The results were expressed as F/OD relative to the control sample.

The second approach (protocol II) followed the basic protocol. After 24 hours of metal treatment, cells were washed with PBB and then dye was added at a final concentration of 10 µM. After a 30-minute incubation in the dark, the cells were washed again with PBB medium. Then, fluorescence and OD were measured with the same parameters using an appropriate microplate reader. The results were presented as F/OD relative to the control sample.

In the third approach, we also followed the basic protocol, but instead of reporting the results as F/OD, we divided the fluorescence intensity with the corresponding cell cultivability. This ensured that the ROS concentration was represented in terms of culturable cells. As such, the results were presented as F/CFU relative to the control sample.

3.4.5 Enzymatic antioxidant defense

3.4.5.1 Cell lysate preparation

After 24-hour metal treatment, yeast cells were washed twice with PBS and the pellet was resuspended in lysis buffer consisting of 0.05 M Tris-HCl (pH 8) with cOmplete™, an EDTA-free protease inhibitor cocktail (Roche, Basel, Switzerland). Cells were homogenized 3 times with zirconium quartz beads (Biospec, USA) on the Bullet Blender tissue homogenizer (Next Advance, USA) at 30 second intervals. After each homogenization step, samples were incubated on ice for the same time. Cell lysates were then centrifuged at 20000 RCF and 4 °C for 20 minutes. Protein concentration in the supernatant was then determined using Bradford assay (Bradford, 1976).

The Bradford method is based on the binding of the dye (Comassie Brilliant Blue G-250) to aromatic amino acids. Upon binding, the color shifts from red to blue, changing the absorption maximum of the dye from 465 nm to 595 nm. The principle of the assay was to first add 196 µL of Bradford reagent (Merck, Germany) to a well of a reader plate, to which

4 μL of an unknown protein sample had to be added. The dye-protein solution was briefly shaken and incubated for 5 minutes. The absorbance could be read within the next hour as the dye-protein solution is very stable. As with any measurement, a calibration curve had to be established by using different concentrations of BSA (Merck, Germany) to which the same amount of Bradford reagent was added. The plate reader measures the absorbance of the sample at 595 nm and the protein concentration of the sample can then be determined from the calibration curve.

3.4.5.2 Superoxide dismutase activity

The protocol for SOD activity was based on the antioxidant ability of the SOD enzyme to inhibit the autoxidation of pyrogallol at alkaline pH, which was first described by Marklund and Marklund (1974). When pyrogallol is oxidized, a yellow colored product (purpurogallin) is formed. When SOD is present, the color change decreases according to the activity of SOD. The difference in color change rate can be determined at 420 nm absorbance. Mesa-Herrera et al. (2019) improved and optimized the method for measurement in 96-well plates.

Volumes of 176 μL of the reaction buffer (50 mM Tris-cacodylic acid, 1 mM DTPA, pH 8.2) and 20 μL of the protein sample were pipetted into a well of a multi-well plate and incubated at room temperature in a plate reader under gentle shaking conditions. Both blank and control wells were used in the assay. After incubation, 4 μL of 30 mM pyrogallol was added to the wells (except the blank well) and the entire plate was shaken for 1 minute. Kinetic measurement of absorbance at 420 nm was performed every 15 s for 5 min in a multiwell plate reader at room temperature. The increase/decrease in absorbance change was determined by the linear slope of the control and unknown sample. The results are expressed as the percentage activity of the enzyme SOD after treatment compared to the enzyme activity of the control sample.

3.4.5.3 Catalase activity

Spectrophotometric determination of CAT activity was first described by Beers and Sizer (1952). As CAT from cell lysates decomposes H_2O_2 , a decrease in absorbance at 240 nm can be observed. The difference in absorbance over time (ΔA_{240}) is derived as a measure of CAT activity (Grilo et al., 2020).

Samples had to be diluted 50x with PBS, and 100 μL of the diluted samples were pipetted into a well of a UV-transparent 96-well plate (Greiner Bio-One, The Netherlands). To start the assay, 100 μL of a 30 mM H_2O_2 solution was added. The initial absorbance had to be between 0.520 and 0.550, otherwise H_2O_2 had to be added to the solution or diluted with PBB. This step ensured a repeatable measurement between replicates. For a control sample, 10 μL of 1 U/mL bovine liver CAT (Merck, Germany) was used. A blank well was also used

consisting of 200 μL of PBB and 100 μL of 30 mM H_2O_2 as a blank. Kinetic measurements were performed every 10 s for 5 min at a wavelength of 240 nm. The results were expressed as the percentage activity of the enzyme CAT after treatment compared to the enzyme activity of the untreated control sample.

3.4.5.4 Glutathione peroxidase activity

The GPx activity was determined by the assay described by Smith and Levander (2002) with minor modification. The assay relies on the GPx enzyme to degrade peroxides. In the first reaction, GSH is oxidized to GSSG, and in the second reaction, it is converted back to GSH by GR, using NADPH for the reduction reaction. Consequently, the oxidation of NADPH may be a good measure of GPx activity.

The adapted assay (Dong et al., 2016) was performed as follows: For a GPx reaction mixture, final concentrations of 6.5 mM EDTA- Na_2 , 1.3 mM NaN_3 , 0.5 mM NADPH, 2.5 mM GSH, and 1.7 U/mL GR were dissolved in 65 mM PBS (all from Merck, Germany), with NADPH and GR added as late as possible to the reaction mixture. Then, 47 μL of the cell sample was mixed with 250 μL of the GPx reaction mixture in a well of a multiwell plate, to which 3 μL of 250 μM H_2O_2 was added to start the reaction. For a blank sample, 50 μL of lysis buffer was used instead of the cell sample. During the addition of H_2O_2 , the change in optical density was measured at 340 nm every 15 s for 5 min. The results obtained were expressed as the percentage activity of GPx enzyme after treatment compared to the enzyme activity of the control sample.

3.4.5.5 Glutathione reductase activity

The GR activity assay was described by Smith et al. (1988) and adapted by Glippa et al., (2018). The principle of the assay is the ability of GR to convert GSSG to GSH using NADPH as a substrate. Instead of measuring the rate of NADPH conversion, the assay measures the concentration of GSH formed, which reacts with 5,5'-dithiobis(2-nitrobenzoic acid) (DTNB) present in the reaction mixture. The formed product 5-thio(2-nitrobenzoic acid) (TNB) is colored yellow and its absorbance can be read at 412 nm.

For the assay, the buffer (100 mM K-phosphate buffer (pH 7.5) containing 1 mM EDTA) had to be prepared. A 2 mM GSSG solution, 2 mM NADPH and 3 mM DTNB were prepared in the above assay buffer. Twenty μL of the cell sample was pipetted into one well first, followed by DNTB. NADPH was added last, and immediately the plate was shaken for 5 s and absorbance was measured at 412 nm every 20 seconds for 6 min. For blank wells, the cell sample was replaced with the same amount of lysing buffer, and 4 μL (10 U/mL) GR of baker's yeast (Merck, Germany) was used for the positive sample. The results obtained were

expressed as the percentage activity of the GR enzyme after treatment compared to the enzyme activity of the control sample.

3.4.5.6 TrxR activity

The TrxR activity assay was also adapted from Smith and Levander (2002) with minor modifications. TrxR catalyzes the reduction of oxidized thioredoxin, but in the assay 5,5-dithiobis (2-nitrobenzoic acid) (DTNB) was used as a suitable and inexpensive substrate. DTNB is reduced to a thio-bis-nitrobenzoic acid anion (TNB) in an NADPH-dependent reaction. The absorbance change of the formed product TNB was measured at 412 nm.

The assay buffer contained 10 mM EDTA- Na_2 , 5 mM DTBN, 240 μM NADPH, and 0.2 mg/mL bovine serum albumin, all dissolved in 100 mM PBS. The lysate samples were added to the two corresponding wells, each containing 54 μL . To one well containing the lysate samples, 6 μL of 5% EtOH was added and to the second 6 μL of 1.47 mM auranofin, an inhibitor of TrxR (Dong et al., 2016) was added and incubated for 10 minutes at room temperature. After incubation, 250 μL of the assay buffer was added and absorbance measurement started 1 min after buffer addition, due to non-enzymatic reduction of DTNB in the lysate sample. The absorbance change was measured at 412 nm every 15 s for 5 min. The slope of the reaction in the presence of auranofin was subtracted from the slope of the reaction in which auranofin was omitted. The results obtained were expressed as the percentage activity of the TrxR enzyme after treatment compared to the enzyme activity of the control sample.

3.4.5.7 Peroxiredoxine activity

Prx activity was determined according to assay described by Ali and Hadwan (2019), also known as ferrous xylenol orange assay (FOX). Prx activity is based on detoxification of peroxides at the expense of either NADPH or NADH. Peroxides are also degraded by CAT and GPx, but due to the addition of sodium azide (NaN_3) to inhibit CAT and the absence of the GPx substrate GSH, the FOX method remains a specific and reliable way to detect Prx activity. The FOX assay utilizes the peroxide-dependent oxidation of Fe(II) to Fe(III), which reacts with xylenol orange. The newly formed product is colored blue/purple and its absorption spectrum can be measured at 560 nm.

For the assay, the reagents FOX -A and FOX -B had to be prepared. For FOX-A, 25 mM $(\text{NH}_4)_2\text{Fe}(\text{SO}_4)_2 \cdot 6\text{H}_2\text{O}$ in 25 M H_2SO_4 had to be prepared and for FOX -B, 100 mM sorbitol and 125 μM concentrations in distilled water were prepared. On the day of the experiment, FOX -A and FOX -B were mixed together in a volume ratio of 1:100, as was a standardized 2.1 mM H_2O_2 solution in 50 mM PBS. 2.1 mM concentration of 1,4-dithio- DL -threitol (DTT) and 10 mM concentration of NaN_3 were also freshly prepared each time the assay

was performed. In a tube, 100 μL of the cell lysate, 200 μL of DTT, 100 μL of NaN_3 , and 600 μL of PBS were mixed. A standard tube in which the lysate was replaced with additional DTT and a blank tube containing no DTT and no lysate sample were also analyzed. 200 μL of H_2O_2 solution was added to each tube, mixed vigorously, and incubated for 3 minutes. Then, 50 μL was aliquoted from each tube, mixed with 950 μL of the freshly prepared FOX-A/B reagent, and incubated for 30 minutes at room temperature. The change in absorbance at 560 nm was recorded and evaluated against the standard and blank. The results were expressed as the percentage activity of the PRDX enzyme after treatment, compared to the enzyme activity of the control sample.

3.4.5.8 In-gel enzyme activity of SOD and CAT

Native gels require ten times less protein samples than spectrophotometric activity assays and provide a qualitative result compared to the quantitative results of the assays. In addition, the visual representation of activity is more presentable to the general public.

The protocol was adopted from Weydert and Cullen (2010) with minor modifications. Reduction of nitroblue tetrazolium (NBT) by the $\text{O}_2^{\cdot-}$ is a key factor in the protocol because the enzyme SOD competes with NBT for $\text{O}_2^{\cdot-}$. Since NBT changes color from yellow to blue when reduced, the color inhibition is related to the SOD activity of sample (Spitz and Oberley 2001). The CAT activity assay was similar to the normal spectrophotometric method in which the principle of activity evaluation was the removal of peroxide. The remaining peroxide reduces the yellow potassium ferricyanide to potassium ferrocyanide, which reacts with ferric chloride to form a Prussian blue (green-yellow) precipitate.

3.4.5.8.1 Electrophoresis gels

A non-denaturing polyacrylamide gel and a 5% stacking gel were prepared for each SOD or CAT activity assay. The difference in gel preparation when evaluating SOD or CAT activity was the separating gel. For SOD activity, a 12% polyacrylamide separation gel was used, and for CAT activity, an 8% separation gel was used.

For the native separation gel, 1.5 M Tris-HCl (pH 8.8), 30% acrylamide/8% bis-acrylamide, 10% ammonium persulfate (APS), and tetramethylethylenediamine (TEMED) were mixed in distilled H_2O and the volume was pipetted into a 1.0 mm spacer glass plate cassette (Bio-Rad, United States) with the top edge only about 1 cm short. A layer of water was added on top of the gel to cover it completely. Within 1 hour, the running gel cured and the water was carefully removed from the top of the gel. A 5% stacking gel consisting of the same reagents as the separating gel, except 0.5 M Tris-HCl (pH 6.8), was poured on top and a 1.0 mm comb was inserted. It took 1 hour for the stacking gel to cure. The cassette was then removed from the casting stand, wrapped in a towel soaked in water, and allowed to polymerize completely overnight in the margins (2 - 8°C).

3.4.5.8.2 Electrophoresis buffers

Three different buffers had to be prepared: a buffer before electrophoresis, a buffer for electrophoresis, and a buffer for loading the samples. It was an absolute necessity to prepare them fresh and keep them all at $< 4\text{ }^{\circ}\text{C}$.

The pre-electrophoresis running buffer ensures that the free persulfate ions are removed from the gels so that they do not interfere with the activity of the antioxidant enzymes. It consisted of 190 mM Tris- HCl and 1.13 mM disodium EDTA. The pH had to be adjusted to pH 8.8 with HCl.

The electrophoresis running buffer provided ions to conduct a current and keep the pH relatively constant. It consisted of 50 mM Tris- HCl, 0.3 M glycine, and 2 mM disodium EDTA. The pH was adjusted to pH 8.3 with HCl.

The sample loading buffer was prepared by mixing 1.5 M Tris-HCl (pH 6.8), glycerol and 5% bromophenol blue solution at a ratio of 1:1:0.02.

3.4.5.8.3 Loading of samples and electrophoresis

After overnight gel polymerization, the combs were removed from the gel assembly, placed in the electrophoresis assembly, and placed in the electrophoresis apparatus (box). The pre-electrophoresis buffer was poured into the reservoir and chamber of the box. To ensure that the pre-electrophoresis proceeded at $< 4\text{ }^{\circ}\text{C}$, the entire electrophoresis box was surrounded with ice. Pre-electrophoresis ran for 1 hour, and the gels ran for 1 hour at 40 mA per gel. This step removed residual APS, TEMED, and incomplete polymerization products that could inactivate native proteins.

Cell lysates of known concentration were mixed 1:1 with the loading buffer. 20 μL of the thoroughly resuspended samples were then pipetted into the appropriate wells.

After the pre-electrophoresis step, the buffer was removed and replaced with electrophoresis buffer. The gels were then run under the same conditions (40 mA, $4\text{ }^{\circ}\text{C}$) until the dye line reached the bottom (between 2-3 hours). The gels were then run for an additional 1 hour.

3.4.5.9 SOD in-gel activity staining

For SOD activity staining, the dye solution consisted of 2.43 mM NBT, 28 mM TEMED, and 22.4 μM riboflavin 5'-phosphate in 50 mM phosphate buffer (pH 7.8). Each gel was stained in the dye solution for 20 min at room temperature with shaking and in the dark. Then the gels were rinsed twice with water and lightly immersed in the water under fluorescent light or in a light box. Depending on the light intensity (up to 2 hours), the gels

turned blue/purple in the areas where there was no SOD activity. The gels were then washed with water and left in water under ambient light for better band development.

The gel/band images were acquired, and the intensity of each gel/band image was determined using ImageJ, an image analysis software (Java-based image processing software, National Institutes of Health, Bethesda, MD, USA). The activity of the treated lysate samples was compared with the control.

3.4.5.9.1 CAT in-gel activity staining

For CAT stain, 2% ferric chloride was prepared in one tube and 2% potassium ferricyanide in distilled water in a second tube.

After electrophoresis, the gels were washed three times in distilled water for 10 minutes. After the washing phase, the gel was incubated in a 0.003% H₂O₂ solution for an additional 10 minutes. The cells were then washed twice for 5 minutes in distilled water. The water was then poured off and the two tubes containing the CAT staining solution were poured onto the gel simultaneously. The staining of the gel took about 30 minutes until achromatic curvatures appeared. All the staining solution was then removed from the dish.

The gel/band images were acquired, and the intensity of each gel/band image was determined using ImageJ, an image analysis software (Java-based image processing software, National Institutes of Health, Bethesda, MD, USA). The activity of the treated lysate samples was compared with the untreated control.

3.4.6 Oxidative damages

3.4.6.1 Oxidative lipid damages

To evaluate oxidative damage to lipids, the thiobarbituric acid reactivity assay (TBARS) was used. The method was described by Ohkawa et al. (1979) and adapted by Aguilar Diaz De Leon and Borges (2020). The TBARS method uses the reaction between MDA, a product of lipid peroxidation, and thiobarbituric acid (TBA). The reaction product, MDA-TBA₂, has a reddish-pink color and absorbs the visible spectrum at 532 nm. After metal treatment, cells were washed twice with PBS and TBARS reagent consisting of 91.8 mM trichloroacetic acid, 2.5 mM thiobarbituric acid, 45.4 μM butylhydroxytoluene (Merck, Darmstadt, Germany) and 25 mM HCl (all from Merck, Germany) was added to the pellet, thoroughly resuspended and homogenized. After homogenization, samples were incubated at 90 °C (Thermomixer R, Eppendorf, Hamburg, Germany) for 30 minutes and then placed on ice for an additional 10 minutes. After ice treatment, butanol was added and the homogenized samples were centrifuged at 10000 RCF for 10 minutes. Fluorescence intensity (515/555

nm) and OD (650 nm) were measured using a Varioskan™ LUX (ThermoFisher, Waltham, MA, USA) microplate reader. Results were expressed as F/OD relative to the untreated control.

3.4.6.2 Oxidative protein damages

The method for determining protein oxidative damages was described by Levine et al. (1990) and modified by Mesquita et al. (2014). The method proposed to use 2,4-dinitrophenylhydrazine (DNPH) to react with the oxidatively formed protein carbonyl groups. For the simplified method, 40 µL of the lysate sample was mixed with 40 µL of DNPH (10 mM in 0.5 M H₃PO₄) and incubated for 10 min. For the blank sample, the protein sample was replaced with the lysis buffer, and for the positive control, the BSA solution with the same protein concentration as the lysate sample was used. After incubation, 20 µL of 6 M NaOH was added, and after 10 min of incubation, absorbance was measured at 450 nm. Incubation after addition of NaOH was strictly controlled due to the instability of DNPH in alkaline media. Results were expressed as the percentage of protein oxidative damage after treatment with specific metals compared with the control sample.

3.5 OXIDATIVE STRESS IN HGF

3.5.1 HGF cell line

The hTERT-immortalized HGF cell line (T0026) was originally purchased from (ABM, Canada) but was kindly provided to us by Prof. Dr. Sue Gibbs (MCBI, Amsterdam UMC, The Netherlands). Fibroblasts were cultured in 10 mL of fibroblast medium consisting of DMEM (Merck, Germany) supplemented with 5% HyClone FetalClone III serum (Cytiva, United States) 1% penicillin-streptomycin (Merck, Germany) in T75 flasks (Merck, Germany) at 37°C and 5% CO₂ atmosphere. After reaching confluence, cells were washed with PBS, trypsinized with 2 mL of 0.05% trypsin-EDTA solution (Merck, Germany), and detached from the flask for approximately 10 minutes in the previously described incubator settings. Then, 8 mL of medium was added, a small sample was taken for cell counting, and the cells were centrifuged at 300 RCF for 5 minutes. The supernatant was discarded and the pellet was resuspended in an appropriate amount of the medium so that the final number of cells was 1.0 x 10⁶ per T75 flask.

3.5.2 Nanoparticle characterization and preparation for treatment

TiO₂-NPs, ZnO-NPs, Ag-NPs and WS₂-NPs were purchased from Nanografi Nano Technology (Ankara, Turkey) in different sizes and in the case of TiO₂-NPs in different shapes: Anatase, Rutile and a mixture of both forms (Table 5). For the treatment, 10 mg/mL stock suspensions of each NP were prepared in deionized water (MilliQ, Millipore, USA).

Before preparation of working suspensions from NP, stock suspensions from NP were sonicated for 15 minutes in an ultrasonic water bath at 250 W and 50 Hz (Sonis 2GT, Iskra Pio, Slovenia). The prepared stock solutions were used for NP characterization.

Characterization of NPs were done by prof. dr. Darko Makovec and asst. prof. dr. Slavko Kralj from the Department for materials synthesis, Institute Jozef Stefan. For the NPs diameter size evaluation, at least 500 NPs were measured with a transmission electron microscope (JOEL, Tokio, Japan). To observe, how NPs behave in an aquatic solution or as in our case, in cell growth medium, dynamic light scattering (DLS) method combined with zeta potential (ZP) measurement were used to measure hydrodynamic diameter of NPs in 100 µg/mL NP solution and to provide information on the aggregation state of nanoparticles in 100 µg/mL NP suspension. The DLS analysis in the liquid phase provides information on the hydrodynamic particle size of the nanoparticles (Lim et al., 2013), whereas ZP provides information of NPs solution stability due to its surface charge (Bhattacharjee, 2016). DLS and the ZP analysis were performed on Litesizer 500 (Anton Paar, Austria).

Table 5: Nanoparticles used in the study.

Nanoparticles	Average Diameter (nm)	Catalog number	Company
TiO ₂ - Anatase/Rutile	18	NG04SO3506G25	
TiO ₂ - Anatase	28	NG04SO3503G25	
TiO ₂ - Rutile	28	NG04SO3507G25	Nanografi Nano
Ag	28-48	NG04EO0105G5	Technology
Ag	48-78	NG04EO0103G5	(Ankara, Turkey)
ZnO	18	NG04SO3803G25	
ZnO	30-50	NG04SO3802G25	
WS ₂	35-75	NG04CO2401G25	

To prepare working solutions, which ranged from 1 µg/mL to 1000 µg/mL, the NP stock solutions were appropriately diluted in fibroblast medium. The NP treatment was performed in either 6-well, 12-well or 96-well plates. For this purpose, we used HGF at a concentration of 2.2×10^4 cells/cm², regardless of the multi-well plate. A volume of 2 mL was added to each well of the multi-well plate for a 6-well plate, 1 mL for a 12-well plate, and 100 µL for a 96-well plate. Freshly seeded cells on a multi-well plate were then placed back into the incubator and left there for 24 hours to attach properly. After attachment, the cells were treated with the working solution NP.

3.5.3 HGF cell viability

To test the viability of the cells, several methods were used because some NP interfered with the analytical methods (Mello et al., 2020).

3.5.3.1 Resazurin assay

Resazurin is a non-toxic, membrane-permeable molecule. It acts as an electron acceptor in cells ETC without interfering with their normal function (Page et al., 1993). When the dye accepts electrons from either mitochondrial reductases or other cytoplasmic enzymes, the blue, nonfluorescent dye is reduced to a pink, highly resorufinated dye. The changes in the fluorescence signal can be observed at an excitation wavelength of 530-560 nm and an emission wavelength of 590 nm (Rampersad, 2012). The method used in this study was described by Elshikh et al (2016).

HGF were seeded on a 96-well plate, with each well containing 100 μL of 2.2×10^4 cells/ cm^2 , and allowed to attach in the incubator for 24 hours. The cells were then exposed to NPs with final concentrations ranging from 1 $\mu\text{g}/\text{mL}$ to 1000 $\mu\text{g}/\text{mL}$, depending on the type of NPs used. After incubation at 37°C and 5% CO_2 for 24 hours, 30 μL of 0.015% resazurin (Merck, Germany) was added to all wells and incubated further for 2.5 hours under the same known conditions. The fluorescence intensity of the samples was then measured at 560/590 nm. Results were expressed as the percentage of fluorescence intensity after a given NP treatment compared to the control sample.

3.5.3.2 Neutral red uptake assay

The neutral red assay was proposed by Repettou et al. (2008). The dye penetrates the cell membrane at a physiological pH and concentrates in the lysosomes where it binds to anionic or phosphate groups of the lysosomal matrix (Nemes et al., 1979). There is a low pH gradient in the lysosomal matrix that prevents the dye from escaping the lysosome. This only happens in viable cells because they are able to maintain acidic pH gradients by producing ATP. The dye is easily extracted with an acidified ethanol solution and the absorbance of the extract can be quantified spectrophotometrically. The dye concentration of the extract is proportional to the number of viable cells.

HGFs were seeded on a 96-well plate, with each well containing 100 μL of 2.2×10^4 cells/ cm^2 , and allowed to attach in the incubator for 24 hours. The cells were then exposed to NPs with final concentrations ranging from 1 $\mu\text{g}/\text{mL}$ to 1000 $\mu\text{g}/\text{mL}$, depending on the type of NPs used. After the 24-hour incubation at 37°C and 5% CO_2 , 18 μL of neutral red dye (Merck, Germany) was added to all wells and incubated further for 2.5 hours under the same known conditions. After the incubation period, the dye-containing medium was discarded and 80 μL of neutral red dye solvent (50% EtOH, 1% CH_3COOH , and 49% ddH₂O) was added to each well. The multiwell plate was then incubated for 20 min at room temperature with occasional shaking. Measurement was then performed using a spectrofluorimeter at excitation and emission wavelengths of 530 and 645 nm, respectively.

Results were expressed as the percentage of fluorescence intensity after a given NP treatment compared to the control sample.

3.5.3.3 Coomassie Blue Assay

The Coomassie blue stain assay is used to determine total protein content. Under acidic conditions, the Coomassie Brilliant Blue G-250 dye binds to arginine, histidine, phenylalanine, tryptophan and tyrosine residues. Upon binding, there is a color shift from 465 nm to 595 nm (Noble, 2014). Theoretically, the cellular protein amount is related to the number of viable cells. The assay used in the study was performed according to Kononenko et al. (2019).

HGF were seeded on a 96-well plate, with each well containing 100 μL of 2.2×10^4 cells/cm², and allowed to adhere in the incubator for 24 hours. The cells were then exposed to NPs with final concentrations ranging from 1 $\mu\text{g/mL}$ to 1000 $\mu\text{g/mL}$, depending on the type of NPs used. After the 24-hour incubation at 37°C and 5% CO₂, the medium was discarded and 50 μL of 0.05% Coomassie Brilliant Blue G250 (Merck, Germany) (30% MeOH, 10% CH₃COOH, 60% ddH₂O) was added to each well and incubated for 20 minutes at room temperature. The dye was then discarded, the wells were washed with Dulbecco's phosphate buffered saline (DPBS), and 50 μL 0.1 M NaOH was added to dissolve the dye. A 20-minute incubation followed and absorbance in the wells was measured at 595 nm. Results were expressed as the percentage of absorbance intensity after a given NP treatment compared to the control sample.

3.5.3.4 The trypan blue cellular debris assay

The trypan blue dye is well known in the laboratory (trypan blue exclusion assay) as it is used as a dye to distinguish between intact live cells and permeable dead cells and debris, usually routinely used to count live cells on a hemocytometer (Strober, 2015). Live cells do not take up the dye, but dead cells and debris do. The viability assay proposed by Lebeau et al. (2019) and also used in this study suggests using bound dye concentrations to determine cell viability.

HGF were seeded on a 6-well plate, with each well containing 2 mL of 2.2×10^4 cells/cm², and allowed to attach in the incubator for 24 hours. The cells were then exposed to NPs with final concentrations ranging from 1 $\mu\text{g/mL}$ to 1000 $\mu\text{g/mL}$, depending on the type of NPs used. After incubation at 37°C and 5% CO₂ for 24 hours, the well medium containing cell debris and dead cells was carefully collected in a tube and centrifuged at 10000 RCF and room temperature for 2 minutes. The medium was then discarded and 100 μL of a 0.4% trypan blue solution (ThermoFisher, USA) was added, shaken vigorously and stained for 5 min. The samples were then centrifuged again for 2 min at 12000 RCF and the dye was removed. Without disturbing the pellet, a washing step was performed with 500 μL of 99%

2-propanol. To the washed pellet, 100 μL of PBS was added to each of the tubes to extract the dye from the pellet. The pellet was shaken again and heated on the ThermoMixer C dry block heater (Eppendorf, Germany) at 80 $^{\circ}\text{C}$ for 10 min. A final centrifugation step was performed at 12000 RCF for 2 min, and a 40 μL volume of the PBS extract was added to a 96-well plate. The optical density of the extract was measured at a wavelength of 590 nm. Results were expressed as the percentage of absorbance intensity after a given NP treatment compared to the control sample.

3.5.4 ROS level determination

The fluorescent probe $\text{H}_2\text{DCF-DA}$ was used to detect the intracellular ROS to evaluate the redox balance in pathological cells. The assay described by El-Hassani and Dupuy (2013) served as a platform for this study. The dye crosses the cell membrane and is converted to a fluorescent product in the presence of ROS. This cleavage of the dye also occurs in dead or senescent cells, so a live/dead cell exclusion assay must be performed simultaneously. The proposed method was to use propidium iodide (PI) to stain the dead and dying cells. PI cannot penetrate the membranes of viable cells, only dead and dying cells, where it binds to nucleic acids. When it attaches to DNA, the fluorescence of PI increases 20-30 fold and the emission and excitation shifts to 535 nm / 617 nm (Rosenberg et al., 2019). Because of the wavelength shift, the use of PI at the same time as $\text{H}_2\text{DCF-DA}$ is possible.

HGF were seeded on a 96-well plate, with each well containing 100 μL of 2.2×10^4 cells/ cm^2 , and allowed to adhere for 24 h in the incubator. The cells were then exposed to NPs, the final concentration of which ranged from 1 $\mu\text{g}/\text{mL}$ to 1000 $\mu\text{g}/\text{mL}$, depending on the type of NPs used. After incubation at 37 $^{\circ}\text{C}$ and 5% CO_2 for 24 hours, the cells were washed three times with PBS. After the last washing step, PBS was discarded and 100 μL of 10 μM $\text{H}_2\text{DCF-DA}$ was added to the wells. The multiwell plates were left in dark conditions for 45 min. After incubation, 15 μL of 1 $\mu\text{g}/\text{mL}$ PI was added and the plates were immediately placed in the spectrophotometer to obtain fluorescence for intracellular ROS (exc/em = 488/527) and PI (exc/em = 535/617). Results were expressed as the percentage of fluorescence intensity after a given NP treatment compared to the control sample.

3.6 STATISTICAL ANALYSIS

For the data analysis of the *in vivo* study, the Statistical Package for Social Sciences Software release 20.0 (SPSS Inc., Chicago, Illinois, USA) was used. To balance the age of each experimental groups, Mann-Whitney U-test was used. After testing the normality of the data with the Shapiro-Wilk test and Q-Q normality plots and the equality of variance among the datasets using a Levene test, nonparametric methods were used for data analysis.

A Friedman test was used to assess the significance of the differences in every parameter (FORT, FORD, and FORT/FORD ratio) over the time points within each group. When significant

interactions were seen, a Bonferroni-corrected Wilcoxon test was used for pairwise comparisons. A Mann-Whitney U-test was used to assess the significance of the differences in every parameter between the two groups within each time point. The results were considered to be significant at p-values below 0.05.

Shapiro–Wilk and D’Agostino and Pearson tests were used to analyze the normal distribution of the acquired data. Normally distributed data were analyzed with one-way ANOVA followed by Dunnett’s post hoc test for multiple comparisons and non-normally distributed data were analyzed with Kruskal–Wallis test followed by Dunn’s post hoc test. Cutoff for the statistical significance of data was considered when $p < 0.05$. Visual presentation and statistical analysis were performed with GraphPad Prism (version 8.02 for Windows, GraphPad Software, La Jolla, CA, USA, www.graphpad.com).

4 RESULTS WITH DISCUSSION

4.1 CHANGES IN OXIDATIVE STRESS PARAMETERS IN THE CAPILLARY BLOOD

In this study, we sought to evaluate whether oxidative stress in blood samples occurs during orthodontic treatment. The predominance of free radicals over antioxidants may be a trigger for periodontal desies (Panjamurthy et al., 2005). Previous studies have used saliva (Buczko et al., 2017; Portelli et al., 2017; Yamyar and Daokar 2019) or gingival crevicular fluid (Atuğ Özcan et al., 2014; Chitra et al., 2022) as diagnostic tools to determine oxidative stress parameters. The oral cavity, especially saliva, has numerous antioxidant defense systems and therefore plays an important role in maintaining redox balance. It can be said that saliva acts as the first antioxidant defense, and salivary markers reflect to some extent the condition of the oral cavity (Buczko et al., 2017). Evaluation of individual oxidative markers provides only specific information, whereas estimation of the overall oxidative status and total antioxidant capacity provides a more objective picture of the given prognosis. By measuring the formation of ROS (FORT) and antioxidant potential (FORD) in capillary blood samples, the normal/abnormal physiology of patients can be more accurately estimated at a systematic level.

Blood samples from the TG and CG groups were collected during the first week of orthodontic treatment, and the values FORT and FORD were determined. No significant difference was found between the baseline values of TG and CG before appliance insertion, neither for FORT ($p > 0.05$) nor for FORD ($p > 0.05$). The only significant difference in the values of FORT was observed for TG after 24 hours of orthodontic treatment ($p < 0.05$), but at the next analysis (at 7 days), the value decreased back to the baseline level. Compared to CG, whose FORT values remained almost the same throughout the study, an increase in radical formation is observed after 24 hours of orthodontic treatment. The FORD values did not change significantly in the first week in either group. The results of the analysis of FORT and FORD are shown in Figure 5 as FORT /FORD ratio, which illustrates the balance between radical formation and antioxidant defense. There was no evidence of periodontal disease or inflammation in any subject throughout the study period.

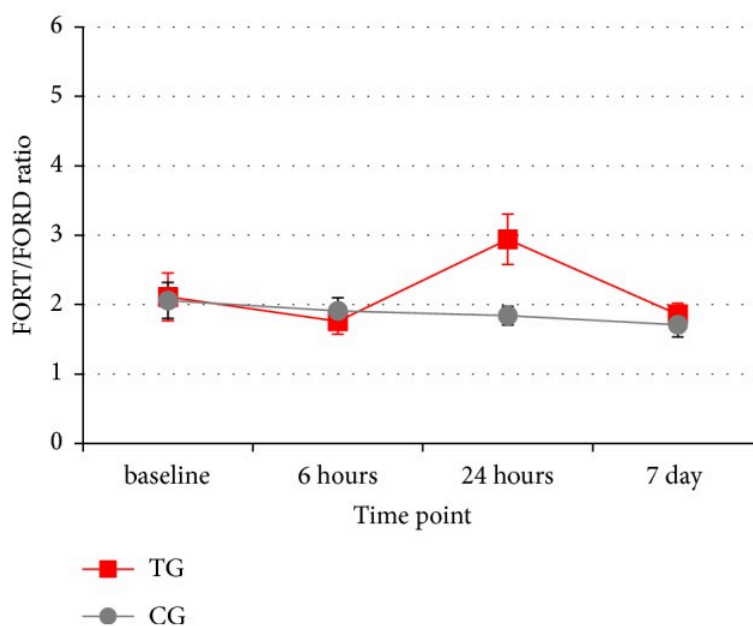


Figure 5: Changes in FORT/FORD oxidative stress parameter during the one week orthodontic treatment. Capillary blood samples of orthodontic patients were taken at different time points. At the 24-hour mark, a significant increase of FORT/FORD ratio was observed in the TG. Results are presented as mean values with standard deviation errors (Kovac et al., 2019).

The result suggests that there is a short-term increase in ROS formation after 24 hours in patients undergoing orthodontic treatment. Yamar and Daokar (2019) and Olteanu et al. (2009) also observed a significant increase in salivary oxidative stress markers after 24 hours of orthodontic treatment and a steady decrease in marker levels after 7 days and 90 days. Several other studies (D'Attilio et al., 2004; Olteanu et al., 2009) suggest that the significant increase in oxidative stress markers is due to the release of metal ions, which is highest in the early stages of orthodontic treatment. The obtained results and many other studies demonstrate the long-term effects that orthodontic treatment can have on patients. The longest *in vivo* experiment to date was conducted by Buczko et al. (2017) who collected saliva samples from orthodontic patients until 24 weeks. They, too, obtained initially higher values for total oxidant status, but after 24 weeks, salivary oxidant status reached the initial basal level obtained before the study. The normalisation of the ROS and antioxidant ratio may be attributed to the organism's adaptation responses or differences in metal ions release within the sampling time period.

However, these results should be taken with caution, because the increase in oxidative levels may also be caused by the inflammation of the gingival tissue during orthodontic treatment (Buljan et al., 2012). The mechanical forces alter the periodontal ligament and alveolar bone structure induce local inflammation around the teeth (Shamaa and Mansour 2019). Atuš Özcan et al. (2014) found no inflammation and pathological changes in healthy tissues during 6 months of orthodontic treatment. In our study, we did not investigate the expression of proinflammatory mediators and we did not perform measurements of metal ions released

in blood. Other sources of ROS such as oral bacteria, food, chocolate, radiation, and cigarette smoking that affect redox balance could also be responsible for an increase in oxidative markers, but could be neglected based on the inclusion/exclusion criteria used in the study and a regular health examination by an orthodontist. Since the FORT /FORD ratio does not provide any indication of the initial increase in ROS, we assumed that the reason for the occurrence of oxidative stress must be from the orthodontic material, from which metal ions can be released and cause oxidative stress (Kovac et al., 2019).

4.2 METAL ION RELEASE FROM DIFFERENT ORTHODONTIC ALLOYS

The orthodontic appliance remains in the oral cavity for about 2 years or until the end of orthodontic treatment (Mavreas and Athanasiou 2008). Based on our previous findings that metallic orthodontic appliances could be the reason for the occurrence of oxidative stress (Kovac et al., 2019), the question arose about the safety of such orthodontic appliances and their permanent use. Although the arches are usually changed every one to three months, the brackets and molar bands are rarely changed throughout the treatment period. In the oral cavity, fixed orthodontic appliances are exposed to constantly changing pH and temperatures, as well as biological and enzymatic environments (Barrett et al., 1993). Electrochemical corrosion, mechanical friction, wear of the appliance, and surface wear are very common in everyday life and lead to increased release of metal ions (Močnik et al., 2017).

The biological effects of certain metals and their ions that make up orthodontic appliances have been linked in the past to certain oral health problems such as glossitis, gingivitis, contact stomatitis, multiforme erythema, and gingival hypertrophy (Ortiz et al., 2011). The most commonly used orthodontic alloys for parts of an orthodontic appliance include SS, Ni-Ti, Co-Cr, and β -Ti, all of which are composed of a combination of metals, some of which are considered allergenic or even toxic (Keinan et al., 2010).

In vitro studies on the released metal ions from orthodontic alloys are conducted in artificial saliva to mimic *in vivo* conditions in terms of pH, temperature, and in some cases even saliva composition (Hanawa, 2004). To better understand the metals that make up orthodontic alloys and the concentrations of metal ions they release under laboratory conditions, we designed a study in which parts of the orthodontic appliance were immersed in artificial saliva for 90 days and their metal composition was evaluated. Table 6 shows the metal composition and combined surface area of each orthodontic alloy used in the study. The orthodontic parts (brackets, archwires, and bands) made from the alloy SS had approximately the same weight percent metal composition of Fe ($57 \pm 2\%$), Ni ($16 \pm 2\%$), and Cr ($25 \pm 2\%$), although they were manufactured by different companies. The only notable difference in the composition of the SS alloys was that the SS version also contained 1.9% Mo. The similarity in metal composition was also evident in the two Ni-Ti alloys,

where the weight fraction of Ni was $73.5 \pm 0.3\%$ and that of Ti was $26.5 \pm 0.3\%$. The single β -Ti alloy used in the study consisted of 91.8% Ti and 8.18% Mo. Although the Co-Cr alloys were similar in terms of Co content (50%), they had some differences in terms of the other constituents, which was to be expected since they are marketed as separate products. We used the manufacturer's Data Sheet (Dentaurum, 2020) to compare our alloy compositions to those prescribed. Since there are many different types of SS wires, the exact range cannot be determined. As a rough estimate, the alloy SS should contain between 17-25% Cr, 8-25% Ni, 0.0-6.5% Mo, and the balance Fe (Tian et al., 2017). Analysis of the composition of our Ni-Ti alloy showed a much higher percentage weight ratio (73% Ni and 26% Ti) compared to the manufacturer's data sheet (55% Ni and 45% Ti). One possible explanation for this situation could be the incomplete dissolution of the alloy, but the dissolution liquid obtained was clear and did not contain solid particles. Another explanation is that the metal composition reported by the manufacturers was evaluated by energy dispersive X-ray spectroscopy, where the amount of elements on the surface can be imaged (Shojaei et al., 2022) which means that the metal composition may be different below the surface, as explained by Lazić et al. (2022). Like SS, Co-Cr alloys do not have a specific composition, and data ranges of 40-50% Co, 18-25% Cr, 15-25% Ni, 3-8% Mo, and 1-15% Fe are described (Alobeid et al., 2014; Wepner et al., 2021).

Table 6: Components of orthodontic appliances used in the study with their corresponding metal composition in weight percentages (%) (Kovač et al., 2022).

Component	Type	Specification	Number of parts	Surface (cm ²)	Fe (%)	Ni (%)	Cr (%)	Co (%)	Mo (%)	Ti (%)
Archwire	SS	Damon .016 x 0.25 Ormco, USA	2	5.104	58.3	14.6	27.1	<0.1	<0.1	<0.1
	Ni-Ti	Biostarter® .016” Forestadent, Germany	2	4.172	<0.1	73.8	<0.1	<0.1	<0.1	26.2
	Ni-Ti	rematitan® super elastic .016” Dentaurem, Germany	2	4.149	<0.1	73.2	<0.1	<0.1	<0.1	26.8
	β-Ti	rematitan® SPECIAL .032” Dentaurem, Germany	2	6.846	<0.1	<0.1	<0.1	<0.1	8.18	91.8
	Co-Cr	Elgiloy® .036” Rocky Mountain Orthodontics, USA	2	9.476	6.12	19.9	21.6	49.7	2.65	<0.1
	Co-Cr	remaloy®.036” Dentaurem, Germany	2	9.217	1.42	26.1	19.4	53.2	<0.1	<0.1
Brackets	SS	Discovery® Dentaurem, Germany	24	14.478	55.4	17.8	24.9	<0.1	1.95	<0.1
Molar bands	SS	W-Fit Form Forestadent, Germany	4	9.881	57	18.2	24.9	<0.1	<0.1	<0.1

The release of metal ions from orthodontic alloys during the 90-day incubation in artificial saliva is shown in Figure 6 and the detailed results can be found in Appendix E. During the incubation, samples were taken for analysis at different time points to better evaluate the released kinetics. Overall, the amount of ions released increased during the study with minor fluctuations likely due to minor sampling or measurement errors. It should be noted that only some of the metals were analyzed in the study, so it cannot be ruled out that certain other metals were also released from the material. For more-suitable results, beakers made of Teflon were used to prevent the absorption of metals on the walls of the containers during the experiment. The pH-neutral artificial saliva is not an exact replica of human saliva, whose pH varies and contains different organisms and biological material, but it allowed us to obtain metal release results only. Galeottiet al. (2013) have shown that pH is an important factor in metal release studies.

In the case of the alloy SS (arches, brackets, and molar bands), the release was mainly Fe ions compared to the other metals studied, remaining almost at the initial level until the 90-day mark, where a slight increase was observed. Since we used upper and lower arches, we also obtained much lower metal concentrations released from the arches compared to the total brackets (24 brackets) and molar bands (4 molar bands). This finding is consistent with the fact that metals are only released from the surfaces and, consequently, with a larger surface area, more ions can be released.

When looking at the metal release concentration for both Ni-Ti arcs, we found it interesting that the amount of Ti released was similar for both ($\text{Ti} \approx 9.5 \text{ ng/mL}$ or 530 ng/cm^2), but the amount of Ni released was not comparable ($\text{Ni}_{(\text{Dentaurum})} \approx 13 \text{ ng/mL}$ or 721 ng/cm^2 and $\text{Ni}_{(\text{Forestadent})} \approx 116 \text{ ng/mL}$ or 6522 ng/cm^2). The Ni-Ti_(Forestadent) archwire released almost ten times as many Ni ions as Ni-Ti_(Dentaurum) at the end of the study. No differences were found between them in the metal composition study, so there must have been a different resonance as to why this situation occurred. It is known that titanium forms a protective oxide layer on the surface of the material that protects against corrosion (Ramazanzadeh et al., 2014) and at the Ti concentrations found in the medium, this could be a sign of deterioration of the protective layer. This was not the case in our study, as Ti concentrations were the same in both arcs. It is believed that surface topography, processing, and finishing techniques used in the fabrication of the sheets are critical to corrosion resistance, as surface roughness and surface imperfections are the main corrosion sites (Hunt et al., 1999). Lazić et al. (2022) stated that the conventional way of manufacturing Ni-Ti wires, unlike modern manufacturing methods, does not ensure a Ni-free zone on the alloy surface, which makes them less stable, less hard, and less resistant to corrosion.

For β -Ti, Mo concentrations were undetectable until day 90 of the study, when the concentration was 0.45 ng/mL or 15 ng/cm^2 . Ti concentrations fluctuated by 1.5 ng/mL or 50 ng/cm^2 throughout the study and until day 90, when a peak value of about 8.3 ng/mL or 279 ng/cm^2 was detected. Suárez et al. (2011) compared the biocompatibility between SS, Ni-Ti and β -Ti wires and showed that the β -Ti alloy was the most corrosion resistant, followed by Ni-Ti and SS was the least corrosion resistant. The same conclusion can be drawn from our study highlighting the importance of the formation of the passive TiO_2 surface layer of β -Ti and Ni-Ti and, to a lesser extent, the passive Cr_2O_3 oxide layer of SS. Due to the passive surface layer, the β -Ti alloy released the least amount of metals from its surface. The Ti concentration in the media was also lower than that of the Ni-Ti alloy. The release of metal ions depends on the properties of the oxide layer formed, which can vary from alloy to alloy. The corrosion resistance of Ti-containing alloys was evaluated by Schiff et al. (2002), who emphasized that the passive oxide layer of the β -Ti alloy was superior to the oxide layer formed on the Ni-Ti alloy. Huang et al. (2005) hypothesized that the Mo present in the β -Ti alloy forms an additional MoO_3 oxide protective layer on the surface, which makes the alloy permanently corrosion resistant. Comparing the corrosion resistance

of the β -Ti alloy with the alloy SS, whose corrosion protection is based on the passive formation of the Cr_2O_3 oxide layer, β -Ti with its TiO_2 surface layer was less susceptible to corrosion (Castro et al., 2015). The protective layer of β -Ti alloy can be removed by local mechanical forces, which greatly decreases the corrosion resistance of the Ti containing alloy. To overcome this problem, protective coatings or other surface treatments could be applied to dental materials (Velasco-Ibáñez et al., 2020). It is not known whether we have used parts of orthodontic appliances whose surface has been modified.

The metal release from both Co-Cr arch wires gradually increased during the study. The concentrations of Co (30 ng/ml or 730 ng/cm²) and Cr (1.5 ng/ml or 35 ng/cm²) reached similar levels in both wires, but some differences were observed in Fe, Ni, and Mo. This was expected since the two Co-Cr arches had different metal compositions of these three metals according to our compositional study. For this reason, more Mo (2.54 ng/mL or 61.8 ng/cm²), Fe (13.77 ng/mL or 335 ng/cm²), and Ni (8.55 ng/mL or 208 ng/cm²) were released from Co-Cr_{Elgiloy} than from Co-Cr_{remaloy}, which released more Ni (11 ng/mL or 267 ng/cm²) and less Fe (4.6 ng/mL or 112 ng/cm²) and contained no Mo. Comparing the metal release from each arch type throughout the study, it appears that the metal concentrations of the Co-Cr wire increased, indicating metal saturation. Since this occurred at the end of the study, we cannot consider this statement conclusive.

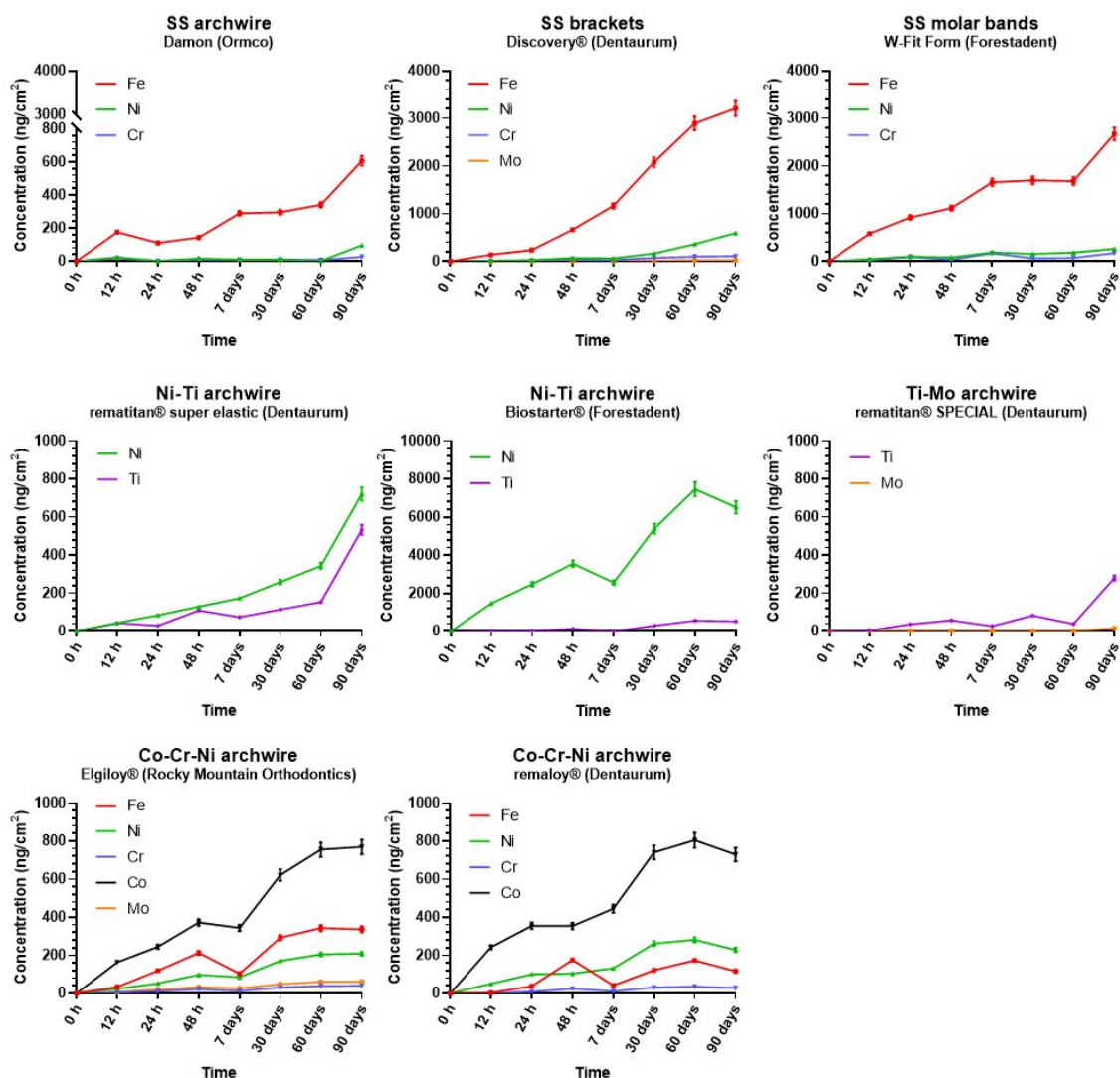


Figure 6: The release of metal ions from different parts of fixed orthodontic appliances.

Parts of a fixed orthodontic appliance made of different alloys were immersed in artificial saliva for 90 days. A set of different parts of the orthodontic appliances was used, and three technical replicates were obtained during each incubation time point, after which the metals released from the samples were quantified three times. Results are shown as means with standard deviation.

Direct comparison of leached metal concentrations between different studies from other authors is not possible due to differences in study design with respect to the material studied, the immersion media, and the analytical equipment used. In previous studies, combinations of wire, brackets, and tapes were used to determine metal ion release. In the present study, the release of metal ions from brackets, molar bands, and arches was measured separately and, in the case of arches, also according to the composition of their material alloys. This could be considered as a limitation of the study, since it excluded the possible corrosive effect and the related ions released by the friction of the material (Staffolani et al., 1999). With the obtained results, we provided information on the minimum concentrations of metal

ions that can be released from orthodontic alloys only by the pure diffusion process without additional mechanical forces. Our study also did not consider salivary flow rate (Iorgulescu, 2009), pH, and temperature changes (Kuhta et al., 2009) at which even more metal could be released. The effect of low pH on increasing metal release was shown by Kuhta et al. (2009) and the increase in metal release due to mechanical and thermal loading of orthodontic alloys was shown by Arndt (2005).

According to Institute of Medicine (US) Panel on Micronutrients (2001), the reported upper intake limits (UL) for each metal are as follows: $UL_{Ni} = 1$ mg/d, $UL_{Fe} = 45$ mg/d, $UL_{Cr} = 0.2$ mg/d, $UL_{Mo} = 2$ mg/d, and $UL_{Ti} = 1.1$ mg/d. The fact that orthodontic alloys release metal ions from their surfaces is undeniable, but although a constant release pattern was observed, the amount of metal ions released is still far below the recommended daily levels for ingestion. Comparing our results with the prescribed UL, even when considering the cumulative concentrations, none of the released metal ions studied exceeded the prescribed daily intake concentration. Caution should be exercised when interpreting metal concentrations because even nontoxic concentrations of some metals may have biological effects on the organism (Anderson et al., 2008; Urban et al., 1994) or could induce synergistic effects. For example, Cr is known to be an allergen and Cr^{6+} is considered toxic and mutagenic (Dayan and Paine 2001). Hypersensitivity to metals, such as Ni, is also present in our population and should not be neglected in orthodontic patients (Santos Genelhu et al., 2005). Hypersensitivity to metals is a type IV delayed immune response, resulting in stomatitis, perioral rashes, loss of taste or metallic taste, burning sensation and soreness of the tongue. Nickel allergies occur more frequently than all other metal allergies combined (Verma and Dhiman, 2015). In addition, delayed nickel allergy reactions are more common in women than in men due to daily contact with nickel in jewelry (Chakravarthi et al., 2012). The European Committee for Standardization has specified in EN 1811:2011 that the release of nickel from products should not exceed $0.5 \mu\text{g}/\text{cm}^2/\text{week}$ (Tsang, 2016). Extrapolating our data, Ni-Ti_(Forestadent) released $2568 \mu\text{g}/\text{cm}^2/\text{week}$ Ni after only one week, and $0.501 \mu\text{g}/\text{cm}^2/\text{week}$ Ni after 13 weeks.

There is a large market for orthodontic appliances, where each part is made of a different composition of metal alloys. It is the responsibility of the dentist to use the right material for the treatment and safety of the patient. Knowledge of the biocompatibility of the materials is an added advantage to meet the needs of patients and address their potential problems (Kovač et al., 2020). Many adverse oral conditions such as gingival hyperplasia, glossitis, erythema multiforme, and labial desquamation have been associated with the released metal ions from orthodontic appliances (Nayak et al., 2015).

Based on the results obtained, we were able to estimate the type and concentration of released metal ions. This allowed us to prepare specific ion combinations and concentrations for further oxidative stress studies.

4.3 CAUSATION OF OXIDATIVE STRESS BY METAL IONS IN *S. CEREVISIAE*

Throughout evolution, all eukaryotes, from yeast to vertebrates, share similarities in mitochondrial respiration, antioxidant enzymes, and accumulation of oxidative damage due to metabolic processes and aerobic life. These similarities, along with ease of access, rapid growth, genetic relevance to human disease, and ROS processing, make *S. cerevisiae* an useful model organism for oxidative stress studies (Lushchak, 2011). In our study, we treated *S. cerevisiae* cells when they were in the stationary phase. In this phase the yeasts switch from fermentative to mitochondrial respiration, which closely resembles the normal respiration of multicellular eukaryotes, and the transitions cause more ROS to be produced (Vázquez et al., 2017). The cells must cope with increasing amounts of ROS by modulating antioxidant defenses and preventing or repairing potential damage that could result from oxidative processes (Longo et al., 1996). If we were to use yeast cells in the exponential phase, all energy would come from glycolysis rather than oxidative phosphorylation reactions, and the cells would continue to decay after being exposed to the ROS stressor for only a short time (Longo and Fabrizio 2012). Stationary *S. cerevisiae*, on the other hand, are exposed to the stressor for a longer period of time, so defense and repair mechanisms are upregulated. Using two *S. cerevisiae* mutants lacking either the antioxidant enzyme SOD (Δ Sod1) or CAT (Δ Ctt1), we were able to see how the loss of antioxidant defense affects yeast cell culturability.

4.3.1 Culturability

As shown above, orthodontic materials do release metal ions from their surfaces, but some authors (Assad et al., 2002; Kao et al., 2007) claim that these released substances are not harmful, yet other authors (Giudice et al., 2016; Pérez-Navero et al., 2009) state that these metal ions are key producers of free radicals and its mediated toxicity. There are several studies in the literature investigating the biocompatibility of orthodontic materials with respect to the cytotoxicity of metal ions (Hafez et al., 2011; Ortiz et al., 2011; Velasco-Ortega et al., 2010), but only two have used yeast to study the cytotoxic effects of orthodontic metals (Gonçalves et al., 2014; Limberger et al., 2011). Limberger et al. (2011) compared the cytotoxicity of orthodontic materials in yeast and other cell lines, providing the necessary information that the yeast cell model is a reliable model for cytotoxicity studies. In the dissertation study, we treated yeast cells for 24 hours with different metal ion mixtures, detailed presented in Table 4, at concentrations of 1 μ M, 10 μ M, 100 μ M, and 1000 μ M. We used metal mixtures of SS, Co-Cr, Ni-Ti, and β -Ti orthodontic alloys because they are most commonly used in clinical practise and their nature was previously described by Arndt et al. (2005) and Kusky (2002).

Figure 7 shows the cell culturability of Wt, Δ Sod1, and Δ Ctt1 yeast as CFU/mL cell counts and relative values compared with the untreated control group. A decrease in culturability

was observed when yeast cells were treated with metal mixtures, although only a significant decrease was observed in all metal mixture treatments at 1000 μM concentrations. Concentrations of SS below 1000 μM did not significantly decrease the culturability of Wt and the mutants. For Wt yeast, all other metal treatments caused a significant decrease in culturability at concentrations below 1000 μM . REM and β -Ti mixtures caused a significant decrease in culturability at 100 μM , and ELG and Ni-Ti mixtures caused a significant decrease at a concentration as low as 10 μM . When the culturability of Wt and the two mutants were compared, a significant difference in culturability was observed, as the CFU/mL of the untreated control samples of the mutant yeast was much lower than that of the untreated control sample of Wt. It appears that, like Wt, the ΔSod1 yeast was affected by all metal mixtures at 1000 μM concentrations, with the exception of 100 μM REM, which also caused a significant decrease in culturability. ΔCtt1 , on the other hand, showed the same significant decrease at 1000 μM SS and 1000 μM TiMo as the other yeast cells, but was much more susceptible to ELG and REM, where a significant decrease was observed at 10 μM . Threatening ΔCtt1 with a Ni-Ti mixture had no effect on cell culturability. El Medawar et al. (2002) treated cell lines with only Ni, Ni-Ti, and only Ti and found that 425 μM concentrations of Ni caused a 50% decrease in viability, whereas Ni-Ti and Ti concentrations had no effect on cell viability even at 3750 μM concentrations. Issa et al. (2008) obtained a 50% decrease in viability of HGF at the following concentrations: Co = 705 μM , Ni = 828 μM , and Cr = 1971 μM . Although the individual metal concentrations are useful, they do not provide information on how the cell responds when exposed to multiple ions simultaneously. As described by Terpilowska and Siwicki (2018), certain metal combinations may have a synergistic or even antagonistic effect on cell viability. This is the information that the individual metal treatments do not provide.

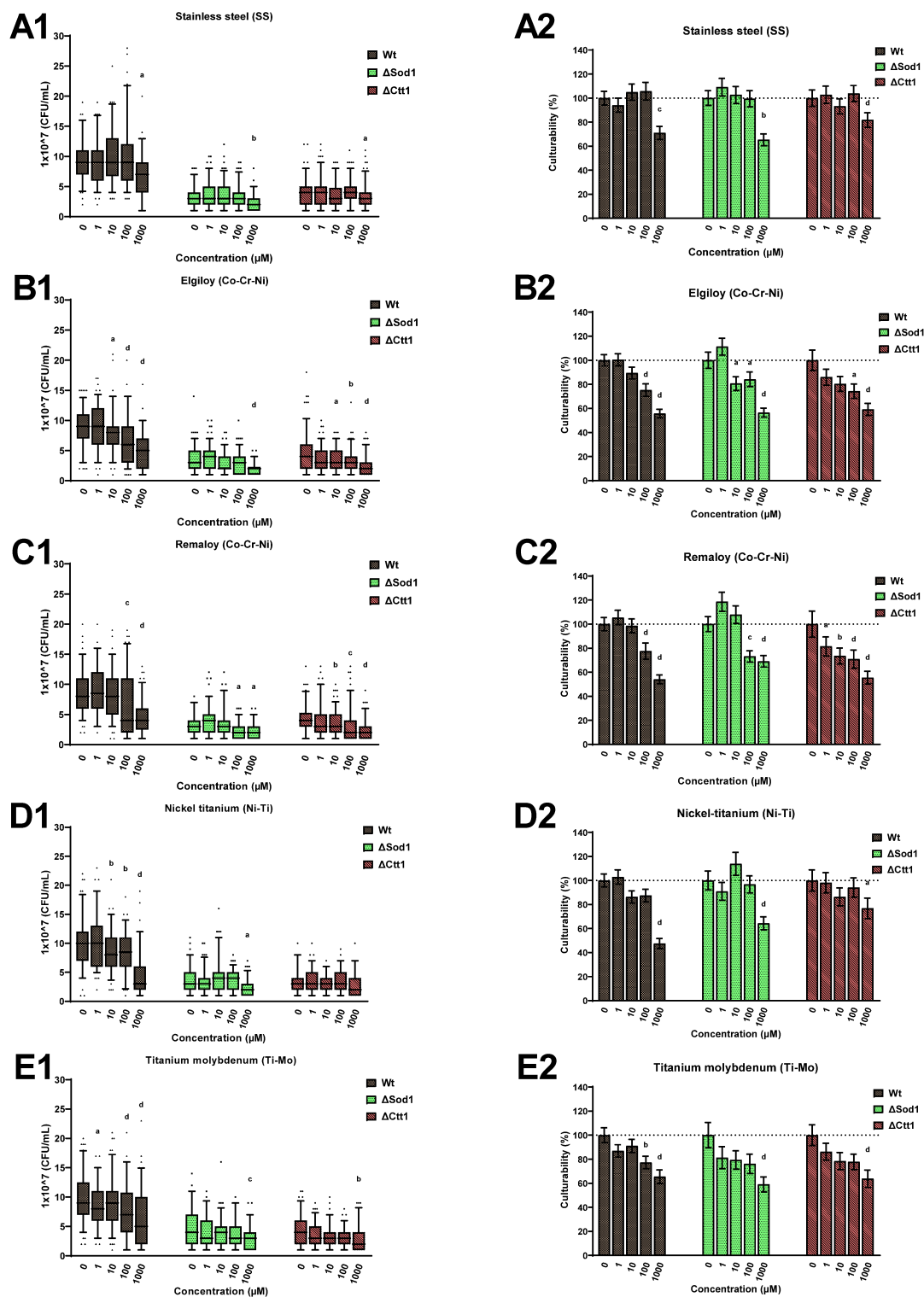


Figure 7: Cell culturability of *Wt*, $\Delta Sod1$ and $\Delta Ctt1$ yeast after 24-hour metal treatment. Yeast cells we treated with (A) SS, Co-Cr (B) ELG and (C) REM, (D) Ni-Ti, and (E) β -Ti metal mixtures for 24-hours. The individual cell culturability is represented as CFU/mL in box-plots (A1–E1) and as percentage culturability according to the control sample in grouped columns (A2–E2). Significant differences are indicated with a = $p < 0.05$, b = $p < 0.01$, c = $p < 0.001$, and d = $p < 0.0001$. (Kovač et al., 2020b).

4.3.2 Metabolic activity

The cell metabolic activity assay, another assay used to test metal ion toxicity, was also used in the presented study. Due to the small number of biological replicates performed, the results did not show clear differences between yeast cells treated differently. For this reason, we believe that no significant differences were detected when the metabolic activity values for each treated sample were compared with the corresponding untreated control (Figure 8). When the Wt yeast cells with different metal solutions were treated, it was observed that higher concentrations actually increase the mean value of metabolic activity. The metabolic assay measures the ATP present in the cell, the quantification of which should be proportional to the metabolically active viable cells. By observing the metabolic activity of Wt yeast, it does not match the results of the cell culturability assay. Under stress conditions, the membrane and the ETC are the first components to be affected by the toxic metals, hence the observed ATP depletion and the decrease in viability (Chen et al., 2014). On the other hand, both yeast mutants tend to decrease their metabolic activity with increasing metal concentration, especially at 1000 μM concentrations. We also compared the metabolic activity between the untreated yeast cells of Wt and the mutants and found that the baseline metabolic activity of the mutants was at least two times higher than that of the untreated control group of Wt yeast. The reason for this observation might be the in the slow response of the mutant yeast to new metal-induced stressors, so that it requires higher energy consumption to maintain its viability. As explained by Huang et al. (2019) under mild stress conditions, cells use ATP to activate the antioxidant defense system and increase gene transcription, whereas under severe stress, ATP loss occurs due to mitochondrial damage. The ATP increase was explained by Akhova and Tkachenko (2014) as a process in which cells shut down all unnecessary energy-consuming processes and tend to produce more energy to meet the necessary requirements for stress defense. These statements explain why our yeast mutants without antioxidant defenses had much higher metabolic activity than Wt yeast.

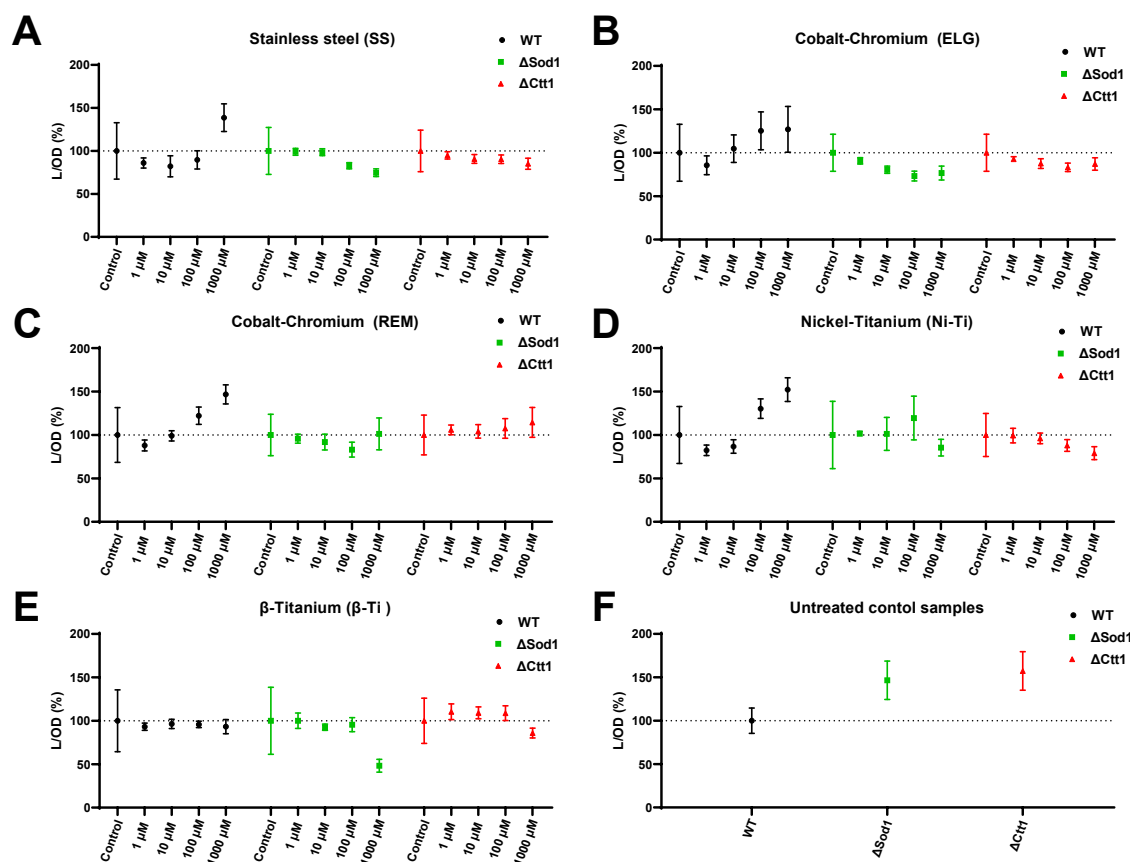


Figure 8: Metabolic activity of Wt, Δ Sod1 and Δ Ctt1 yeast treated with different metal mixtures. Yeast cells were treated with SS (A), Co-Cr ELG (B), REM (C), Ni-Ti (D), and β -Ti (E) metal mixtures for 24 hours. The cell metabolic activity is presented as luminescent signal, which is proportional to the number of metabolic active cells in the culture. Values of untreated yeast cells were set at 100% and the treated samples were compared to it. A comparison among untreated control groups of each yeast strain is shown in the graph (F). Results were shown as means with standard mean errors where no significant differences were obtained.

4.3.3 Intracellular ROS level

As indicated by the cell viability assessment, the metal mixtures were stressors for the yeast cells. Since all the metals used in the study were transition metals capable of generating ROS through Fenton and Haber-Weiss reactions (Zhao, 2019), we assumed that the reason for the decrease in cell viability was due to the oxidative stress that occurred although other causes are possible. When the metal is present in manageable concentrations, the antioxidant defense system ensures that no oxidative stress damage occurs. Among the endogenous antioxidant enzymes, SOD and CAT are the two major defense enzymes that remove $O_2^{\cdot-}$ and H_2O_2 , respectively (Ighodaro and Akinloye 2018). The Δ Sod1 yeast lacked the cytosolic SOD, which hindered the scavenging of ETC formed $O_2^{\cdot-}$ (Turrens, 2003), and the Δ Ctt1 yeast, which lacked the cytosolic CAT, was unable to degrade H_2O_2 (Farrugia et al., 2012).

To determine whether metal mixtures had caused oxidative stress in the yeast, an assay was performed to determine the ROS formation. Two different approaches were used to evaluate the intracellularly formed ROS (Figure 9). In the first method, the fluorescent dye was added immediately after the yeast was treated with metal mixtures, and in the second method, the dye was not added until 24 hours after treatment with the metal mixture. As expected, the addition of the dye after treatment with metal mixtures increases the fluorescence signal of all yeast cells, regardless of the metal treatment used. Much higher fluorescence intensity was also observed in the yeast mutants lacking antioxidant defense enzymes, which could be due to the fact that the ROS were probably not efficiently removed and caused higher fluorescence intensity than in the Wt yeasts. It is worth noting that the organism has several isoenzymes of SOD and CAT, so it can thrive under oxidative stress conditions (Ighodaro and Akinloye 2018).

The comparison of the different methods in Wt yeast gave different results. When the dye is added immediately after the addition of the metal, an increase in fluorescence is observed in the treatments with 1000 μM SS, ELG and REM, but when the dye is added after the 24-hour treatment, a decreasing trend in fluorescence was observed, and a statistically different decrease was observed in the case of 1000 μM REM and Ni-Ti. The β -Ti treatment of Wt yeast showed no effect on the intracellular formation of ROS. The SS and ELG treatment of ΔSod1 and ΔCtt1 yeast mutants had the same effect as the threat of Wt yeast; after the medium-term addition of the dye, only 1000 μM concentrations showed a statistically detectable increase in the fluorescence signal, while the addition of the dye after the 24-hour treatment resulted in no change in fluorescence compared to the untreated control sample. Similarly, when treated with REM, although the increase was detected at a concentration of 1000 μM , it was not statistically significant. Interestingly, treatment of the mutant yeast with Ni-Ti showed a statistically significant decrease in fluorescence intensity at a concentration of 1000 μM . Just as in Wt yeast, the fluorescence intensity of the mutants was not affected, except for the ΔCtt1 mutant, where a decrease was observed at 100 μM and 1000 μM concentrations.

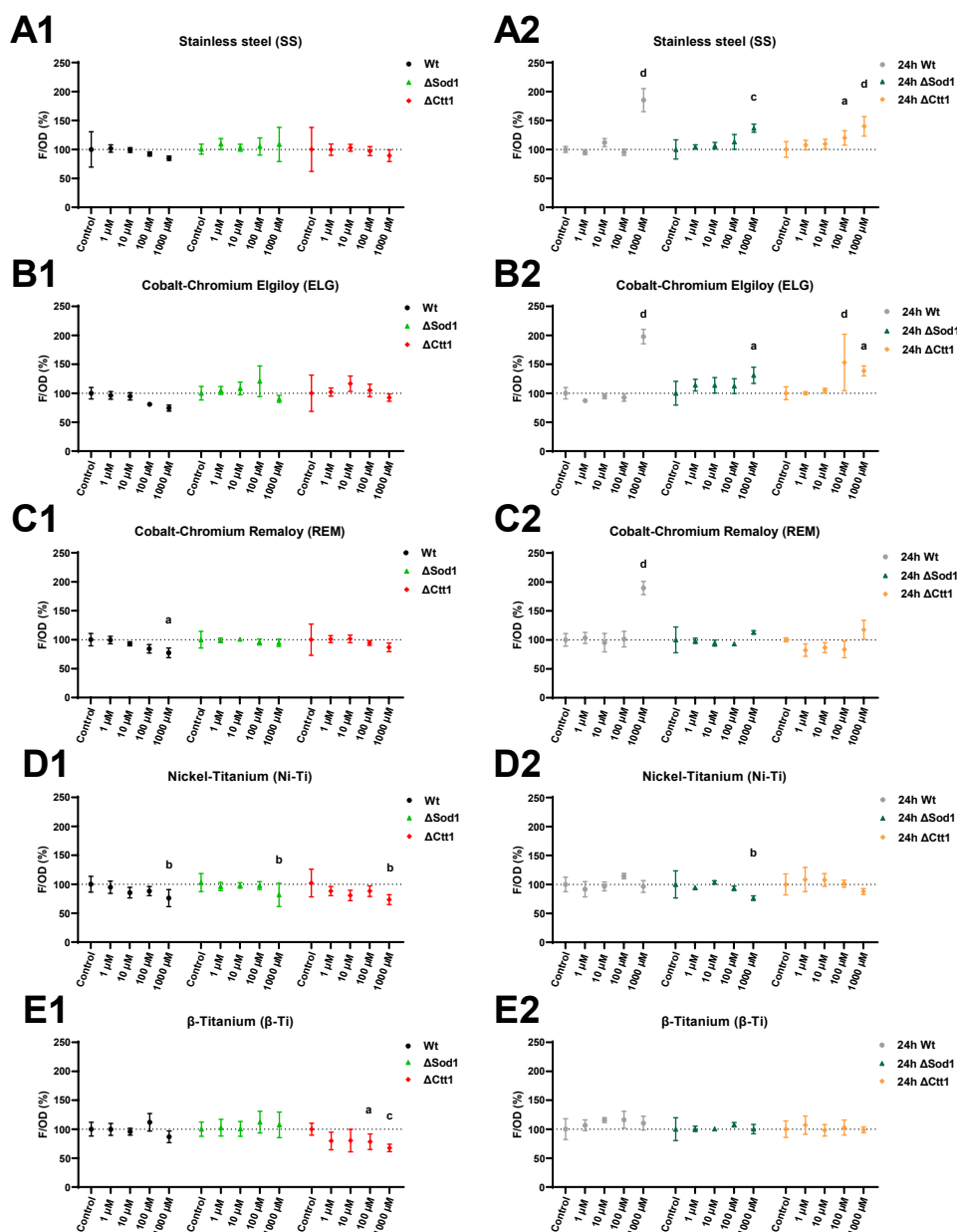


Figure 9: Intracellular ROS level of Wt, ΔSod1 and ΔCtt1 yeast was performed with two different methods, each with a different time point of H₂DCFDA dye addition.

All yeast cells were treated with either SS (A), Co-Cr ELG (B), REM (C), Ni-Ti (D) and β-Ti (E) metal mixtures for 24 hours. Two different protocols to determine the ROS level were performed, each having a different time point of H₂DCFDA dye addition. In the first protocol (suffix 1), the fluorescent dye was added after 24-hour metal treatment, and in the second protocol (suffix 2) the fluorescent dye was added simultaneously with the metal mixture. In the cell, the dye is reduced by ROS and the intensity of the fluorescent signal is proportional to the cell ROS level. The results are presented as means with 95% confidence intervals. Significant differences are indicated with a = p < 0.05, b = p < 0.01, c = p < 0.001, and d = p < 0.0001.

The results obtained were contradictory, because it appeared that the addition of the dye immediately after the addition of the metal mixture provided information about the ROS

generated intracellularly by the treatment with the metal mixture, whereas the addition of the dye after the treatment with the 24 metals did not. In fact, the addition of the dye after the 24-hour treatment decreased the fluorescence signal. If the metal mixtures were the stressor resulting in the formation of ROS, the two methods used should show similar results. Since H₂DCFDA is not fluorescent, it must first pass through the cell membrane, where it could be cleaved by intracellular esterase's and oxidized by ROS to become fluorescent (Wang and Roper 2014). This means that the process of converting a non-fluorescent dye into a fluorescent product is only possible in living cells (Tanaka et al., 2020). Valiakhmetov et al. (2019) showed a correlation between ROS fluorescence and viable cell population. After the 24-hour metal treatment, the dye has fewer viable cells for its fluorescence conversion, hence the decreasing fluorescence signature. From our previous culturability measurements, we could see that the culturability of the cells decreased with the increase of the metal concentration. Therefore, we applied the third method, in which we treated the Wt yeast cells for 24 hours, took a small sample and determined the cell culturability, and plotted the obtained fluorescence signal against the number of culturable cells (Figure 10).

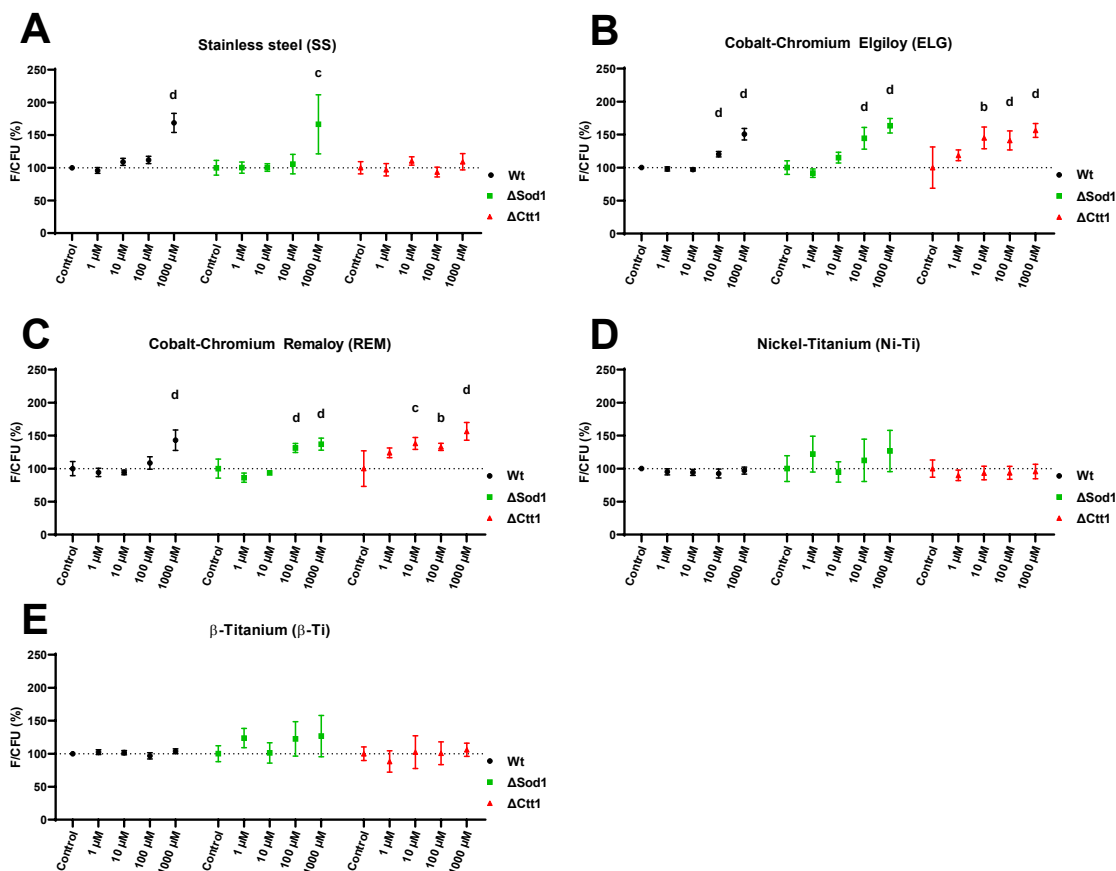


Figure 10: Intracellular ROS level in culturable Wt, Δ Sod1 and Δ Ctt1 yeast cells after the 24-hour metal treatment.

Yeast cells were treated with SS (A), Co-Cr ELG (B), REM (C), Ni-Ti (D) and β -Ti (E) metal mixtures for 24-hours. Before the addition of the fluorescent dye H_2 DCFD, the culturability of each metal treated yeast was obtained. The fluorescence intensity and the CFU count show the ROS level of culturable cells. The results are presented as means with 95% confidence intervals. Significant differences are indicated with a = $p < 0.05$, b = $p < 0.01$, c = $p < 0.001$, and d = $p < 0.0001$.

Examination of the intracellular ROS in only culturable cells gave a clearer picture of intracellular oxidation level that occurs under metal stress treated conditions. SS Metal mixtures with a concentration of 1000 μ M had a significant effect on Wt yeast and Δ Sod1, while the Δ Ctt1 mutant did not seem to be affected by treatment with the SS mixture. On the other hand, the Co-Cr metal mixtures of ELG and REM had a strong effect on the generation of ROS in the Δ Ctt1 mutant, as there was an increase in the fluorescence signal already at 10 μ M, which only became more intense with increasing concentration. The Wt and the Δ Sod1 mutant also exhibited a significant increase in ROS generation at 100 μ M and 1000 μ M concentrations. The improved method showed a significant increase in intracellular ROS generation in viable cells after 24 hours of treatment, while there was no change in

fluorescence intensity when any type of yeast cell was treated with Ni-Ti or β -Ti metal mixture. Compared with other methods, no decrease in fluorescence signal was observed when ROS was probed only in culturable cells. Terpilowska and Siwicki (2019) showed that 1000 μ M concentrations of Fe, Cr, Ni, and Mo ions decreased cell viability and induced apoptosis. Caicedo et al. (2008) examined the effects of these metal ions on Jurkat cells and concluded that in terms of inducing apoptosis and DNA damage, Ni was the most detrimental of all, followed by Co, then Mo, then Cr, and finally Fe. Since the Co-Cr metal mixtures contained more of the higher toxic metal ions such as Ni and Co compared to the mixture SS, the increase in intracellularly produced ROS was observed at lower concentrations. If Ni is the most toxic metal ion, the Ni-Ti mixture that contained 45% Ni ions should be the most toxic metal mixture of all, and our results with Wt yeast confirm this. Viability decreased significantly when cells were treated with concentrations as low as 10 μ M, but interestingly, no intracellular ROS formation was observed.

4.3.4 Lipid oxidation

It is known that certain high concentrations of metal ions actually trigger the formation of ROS in yeast cells. But with an efficient antioxidant defense system, the deleterious effect of ROS overproduction can be prevented. To determine whether the ROS generated by the metal mixture actually causes oxidative damage of molecules and not just increased ROS formation, we used the TBARS assay to examine lipid oxidation damage (Figure 11). Comparing the assessment of intracellular ROS (Figure 10) and the assessment of oxidative damage of lipids, a clear correlation can be seen, i.e., when the formation of ROS was increased, lipids were also oxidatively damaged. SS and the Co-Cr mixture caused lipid oxidation at higher concentrations, at 1000 μ M for Wt and even at 100 μ M for the mutant. Pallero et al. (2010) also confirmed that the SS mixture, consisting of Fe, Cr, Ni, and Mo ions, increased the formation of ROS in vascular smooth muscle cells. No signs of lipid damage were observed when yeast cells were treated with the Ni-Ti or β -Ti metal mixture. According to previous studies, metal ions compromising, Ni (Chen et al., 2010), Ti (Gholinejad et al., 2019) and Mo (Siddiqui et al., 2015) metal mixtures are capable of inducing ROS formation and lipid oxidation, but this was not revealed in our study. Spalj et al., (2012) showed, that Ni and Ti salts induce ROS formation in gastrointestinal cell lines (Rincic Mlinaric et al., 2019). We also compared lipid oxidation levels between Wt yeast and the two mutant yeasts and found a significant difference between them. It appears that the mutant yeast undergoes mild lipid oxidation even in the absence of metal ions because of the lack of antioxidant enzymes.

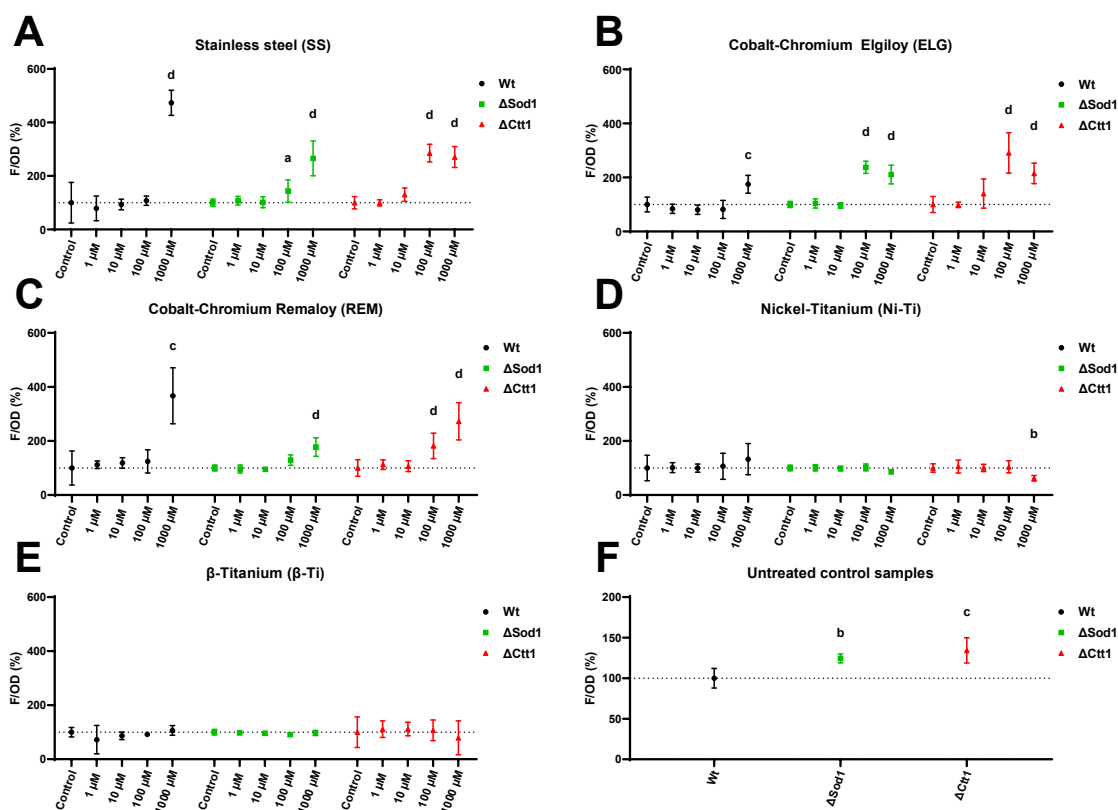


Figure 11: Influence of 24-h metal treatment on the formation of oxidative lipid damage in yeast cells. Wt, Δ Sod1, and Δ Ctt1 yeast strains were treated with different concentrations of SS (A), Co-Cr ELG (B) and REM(C), Ni-Ti (D), and β -Ti (E) metal mixtures. The fluorescent product of the TBARS method directly indicates the amount of lipid oxidation damages. Graph (F) compares untreated control groups of different yeast strains relative to the wild type. The results are presented as means with 95% confidence intervals. Significant differences are indicated with a = $p < 0.05$, b = $p < 0.01$, c = $p < 0.001$, and d = $p < 0.0001$.

4.3.5 Antioxidative defense

We have shown that there is a relationship between the metal ions and the occurrence of oxidative stress in yeast cells. Each organism is equipped with an appropriate antioxidant defense mechanism to maintain redox levels. Because the Δ Sod1 and Δ Ctt1 yeast mutants do not have the full defense arsenal to successfully remove excess oxygen radicals and their products, intracellularly generated ROS and lipid oxidation damage were observed at lower concentrations than in Wt yeast. This prompted us to investigate the enzymatic antioxidant system in *S. cerevisiae*, particularly the major enzymes SOD and CAT. When the levels of ROS are too high, the enzymatic activity is increased, which gives a better indication of the occurrence of oxidative stress. Figure 12 shows the results of native electrophoresis. No significant differences in SOD activity were observed when yeast cells were treated with different concentrations of metal mixtures, although some differences in main values were observed. The same was true for the activity of CAT. However, when yeast cells were treated with SS metal mixtures, a decreasing trend in mean values was observed, and the activity

was significantly different from the untreated control sample at a concentration of 1000 μM SS.

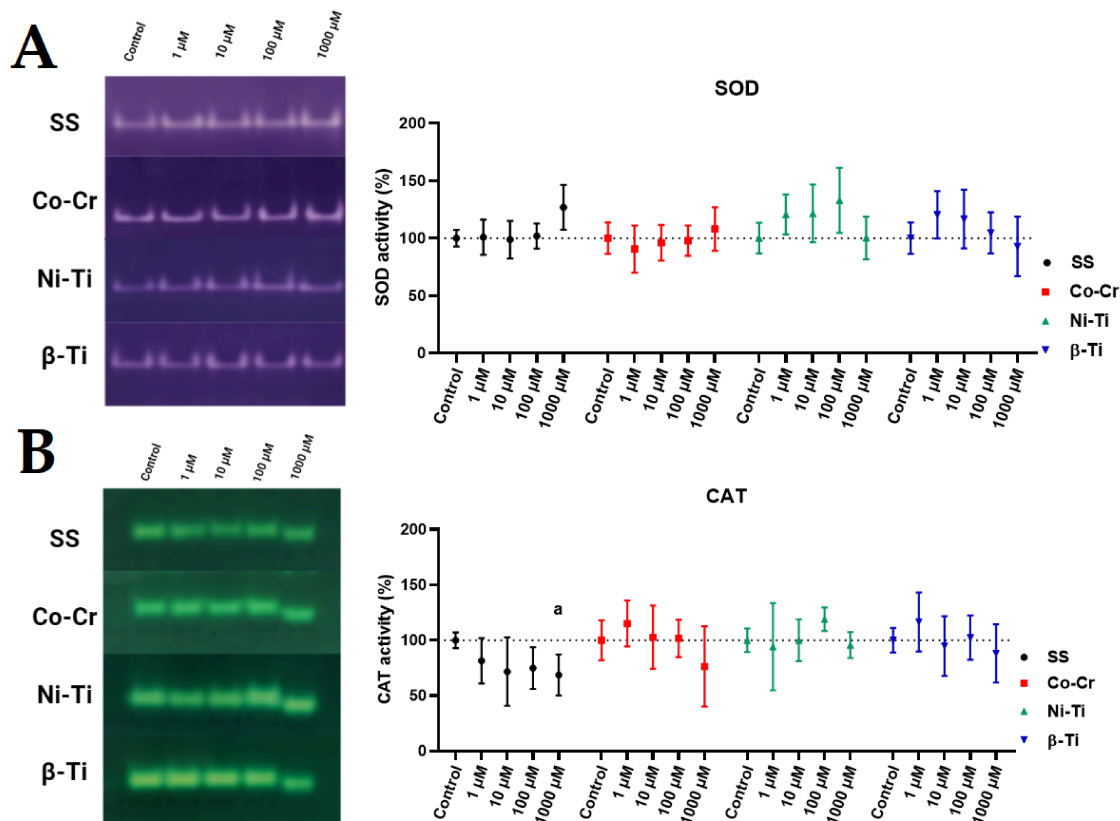


Figure 12: In-gel antioxidative activity of SOD (A) and CAT (B) enzyme after metal ion mixture treatment. *S. cerevisiae* was treated with metal mixtures for 24-hours. The most representative images ($n = 5$) of native electrophoretic bands movement for each metal mixture concentrations are shown the left picture, whereas the intensity of the bands was quantified with ImageJ and presented in the graphs on the right. The results are presented as means with 95% confidence intervals. Statistically different results in the graph are labeled with $a = p < 0.05$.

Due to the high variability of SOD and CAT in-gel activity, we also performed simultaneous spectrophotometric activity measurements, which also measured other enzyme activities related to antioxidant defense, such as GPx, GR, Prx, and TrxR activity (Figure 13). The SOD function is based on the conversion of $\text{O}_2^{\cdot-}$ to H_2O_2 , and the activity was significantly increased when the cells were treated with 1000 μM SS concentration. Other types of metal mixtures at different concentrations had no effect on SOD activity. As it was shown before, the concentration of 1000 μM SS significantly increases the metabolic activity and thus the possible leakage of $\text{O}_2^{\cdot-}$ from the mitochondrial ETC. To maintain proper redox balance, the SOD activity should remove excess $\text{O}_2^{\cdot-}$. The H_2O_2 formed in the dismutase reaction is further converted to H_2O by the enzyme CAT. When the activity of CAT was assessed, a significant decrease was observed after treatment with 1000 μM SS and 1000 μM Ni-Ti. Interestingly, as the concentration of the metal mixture was increased, a non-significant

decrease in activity levels was observed. This observation was contrary to what we expected based on the activity of SOD, as we assumed that with the increase in the activity of SOD, the CAT activity would also increase. The H₂O₂ could also be converted to H₂O by GPx enzyme (Arthur, 2000) and its activity was not affected by the addition of SS and Co-Cr mixture, but a significant increase in activity was observed in the presence of 1000 μM Ni-Ti and β-Ti metal mixture. Since GPx uses GSH as a substrate for its redox reaction, the GR enzyme activity must be consistent with the GSH requirement. The GR activity of 1000 μM SS samples had decreased, whereas the activity was increased after 1000 μM Co-Cr treatment and 10 μM, 100 μM and 1000 μM β-Ti treatment. The thiol-containing enzymes, TrxR and Prx, are also involved in H₂O₂ removal. The TrxR enzyme requires NADPH as a reducing agent to provide reduced thioredoxin for Prx function (Gromer et al., 2004). While Prx activity also decreased significantly after treatment with 1000 μM SS, other metal mixtures caused no changes in enzymatic activity. TrxR activity also decreased when cells were treated with 1000 μM SS, while metal mixtures of Co-Cr, Ni-Ti and β-Ti had an increasing effect on enzyme activity even at a concentration of 100 μM.

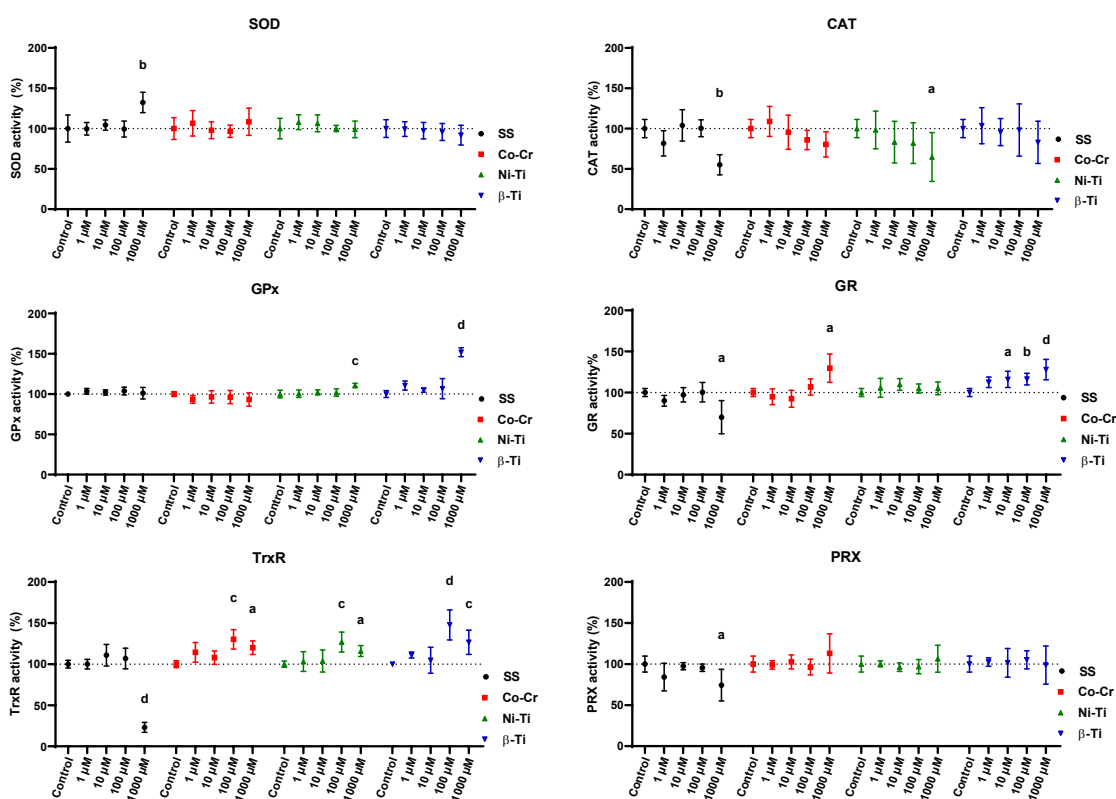


Figure 13: Yeast antioxidant enzyme activity after 24-hour metal mixture treatment. Yeast cell were treated with different concentrations of metal mixtures, and the activity of SOD (A), CAT (B), GPx (C), GR (D), TrxR(E), and Prx (F) was compared to the untreated sample, which enzyme activity was set at 100% for easier comparison between the enzyme activity changes. The activity results are represented as means with 95% confident intervals. Significant differences are indicated with a = p < 0.05, b = p < 0.01, c = p < 0.001, and d = p < 0.0001.

When yeast cells were treated with the SS alloy mixture, the increased O_2 - dismutation by SOD to H_2O_2 should be a trigger for CAT, Gpx and Prx to increase their activity, but this was not the case in presented study, where a decrease in enzyme activity was found. The activity of TrxR, a general mediator of the antioxidant defense system (Lopert et al., 2012), was almost completely inhibited. It is possible that majority of the H_2O_2 generated immediately enters the Fenton and Haber-Weiss reactions, forming OH^\bullet in the presence of metal ions. As reported in the previous section the presence of high concentrations of metal ions reduces cell viability and induces intracellular formation of ROS and causes lipid oxidation. The same deleterious effects were seen when cells were treated with a Co-Cr metal mixture, but the antioxidant enzyme defense system did not show the same response. There was a noticeable increase in SOD activity, but this could not be statistically demonstrated. Again, CAT activity showed a dose-dependent decrease after treatment with Co-Cr, Ni-Ti, and β -Ti. The same observation was made by Atli and Canli (2010) who suggested that the inhibition of CAT activity could be due to the binding of the metal ion to the protein - SH groups. Scharf et al. (2014) also described that the Cr ions could replace Fe in the active site of the enzyme and inhibit the activity of CAT. Another explanation of why the activity of CAT might be decreased comes from Bayliak et al. (2006) who attributed the decreasing effect to high H_2O_2 concentrations, implying that there is a critical H_2O_2 level above which the CAT enzymes no longer function properly. Our in-gel assay of CAT could prove otherwise, as the CAT enzymes from lysates treated with 1000 μ M showed higher electrophoretic mobility, indicating possible oxidation of the enzyme. This was also demonstrated by Rodríguez-Ruiz et al. (2019) who found similar increase in band mobility after H_2O_2 treatment.

Since GPx enzymes require GSH for their reactions and GR obtains it from the conversion of GSSG to GSH, their activity is closely related to the GSH/GSSG ratio, a commonly recognized marker of oxidative stress (Kubrak et al., 2010). There was no increase in GPx activity after SS and Co-Cr treatment, but the activity was increased after Ni-Ti and β -Ti treatment. It was expected that the results for GPx activity would translate to GR activity, but this was not the case in our results. In fact, no clear link could be established between GPx and GR activity. Tandoğan and Ulusu (2008) suggested that Ni ions compete with GSS for the GR ctivity sites and possibly decrease enzyme activity. Ni-Ti treatment, whose Ni ion content was the highest among all metal mixtures, had no effect on GR activity, while SS treatment showed a decrease and Co-Cr and β -Ti treatment showed an increase in GR activity.

Like GPx, the enzyme Prx can reduce organic and inorganic H_2O_2 and often competes with GPx for H_2O_2 dissociation (Mitozo et al., 2011), but no such competition was observed in our study. Treatment of cells with SS induced inactivation of Prx as well as a decrease in TrxR activity, which provides TrxR with the necessary electron donor for its enzyme reaction.

Terpilowska and Siwicki (2019) treated the cell lines BAKB/3T3 and HepG2 with different concentrations of Cr, Fe, Ni, and Mo and investigated the intracellular ROS level, lipid oxidation, and SOD, CAT and GPx activity. The authors concluded that each of the metal ions at concentrations greater than 200 μM can induce oxidative stress and lipid oxidation and decrease the activity of all antioxidant enzymes. The same result was obtained by Kalaivani et al. (2014), who treated A549 cell line with Ni, and by Siddiqui et al. (2015), who treated L929 cell line with Mo ions.

Assessment of Co-Cr metal mixture, Co^{2+} , Cr^{3+} and Cr^{6+} , has different effects on cell viability and enzyme activity. In a cell-free study by Chen et al. (2018) was shown, that 0–50 μM Cr^{3+} concentrations increased CAT activity and concentrations above 50 μM had a decreasing effect on CAT activity. Feng et al. (2017) and Lazarova et al. (2014) found an increase in SOD and CAT activity when yeast cells were treated with low concentrations of Cr^{6+} for a short period of time, whereas prolonged Cr exposure and higher concentrations decreased enzyme activity, suggesting that antioxidant enzymes can only handle a certain amount and time of oxidative stressor. Treatment of cells with Co^{2+} , Cr^{3+} , and Cr^{6+} ions showed a dose-dependent decrease in viability, with Co^{2+} being the most toxic, followed by Cr^{6+} and then Cr^{3+} . The reason why the Cr^{6+} ions were more toxic than Cr^{3+} is because Cr^{6+} can easily pass the cell membrane through anion channels, whereas Cr^{3+} must be taken up by phagocytosis (Wang et al., 2017b). We chose Co^{2+} and Cr^{3+} chlorides to simulate Co-Cr alloys in our study because the Co^{3+} and Cr^{6+} tend to reduce to lower oxidation states under physiological conditions (Baskey et al., 2017).

4.3.6 Protein oxidation

Measuring the carbonyl content of proteins, an end product of protein oxidation in biological samples, is a useful biomarker for evaluating metal-induced oxidative stress because the reaction is irreversible (Lazarova et al., 2014). In our study, it was found that the concentrations of the metal mixtures that induced intracellular ROS generation and lipid oxidation (1000 μM SS, 100 μM , and 1000 μM Co-Cr) also caused oxidative damage to proteins, whereas other metal mixtures had no effect (Figure 14). These results are consistent with those of Scharf et al. (2014) who also treated cells with Co^{2+} and Cr^{3+} ions and found protein carbonylation at concentrations of 100 μM and 1000 μM . Lazarova et al., (2014) also treated yeast cells with 1000 μM Cr^{3+} concentrations and observed an increase in protein carbonyl content.

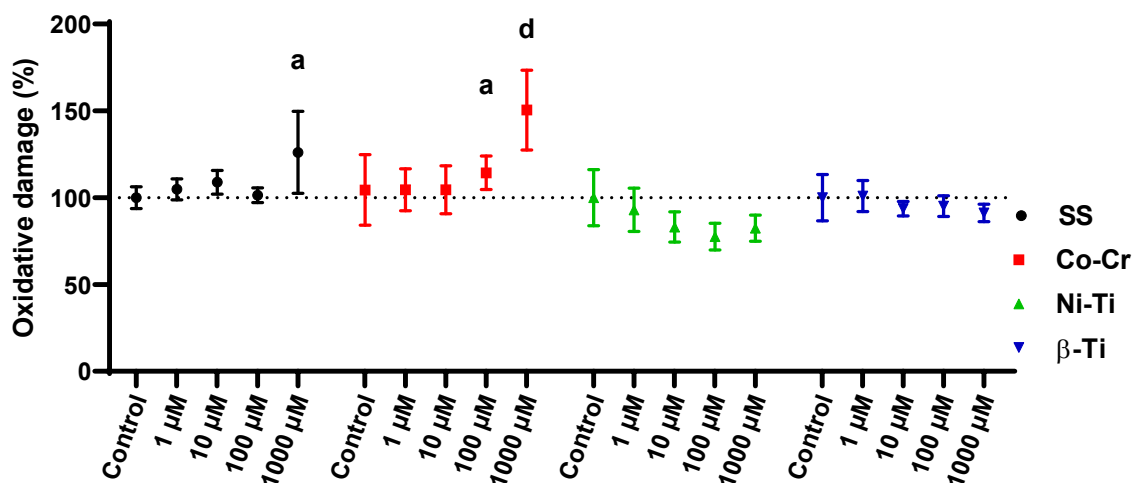


Figure 14: Protein carbonyl content as a result of oxidative protein damage in *S. cerevisiae* after 24-hour metal mixture treatment.

Yeast cells were treated with different concentrations of SS, Co-Cr, Ni-Ti, and β-Ti metal mixtures. The change in absorbance spectrum after the DNPH reacted with the protein carbonyl groups and the OD indicates the amount of protein oxidation damages. Graph (F) compares untreated control groups of different yeast strains relative to the wild type. The results are presented as means with 95% confidence intervals. Significant differences are indicated with a = $p < 0.05$, b = $p < 0.01$, c = $p < 0.001$, and d = $p < 0.0001$.

4.4 THE EFFECT OF METAL MIXTURES ON HGF CELL LINE

The oral mucosa is a mucous membrane consisting of a stratified squamous epithelium – layers of flattened epithelial cells – supported by underlying connective tissue called “lamina propria” (Nanci, 2016). The oral mucosa and gums are the first tissues to come into contact with the released metal ions from orthodontic appliances. The outer epidermal layer of the gingiva is keratinized and protects the inner connective tissue, which consists of gingival fibroblasts. The fibroblasts of the gingiva are responsible for tissue repair and initiating inflammatory responses (Smith et al., 2019). By using human gingival fibroblasts (HGF), we can obtain information about how the cells might respond to certain metals at different concentrations in oral cavity.

To confirm that the use of *S. cerevisiae* as a model organism was justified, we treated the HGF cells with the same metal mixtures for the same period of time with the same concentrations as the yeast cells. As with the yeast cells, we first had to check the viability of the cells (Figure 15). We hoped to obtain more accurate results by using three different methods simultaneously to assess cell viability, but in the case of the Coomassie assay, it was difficult to interpret the results. The Coomassie assay only shows the amount of proteins present; it does not directly describe the viability of the cells. The theory behind this is that the more cells are present, the more proteins are present, and because we discarded the dead cells with the medium, only living cells were dyed. However, for each treatment, we found that the protein content decreased rapidly after treating the HGF cells with low concentration

mixtures and increased again with increasing treatment concentration. We used only the resazurin assay and neutral red uptake results to interpret the cell viability results. The results presented show that treatment of HGF cells with SS and Co-Cr metal mixtures had no effect on HGF cell viability, while Ni-Ti and β -Ti mixtures had a significant effect on viability at 250 μ M for Ni-Ti and at 500 μ M for β -Ti. It appears that the resazurin assay is slightly more sensitive than the neutral red assay, as we found significant differences at lower concentrations compared to the neutral red assay.

Based on the previous results with yeast cells, we had expected the HGF viability results to be just the opposite, with the SS and Co-Cr mixtures decreasing cell viability and Ni-Ti and β -Ti mixtures having no effect. There still remains the question of what happens to the amount of protein in the samples. By definition, cell viability shows the amount of healthy cells in the sample (Kamiloglu et al., 2020). We used the resazurin assay, which measures viability based on the metabolic activity of the cell to reduce resazurin into a fluorescent product (Riss et al., 2016) and the neutral red uptake assay, which measures the uptake of the dye by functioning lysosomes (Fotakis and Timbrell 2006). It is possible that the viability of the HGF cells did not change because the viability assays only measure the final product colorimetrically, which may have come from less viable cells with greater metabolic functions. This could also explain why we obtained such different results for protein levels. These observations prompted us to use the trypan blue cell debris assay to quantify cell death after treatment with the metal mixture (Figure 16). Trypan blue is commonly used in laboratories to count live cells because the dye is only permeable to dead cells and cell debris (Strober, 1997), but isolating and measuring cell debris could provide important information about the amount of dead cells.

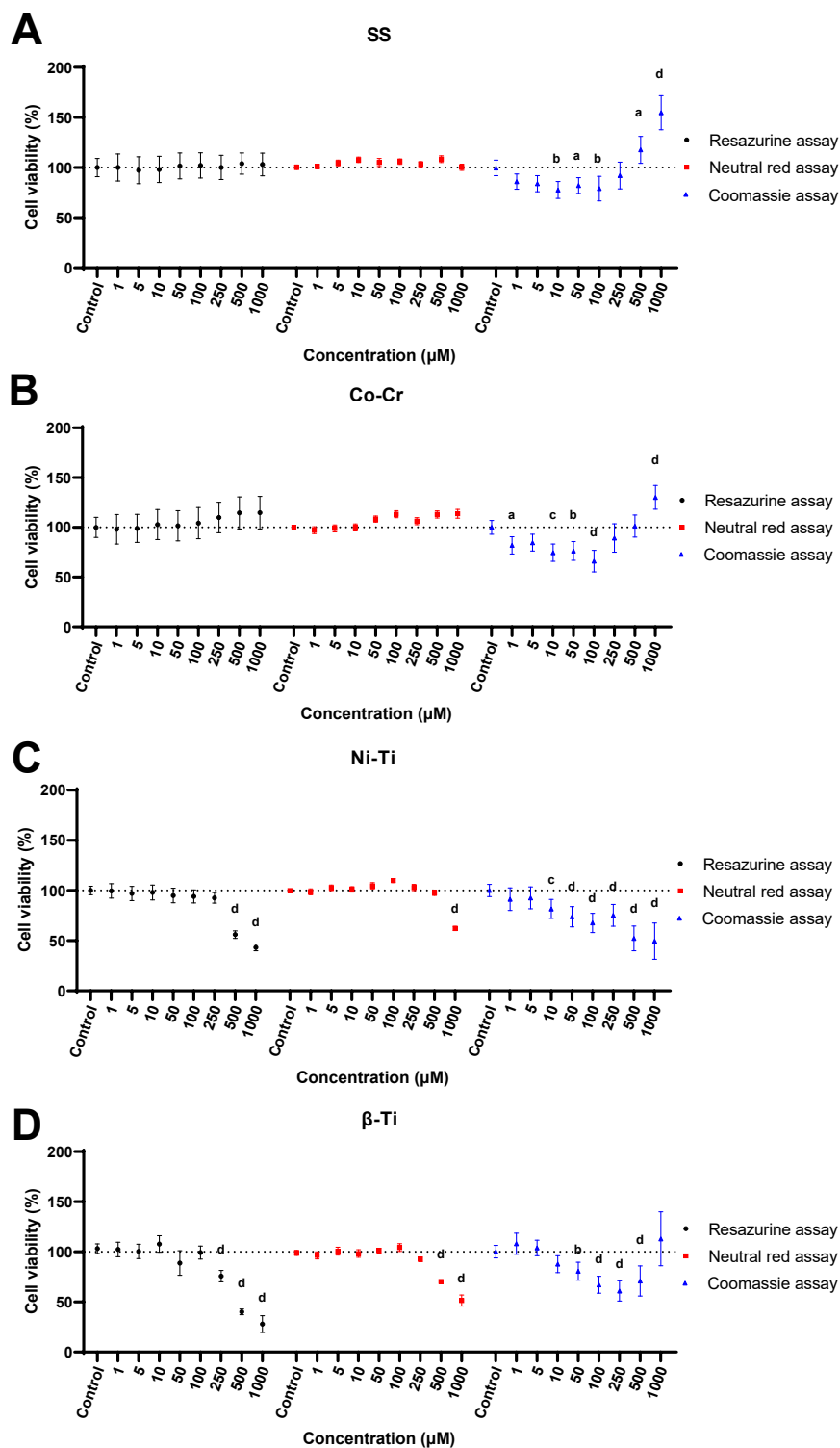


Figure 15: HGF cell viability after 24-hour treatment with metal mixtures
 HGF cell were treated with SS (A), Co-Cr (B), Ni-Ti (C) and β -Ti (D) metal mixtures for 24-hours and the cell viability was assessed with resazurine assay, neutral red assay, and Coomassie assay. The results are presented as means with 95% confidence intervals. Significant differences are indicated as follows; a = $p < 0.05$, b = $p < 0.01$, c = $p < 0.001$, and d = $p < 0.0001$.

As shown in Figure 16, treatment of HGF with SS and Co-Cr mixtures rapidly induces cell death with increasing concentration. A first significant sign of cell death can be observed at a concentration of 100 μM in the case of SS, at a concentration of 400 μM in the case of Co-Cr and at a concentration of 500 μM in the case of Ni-Ti and β -Ti. The trypan blue cell debris assay showed a significant increase in cell death after treatment of cells with SS and Co-Cr mixtures, while the previous methods showed no change in cell viability. These results suggest that metal mixtures of SS and Co-Cr cause HGF cells to increase their metabolic activity and in some cases even increase lysosome volume (Repetto and Sanz 1993) to maintain the same viability in a smaller cell population.

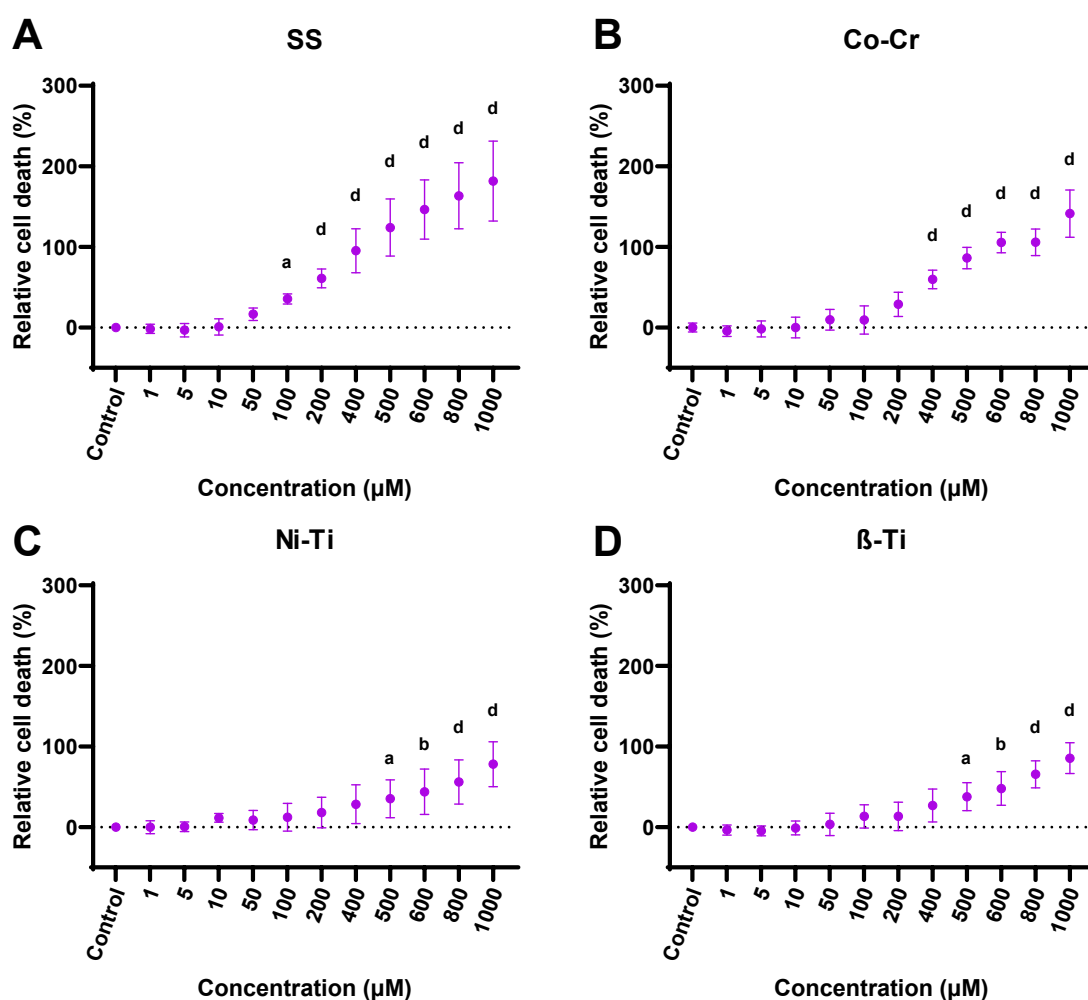


Figure 16: Relative cell death of HGF cells after 24-hour metal mixture treatment. HGF cell were treated with SS (A), Co-Cr (B), Ni-Ti (C) and β -Ti (D) metal mixtures for 24-hours and the relative percentage of dead cells was assessed with trypan cell debris assay. The results are presented as means with 95% confidence intervals. Significant differences are indicated as follows; a = $p < 0.05$, b = $p < 0.01$, c = $p < 0.001$, and d = $p < 0.0001$.

Studies exposing cells to metal ions and metal alloy corrosion products *in vitro* have shown that the toxic effects of the stressor take the form of a reduction in cell viability, alteration of proliferation, inhibition of enzymes, membrane damage, and impairment of DNA and RNA synthesis (Messer and Lucas, 2000; Takano et al., 2002). A study by Issa et al. (2008) showed that different cell types respond differently to the same metal exposure and that even the response of the same cell types to the stressor can vary, mainly because of differences in passage number and cell density. This makes it very difficult to compare our results with those previously obtained from other studies.

Some elements, such as Fe and Ni, are more likely to be released from dental alloys, but not proportionally to the alloy composition (Kovač et al., 2021; Wataha et al., 1991). Issa et al., (2008) found that the viability of HGF cells decreased by 50% after individual treatment with 705.8 μM Co^{2+} , 827.9 μM Ni^{2+} and 1971 μM Cr^{3+} . The high effective concentrations of Cr^{3+} indicate the inability of the ion to enter the cell (Shrivastava et al., 2005). This study is consistent with the study by Messer and Lucas (1999) in which they evaluated the toxic effects of some metal ions as follows: $\text{Cr}^{6+} > \text{Ni}^{2+} > \text{Cr}^{3+} \approx \text{Mo}^{6+}$, while viability was not altered after 1923 μM concentrations of Cr^{3+} and Mo^{6+} . Similar results were also reported by Hallab et al. (2005) who concluded that Co^{2+} and Ni^{2+} were cytotoxic ($\text{LC}_{50} < 1000 \mu\text{M}$), whereas Cr^{3+} and Mo^{6+} posed no toxic hazard at 1000 μM . In our study, we used combinations of metal ions, so we cannot fully compare the cytotoxicity of individual metal ions. Terpilowska et al., (2018) used Fe^{3+} and Ni^{2+} to treat BALB/3T3 fibroblasts and examined cell viability, which decreased with increasing concentration. At lower concentrations (100 and 200 μM), they also observed a slight increase in viability, but any concentration above this decreased cell viability. Iron is an essential element for cell metabolism, but at higher concentrations it is thought to alter membrane stability, trigger the production of ROS through the Fenton reaction, and further damage the biological macromolecules. San Miguel et al. (2013) treated HGF with 1000 μM Ni^{2+} and found a significant decrease in viability, as we did in our study. Ni^{2+} can also induce the formation of ROS through Fenton and Haber-Weiss reactions and cause lipid oxidation, but it must first be oxidized to Ni^{3+} (Chen et al., 2003). The ability of Ni^{2+} to form ROS was put to the test when San Miguel et al. (2013) added synthetic antioxidants to the metal treatment. The viability of HGF cells in the presence of antioxidants increased and the intracellularly generated ROS decreased, suggesting that Ni^{2+} ions have a ROS generating potential. The surfaces of β -Ti alloys are considered resistant to corrosion, but prolonged exposure to acids and in the presence of fluoride, as in the oral cavity, tend to release Ti ions (Nakagawa et al., 2002). Mikihiro et al., (2010) treated gingival epithelia like cells with Ti ions and found a decrease in cell viability at concentrations greater than 250 μM . Because the treatment lasted only 6 hours, compared with our 24 hours, it is reasonable to speculate that viability might change at lower concentrations if the cells were exposed to the Ti ions for a longer period of time. This was demonstrated by Liao et al, who found that treatment of primary osteoblast cells from rat calvaria with 210 μM Ti ions for 24 hours resulted in a decrease in

viability. Treatment of CAL27, HepG2, and Caco-2 cell lines with only Ni²⁺, Ti⁴⁺, or a combination of both ions for 24, 48 and 72 hours resulted in a significant decrease in cell viability (Rincic Mlinaric et al., 2019).

The cause of the decrease in cell viability and cell death was unclear, but we hypothesised that this could be due to the ability of the metal mixtures to generate ROS because all components of the metal mixtures belong to the transition metal group (Jomova and Valko 2011). As before, we used the same protocol of fluorescent dye H₂DCFDA addition to see if the metal mixtures increased the intracellular production of ROS in HGF. The results are shown in Figure 17.

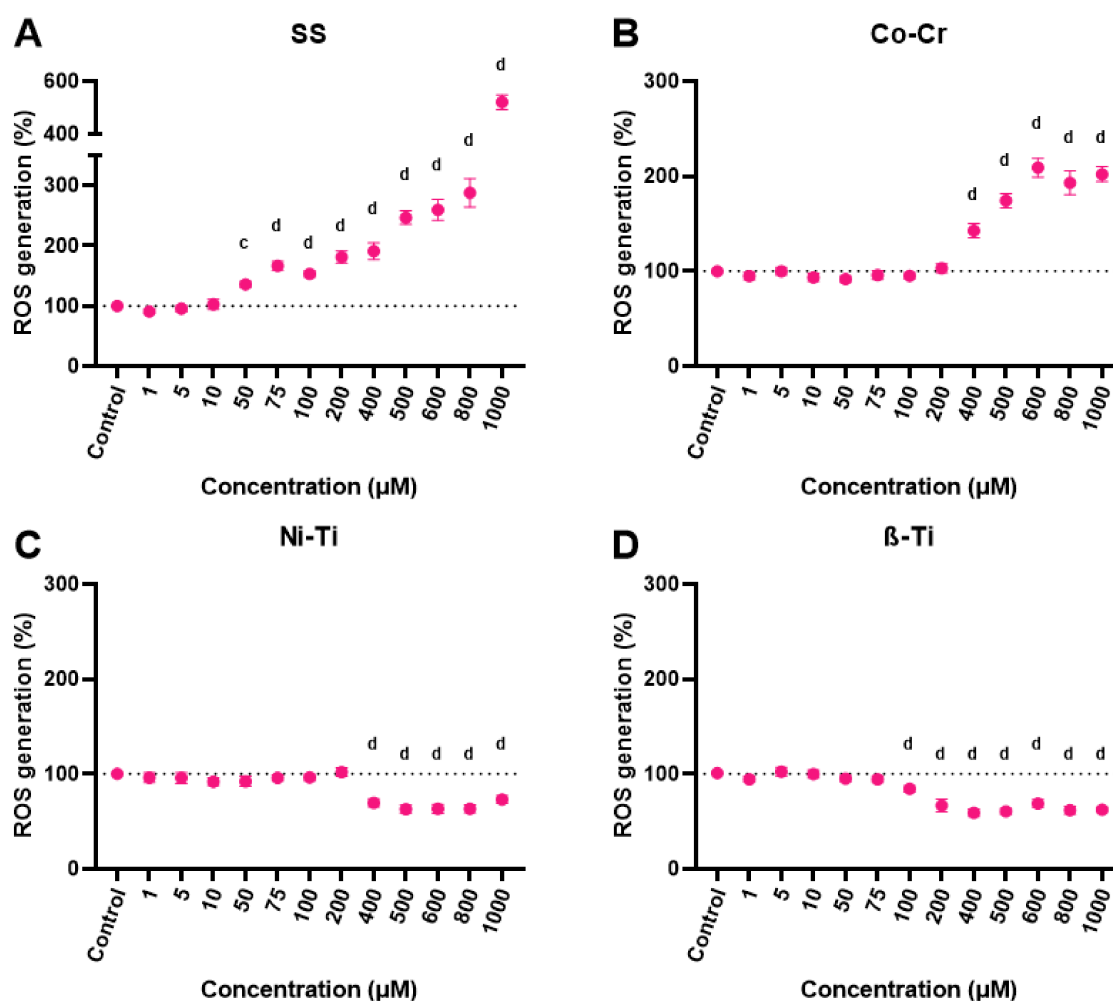


Figure 17: HGF cell intracellular oxidation level after metal mixture treatment. HGF cell were treated with SS (A), Co-Cr (B), Ni-Ti (C) and β-Ti (D) metal mixtures for 24-hours and the intracellular ROS level was observed as change of fluorescence intensity after the addition of the dye H₂DCFDA. The results are presented as means with 95% confidence intervals. Significant differences are indicated as follows; a = p < 0.05, b = p < 0.01, c = p < 0.001, and d = p < 0.0001.

Treatment of HGF cells with different metal mixtures produced different results in terms of intracellular ROS production. The first significant differences in ROS production occurred at a concentration of 50 μM for the SS mixture, a concentration of 400 μM for the Co-Cr mixture, a concentration of 400 μM for the Ni-Ti mixture, and a concentration of 100 μM for the β -Ti mixture. Treatment of HGF cells with the metal mixtures SS and Co-Cr increased the ROS production, whereas after the threat with Ni-Ti and β -Ti, ROS production decreased. When we compared the results of intracellular ROS production with the results of the type blue cell debris assay, we find that in the case of SS and Co-Cr, the ROS level increased with cell death, whereas this effect was reversed in the case of Ni-Ti and β -Ti. The results suggest that SS and Co-Cr mixtures induce oxidative stress and cause cell death in the HGF cell line, whereas cell death after treatment with Ni-Ti and β -Ti does not appear to be due to the generation of ROS.

The ability to generate intracellular ROS Fe^{3+} , Cr^{3+} , Ni^{2+} and Mo^{6+} above a concentration of 200 μM was demonstrated in the BALB/3T3 and HepG2 cell lines in a dose-dependent manner (Terpilowska and Siwicki 2019). Fe^{3+} induced intracellular formation of ROS at a concentration as low as 10 μM in HeLa cell lines (Poljak-Blazi et al., 2011). The effect of individual metal ion treatments cannot be compared because the metal mixtures may have synergistic or antagonistic effects. This was also shown by Terpilowska and Siwicki (2019) that mixtures of 200 μM Cr^{3+} and 1000 μM Fe^{3+} or 1000 μM Cr^{3+} and another metal ion at a concentration of 200 μM have a synergistic effect on ROS formation. On the other hand, a metal mixture of 200 μM Cr^{3+} and 1000 μM Ni^{2+} as well as a mixture of 200 μM Cr^{3+} and 1000 μM Mo^{6+} has an antagonistic effect on ROS generation. Also, a study by Patel et al., (2012) showed that Co^{2+} and Ni^{2+} , alone and in combination, increased ROS production. Assuming that the metal mixtures we prepared did not have synergistic or antagonistic effects, we could obtain some conclusions. The ability to produce ROS in the SS metal mixture of Fe^{3+} , Cr^{3+} and Ni^{2+} could be due only to Fe^{3+} and Cr^{3+} since Ni^{2+} could not have induced the production of ROS, as shown in the case of the Ni-Ti mixture of Ni^{2+} and Ti^{4+} since no increase in ROS was obtained. The question remains to what extent Cr^{3+} causes the formation of ROS, because it is known that it cannot freely cross the cell membrane although a study by Fleury et al. (2006) showed that Cr^{3+} can be taken up by phagocytosis. The ability of Fe^{3+} to generate ROS via the Fenton reaction has been mentioned in several previous studies (Jia et al., 2012; Keenan et al., 2009). It is important to note that all metals used in the mixture are capable of generating ROS, although the efficiency to generate free radicals varies greatly. For example, the efficiency of Co^{2+} and Ni^{2+} in generating ROS is very low due to the high oxidation/reduction potential (Leonard et al., 2004). This brings us to the question of which metal ion is responsible for the generation of ROS in the Co-Cr mixture consisting of Co^{2+} , Cr^{3+} , Fe^{3+} , Ni^{2+} and Mo^{6+} ions. As before, we can exclude Cr^{3+} , Ni^{2+} and Mo^{6+} ions, leaving Co^{2+} and Fe^{3+} ions as potential oxidative stressors. Most of the decrease in viability and formation of ROS can be attributed to Co^{2+} , as it makes up 40% of the Co-Cr mixture compared to the 18% of Fe^{3+} . As mentioned above, the ability of Co^{2+} to catalyze

the Fenton reaction is lower compared to Fe^{3+} , so the single fluorescence obtained after Co-Cr treatment was also lower than that of SS. Co^{2+} has also been shown to induce the formation of ROS and to cause oxidative stress-induced damage to biological molecules (Fleury et al., 2006; Gault et al., 2010; Tripathi et al., 2019). No increase in ROS was observed in the β -Ti mixture composed of Ti and Mo ions, so these two metals could be ruled out as potential ROS generators, although some studies have shown that Ti ions can generate free radicals (Rincic Mlinaric et al., 2019).

When comparing the 24-hour effect of metal mixtures between the yeast *S. cerevisiae* and the HGF cell line, some findings were obtained. Regarding the concentration of metal mixtures, 100 μM concentrations could not affect the viability of HGF cells, but some metal mixtures (Co-Cr) also had a decreasing effect on the culturability of *S. cerevisiae* at this concentration. Of course, when the concentration of the metal mixture exceeded the 100- μM concentration, the death of HGF cells was observed in all metal mixtures. Assuming that the decrease in culturability/viability was due to the ability of the metals to generate ROS, we found interesting similarities between the yeast and the cell line. Both showed an increase in the levels of ROS when treated with SS or a Co-Cr metal mixture, and a dose-dependent increase in the levels of ROS was observed in the cell line. No increase in ROS levels was observed with the other two metal mixtures, Ni-Ti and β -Ti. Rather, a decrease in the ROS level was observed. This means that the Ni-Ti and β -Ti mixtures do not cause ROS-related decrease in cell viability. The comparison suggests that *S. cerevisiae* is a useful model organism for oxidative stress studies.

4.5 EFFECT OF NANOPARTICLE EXPOSURE TO HGF CELL LINE

4.5.1 Nanoparticle characteristics

The detailed results of the individual measurements of NP are given in Table 7. The main problem with the stability of NPs is their tendency to agglomerate and sediment (Wu et al., 2011). Because of their small size, they have a high surface energy and to reduce the energy distribution, they agglomerate. To solve this problem, nonionic or ionic surfactants are usually added to NP suspensions to form a protective layer around the NP (Rabinow, 2004). Parameters of the medium such as pH, salts and the presence of proteins (serum) can also cause agglomeration (Joris et al., 2013). Sedimentation due to gravity is also common to all NPs. Other factors such as size, density, and zeta potential (ZP) of the NPs can affect sedimentation. For example, the higher the absolute ZP value, the more the NPs tend to settle to the bottom. It should be mentioned that all tested NPs sedimented very quickly. Since the dynamic light scattering (DLS) and ZP measurements had to be performed in suspension, the measurements were not completely accurate because only small NPs dispersed in the solution could be measured, but not the sedimented NPs. After the DLS measurement, the hydrodynamic size of the NPs increased dramatically.

All three TiO₂-NPs samples are very similar after transmission electron microscope (TEM) visualization (Appendix F). Mainly spherical particles ranging in size from 200 nm to several µm are seen, with some larger single crystals. These spherical particles consist of tightly bound small NP crystals and are not expected to be dispersed in the suspension after ultrasonic treatment. In the case of the TiO₂ anatase/rutile sample, these small crystals are in the size range of 30-100 nm, in the case of TiO₂ anatase in the range of 5 to 100 nm, and in the case of TiO₂ rutile in the range of 3-100 nm. The ZP of TiO₂-NPs showed negatively charged NPs in both H₂O and Fib medium.

Most of the Ag-NP material was present in large crystal aggregates. Smaller NP crystals of various sizes were also found among the larger aggregates (Appendix G). When the NPs were placed on a carbon surface for the TEM measurement, the Ag-NPs tended to self-regulate and form clusters in which larger NPs were found in the center of the clusters and the size of the NP decreased toward the edge of the cluster. In the Ag 28-48 nm sample, the size of the NPs ranged from 2-20 nm and in the Ag 48-78 nm sample, the size of the NPs was 3-10 nm. In addition, very small NP were seen in the Ag 48-78 nm sample, which were probably formed from Ag⁺ ions of the NP solution. The ZP measurement showed negatively charged NP.

The two ZnO-NPs look very similar TEM (Appendix H). Again, the smaller NPs tend to agglomerate and form crystals of about 50 nm in size. Smaller agglomerates of larger ones, about 100 nm in size, NP were also seen. After the ZP measurements of H₂O, positively charged NP were analyzed, and in the case of fib medium, negatively charged NP were seen. The WS₂ sample also showed a tendency to agglomerate into larger structures (Appendix I). All sizes of NPs could be found in the samples, among the larger ones we were larger than 1000 nm and the smaller ones around 200 nm, while no monocrystalline NPs were seen. The ZPs of the WS₂-NPs were found to be negatively charged.

Table 7: Size and surface charge of used nanoparticles

NP	Declared size (nm)	TEM (nm)	DLS H ₂ O (nm)	DLS Fib-medium (nm)	ZP H ₂ O	ZP Fib-medium
TiO ₂ Anatase/Rutile	18 nm	Small crystals of 30 nm aggregate to form globular particles (<1000 nm)	1787 nm (pH = 7.2)	853 nm (pH = 8.2)	-15.9 (pH = 7.2)	-11.2 (pH = 8.1)
TiO ₂ Anatase	28 nm	Small crystals of 5 nm aggregate to form globular particles (<1000 nm)	1919 nm (pH = 7.6)	691 nm (pH = 7.9)	-8.3 (pH = 7.9)	-11.9 (pH = 7.9)
TiO ₂ Rutile	28 nm	Small crystals of 3 nm aggregate to form globular particles (<1000 nm)	751 nm (pH = 7.6)	865 nm (pH = 7.7)	-18.9 (pH = 7.2)	-11.4 (pH = 7.7)
Ag	28-48 nm	Small crystals of 2 - 20 nm aggregate to form globular particles (< 1000 nm)	582 nm (pH = 7.6)	437 nm (pH = 8.1)	-31.2 (pH = 7.6)	-12.1 (pH = 8.1)
Ag	48-78 nm	Small crystals of 3 - 10 nm aggregate to form globular particles (< 1000 nm)	748 nm (pH = 7.6)	1343 nm (pH = 7.8)	-25.4 (pH = 7.6)	-10.3 (pH = 7.8)
ZnO	18 nm	Small crystals of 50 nm aggregate to form globular particles (< 100 nm)	735 nm (pH = 8.1)	7486 nm (pH = 8.1)	24.1 (pH = 8.1)	-10.9 (pH = 8.1)
ZnO	30-50 nm	Small crystals of 50 nm aggregate to form globular particles (< 100 nm)	998 nm (pH = 8.0)	4691 nm (pH = 8.2)	22.2 (pH = 8.0)	-11.7 (pH = 8.2)
WS ₂	35-75 nm	Small crystals of 50 nm aggregate to form globular particles (< 1000 nm)	749 nm (pH = 3.5)	3356 nm (pH = 7.7)	-21.6 (pH = 3.5)	-11.2 (pH = 7.7)

4.5.2 Cytotoxicity of NPs

Due to their physical and chemical properties, NPs are becoming increasingly important in the research and development of new materials, which include orthodontic materials. However, with the new properties and industrial production of NPs, concerns about possible adverse health effects have also arisen. Therefore, it is first necessary to understand the effects of NPs on living cells in order to recognize them as safe for further use in any applications. As there are more and more NPs of different types, sizes, and shapes, the number of reagents for their safety increases to (Drasler et al., 2017). Based on the 3Rs principle replacement, reduction, and refinement, *in vivo* safety studies in animals are slowly being replaced by *in vitro* studies in primary cells or cell lines (Krewski et al., 2010a).

TiO₂-NPs are the most commonly produced NPs and their use is very versatile, but is mainly used as a white pigment in food additives, medicine, cosmetics, and sunscreens (Hamzeh and Sunahara 2013). Ti materials are widely used in dentistry due to their high corrosion resistance and biocompatibility. The oxide layer formed on the surface of titanium materials is the reason for their excellent properties. However, in the oral environment, tribocorrosion of the layer can occur, reducing the biocompatibility of Ti materials and releasing metal ions

and abrasion from the surface (Apaza-Bedoya et al., 2017). TiO₂-NPs can occur in two crystalline forms: anatase or rutile, and anatase has been shown to be more cytotoxic than rutile (Sayes et al., 2006). In our study, we used anatase, rutile, and a mixture of both to investigate the effects of these NPs on the HGF cell line (Figure 18).

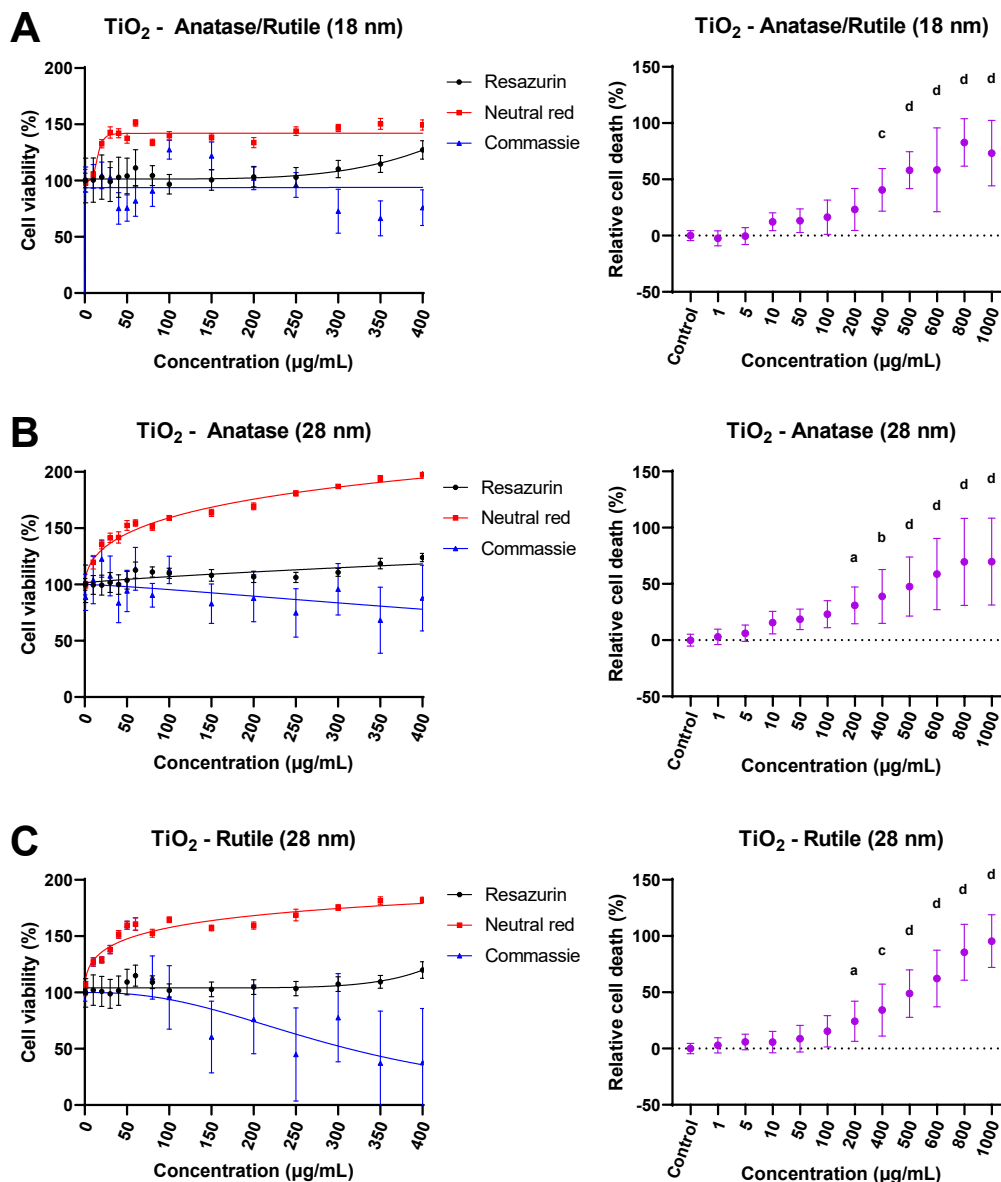


Figure 18: Cell viability of HGF after treatment with three types of TiO₂-NPs. After treating HGF cells with different concentrations of TiO₂ Anatase/Rutile (18 nm) (A), TiO₂ Anatase (28 nm) (B) and TiO₂ Rutile (28 nm) (C) for 24-hours, the resazurine assay, neutral red uptake assay and Coomassie assay were used to assess the cell viability. To obtain the relative cell death after the NP treatment, typan blue cell debris assay was employed. The results are presented as means with 95% confidence intervals. Significant differences are indicated as follows; a = p < 0.05, b = p < 0.01, c = p < 0.001, and d = p < 0.0001.

The oral cavity is a portal of entry into the respiratory and gastrointestinal tracts and is the first to be affected by the release of nanoparticles from orthodontic materials. If NPs have an effect on cells of the oral cavity, then it is also worth considering that NPs may migrate to other tissues and have an effect there as well. To test the viability of HGF cells, we used different concentrations of NPs and examined the viability of the cells after 24 hours of treatment of HGF with TiO₂-NPs using four different methods. The use of the neutral red uptake assay to determine cell viability was found to be inappropriate because the TiO₂-NPs interfered with the assay and gave erroneous results. It was noted by Jalili et al. (2018) and Bessa et al. (2017) that TiO₂-NP can interfere with NR assay due to the light reflecting/absorbing of TiO₂-NPs at wavelengths used for NR quantification. No change in viability was observed when the resazurin assay was used. Mello et al. (2020) suggest that resazurine assay should be the preferred assay, when assessing NP related cytotoxicity, due to minimal interference of the NP. After treatment of HFG cells with a concentration of 300 µg/mL, an increase in viability was even observed, but this may also be due to the interference of the NPs with the assay. The Coomassie assay indicated the amount of protein in the cells, which was volatile up to the 100 µg/mL concentration of NPs but then decreased significantly. In the case of TiO₂ anatase/rutile, the protein concentration was significantly reduced at a concentration of 300 µg/mL, and in the case of TiO₂ anatase and TiO₂ rutile, the significant decrease was reached at 200 µg/mL. Because each of these three viability assays gave different results, we used the Typan cell debris assay to compare the amount of dead cells after treatment with the untreated cell sample. Dose-dependent cell death was detected in all samples treated with TiO₂-NPs. The extent of cell death of the samples treated with TiO₂ anatase/rutile was significantly different at 300 µg/mL and higher concentrations compared with the untreated control sample, whereas TiO₂ anatase and TiO₂ rutile significantly increased cell death at 200 µg/mL and higher. The observations of cell death were consistent with the results of the Coomassie assay, and it could be concluded that high concentrations of TiO₂-NP interfered with normal cell activity. Li et al. (2010) also found that the same dose of 200 µg/mL increased cell death in fibroblast cultures.

A systematic review by Suárez-López del Amo et al., (2018) reported that TiO₂-NPs and TiO₂ microparticles (TiO₂-MPs) ranging in size from 15 nm to 45 µm were found in animal models and from 100 nm to 54 µm in human tissues as a consequence of particle release from dental materials, as well as dental material wear debris in oral tissues. The Ti particles can cause cytotoxicity (Happe et al., 2019), genotoxicity, inflammation (Pettersson et al., 2017), changes in cytoskeletal structures (Saldaña and Vilaboa 2010). It is difficult to assess the cytotoxicity of NPs, which tend to aggregate into MPs because they are larger than the cell organelles and cannot be taken up by the cell membrane as the NPs below 100 nm do (Singh et al., 2007). Actually, the agglomerated particles should be dispersed before treatment with ultrasound, but in our case, the TiO₂-NPs could not be dispersed properly. The agglomerated particles could have a different bioactivity on the cells, but at the same time, these agglomerated crystals are not uniform and usually consist of submicron particles

and can also release some NPs from their structure into the environment. Li et al., (2022) have shown that after treatment of HGF with TiO₂-MPs and TiO₂-NPs, TiO₂-NPs were found to be more cytotoxic than TiO₂-MPs, as they decreased cell viability at 250 µg/mL, in contrast to TiO₂-MPs, which significantly decreased cell viability at 1000 µg/mL. Similar results were observed with other cell types such as epithelium (Suárez-López del Amo et al., 2018), fibroblast (Garcia-Contreras et al., 2015), macrophages (Ding et al., 2012) and osteoblasts (Zhang et al., 2020). Lin's group also showed that both NPs and MPs were taken up by the cells, but MPs were distributed only in the cytoplasm, whereas NPs were also found in the nuclei. Importantly, even non-cytotoxic concentrations of NPs and MPs can alter the organization of the cytoskeleton and thus affect the biological behavior of the cell. Cytoskeletal organization regulates cell shape, adhesion, growth, maturation, and migration (Pollard and Cooper 2009; Thievensen et al., 2013). In contrast, Barrak et al. (2020) showed no reduction in viability after treatment of HGF with a mixture of TiO₂-NPs and TiO₂-MPs, but the average size of MPs was 77.4 ± 9.1 µm, twenty times larger than those we used.

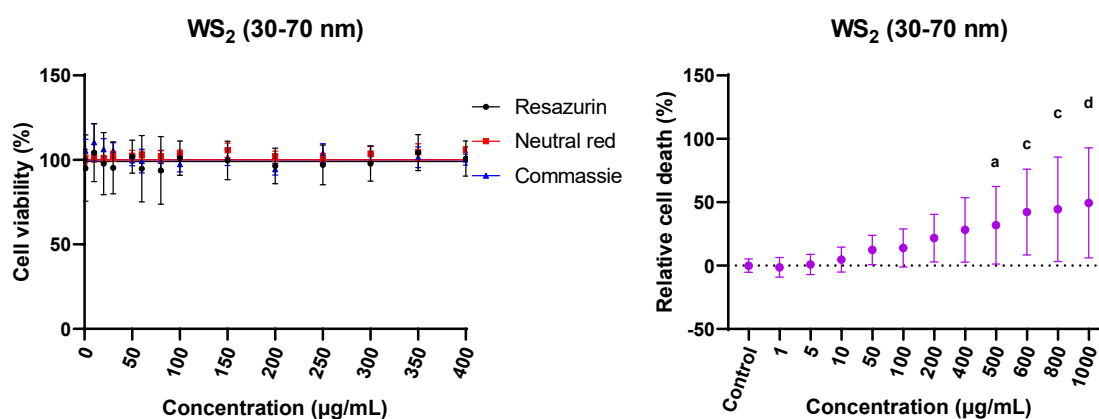


Figure 19: Cell viability of HFG after treatment with WS₂-NPs.

After treating HGF cells with different concentrations of WS₂-NPs for 24-hours, we used resazurine assay, neutral red uptake assay and Coomassie assay to assess the cell viability. To obtain the relative cell death after the NP treatment, trypan blue cell debris assay was employed. The results are presented as means with 95% confidence intervals. Significant differences are indicated as follows; a = $p < 0.05$, b = $p < 0.01$, c = $p < 0.001$, and d = $p < 0.0001$.

Due to its high strength and low coefficient of friction, WS₂-NPs are gaining interest in dentistry, especially in orthodontics. Therefore, understanding their potential toxicological effects is necessary, but not yet sufficiently explored. Treatment of HGF cells with increasing concentrations of WS₂-NPs had no effect on cell viability in all assays up to 400 µg/mL, but the trypan blue cell debris assay showed a dose-dependent increase in dead cells that was significant at a concentration of 500 µg/mL (Figure 19). While Domi et al. (2021) observed no decrease in viability after treatment of A549 cells with a concentration of 160 µg/mL, Domi et al. (2021) and Teo et al., (2014) observed a decrease in cell viability after treatment of cells with a concentration of 400 µg/mL WS₂-MPs and WS₂-NPs, but this is

considered mild cytotoxicity. The reason for the mild cytotoxicity of WS₂-NPs might be due to the agglomeration of NPs in the presence of the growth medium. Turkez et al. (2014) have shown that high concentrations of NPs disrupt the integrity of cell membranes, leading to cell death, but the actual toxicity of NPs may depend not only on the numerical nominal exposure (concentration) but also on the properties of NPs, such as mass, surface area, and dissolution of ions (Pardo et al., 2014). The exact mechanism of toxicity of WS₂-NPs at high concentrations is not defined, but Liu et al. (2017) suggested that proteins in the medium are absorbed onto the WS₂-NPs surface and form a protein corona that can reduce cell viability. In our study, the interaction of proteins from fibroblast serum with WS₂-NPs may have been the reason why we observed a significant increase in cell death at 500 µg/mL compared with the control sample. From a chemical point of view, there is an intrinsic electron transfer from W to S atoms that makes WS₂ hydrophilic and reduces the likelihood of other molecules such as phospholipids being distributed in the membrane (Liu et al., 2017).

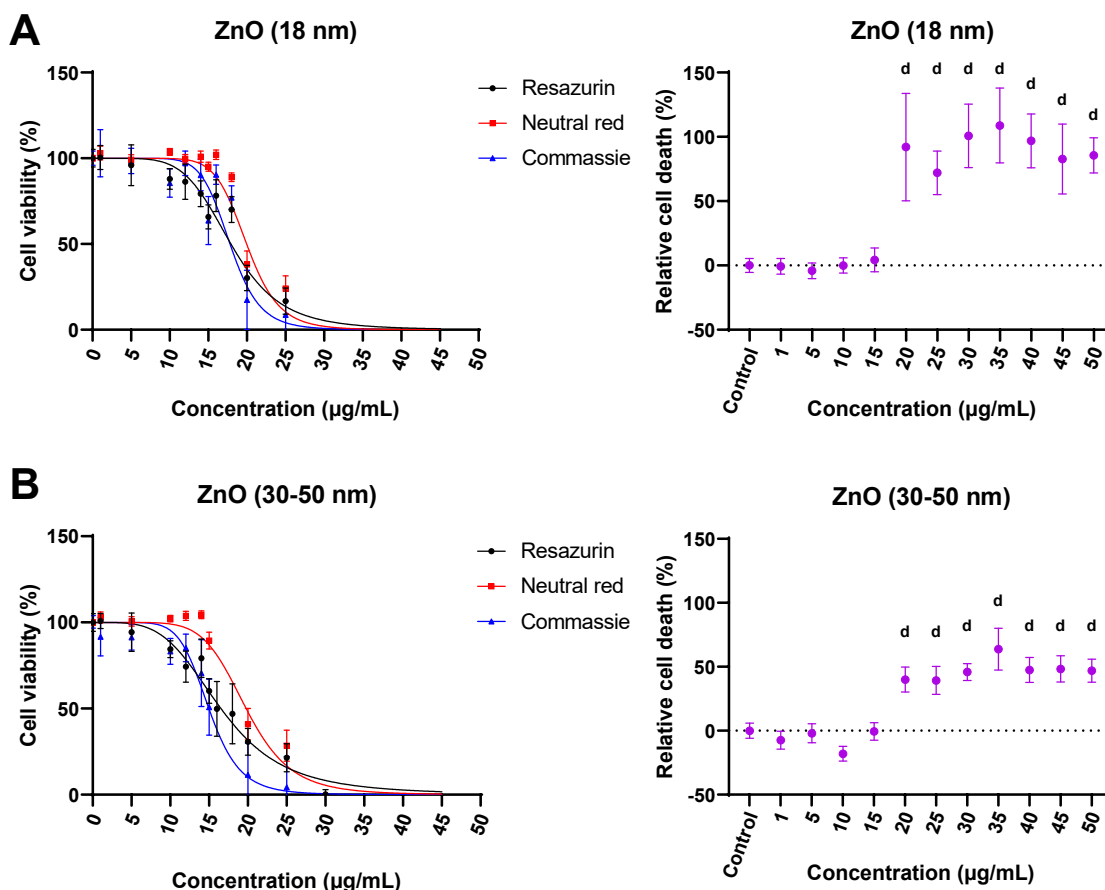


Figure 20: Cell viability of HGF after treatment with two different ZnO-NPs.

After treating HGF cells with different concentrations of ZnO (18 nm) (A) and ZnO (30-50 nm) (B) for 24-hours, we used resazurine assay, neutral red uptake assay and Coomassie assay to assess the cell viability. To obtain the relative cell death after the NP treatment, typan blue cell debris assay was employed. The results are presented as means with 95% confidence intervals. Significant differences are indicated as follows; a = $p < 0.05$, b = $p < 0.01$, c = $p < 0.001$, and d = $p < 0.0001$.

Like TiO₂-NPs, ZnO-NPs are increasingly used in industrial and commercial applications, especially as pigments and for protection against UV radiation in sunscreens. ZnO-NPs also have good antibacterial, anticorrosive, and antifungal properties, which are in high demand in the field of orthodontics (Service, 2003). To investigate the possibility of toxic damage to HGF cells by ZnO-NPs, we performed various tests to explore the toxic effect (Figure 20). The cell viability data show a strong decrease in viability after treatment with 15 µg/mL and above for both ZnO-NPs used in the study. We also obtained the same results on cytotoxicity as Choudhury et al. (2017) who also found a strong effect of ZnO on the cytoskeleton of the cells. When the used ZnO NPs agglomerate in the aqueous medium, they clump together and form larger crystals. A wide range of crystals of different sizes can bind to a wider range of biomolecules and potentially cause multimodal damage (Rana et al., 2013). Not only MPs and NPs, but also ions could affect cell viability because ZnO-NPs release Zn²⁺ ions to the environment (Ng et al., 2017; Yin et al., 2010). We found no difference in the cytotoxicity of ZnO-NPs with sizes of 18 nm and 30-50 nm, but these were only the reported sizes, which turned out to be much larger after theoretical characterization. On the other hand, study of Bhattacharya et al. (2016) shows that ZnO NPs of different sizes and shapes have different effects on the cell.

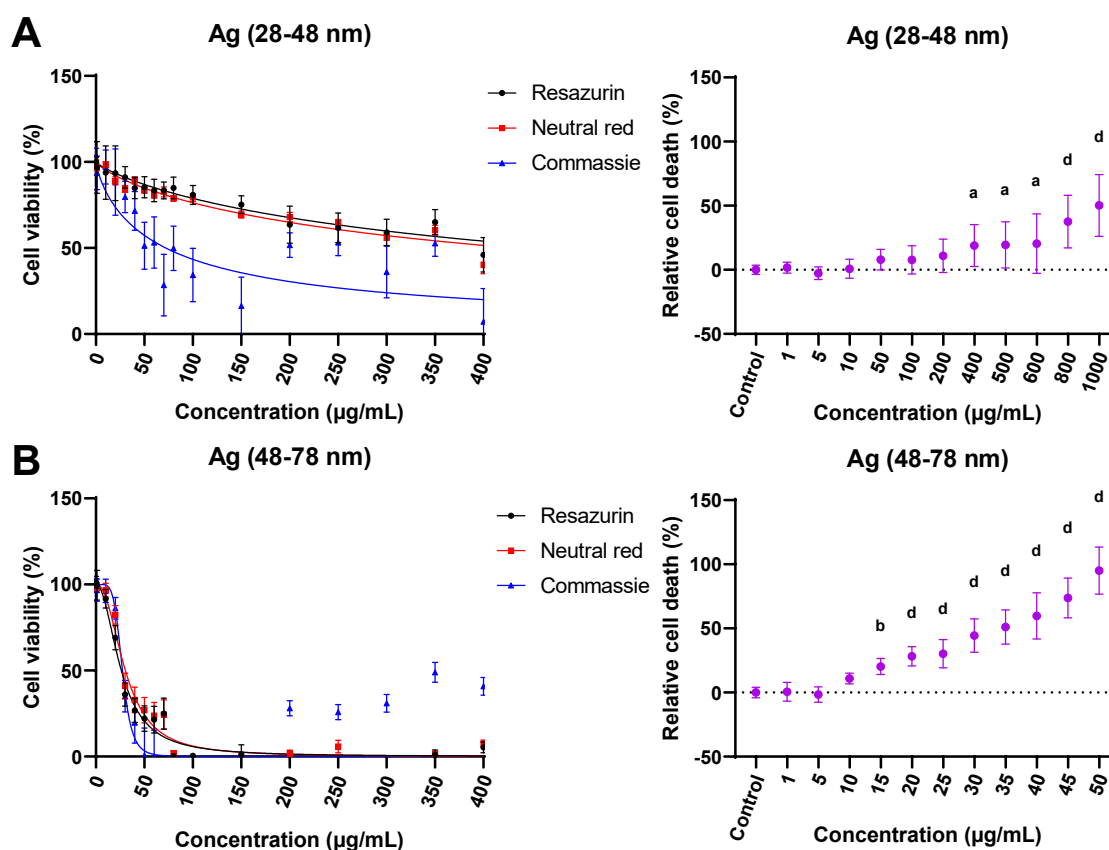


Figure 21: Cell viability of HGF after treatment with different concentrations of Ag-NPs. After treating HGF cells with different concentrations of Ag (28-48 nm) (A) and Ag (48-78 nm) (B) for 24-hours, we used resazurine assay, neutral red uptake assay and Coomassie assay to assess the cell viability. To

obtain the relative cell death after the NP treatment, typan blue cell debris assay was employed. The results are presented as means with 95% confidence intervals. Significant differences are indicated as follows; a = $p < 0.05$, b = $p < 0.01$, c = $p < 0.001$, and d = $p < 0.0001$.

Ag-NPs are a kind of double-edged sword when exposed to humans, as producing both beneficial effects such as antimicrobial effects and harmful effects such as cytotoxicity. Exposure of the HFG cell line to two different Ag-NPs led to different results in cell viability (Figure 21). In the case of the 28-48 nm size NPs, viability slowly decreased with increasing NP concentration, and a significant increase in cell death was observed at 400 $\mu\text{g/mL}$. In contrast, for the 48-78 nm size NPs, the effect was much more pronounced, as cell viability dropped below 50% when treated with a concentration of 30 $\mu\text{g/mL}$, and cell death was significantly increased at a concentration of 15 $\mu\text{g/mL}$. The different effect of the two Ag-NPs could not be related to the properties, because both Ag-NPs have similar properties, but when the size was assessed on TEM, very small particles were seen (< 1 nm), which could be the Ag^+ ions. The larger presence of Ag^+ ions in the 48-78 nm Ag-NPs suspension could be the reason for the strong cytotoxic effect of these NPs. After entering the cell, Ag-NPs and Ag^+ ions can have deleterious consequences, ranging from the generation of ROS and oxidative damage to mitochondrial damage and apoptosis (Akter et al., 2018). Depending on the properties, some Ag-NPs are taken up by endocytosis and dissolved into Ag^+ ions due to the acidic medium in the lysosomes. Other Ag-NPs diffuse into the cytoplasm, where they are oxidized by cytoplasmic enzymes and release Ag^+ ions (Sabella et al., 2014). The released ions interact with mitochondrial proteins, disrupting mitochondrial flux and generate ROS.

The cytotoxic mechanism of NPs is still controversial, but several lines of evidence suggest the possible role of ROS and oxidative stress on induced cytotoxic effects (Singh et al., 2007). To investigate the ability of NPs to stimulate the formation of ROS, the dye H_2DCFDA was used as an indicator of intracellularly formed ROS (Figure 22). Treatment with TiO_2 -NP showed a dose increasing effect of intracellularly ROS formation. Even a TiO_2 -NP concentration of 20 $\mu\text{g/mL}$ resulted in a significant increase in ROS production compared with the control group. As it was already seen in the assessment of cell viability, higher concentrations led to membrane damage, so that the fluorescence signal was also significantly attenuated. The same observation was also reported by Liu et al. (2010). Periasamy et al. (2015) linked the generation of ROS to mitochondrial damage because ROS disrupted the mitochondrial membrane potential, resulting in even more ROS being generated.

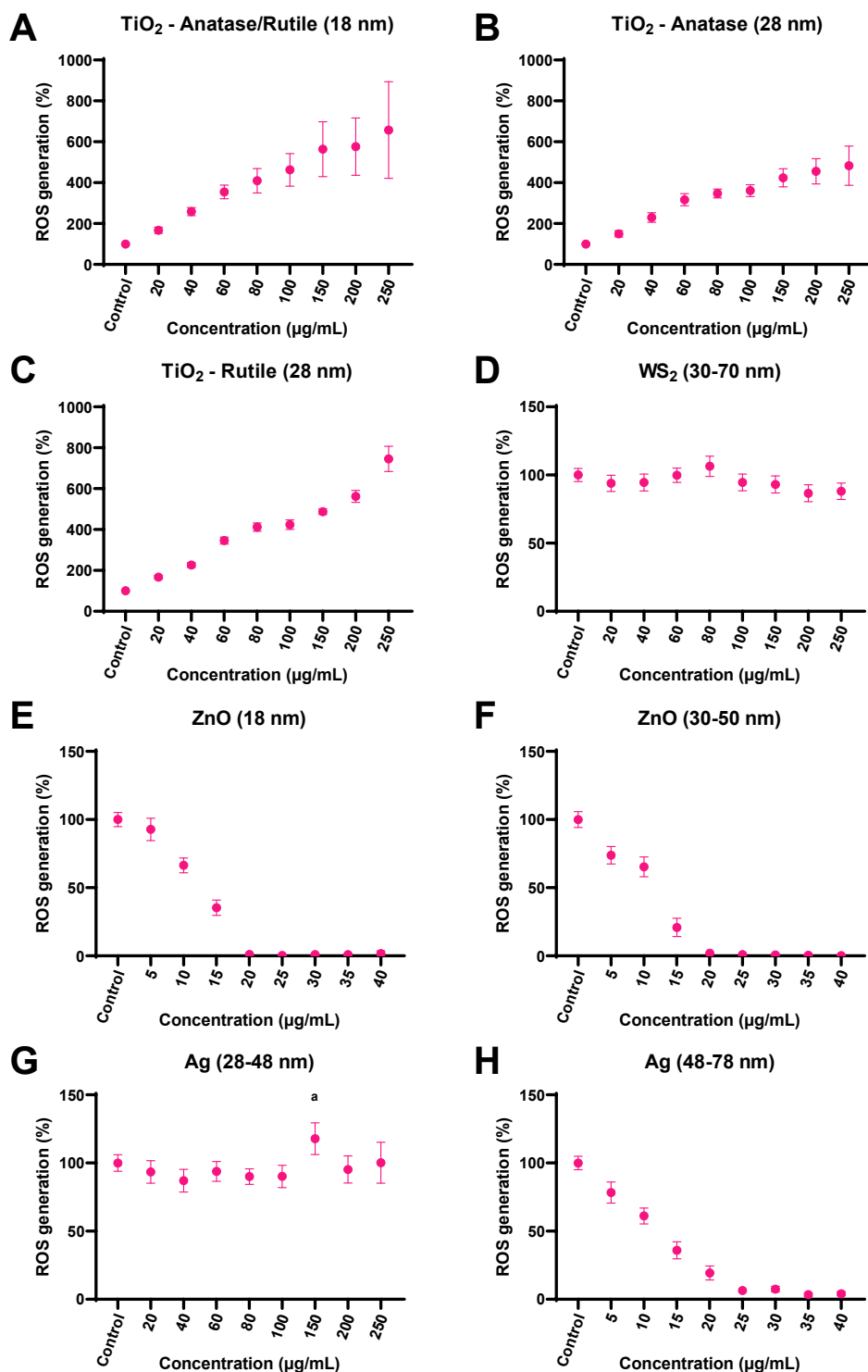


Figure 22: Intracellular ROS generation of HGF cells, treated with different types and concentrations of NPs. After treating HGF cells with different concentrations of TiO_2 (Anatase/Rutile 18 nm) (A), TiO_2 (Anatase 28 nm) (B), TiO_2 (Rutile 28 nm) (C), WS_2 (D), ZnO (18 nm) (E), ZnO (30-50 nm) (F), Ag (28-78 nm) (G) and Ag (48-78 nm) (H) for 24-hours, the fluorescent dye H_2DCFDA was added to observe the intracellular ROS level. The results are presented as means with 95% confidence intervals.

As much as TiO₂-NPs are praised for their use as UV light blockers in sunscreens, their property also has a downside, because when photoexcited, they can generate ROS (Konaka et al., 2001). Excitation of valence electrons by UV light leaves positively charged spaces that generate ROS in the presence of aqueous media and O₂ (Fujishima et al., 2000). Treating HGF cells with as low as 20 µg/mL concentration of TiO₂-NPs has significantly risen the fluorescence intensity of the sample and the fluorescence intensity only enhanced when the NPs concentration was increased. Whether the increase in fluorescence intensity was due to the generation of ROS or only to the interference of TiO₂-NPs with the H₂-DCFDA assay is not known. The viability results indicate that some kind of cytotoxic effect causes the increased cell death in the presence of TiO₂-NPs. The results of the intracellular oxidation assay suggest that viability decreased because of ROS-induced cytotoxicity, but in this case, viability should decrease before treatment with 250 µg/mL TiO₂-NPs. A more plausible explanation could be supported by the results of Wang et al. (2015), who reported that excess TiO₂-NPs on the cell membrane caused blockage of ion pathways, disrupting ion exchange and causing cell death. Zhang et al. (2013) showed that there was a correlation between the increased ROS levels and cytotoxicity after the addition of TiO₂-NPs to cell lines, but the ROS generation might not only be based on the inherent oxidative capacity of TiO₂-NPs, as it might also be related to mitochondrial damage due to the interaction of TiO₂-NPs with the cell membrane. So far, many studies suggest various toxic mechanisms of toxicity induced by TiO₂-NPs, but a precise mechanism remains to be determined. We could not accurately determine the viability of the HGF cell line after treatment with TiO₂-NPs, but based on our previous *in vitro* study on yeast cell model, we have shown that oxidative damage occurs when the ROS level increases, strongly suggesting that a ROS-dependent mechanism of cell death augmented by TiO₂-NPs (Kongseng et al., 2016) could be seen in HGF cell line.

Although WS₂-NPs showed no reduction in cell viability at 400 µg/mL, the possible ROS generation was still plausible, but as shown by Corazzari et al. (2014), oxidative potential of WS₂-NPs is negligible. Treatment of cells with increasing concentrations of WS₂-NP did not result in the generation of ROS. The inability to generate ROS was also demonstrated by Corazzari et al. (2014) when treating A549 and by Appel et al. (2016b) when treating epithelial cells with WS₂-NPs concentrations. Domi et al. (2021) observed only a slight increase in intracellular oxidation, which may not even be due to the NPs themselves.

ZnO-NPs were found to be the most cytotoxic NPs used in our study because they exerted their effects at very low concentrations. The same results were hindered when evaluating the intracellularly generated ROS. The lowest ZnO-NP concentration used (5 µg/mL) did not increase ROS production, nor did the higher concentrations. Interestingly, the production of ROS and cell viability correlated well, with low ZnO-NPs concentrations shown to decrease viability. Studies report that citrate toxicity could be due to the Zn²⁺ ions released by ZnO NPs or the ability of ZnO-NP to induce the formation of ROS. It is important to note that Zn²⁺ itself cannot undergo electron reduction to generate ROS, but it can inhibit antioxidant

molecules and thus induce oxidative stress indirectly (Shen et al., 2013). Like TiO₂-NPs, ZnO-NPs are also considered photocatalysts that generate electron-hole pairs in the presence of light energy and consequently convert O₂ into [•]OH (Yin et al., 2010). Whether the intracellularly generated ROS molecules are the cause of cytotoxicity of ZnO-NPs or just a consequence of mitochondrial damage caused by Zn²⁺ ions is unclear. Ng et al. (2017) concluded that ROS is the cause of cell death induced by ZnO-NP. On the other hand, Choudhury et al. (2017) found that ZnO NPs disperse inside the cell, deforming the cytoskeleton and thus affecting mitochondrial function and membrane protein. This leads to caspase activation and increased ROS production (Ricci et al., 2003).

Due to the strong oxidative activity of Ag-NPs and the silver ions released by the NPs from their surfaces, Ag-NPs are widely used as antimicrobial agents in medicine (He et al., 2012). Most of the Ag- NP cellular and biochemical changes in the cell are considered to be caused by ROS. In our study, Ag-NPs with size of 28-48 nm did not increase the formation of ROS and Ag-NPs with size of 48-78 nm decreased the production of ROS. It is generally believed that the formation of ROS is the main mechanism for the toxicity of Ag-NPs, as a correlation between the formation of ROS and cytotoxicity has been established in many studies (Xue et al., 2016). What exactly caused Ag-NPs cytotoxic effect in our study, if not increased formation of ROS, should be investigated in further studies to make a definitive statement.

Investigating the effect of NPs on immortalized cell lines gave us insight into the field of nanotoxicology. Although some concentrations of NPs are unlikely to occur *in vivo*, they provided a dose-response analysis for further toxicological studies. So far, we do not know the amount, size, and shape of NPs used in the field of orthodontics, how they are applied (coatings, adhesives, materials) and how they are released into oral cavity. Despite their increasing popularity, certain questions regarding the toxicity and biocompatibility of NPs have yet to be investigated. Toxicity and biocompatibility are two absolute necessities that must be determined when evaluating safety of orthodontic appliances used in healthcare settings. With the advent of nanotechnology and its applications, concerns have been raised about toxic effects on humans (Allaker, 2010). It is not possible to compare toxic levels of bulk materials with those of nanomaterials because the area-to-volume ratio is greater for nanoparticles, making it more likely that potentially toxic substances will elute or particles will be released. Because metal nanoparticles differ in their toxic-kinetic properties from metals without nanoparticles, additional ADME (absorption, distribution, metabolism, and excretion) information must be obtained (Hagens et al., 2007). Of particular concern is their safety status after a prolonged period of exposure and possible dissolution of NPs in living organisms, whether through the chemical aspects of saliva, erosion, chewing, bacterial accumulation, or some other form of destruction of the NPs. Such released metals NP or metal ions can freely enter the bloodstream and cause toxic damage at the systemic level (Behzadi et al., 2017). Therefore, short-term *in vitro* studies are not sufficient to fully assess the human health risk.

The toxicity of NP is not yet fully understood, but depends mainly on NP parameters such as shape, size, surface area, composition and stability. The use of NPs in orthodontics involves direct contact with the teeth and surrounding cells and tissues in the oral cavity. Therefore, the handling of the potentially harmful effects of NPs must be carefully managed.

4.6 STUDY LIMITATIONS AND FUTURE PERSPECTIVES

When assessing oxidative stress status, two or more assays should be used to increase validity because each method has its own limitations and no method alone can accurately measure antioxidant status and ROS formation (Poljsak and Jamnik, 2010). In the present study, the FORT and FORD methods were used to determine the ROS/AD ratio. Although changes in the ROS/AD ratio were observed over time, their main cause could not be determined because the observed change in the ROS/AD ratio could be related to many factors (i.e., activation of endogenous antioxidants, inflammation, and metal ions in the blood). We excluded the possibility that periodontal inflammation had an effect on the measured systemic oxidative stress parameters because no signs of inflammation were detected in the patients during the study. However, we could not exclude inflammation as a cause of the increased ROS due to the metal ion release and metal content in the blood. The detection of inflammatory mediators and metal concentrations in blood samples could provide very important information for our study, but for ethical reasons it was not possible to collect consecutive larger venous blood samples throughout the study period. In addition, previous studies (Mikulewicz and Chojnacka, 2010) reported that heavy metal ions (e.g., nickel) are detectable in blood only after long-term exposure. Finding out the exact reason for short-term increase in systemic oxidative stress parameters (ROS/AD levels) in capillary blood was beyond the scope of the present study but real reason of increased ROS/AD ratio would be interesting to determine in further studies as well as the potential of endogenous antioxidative defenses induction in patients

In vitro experiments are not able to fully simulate the *in vivo* environment, such as saliva biological composition, salivary flow rate, temperature fluctuations, pH differences, and microbiological flora (Wendl et al., 2017). For example, corrosion is considered to be the main reason for the release of metal ions, and the extent of corrosion depends on the formation of passive oxide layers on the surfaces of orthodontic materials. These oxide layers effectively prevent corrosion (Eliades et al., 2004), but are strongly influenced by changes in the oral environment, such as pH and temperature level. In our study, a constant pH, temperature and non-shaking conditions were maintained to avoid a potential increase in ion release, but in the *in vivo* environment, the oxide layers could be degraded more rapidly due to the instability of the environment (Kuhta et al., 2009).

Instead of using primary cells isolated from excised tissue *in vivo* and proliferating in culture until natural senescence occurs, we used immortalized cell lines. They are produced either by artificial transformation of primary cell cultures with viral vectors to transfer genetic material or by natural transformation and derivation of cancer tissue cells (Nanci, 2016). While primary cells better represent the *in vivo* environment than immortalised cells, obtaining ethical approval and processing samples for cell isolation is a time-consuming process. In addition, when using primary cells, the amount of samples is very limited and there are large differences between samples because the primary cells come from different individuals (sex, age, disease status, the depth of the removed layer) (Nanci, 2016). On the other hand, immortalized cell lines are ready to use and can be easily cultured indefinitely. However, this comes at a price, as immortalised cell lines may have altered metabolism and phenotype compared to primary cells. Therefore, they may not provide representative *in vivo* results, thus results should be interpreted with some caution or not directly extrapolated to humans.

It should be noted that the metal mixtures may not fully reflect the release of metal ions by orthodontic appliances (Kovač et al., 2022). The release of metals *in vivo* is very difficult to simulate because many factors influence the release process. We have used specific ratios of metal ions to simulate orthodontic alloys, while these concentration ratios of metal ions may be different *in vivo*. The use of metal mixtures instead of the released metal ions from our *in vitro* release study could be considered a limitation. The reason we chose to use metal mixtures was that a large sample volume was needed for a large-scale study and higher metal concentrations were desirable for predicting toxicological effects and risk assessment of metal ions. We could have evaporated the samples from the *in vitro* release study to obtain higher metal concentrations, but even then they would not have reached the desired concentrations and we would still have less sample volume to test toxic effects in the study.

The choice of the HGF cell line may not initially seem reasonable from an *in vivo* perspective, since fibroblasts among epithelial cells, like keratinocytes, promote connective tissue that is most likely to be the first to come into contact with the released metal ions. However, orthodontic appliances are in the oral cavity for a long period of time, and the continuous release of metal ions eventually reaches the inner layer of the oral mucosa (Milheiro et al., 2016). In orthodontic patients, metal accumulation in the oral mucosa has been observed even 12 months after orthodontic treatment (Orozco-Páez et al., 2021). Although the metal ions released from orthodontic appliances are lower than the concentrations of metal mixtures and Schmalz et al., (1998) indicated that the metal ions released from dental alloys are less cytotoxic compared to the same salt solutions, the potential long-term local toxic effect should not be forgotten.

5 CONCLUSIONS

1. A short-term increase in systemic oxidative stress parameters (ROS/AD levels) in capillary blood was observed at 24 hours after orthodontic treatment with fixed appliances.
2. All orthodontic alloys released metal ions during a 90-day exposure to artificial saliva, but the final concentrations did not exceed the recommended upper limits for daily metal intake.
3. The β -Ti alloy released the fewest metal ions of all orthodontic alloys tested.
4. All metal mixtures simulating the orthodontic alloys SS, Co-Cr, Ni-Ti, and β -Ti decreased *Saccharomyces cerevisiae* culturability, but only at high concentrations. The SS and Co-Cr metal mixture induced the formation of ROS and caused oxidative protein and lipid damage at high concentrations, whereas Ni-Ti and β -Ti mixtures did not.
5. The treatment of *Saccharomyces cerevisiae* with metal mixtures induced a complex response observed as changes in endogenic enzymatic antioxidative defense systems
6. Concentrations of the released metal ions from orthodontic appliances cannot induce oxidative stress and its related damages in the yeast *Sacharomyces cerevisiae*.
7. All metal mixtures induced HGF cell death at high concentrations, but only SS and Co-Cr metal mixtures were able to generate increased intracellular ROS formation.
8. Characterization of NPs shows aggregation and agglomeration of NPs in aquatic media, meaning that the NPs size increased to micro meter level.
9. Three selected types of TiO_2 -NPs caused ROS-induced cytotoxicity at high concentrations. WS_2 -NP did not cause cytotoxicity nor the formation of ROS. The two selected ZnO-NP were found to be cytotoxic already at low concentrations, but their toxic effects could not be associated with the increased formation of ROS. The two selected Ag-NPs gave different cytotoxic results, with the 28-48 nm Ag-NPs being much less cytotoxic compared to the 48-78 nm Ag-NPs. No increase in ROS generation was detected after threatening HGF cells with Ag-NPs.
10. Of the selected nanoparticles, WS_2 nanoparticle was the least toxic to human gingival cells and as such has potential to be considered in nano-medical applications.

6 SUMMARY (POVZETEK)

6.1 SUMMARY

Misaligned teeth, also known as malocclusion, have a significant impact on oral and dental health. The most effective method of correcting the problem is orthodontic treatment with fixed orthodontic appliances. However, over time and with the ever-changing conditions in the oral environment, orthodontic appliances are also affected. Electrochemical reactions, mechanical forces and general wear of the material in the oral cavity lead to corrosion, a process of wear of the orthodontic metals.

During orthodontic treatment with fixed appliances, subjects are exposed to metals released from the corroded appliances that can in theory increase levels of ROS through metal-catalyzed free radical reactions. If the constantly increasing ROS molecules are not maintained at physiological levels, excessive amounts of ROS generated can lead to oxidative stress that disrupts cellular redox homeostasis and consequently damages lipids, proteins, and DNA. To counteract these harmful effects and intercept overproduced ROS, each cell has a defense system that includes enzymatic and non-enzymatic antioxidant defenses.

Nanotechnology represents a great opportunity for improving dental properties such as strength and durability. The nanoparticles are applied to the orthodontic appliances as a coating, but they can degrade or corrode in the oral cavity during the course of treatment. The lack of knowledge about the safety of nanoparticles after prolonged exposure and the possible dissolution of nanoparticles in living organisms are of concern and should be properly investigated.

The objective of this work was to investigate the level of selected systemic oxidative stress parameters during orthodontic treatment, the composition of selected orthodontic alloys, the release of metal ions, and the oxidative consequences that the metal ions may have on the model organism *Sacharomyces cerevisiae*. The work also aimed to investigate the effects of nanoparticles on the human gingival cell line. Fifty-four male patients with malocclusions who underwent orthodontic treatment had their capillary blood levels ROS and ROS /AD examined. Different parts of orthodontic appliances were analyzed for their metal composition and incubated in artificial saliva for 90 days to quantify metal release. Metal mixtures were prepared according to metal composition and used to treat yeast cells to determine the occurrence of oxidative stress, antioxidant enzyme defense system, and oxidative damage. Selected nanoparticles were prepared at different concentrations and used to treat human gingival fibroblasts to study cell viability and their ability to form ROS.

Our study shows that the induction of systemic oxidative stress in the capillary blood of orthodontic patients occurs only after 24 hours, after which the oxidative stress parameters in capillary blood normalize to the initial level. Whether the increase in systemic oxidative stress levels is due to metal release from orthodontic appliances was not defined. We have shown, that the release of metal ions from orthodontic appliances into artificial saliva is constant, but the metal concentrations released are still below the maximum tolerated daily dose. Of the selected orthodontic alloys, the lowest concentration of metal ions was released from the β -Ti alloy. Based on the metal composition of orthodontic alloys, metal ion mixtures were prepared and used to treat yeast *Sacharomyces cerevisiae*. Only high metal ion concentrations were able to generate large amounts of reactive oxygen species, which the antioxidant system was unable to regulate adequately, resulting in oxidative stress and its damage to biological molecules. Only SS and Co-Cr metal mixtures caused the formation of reactive oxygen species and caused oxidative damage to lipids and proteins. The comparison between the yeast cell model and the human gingival fibroblast cell line proved the suitability of the yeast *Sacharomyces cerevisiae* as a model organism for oxidative stress research. NP characterization showed that NPs aggregate and agglomerate in culture medium and water, increasing their size from the nanometer scale to the micrometer scale. The toxicity of selected nanoparticles and their ability to generate reactive oxygen species in human gingival fibroblasts mainly depends on the type, concentration, and properties of the nanoparticles. All three selected types of TiO₂-NPs were cytotoxic at high concentrations, due ROS formation. Both selected ZnO-NPs were found to be cytotoxic even at low concentrations, but their toxic effects could not be linked to increased ROS formation. The two selected Ag-NPs gave different cytotoxic results, with Ag-NPs 28-48 nm being much less cytotoxic compared to Ag-NPs 48-78 nm. After treating HGF cells with Ag-NPs, no increased generation of ROS was detected. Among the selected nanoparticles, the WS₂ nanoparticle was the least toxic to human gingival cells, as it did not cause cytotoxicity or ROS formation, and is therefore the most suitable for potential medical use.

6.2 POVZETEK

Nepravilno poravnani zobje, znani tudi kot malokluzija, imajo pomemben vpliv na zdravje ustne votline in zob. Tudi iz psihološkega vidika malokluzije vplivajo na človekovo počutje in samozavest (Nguee in sod., 2020). Najučinkovitejša metoda za odpravo težave je ortodontsko zdravljenje z nesnemnimi ortodontskimi aparati, ki se uporabljajo za različne premike zob po alveolarni kosti. Učinkovitost ortodontskega zdravljenja je odvisna od dovzetnosti obzobnih tkiv za zdravljenje in značilnosti delov nesnemnega ortodontskega aparata, ki ga sestavljajo nosilci, loka, obročki in ligature (Proffit et al., 2007). Deli ortodontskega aparata so lahko iz različnih materialov, vendar se zaradi dobrih mehanskih lastnosti, trdnosti ter toplotne in električne prevodnosti najbolj uporabljajo zlitine kovin (Park in Lakes, 2007). Ortodontsko zdravljenje z biokompatibilnimi aparati je ključnega pomena za učinkovitost zdravljenja in varnost pacienta. Za biokompatibilne se štejejo

materiali, ki ne povzročajo negativnih učinkov na zdraje, kar pomeni, da niso strupeni, rakotvorni in ne morejo povzročiti alergijskih reakcij (Widu in sod., 1999). Druga pomembna lastnost biokompatibilnih materialov je, da se njihove fiziološke in mehanske lastnosti ne spremenijo v pogojih *in vivo*. Biomateriali so v tesnem stiku s telesnimi tekočinami, ki lahko vplivajo na površino materiala. V prisotnosti sline ali drugih tekočin se ortodontske zlitine sčasoma nagibajo k koroziji, kar povzroči sproščanje kovine s površine zlitine in osnovno oslabitev lastnosti zlitin (Mathew in Wimmer, 2011). V procesu, imenovanem korozija, kjer pride do fizikalno-kemijske (elektrokemične) interakcije med kovino in njenim okoljem, se lahko pojavijo spremembe v lastnostih kovine. Glavna pomanjkljivost kovinskih zlitin je prav v nagnjenosti k koroziji v prisotnosti bioloških tekočin.

Nanotehnologija predstavlja dobro priložnost za nadaljnje izboljšave lastnosti medicinskih in dentalnih materialov kot sta trdnost in vzdržljivost. Nanodelci imajo ugodne lastnosti, kot so visoko razmerje med površino in prostornino za boljšo interakcijo z okoljem, zeta potencial, velikost in oblika delcev, površinska kemija, aglomeracija, raztapljanje in sproščanje ionov (Fernando in sod. 2018). Zaradi svojih katalitičnih, optičnih in elektromagnetnih lastnosti se kovinski nanodelci (NP) pogosto uporabljajo v bioloških in medicinskih aplikacijah (Mamunya in sod. 2004), vključno v ortodontiji. NP, zlasti kovinski NP s svojimi fizikalno-kemijskimi, mehanskimi in antibakterijskimi lastnostmi, bi lahko močno vplivali na trajanje ortodontskega zdravljenja in izboljšali ustno zdravje (Sharan in sod., 2017). Eden od načinov nanašanja NP na ortodontske pripomočke je v obliki prevlek, s katerimi bi lahko izboljšali površinske in mehanske lastnosti kovinskih zlitin.

Izraz oksidativni stres je prvi uvedel Helmut Sies kot neravnovesje med prooksidanti in antioksidanti v korist prvih (Sies, 2020). Tako imenovano redukcijsko-oksidacijsko (redoks) ravnovesje se lahko poruši bodisi zaradi prekomernega nastanka prooksidantov, bodisi zaradi pomanjkanja antioksidantov ali celo zaradi obojega hkrati. Manjša nihanja redoks ravnovesja ne povzročajo večjih težav, saj se organizem lahko nanje prilagaja, velika nihanja, zlasti povečano nastajanje reaktivnih kisikovih zvrsti pa vodijo do nepopravljivih bioloških poškodb celičnih komponent in celo celične smrti (Burton in Jauniaux, 2011). V fizioloških pogojih velja, daje redoks ravnovesje le malenkost premaknjeno v korist prooksidantov, saj so ti nujni za normalno delovanje organizma. Ko pa se ravnotežje vedno bolj nagiba v korist prooksidantov, lahko opazimo poškodbe organelov in razgradne procese (Auten in Davis, 2009).

Med reaktivne kisikove zvrsti (ang. ROS) spadajo prosti radikali, ki imajo nepopolno zunanjo elektronsko plast in imajo enega ali več neparnih elektronov, kar jih naredi zelo reaktivne. ROS se lahko kovalentno povežejo z drugo molekulo preko neparne elektrona ali pa lahko nastanejo z dajanjem neparne elektrona (redukcijski radikal) ali s sprejemanjem elektronov (oksidacijski radikal) (Halliwell, 1991). Izraz ROS vključuje tudi

nekatero neradikalne molekule, kot sta vodikov peroksid in ozon, ki pa se smatrata kot ROS, saj se zlahka pretvorita v radikale (Irani, 2007). ROS se nenehno proizvajajo v normalnih fizioloških pogojih, njihova homeostaza pa se nenehno spremlja in vzdržuje. Teorija prostih radikalov in oksidativnega stresa je bila ustanovljena pred več kot pol stoletja in sprva so ROS veljali za škodljive stranske produkte aerobne presnove, sedaj pa velja, da imajo ROS bistveno vlogo v različnih bioloških procesih (Finkel, 2011), kot je fagocitoza in prenos celičnih signalov. Primarni ROS nastanejo tekom štiristopenjskega procesa redukcije O_2 v H_2O (Halliwell in Gutteridge, 2015). Molekula kisika, ki ima dva neparne elektrona, je neškodljiva, razen če se energijsko aktivira. Aktivacija se lahko pojavi, ko je zagotovljena dovoljšna mera energije, da se obrne vrtenje neparne elektrona, pri čemer nastane singletni kisik (1O_2). Ko pa se molekuli kisika dodajajo elektroni, pa nastajajo superoksidni radikal ($O_2^{\cdot-}$), vodikov peroksid (H_2O_2) in hidroksilni radikal ($\cdot OH$) (Apel in Hirt, 2004).

Kovinski ioni imajo pomembno vlogo pri različnih celičnih funkcijah, kot so prenos elektronov po dihalni verigi, sinteza in popravilo DNA ter celični metabolizem. Kovine z delno napolnjeno d podlupino in zmožnostjo tvorbe kationov imenujemo prehodni elementi ali prehodne kovine (McNaught and Wilkinson, 1997). Prehodne kovine najdemo v skupini 4-11 periodnega sistema in imajo veliko število kompleksnih ionov v številnih pozitivno nabitih oksidacijskih stanjih z različnimi katalitskimi lastnostmi. Nekatere prehodne kovine so bistveni elementi in ključne komponente za številne metaloproteine, vključene v proces tvorbe kisika in odkrivanja hipoksije. Kovinski ioni se pojavljajo v različnih oksidacijskih stanjih in kot taki lahko preidejo v redoks reakcijo, se povežejo s fosfolipidi, spremenijo stabilnost membrane in spodbujajo peroksidacijo lipidov. Ker je nastajanje ROS tesno povezano z vključevanjem redoks aktivnih kovin, se njihove koncentracije vzdržujejo strogo pri fizioloških koncentracijah (Valko in sod., 2005). Eden od mehanizmov nastajanja ROS, v katerega se vključujejo prehodne kovine je Fentonova reakcija, ki je bila prvič predstavljena leta 1894 (Fenton, 1894) in kasneje popravljena in dopolnjena do danes znane reakcije (Haber in sod., 1934). V Fentonovi reakciji železo (Fe^{2+}) katalizira reakcijo pretvorbe H_2O_2 v $\cdot OH$. Namesto železa lahko v reakciji sodelujejo tudi druge prehodne kovine z visoko valenco, kot so baker (Cu), cink (Zn) in aluminij (Al). Kadar reakcija vključuje kovine, ki niso Fe ali Cu, ligande ali perokside, se reakcija imenuje Fentonu-podobna reakcija (Meyerstein, 2021). Dodatek k prvotni Fentonovi reakciji je Haber-Weissova reakcija, ki domneva da $O_2^{\cdot-}$ ponovno reagira s H_2O_2 in tvori $\cdot OH$ ter hidroksilni anion (OH^-) (Das in sod., 2015).

Zaradi svojih edinstvenih lastnosti, kot so katalitične, optične in elektromagnetne lastnosti, se NP in nanomateriali široko uvajajo za biološko in medicinsko uporabo (Mamunya in sod., 2004). NP, zlasti kovinski NP s svojimi fizikalno-kemijskimi, mehanskimi in antibakterijskimi lastnostmi, bi lahko močno vplivali na trajanje ortodontskega zdravljenja, odpravili nekatere z zdravljenjem povezane težave in izboljšali ustno zdravje (Sharan in sod., 2017). Ne glede na to, kako koristne so edinstvene lastnosti, NP veljajo tudi za potencialno

strupene snovi. Visoko razmerje med površino in prostornino jih naredi zelo reaktivne (Drasler in sod, 2017), njihova majhna velikost pa omogoča enostavno prodiranje skozi celično membrano (Yin in sod., 2012). Prisotnost NP in njihovih kovinskih ionov lahko povzročita nastanek ROS, ki je glavni vzrok njihove citotoksičnosti (Yu in sod., 2013). Da NP lahko ustvarjajo ROS na tri načine: prvi mehanizem je interakcija med NP in celico, drugi je raztapljanje in sproščanje kovinskih ionov s površine NP, tretji pa tvorba prooksidantnih funkcionalnih skupin na površini NP (Yanli Wang in sod., 2017). Mehanizem generiranja ROS, ki je specifičen za posamezen NP, še ni popolnoma razumljen.

ROS imajo lahko blagodejen ali škodljiv učinek na biološki sistem. Kadar ROS nastajajo v presežku se smatra, da ROS oslabi biološke molekule in celične strukture. Takrat govorimo o pojavu oksidativnega stresa. Celica oziroma organizem ima sposobnost zmanjšanja ROS in njegovih poškodb, vendar se te oksidativne poškodbe kopičijo in sčasoma dodatno poškodujejo DNA, beljakovine ali lipide (Valko in sod., 2006). Celične komponente, ki vsebujejo polinenasičene maščobne kisline (PUFA), kot je celična membrana in membrane organelov, so zelo občutljive na oksidacijo. Hrbtenica PUFA ima dve ali več dvojnih vezi, s katerimi lahko ROS reagira. Več dvojnih vezi kot ima PUFA, večja je verjetnost, da bo prišlo do oksidacije v prisotnosti ROS (Su in sod., 2019). Poleg lipidne peroksidacije lahko ROS poruši tudi lipidni dvosloj in inaktivira nekatere membransko vezane beljakovine ter na splošno poveča prepustnost membrane (Birben in sod., 2012). Poškodbe DNA, ki jih povzročajo prosti radikali, so vir mutageneze, karcinogeneze in staranja celic. Genetski material bioloških sistemov je nenehno ogrožen zaradi poškodb ROS. $\cdot\text{OH}$ velja za najbolj reaktiven radikal v bioloških sistemih, ker reagira s purinom, pirimidinom ali deoksiriboza v hrbtenici DNA (Dizdaroglu in sod., 2002). Druga ROS, kot sta H_2O_2 in $\text{O}_2^{\cdot-}$, nista neposredno vključena v nastanek oksidativnih poškodb DNA, ampak le posredno. Poškodbe, ki jih povzroča ROS, so eno- ali dvoverižni prelomi DNA in navzkrižne povezave DNA (Cooke in sod., 2003). Oksidacija beljakovin je kovalentno spremenjen proces, pri katerem ROS ali sekundarni stranski produkti oksidativnega stresa reagirajo z beljakovinsko molekulo (Shacter, 2000). Posledice oksidacije beljakovin se kažejo z izgubo aktivnosti beljakovin (receptorja, encima, transporta ali strukture) in nagnjenostjo k proteolizi ali denaturaciji beljakovine. Osnovne sestavine beljakovin, aminokislina, so primarna tarča ROS, zlasti cistein, metionin in aromatske aminokislina (tirozin, fenilalanin in triptofan) (Kehm in sod., 2021).

Ker so aerobni organizmi nenehno izpostavljeni ROS, se je med evolucijo razvil učinkovit obrambni sistem, sestavljen iz obrambnih, nevtralizacijskih in popravljalnih mehanizmov. Prekomerno nastajanje ROS in z njimi povezane škodljive učinke blažijo antioksidanti, bodisi encimski antioksidanti ali neencimski antioksidanti. Obstajajo štiri glavni obrambni encimi, ki so odgovorni za vzdrževanje ROS na za celico neškodljivih ravneh: superoksid dismutaza (SOD), katalaza (CAT), glutation peroksidaza (GPx) in sistem tioredoksin reduktaze (TrxR). SOD katalizira pretvorbo $\text{O}_2^{\cdot-}$ v O_2 in H_2O_2 . CAT je odgovorna za

znotrajcelično pretvorbo H_2O_2 v H_2O in O_2 . Drug encim, ki je odgovoren za razgradnjo H_2O_2 je GPx (Arthur, 2000). Čeprav ni neposredno vključena v obrambo ROS, ima glutation reduktaza (GR) pomembno vlogo pri presnovi GSH in je kot taka tesno povezana z redoks sistemom glutationa. Peroksiredoksin (Prx) je član družine tiol peroksidaze in je tesno povezan s sistemom Trx, ki zagotavlja elektrone, potrebne za njegovo delovanje (Du in sod., 2012). Med neencimske antioksidante spadajo snovi z nizko molekulsko maso, polipeptidi in beljakovine, ki jih organizem proizvaja ali zaužije z vsakodnevno prehrano. Vključujejo vitamin A in vitamin C, β -karoten, sečno kislino, melatonin in GSH.

Modelni organizmi so nenadomestljivo orodje v osnovnih bioloških in kliničnih raziskavah (Hunter, 2008), kadar se preučuje škodljive učinke iz okolja na biološke sisteme. Modelni organizmi so pogosto izbrani, ker premagujejo etične in eksperimentalne omejitve, zagotavljajo model za razvoj, optimizacijo in standardizacijo določenih analiz in so jasen predstavnik večje skupnosti vrst z enakimi ali podobnimi biološkimi procesi (Karathia in sod., 2011). *Saccharomyces cerevisiae* (*S. cerevisiae*) je med evkariontskimi organizmi najbolj znan, preučen in karakteriziran model, saj so osnovni celični procesi in celična organizacija podobni celicam sesalcem (Karathia in sod., 2011). Celotno zaporedje genoma kvasovk razkriva dobro ohranjeno zaporedje aminokislin in funkcijo beljakovin med evkariontskimi vrstami (Botstein in Fink, 2011). Zaradi visoke homologije s človeškim genomom, primerljive homologije funkcij beljakovin, širokega nabora poceni genetskih manipulacij, enostavne in poceni pridelave in rasti, preučevanja več procesov hkrati in skoraj popolne baze podatkov, je *S. cerevisiae* eden izmed idealnih modelnih mikroorganizmov za preučevanje oksidativnega stresa in odziva nanj (de la Torre-Ruiz in sod., 2015). Kar je pa za našo študijo najbolj pomembno pa je to, da je tvorba ROS na ETC ter mehanizem odziva oziroma obrambe na povečan nivo ROS pri kvasovkah podoben kot pri sesalcih (Herrero in sod., 2008).

Skladno z načelom 3Rs (zamenjava, zmanjšanje in izboljšanje) alternative poskusom na živalih in vivo uporabljamo primarne celice ali celične linije (Krewski in sod., 2010). Celične linije imajo na splošno prednost pred primarnimi celicami, ker so bolj stabilne, homogene in splošno dostopne, kar ima za posledico boljšo replikacijo in primerjavo znanstvenih podatkov. Vendar imajo prednosti uporabe celičnih linij svojo ceno, saj se ne diferencirajo in tako v celoti ne predstavljajo in vivo razmer (Gstraunthaler in Hartung, 2002). Človeški gingivalni fibroblasti (HGF) so najpogostejši predstavniki ustne sluznice in se zato pogosto uporabljajo v poskusih za oceno toksičnosti (Mah in sod., 2014) pri oralni izpostavljenosti škodljivemu agensu. Ker so v neposredni bližini ortodontskih zlitin, so klinično pomemben model za ugotavljanje vpliva izluževanja kovinskih ionov. Ker se z vsako delitvijo celice se telomeri skrajšajo in s tem tudi življenjska doba celice, smo v študiji smo uporabili imortalizirano celično linijo HFG, ki z izražanjem reverzne transkriptaze človeške telomeraze (hTERT) preprečuje skrajšanje telomere. Tako lahko dobimo dolgoživo celično linijo, kateri se fiziologija in fenotip ne spreminjata (Reijnders in sod., 2015).

Namen disertacije je bil raziskati, ali bi sproščanje kovinskih ionov iz nesnemnih ortodontskih aparatov lahko vodilo do povečanja nivoja ROS in posledično oksidativnih poškodb na modelnem organizmu. Najprej smo opazovali, ali se parametri oksidativnega stresa spreminjajo med ortodontskim zdravljenjem, nato pa smo načrtovali poskus sproščanja kovin *in vitro*, da bi v celoti razumeli, kateri in koliko kovinskih ionov se sprostijo iz ortodontskih zlitin in kako njihova izpostavljenost vpliva na celice. V raziskavi je sodelovalo 54 zdravih moških bolnikov, starih od 19 do 28 let, pri katerih je bila diagnosticirana malokluzija. Zdrave moške bolnike smo naključno razdelili v dve skupini, tarčno skupino (TG), ki je bila podvržena ortodontskemu zdravljenju, in kontrolno skupino (CG), v kateri ortodontski aparat ni bil nameščen v ustni votlini. Ortodontski aparat, ki se uporablja za zdravljenje malokluzije TG, je bil sestavljen iz SS nosilcev. Kapilarna kri je bila odvzeta iz TG in CG v štirih različnih časovnih intervalih: pred vstavitvijo ortodontskega aparata (čas 0), 6 ur po vstavitvi, 24 ur po vstavitvi in po 7 dneh. Z merjenjem tvorbe ROS (FORT test) in antioksidantnega potenciala (FORD test) v vzorcih kapilarne krvi je mogoče stanje oksidativnega stresa v krvi bolnikov natančneje oceniti na sistemski ravni. V tej študiji smo želeli oceniti, ali med ortodontskim zdravljenjem pride do povečanja nivoja ROS v vzorcih kapilarne krvi. Statistično značilna razlika v vrednostih FORT in FORD je bila opažena v TG po 24 urah ortodontskega zdravljenja, vendar se je pri naslednji analizi (po 7 dneh) vrednost znižala nazaj na izhodiščno raven.

Na podlagi ugotovitev, da bi lahko bili kovinski aparati vzrok za povečanje nivoja ROS (Kovac in sod., 2019), se je postavilo vprašanje o varnosti tovrstnih ortodontskih aparatov po trajni uporabi (Hanawa, 2004). Da bi bolje razumeli kovine, ki sestavljajo ortodontske zlitine, in koncentracije kovinskih ionov, ki se sproščajo v laboratorijskih razmerah, smo zasnovali študijo, v kateri so bili ortodontski materiali potopljeni v umetno slino za 90 dni. Njihova kovinska sestava je bila ovrednotena z ICP-MS. V primeru zlitine SS (loki, nosilci in obročki) so se sproščali predvsem Fe ioni, koncentracije ostalih preučevanih kovin pa so ostale skoraj na začetni koncentracijski ravni vse do 90 dni, ko je bilo opaziti rahlo povečanje. Ko smo pogledali koncentracijo sproščanja kovine za oba Ni-Ti loka, je bila količina sproščenega Ti pri obeh podobna, vendar količina sproščenega Ni pa ni bila primerljiva, saj je Ni-Ti_(Forestadent) sprostil dvakrat več Ni ionov kot Ni-Ti_(Dentaurum). Za β -Ti lok koncentracije Mo niso bile zaznavne vse do 90. dneva študije, ko je bila koncentracija 0.45 ng/mL. Koncentracije Ti iz β -Ti loka so nihale za 1.5 ng/mL skozi celoten potek študije vse do 90. dneva, ko je bila zaznana najvišja vrednost približno 8.3 ng/mL. Med študijo se je sproščanje kovin iz obeh Co-Cr žic postopoma povečevalo. Koncentracije Co in Cr so dosegle podobne ravni v obeh žicah, vendar so bile opažene nekatere razlike v Fe, Ni in Mo. S pridobljenimi rezultati smo podali podatke o minimalnih koncentracijah kovinskih ionov, ki se lahko sprostijo iz ortodontskih zlitin izključno s čistim difuzijskim postopkom brez dodatnih mehanskih sil. Dejstvo, da ortodontske zlitine sproščajo kovinske ione s svojih površin je nesporno, a čeprav je bil opažen stalen vzorec sproščanja, je količina sproščenih

kovinskih ionov še vedno daleč pod dnevno priporočenimi zaužitimi vrednostmi. Če primerjamo naše rezultate s predpisanimi priporočenimi dnevnimi ravni za zaužitje, noben od preučenih sproščenih kovinskih ionov ni presegel zgornje predpisane meje dnevne koncentracije vnosa, tudi če upoštevamo kumulativne koncentracije. Na podlagi dobljenih rezultatov smo lahko ocenili vrsto in koncentracijo sproščenih kovinskih ionov. Glede na kovinsko sestavo ortodontskih zlitin smo pripravili mešanice kovinskih ionov za nadaljnje študije oksidativnega stresa.

Prikazali smo, da ortodontski materiali sicer sproščajo kovinske ione s svojih površin. S pridobljenimi rezultati smo na modelnem organizmu *S. cerevisiae* preučili toksičnost in nastanek oksidativnega stresa po izpostavljenosti celic različnim kombinacijam kovinskih ionov v različnih koncentracijah. Z uporabo dveh mutant *S. cerevisiae* brez antioksidantnega encima SOD (Δ Sod1) ali CAT (Δ Ctt1) smo lahko prepoznali, kako delna izguba endogene antioksidativne obrambe vpliva na sposobnost preživetja celic. V disertacijski študiji smo celice kvasovk za 24 ur izpostavili različnim mešanicam kovinskih ionov v koncentracijah 1 μ M, 10 μ M, 100 μ M in 1000 μ M. Z mešanici kovin smo posnemali kovinsko sestavo ortodontskih zlitin SS, Co-Cr, Ni-Ti in β -Ti. Pri tretiranju celic kvasovk z naraščajočimi koncentracijami kovinskih mešanic smo opazili zmanjšanje kulturabilnosti, saj pri vseh tretmajih s 1000 μ M koncentracijami lahko opazimo statistično značilno zmanjšanje. Ko smo primerjali kulturabilnost Wt in dveh mutant, so opazili pomembno razliko v kulturabilnosti, saj je bila vrednost CFU/mL neobdelanih kontrolnih vzorcev mutant kvasnih celic veliko nižja kot pri netretiranem kontrolnem vzorcu Wt. V predstavljeni študiji je bil uporabljen tudi test celične metabolne aktivnosti, ampak zaradi majhnega števila opravljenih testov rezultati niso pokazali jasnih razlik med različno tretiranimi celicami kvasovk. Ko smo celice kvasovk Wt tretirali z različnimi koncentracijami mešanic kovinskih ionov, je bilo ugotovljeno, da višje koncentracije povečajo povprečno vrednost metabolne aktivnosti. Po drugi strani pa se mutante kvasnih celic nagibajo k zmanjšanju svoje presnovne aktivnosti z naraščajočo koncentracijo kovinskih ionov, zlasti pri 1000 μ M koncentracijah. Primerjali smo tudi metabolno aktivnost med netretiranimi celicami kvasovk Wt in mutanti in ugotovili, da je bila izhodiščna metabolna aktivnost mutant vsaj dvakrat višja kot pri netretirani kontrolni skupini kvasovk Wt.

Kot je razvidno iz ocene kulturabilnosti celic, so bile kovinske mešanice stresorji za celice kvasovk. Ker so bile vse v študiji uporabljene prehodne kovine, ki so sposobne ustvarjati ROS preko Fentonove in Haber-Weissove reakcije (Zhao, 2019), smo domnevali, da je razlog za zmanjšanje kulturabilnosti celic posledica povečanega znotrajceličnega nivoja ROS. Da bi ugotovili, ali so kovinske mešanice povzročile povečanje znotrajceličnega nivoja ROS v kvasovkah, smo izvedli test znotrajcelične oksidacije za določitev nastalih ROS. Metoda znotrajcelične oksidacije z barvilom H₂DCFDA je pokazala znatno povečanje znotrajcelične tvorbe ROS v kulturabilnih celicah po 24 urah tretiranja s SS in Co-Cr, medtem ko ni bilo zaznanih sprememb v intenzivnosti fluorescence, ko je bila katera koli

vrsta celic kvasovk tretirana s kovinsko mešanico Ni-Ti ali β -Ti. Da bi ugotovili, ali ROS, ki ga ustvari kovinska mešanica, povzroči oksidativne poškodbe molekul in ne le povečano tvorbo ROS, smo uporabili test TBARS za preučitev nastanka lipidnih poškodb in opravili analizo za odkrivanje oksidativnih poškodb beljakovin. Če primerjamo oceno znotrajceličnega nastanka ROS in oceno oksidativnih poškodb lipidov, je med njima razvidna jasna povezava, saj ko je bila tvorba ROS povečana, so bili tudi lipidi oksidativno poškodovani. SS in Co-Cr kovinski mešanici sta povzročili oksidacijo lipidov pri 1000 μ M koncentraciji v Wt in celo pri 100 μ M pri mutantah.

Vsak organizem poseduje antioksidativne obrambne mehanizme za vzdrževanje ravnih redoks ravnotežja. Ker mutante kvasovk Δ Sod1 in Δ Ctt1 nimajo vseh endogenih antioksidativnih encimov za uspešno odstranjevanje presežnikov ROS in njihovih produktov, so znotrajcelično ustvarjene poškodbe ROS opazne pri izpostavljenosti nižjim koncentracijam kovinskih mešanic kot pri Wt. To nas je spodbudilo k raziskovanju encimskega antioksidantnega sistema v *S. cerevisiae*. Zaradi velike variabilnosti encimske aktivnosti v gelu smo sočasno izvedli še spektrofotometrične meritve encimske aktivnosti povezane z antioksidativno obrambo. Aktivnost SOD se je znatno povečala, ko smo celice tretirali s koncentracijo 1000 μ M SS. Druge vrste kovinskih zmesi pri različnih koncentracijah pa niso vplivale na aktivnost SOD. Ko smo ocenili aktivnost CAT, smo opazili znatno zmanjšanje aktivnosti po tretiranju s 1000 μ M SS in 1000 μ M Ni-Ti. H_2O_2 lahko pretvori v H_2O encim CAT, kot tudi z encim GPx (Arthur, 2000). Dodajanje zmesi SS in Co-Cr ni vplivalo na njegovo aktivnost, vendar smo opazili znatno povečanje aktivnosti v prisotnosti 1000 μ M Ni -Ti in β -Ti. Aktivnost GR 1000 μ M SS vzorcev se je zmanjšala, medtem ko se je aktivnost povečala po tretiranju s 1000 μ M Co-Cr in tretiranju z 10 μ M, 100 μ M in 1000 μ M β -Ti. Medtem ko se je aktivnost Prx tudi znatno zmanjšala po izpostavljenosti s 1000 μ M SS, druge kovinske mešanice niso povzročile sprememb v encimski aktivnosti. Aktivnost TrxR se je zmanjšala tudi, ko smo celice obdelali s 1000 μ M SS, medtem ko so imele kovinske mešanice Co-Cr, Ni-Ti in β -Ti vse večji učinek na encimsko aktivnost tudi pri koncentraciji 100 μ M.

Merjenje vsebnosti karbonilov kot oksidativnih poškodb beljakovin, končnem produktu oksidacije beljakovin v bioloških vzorcih, je uporaben biološki označevalec za ocenjevanje oksidativnega stresa, ki ga povzroči kovina, saj je reakcija nepovratna (Lazarova in sod., 2014). V naši študiji je bilo ugotovljeno, da koncentracije kovinskih zmesi, ki povzročajo znotrajcelično tvorbo ROS in oksidacijo lipidov (1000 μ M SS, 100 μ M in 1000 μ M Co-Cr), povzročajo tudi oksidativne poškodbe beljakovin, medtem ko druge kovinske zmesi niso imele učinek na oksidacijo beljakovin.

Ustna sluznica in dlesni so prva tkiva, ki pridejo v stik s sproščenimi kovinskimi ioni iz ortodontskih aparatov. Zunanja epidermalna plast dlesni je keratinizirana in ščiti notranje vezivno tkivo, ki je sestavljeno iz fibroblastov dlesni. Z uporabo človeških gingivalnih

fibroblastov (HGF) lahko pridobimo informacije o tem, kako se celice lahko odzivajo na izbrane kovine v različnih koncentracijah v ustni votlini. Da bi potrdili, da je bila uporaba *S. cerevisiae* kot modelnega organizma upravičena, smo celice HGF obdelali z istimi kovinskimi mešanici v istem časovnem obdobju in z enakimi koncentracijami kot celice kvasovk. Predstavljeni rezultati kažejo, da izpostavljenost celic HGF z mešanici kovin SS in Co-Cr ni vplivala na sposobnost preživetja celic HGF, medtem ko so imele zmesi Ni-Ti in β -Ti pomemben učinek na sposobnost preživetja pri 250 μ M za Ni-Ti in pri 500 μ M za β -Ti. Vzrok za zmanjšanje sposobnosti preživetja celic in celične smrti je bil nejasen, vendar smo domnevali, da je to lahko posledica sposobnosti kovinskih zmesi za ustvarjanje ROS, ker vse komponente kovinskih zmesi spadajo v skupino prehodnih kovin. Tretiranje celic HGF s kovinskimi mešanici SS ali Co-Cr poveča proizvodnjo ROS, medtem ko se po izpostavitvi Ni-Ti ali β -Ti kovinskim mešanici proizvodnja ROS zmanjša.

Zaradi svojih fizikalnih in kemijskih lastnosti postajajo NP vse pomembnejši pri raziskavah in razvoju novih materialov, med katere spadajo tudi ortodontski materiali. Z novimi lastnostmi in industrijsko proizvodnjo NP pa so se pojavili tudi pomisleki glede možnih škodljivih učinkov na zdravje. Zato je najprej potrebno razumeti učinke NP na žive celice, da bi jih prepoznali kot varne za nadaljnjo uporabo v kakršni koli aplikaciji. Ustna votlina je vstopno mesto v dihala in gastrointestinalni trakt in je prvo mesto, na katero vpliva sproščanje nanodelcev iz ortodontskih materialov. Če NP vplivajo na celice ustne votline, je potrebno razmisliti tudi o tem, da lahko NP migrirajo v druga tkiva in tam tudi povzročajo škodljive učinke. Uporaba nanodelcev v ortodontiji ni natančno opredeljena. Zato smo morali ovrednotiti razpon toksičnosti za izbrane kovinske nanodelce in oceniti njihovo sposobnost ustvarjanja ROS. Za testiranje sposobnosti preživetja celic HGF smo uporabili različne koncentracije NP in preučili sposobnost preživetja celic po 24 urah tretiranja HGF z NP TiO₂-NP, WS₂-NP, ZnO-NP in Ag-NP. V primeru tretiranja celic s TiO₂ anataze/rutila se je delež umrlih celic znatno povečal pri koncentraciji 300 μ g/mL, v primeru TiO₂ anataze in TiO₂ rutila pa je bilo povečanje deleža mrtvih celic vidno že pri koncentraciji 200 μ g/mL. Tretiranje celic HGF z naraščajočimi koncentracijami WS₂-NP ni imelo vpliva na sposobnost preživetja celic v vseh testih do 400 μ g/mL, vendar je kljub temu bilo opazno povečanje deleža mrtvih celic, ki je bilo statistično značilno pri koncentraciji 500 μ g/mL. Podatki o preživetju celic po tretiranju z obema tipoma ZnO-NP kažejo močno zmanjšanje sposobnosti preživetja po tretiranju s 15 μ g/mL. Izpostavljenost celične linije HFG dvema različnima Ag-NP je povzročila različne rezultate v analizi sposobnosti preživetja celic. V primeru Ag-NP velikosti 28-48 nm se je sposobnost preživetja počasi zmanjševala z naraščajočo koncentracijo NP, pri 400 μ g/mL pa so opazili statistično značilno povečanje deleža mrtvih celic. Nasprotno pa je bil pri Ag-NP velikosti 48-78 nm kjer je učinek veliko bolj izrazit, saj je sposobnost preživetja celic padla pod 50 % pri tretiranju s koncentracijo 30 μ g/mL, delež mrtvih celic pa se je statistično značilno povečal pri koncentraciji 15 μ g/mL.

Citotoksični mehanizem NP je še vedno sporen in nedorečen, vendar več vrst dokazov kaže na možno vlogo ROS in oksidativnega stresa na induciranje citotoksičnih učinkov (Singh et al., 2007). Da bi raziskali sposobnost NP, da stimulirajo tvorbo ROS, je bilo uporabljeno barvilo H₂DCFDA kot indikator znotrajcelično tvorjenih ROS. Tretiranje s TiO₂-NP je pokazalo učinek povečanja znotrajceličnega nastanka ROS. Tretiranje celic HGF s samo 20 µg/mL koncentracijo TiO₂-NP je znatno povečalo intenzivnost fluorescence izmerjenega vzorca. Intenzivnost fluorescence se je povečala le, ko je bila koncentracija NPs povečana. Obdelava celic z naraščajočimi koncentracijami WS₂-NP ni povzročila zaznavne tvorbe ROS. Najnižja uporabljena koncentracija ZnO-NP (5 µg/mL) ni povečala proizvodnje ROS, prav tako ne višje koncentracije. Izpostavljenost Ag-NP z velikostjo 28-48 nm ni povečala tvorbe ROS in Ag-NP z velikostjo 48-78 nm je zmanjšala proizvodnjo ROS v celicah.

Naša raziskava je pokazala, da v kapilarni krvi ortodontskih pacientih prihaja do indukcije sistemskega oksidativnega stresa po 24 urah, čigar parametri pa se po 7 dneh zopet normalizirajo na začetno raven. Ali se stopnja sistemskega oksidativnega stresa poveča zaradi sproščanja kovinskih ionov iz ortodontskih aparatov, ni bilo definirano. Izkazalo se je, da je sproščanje kovinskih ionov iz ortodontskega aparata v umetno slino konstantno, vendar so koncentracije sproščenih kovin še vedno pod največjim dovoljenim dnevnim odmerkom. Od izbranih ortodontskih zlitin se je iz zlitine β-Ti sprostilo najmanj kovinskih ionov. Na podlagi kovinske sestave ortodontskih zlitin smo pripravili mešanice kovinskih ionov in jih uporabili za tretiranje kvasovk *S. cerevisiae*. Le visoke koncentracije kovinskih ionov so lahko ustvarile velike količine ROS, ki jih antioksidativni sistem ni mogel ustrezno regulirati, kar je povzročilo oksidativni stres in z njim povezane poškodbe bioloških molekul. Le SS in Co-Cr kovinski mešanici sta povzročili nastanek reaktivnih kisikovih zvrsti in povzročili oksidativne poškodbe lipidov in proteinov. Primerjava nastanka ROS v kvasnih celicah in celični liniji človeških gingivalnih fibroblastov je dokazala primernost kvasovke *S. cerevisiae* kot modelnega organizma za raziskave oksidativnega stresa. Karakterizacija NP je pokazala, da NP v gojišču in vodi agregirajo in aglomerirajo, kar poveča njihovo velikost iz nano metrske lestvice na mikro metersko. Toksičnost izbranih nanodelcev in njihova sposobnost tvorjenja reaktivnih kisikovih zvrsti v človeških gingivalnih fibroblastih sta odvisni od vrste, koncentracije in lastnosti nanodelcev. Vse tri izbrane vrste TiO₂-NP so bile pri visokih koncentracijah citotoksične, zaradi nastajanja molekul ROS. Ugotovljeno je bilo, da sta oba izbrana ZnO-NP citotoksična že pri nizkih koncentracijah, vendar njunih toksičnih učinkov ni bilo mogoče povezati s povečano tvorbo ROS. Dva izbrana Ag-NP sta dala različne citotoksične rezultate, pri čemer so bili Ag-NP 28-48 nm veliko manj citotoksični v primerjavi z Ag-NP 48-78 nm. Po tretiranju celic HGF z Ag-NP nismo zaznali povečanega nastanka ROS. Izmed izbranih nanodelcev so bili nanodelci WS₂ najmanj toksični za človeške gingivalne celice, saj ni povzročil citotoksičnosti niti tvorbe ROS, in so zato najbolj ustrezni za potencialno uporabo v medicinske namene.

7 REFERENCES

- Abreu I. A., Cabelli D. E. 2010. Superoxide dismutases—a review of the metal-associated mechanistic variations. *Biochimica et Biophysica Acta (BBA) - Proteins and Proteomics*, 1804, 2: 263–274
- Aguilar Diaz De Leon J., Borges C. R. 2020. Evaluation of oxidative stress in biological samples using the thiobarbituric acid reactive substances assay. *Journal of Visualized Experiments*, 159, e61122, doi.org/10.3791/61122: 10 p.
- Akhova A. V., Tkachenk, A. G. 2014. ATP/ADP alteration as a sign of the oxidative stress development in *Escherichia coli* cells under antibiotic treatment. *FEMS Microbiology Letters*, 353, 1: 69–76
- Akter M., Sikder M. T., Rahman M. M., Ullah A. K. M. A., Hossain K. F. B., Banik S., Hosokawa T., Saito T., Kurasaki M. 2018. A systematic review on silver nanoparticles-induced cytotoxicity: Physicochemical properties and perspectives. *Journal of Advanced Research*, 9: 1–16
- Ali S. K., Hadwan M. H. 2019. Precise Spectrophotometric Method for measurement of Peroxiredoxin activity in Biological Samples. *Research Journal of Pharmacy and Technology*, 12, 5: 2254-2260
- Allaker R. P. 2010. Critical review in oral biology medicine: The use of nanoparticles to control oral biofilm formation. *Journal of Dental Research*, 89, 11: 1175–1186
- Alobeid A., Hasan M., Al-Suleiman M., El-Bialy T. 2014. Mechanical properties of cobalt-chromium wires compared to stainless steel and β -titanium wires. *Journal of Orthodontic Science*, 3, 4: 137–141
- Ameziane-El-Hassani R., Dupuy C. 2013. Detection of Intracellular Reactive Oxygen Species (CM-H2DCFDA). *Bio-Protocol*, 3, 2: doi:10.21769/BIOPROTOC.313: 5 p.
- Amro N. A., Kotra L. P., Wadu-Mesthrige K., Bulychev A., Mobashery S., Liu G. Y. 2000. High-resolution atomic force microscopy studies of the *Escherichia coli* outer membrane: structural basis for permeability. *Langmuir*, 16, 6: 2789–2796
- Anderson J., Rodriguez A., Chang D. 2008. Foreign body reaction to biomaterials. *Seminars in Immunology*, 20, 2: 86–100
- Apaza-Bedoya K., Tarce M., Benfatti C. A. M., Henriques B., Mathew M. T., Teughels W., Souza J. C. M. 2017. Synergistic interactions between corrosion and wear at titanium-based dental implant connections: A scoping review. *Journal of Periodontal Research*, 52, 6: 946–954
- Apel, K., Hirt H. 2004. Reactive oxygen species: Metabolism, Oxidative Stress, and Signal Transduction. *Annual Review of Plant Biology*, 55, 1: 373–399
- Appel J. H., Li D. O., Podlevsky J. D., Debnath A., Green A. A., Qing Wang, H., Chae J. 2016. Low Cytotoxicity and Genotoxicity of Two-Dimensional MoS₂ and WS₂. *ACS Biomaterials*, 2, 3: 361–367

- Arango S., Peláez-Vargas A., García C. 2012. Coating and Surface Treatments on Orthodontic Metallic Materials. *Coatings*, 3, 1: doi:10.3390/coatings30100011–15: 15 p.
- Arango Santander S., Luna Ossa C. M. 2015. Stainless Steel: Material Facts for the Orthodontic Practitioner. *Revista Nacional de Odontología*, 11, 20: 71-82
- Arjunan K. P., Sharma V. K., Ptasinska S. 2015. Effects of Atmospheric Pressure Plasmas on Isolated and Cellular DNA-A Review. *International Journal of Molecular Sciences*, 16, 2: 2971–3016
- Arndt M., Bruck A., Bruck B., Scully T., Ager A. J., Bourauel C., Brück A., Scully T., Jäger A., Bourauel C. 2005. Nickel ion release from orthodontic NiTi wires under simulation of realistic in-situ conditions. *Journal of Materials Science*, 40, 14: 3659–3667
- Arthur J. 2000. The glutathione peroxidases. *Cellular and Molecular Life Sciences*, 57, 13: 1825–1835
- Articolo L. C., Kusy R. P. 1999. Influence of angulation on the resistance to sliding in fixed appliances. *American Journal of Orthodontics and Dentofacial*, 115, 1: 39–5
- Assad M., Chernyshov A., Leroux M. A., Rivard C. H. 2002. A new porous titanium–nickel alloy: Part 1. Cytotoxicity and genotoxicity evaluation - IOS Press. *Bio-Medical Materials and Engineering*, 12, 3: 225–237
- Atli G., Canli M. 2010. Response of antioxidant system of freshwater fish *Oreochromis niloticus* to acute and chronic metal (Cd, Cu, Cr, Zn, Fe) exposures. *Ecotoxicology and Environmental Safety*, 73, 8: 1884–1889
- Atuğ Özcan S. S., Ceylan I., Özcan E., Kurt N., Dağsuyu I. M., Çanakçı C. F. 2014. Evaluation of oxidative stress biomarkers in patients with fixed orthodontic appliances. *Disease Markers*, 597892, doi: 10.1155/2014/597892: 7 p.
- Auten R. L., Davis J. M. 2009. Oxygen Toxicity and Reactive Oxygen Species: The Devil Is in the Details. *Pediatric Research*, 66, 2: 121–127
- Ayala A., Muñoz M. F., Argüelles S. 2014. Lipid peroxidation: Production, metabolism, and signaling mechanisms of malondialdehyde and 4-hydroxy-2-nonenal. *Oxidative Medicine and Cellular Longevity*, 360438, doi: 10.1155/2014/360438: 31 p.
- Bagchi D., Stohs S. J., Downs B. W., Bagchi M., Preuss H. G. 2002. Cytotoxicity and oxidative mechanisms of different forms of chromium. *Toxicology*, 180, 1: 5–22
- Ballatori N., Krance S. M., Notenboom S., Shi S., Tieu K., Hammond C. L. 2009. Glutathione dysregulation and the etiology and progression of human diseases. *Biological Chemistry*, 390, 3: 191-214
- Balsera M., Buchanan B. B. 2019. Evolution of the thioredoxin system as a step enabling adaptation to oxidative stress. *Free Radical Biology and Medicine*, 140: 28–35
- Bao J., Shalish I., Su Z., Gurwitz R., Capasso F., Wang X. Ren, Z. 2011. Photoinduced oxygen release and persistent photoconductivity in ZnO nanowires. *Nanoscale Research Letters*, 6, 1: 1–7

- Barbouti A., Doulias P. T., Zhu B. Z., Frei B., Galaris D. 2001. Intracellular iron, but not copper, plays a critical role in hydrogen peroxide-induced DNA Damage. *Free Radical Biology and Medicine*, 31, 4: 490–498
- Barrak F. N., Li S., Muntane A. M., Jones J. R. 2020. Particle release from implantoplasty of dental implants and impact on cells. *International Journal of Implant Dentistry*, 6, 1: 50, doi:10.1186/s40729-020-00247-1: 9 p.
- Barrera G., Pizzimenti S., Daga M., Dianzani C., Arcaro A., Cetrangolo G. P., Giordano G., Cucci M. A., Graf M., Gentile F. 2018. Lipid peroxidation-derived aldehydes, 4-hydroxynonenal and malondialdehyde in aging-related disorders. *Antioxidants*, 7, 8: 102, doi: 10.3390/antiox7080102: 17 p.
- Barrett R. D., Bishara S. E., Quinn J. K. 1993. Biodegradation of orthodontic appliances. Part I. Biodegradation of nickel and chromium in vitro. *American Journal of Orthodontics and Dentofacial Orthopedics*, 103, 1: 8–14
- Baskey S., Lehoux E., Catelas I. 2017. Effects of cobalt and chromium ions on lymphocyte migration. *Journal of Orthopaedic Research: Official Publication of the Orthopaedic Research Society*, 35, 4: 916–924
- Batra P. 2018. Applications of nanoparticles in orthodontics. In: *Dental Applications of Nanotechnology*. Ramesh S. C. (eds.). Springer International Publishing: 81–105
- Bayliak M., Semchyshyn H., Lushchak V. 2006. Effect of hydrogen peroxide on antioxidant enzyme activities in *Saccharomyces cerevisiae* is strain-specific. *Biochemistry*, 71, 9: 1013–1020
- Beers R. F., Sizer I. W. 1952. A spectrophotometric method for measuring the breakdown of hydrogen peroxide by catalase. *Journal of Biological Chemistry*, 195, 1: 133–140
- Behzadi S., Serpooshan V., Tao W., Hamaly M. A., Alkawareek M. Y., Dreaden E. C., Brown D., Alkilany A. M., Farokhzad O. C., Mahmoudi M. 2017. Cellular uptake of nanoparticles: Journey inside the cell. *Chemical Society Reviews*, 46, 14: 4218–4244
- Berkholz D. S., Faber H. R., Savvides S. N., Karplus P. A. 2008. Catalytic Cycle of Human Glutathione Reductase Near 1 Å Resolution. *Journal of Molecular Biology*, 382, 2: 371–384
- Bertini I., Gray H. B., Lippard S. J., Selverstone Valentine J., Lippard S., Valentine J. 1994. *Bioinorganic Chemistry*. Mill Valley, University Science Books: 628 p.
- Bessa M. J., Costa C., Reinoso J., Pereira C., Fraga S., Fernández J., Bañares M., Teixeira J. P. 2017. Moving into advanced nanomaterials. Toxicity of rutile TiO₂ nanoparticles immobilized in nanokaolin nanocomposites on HepG2 cell line. *Toxicology and Applied Pharmacology*, 316: 114–122
- Bhattacharjee S. 2019. ROS and Oxidative Stress: Origin and Implication. In: *Reactive Oxygen Species in Plant Biology*. Springer, New Delhi: 1–31
- Bhattacharjee S. 2016. DLS and zeta potential – What they are and what they are not? *Journal of Controlled Release*, 235: 337–351
- Bhattacharya D., Bhattacharyya A., Karmakar P. 2016. Evaluation of Different Oxidative Stress Parameters and Apoptosis in Human Cervical Cancer Cells Exposed to Rod and Spherical Shaped Zinc Oxide Nanoparticles. *BioNanoScience*, 6, 1: 1–14

- Birben E., Sahiner U. M., Sackesen C., Erzurum S., Kalayci O. 2012. Oxidative Stress and Antioxidant Defense. *The World Allergy Organization Journal*, 5, 1: 9-19
- Botstein D., Fink G. R. 2011. Yeast: An Experimental Organism for 21st Century Biology. *Genetics*, 189, 3: 695-704
- Boverhof D. R., Bramante C. M., Butala J. H., Clancy S. F., Lafronconi W. M., West J., Gordon S. C. 2015. Comparative assessment of nanomaterial definitions and safety evaluation considerations. *Regulatory Toxicology and Pharmacology*, 73, 1: 137–150
- Bradford M. 1976. A Rapid and Sensitive Method for the Quantitation of Microgram Quantities of Protein Utilizing the Principle of Protein-Dye Binding. *Analytical Biochemistry*, 72, 1–2: 248–254
- Bragg P. D., Rainnie D. J. 1974. The effect of silver ions on the respiratory chain of *Escherichia coli*. *Canadian Journal of Microbiology*, 20, 6: 883–889
- Buczko P., Knaś M., Grycz M., Szarmach I., Zalewska A. 2017. Orthodontic treatment modifies the oxidant–antioxidant balance in saliva of clinically healthy subjects. *Advances in Medical Sciences*, 62, 1: 129–135
- Buljan Z. I., Ribaric S. P., Abram M., Ivankovic A., Spalj, S. 2012. In vitro oxidative stress induced by conventional and self-ligating brackets. *Angle Orthodontist*, 82, 2: 340–345
- Burton G. J., Jauniaux E. 2011. Oxidative stress. *Best Practice Research. Clinical Obstetrics Gynaecology*, 25, 3: 287-299
- Cadenas E., Davies K. J. A. 2000. Mitochondrial free radical generation, oxidative stress, and aging. *Free Radical Biology Medicine*, 29, 3–4: 222–230
- Castro S., Ponces M., Lopes J., Vasconcelos M., Pollmann M. C. F. 2015. Orthodontic wires and its corrosion—The specific case of stainless steel and beta-titanium. *Journal of Dental Sciences*, 10, 1: 1-7
- Caicedo M., Jacobs J. J., Reddy A., Hallab N. J. 2008. Analysis of metal ion-induced DNA damage, apoptosis, and necrosis in human (Jurkat) T-cells demonstrates Ni²⁺ and V³⁺ are more toxic than other metals: Al³⁺, Be²⁺, Co²⁺, Cr³⁺, Cu. *Journal of Biomedical Materials Research Part A*, 86A, 4: 905–913
- Chakravarthi S., Padmanabhan S., Chitharanjan A. 2012. Allergy and orthodontics. *Journal of Orthodontic Science*, 1, 4: 83-87
- Chang L., Yang H., Fu W., Yang N., Chen J., Li M., Zou G., Li J. 2006. Synthesis and thermal stability of W/WS₂ inorganic fullerene-like nanoparticles with core–shell structure. *Materials Research Bulletin*, 41, 7: 1242–1248
- Chaturvedi T. P., Upadhayay S. N. 2010. An overview of orthodontic material degradation in oral cavity. *Indian Journal of Dental Research*, 21, 2: 275-284
- Chen A., Zeng G., Chen G., Liu L., Shang C., Hu X., Lu L., Chen M., Zhou Y., Zhang Q. 2014. Plasma membrane behavior, oxidative damage, and defense mechanism in *Phanerochaete chrysosporium* under cadmium stress. *Process Biochemistry*, 49, 4: 589–598
- Chen C. Y., Lin T. K., Chang Y. C., Wang Y. F., Shyu H. W., Lin K. H., Chou M. C. 2010. Nickel(II)-Induced Oxidative Stress, Apoptosis, G₂/M Arrest, and Genotoxicity in

- Normal Rat Kidney Cells. *Journal of Toxicology and Environmental Health, Part A*, 73, 8: 529–539
- Chen C. Y., Wang Y. F., Lin Y. H., Yen S. F. 2003. Nickel-induced oxidative stress and effect of antioxidants in human lymphocytes. *Archives of Toxicology*, 77, 3: 123–130
- Chen L., Zhang J., Zhu Y., Zhang Y. 2018. Interaction of chromium(III) or chromium(VI) with catalase and its effect on the structure and function of catalase: An in vitro study. *Food Chemistry*, 244: 378–385
- Chen Q., Thouas G. 2015. *Biomaterials: A Basic Introduction*. 1st ed. Taylor Francis Group
- Chen X., Schluesener H. J. 2008. Nanosilver: A nanoparticle in medical application. *Toxicology Letters*, 176, 1: 1–12
- Chevion M. 1988. A site-specific mechanism for free radical induced biological damage: the essential role of redox-active transition metals. *Free Radical Biology Medicine*, 5, 1: 27–37
- Chitra P., Prashantha G. S., Rao A. 2022. In vivo investigation of gingival health and oxidative stress changes in patients undergoing orthodontic treatment with and without fluoride use. *Journal of Indian Society of Periodontology*, 26, 2: 123-129
- Choudhury S. R., Ordaz J., Lo C. L., Damayanti N. P., Zhou F., Irudayaraj J. 2017. From the Cover: Zinc oxide Nanoparticles-Induced Reactive Oxygen Species Promotes Multimodal Cyto- and Epigenetic Toxicity. *Toxicological Sciences*, 156, 1: 261–274
- Collin F. 2019. Chemical Basis of Reactive Oxygen Species Reactivity and Involvement in Neurodegenerative Diseases. *International Journal of Molecular Sciences*, 20, 10: 2407, doi: 10.3390/ijms20102407: 17 p.
- Cooke M. S., Evans M. D., Dizdaroglu M., Lunec, J. 2003. Oxidative DNA damage: mechanisms, mutation, and disease. *FASEB Journal*, 17, 10: 1195–1214
- Corazzari I., Deorsola F. A., Gulino G., Aldieri E., Bensaid S., Turci F., Fino D. 2014. Hazard assessment of W and Mo sulphide nanomaterials for automotive use. *Journal of Nanoparticle Research*, 16, 5: 1–14
- Covarrubias L., Hernández-García D., Schnabel D., Salas-Vidal E., Castro-Obregón S. 2008. Function of reactive oxygen species during animal development: passive or active? *Developmental Biology*, 320, 1: 1–11
- D'Attilio M., Di Maio F., D'Arcangela C., Filippi M. R., Felaco M., Lohinai Z., Festa F., Perinetti G. 2004. Gingival Endothelial and Inducible Nitric Oxide Synthase Levels During Orthodontic Treatment: A Cross-Sectional Study. *Angle Orthodontist*, 74, 6: 851–858
- Daimon T., Nosaka Y. 2007. Formation and Behavior of Singlet Molecular Oxygen in TiO₂ Photocatalysis Studied by Detection of Near-Infrared Phosphorescence. *Journal of Physical Chemistry C*, 111, 11: 4420–4424
- Dalle-Donne I., Giustarini D., Colombo R., Rossi R., Milzani A. 2003. Protein carbonylation in human diseases. *Trends in Molecular Medicine*, 9, 4: 169–176
- Dalle-Donne I., Rossi R., Giustarini D., Milzani A., Colombo R. 2003. Protein carbonyl groups as biomarkers of oxidative stress. *Clinica Chimica Acta*, 329, 1–2: 23–38

- Das T. K., Wati M. R., Fatima-Shad K. 2015. Oxidative Stress Gated by Fenton and Haber Weiss Reactions and Its Association with Alzheimer's Disease. *Archives of Neuroscience*, 2, 2: e60038, doi: 10.5812/archneurosci.20078: 8 p.
- Datta A. K., Misra M., North S. L., Kasprzak K. S. 1992. Enhancement by nickel(II) and L-histidine of 2'-deoxyguanosine oxidation with hydrogen peroxide. *Carcinogenesis*, 13, 2: 283-287
- Dayan A., Paine A. 2001. Mechanisms of chromium toxicity, carcinogenicity and allergenicity: Review of the literature from 1985 to 2000. *Human Experimental Toxicology*, 20: 439-451
- de la Torre-Ruiz M., Pujol N., Sundaran V. 2015. Coping With Oxidative Stress. *The Yeast Model*. *Current Drug Targets*, 16, 1: 2-12.
- Dentaurum. 2020. Materials for orthodontic products.
<https://www.dentaurum.de/files/KFO-Werkstoffliste-20.pdf> (5.6.2022)
- Deponte M. 2013. Glutathione catalysis and the reaction mechanisms of glutathione-dependent enzymes. *Biochimica et Biophysica Acta (BBA) - General Subjects*, 1830, 5: 3217-3266
- Dickinson D. A., Forman H. J. 2002. Cellular glutathione and thiols metabolism. *Biochemical Pharmacology*, 64, 5-6: 1019-1026
- Ding H., Zhu Z., Tang T., Yu D., Yu B., Dai, K. 2012. Comparison of the cytotoxic and inflammatory responses of titanium particles with different methods for endotoxin removal in RAW264.7 macrophages. *Journal of Materials Science. Materials in Medicine*, 23, 4: 1055-1062
- Dizdaroglu M., Jaruga P., Birincioglu M., Rodriguez H. 2002. Free radical-induced damage to DNA: mechanisms and measurement, *Free Radical Biology and Medicine*, 32, 11: 1102-1115
- Domi B., Bhorkar K., Rumbo C., Sygellou L., Marti, S. M., Quesada R., Yannopoulos S. N., Tamayo-Ramos J. A. 2021. Toxicological assessment of commercial monolayer tungsten disulfide nanomaterials aqueous suspensions using human A549 cells and the model fungus *Saccharomyces cerevisiae*. *Chemosphere*, 272: 129603, doi:10.1016/j.chemosphere.2021.129603: 10 p.
- Dong R., Wang D., Wang X., Zhang K., Chen P., Yang C. S., Zhang J. 2016. Epigallocatechin-3-gallate enhances key enzymatic activities of hepatic thioredoxin and glutathione systems in selenium-optimal mice but activates hepatic Nrf2 responses in selenium-deficient mice. *Redox Biology*, 10: 221-232
- dos Santos A. A., Ferrer B., Gonçalves F. M., Tsatsakis A. M., Renieri E. A., Skalny A. V., Farina M., Rocha J. B. T., Aschner M. 2018. Oxidative Stress in Methylmercury-Induced Cell Toxicity. *Toxics*, 6, 3: 47, doi:10.3390/toxics6030047: 15 p.
- Drasler B., Sayre P., Steinhäuser K. G., Petri-Fink A., Rothen-Rutishauser B. 2017. In vitro approaches to assess the hazard of nanomaterials. *NanoImpact*, 8: 99-116

- Du Y., Zhang H., Lu J., Holmgren A. 2012. Glutathione and Glutaredoxin Act as a Backup of Human Thioredoxin Reductase 1 to Reduce Thioredoxin 1 Preventing Cell Death by Aurothioglucose. *Journal of Biological Chemistry*, 287, 45: 38210–38219
- El Medawar L., Rocher P., Hornez J. C., Traisnel M., Breme J., Hildebrand, H. F. 2002. Electrochemical and cytocompatibility assessment of NiTiNOL memory shape alloy for orthodontic use. *Biomolecular Engineering*, 19, 2–6: 153–160
- Eliades T, Pratsinis H, Kletsas D, Eliades G, Makou M. 2004. Characterization and cytotoxicity of ions released from stainless steel and nickel-titanium orthodontic alloys. *American Journal of Orthodontics and Dentofacial Orthopedics*, 125, 1: 24–9
- Elshikh M., Ahmed S., Funston S., Dunlop P., McGaw M., Marchant R., Banat I. M. 2016. Resazurin-based 96-well plate microdilution method for the determination of minimum inhibitory concentration of biosurfactants. *Biotechnology Letters*, 38, 6: 1015–1019
- Farrugia G., Balzan R. 2012. Oxidative stress and programmed cell death in yeast, *Frontiers in Oncology*, 2, 64, doi:10.3389/fonc.2012.00064: 22 p.
- Feldman Y., Wasserman E., Srolovitz D. J., Tenne, R. 1995. High-rate, gas-phase growth of MoS₂ nested inorganic fullerenes and nanotubes. *Science*, 267, 5195: 222–225
- Feng M., Yin H., Peng H., Liu Z., Lu G., Dang, Z. 2017. Hexavalent chromium induced oxidative stress and apoptosis in *Pycnoporus sanguineus*. *Environmental Pollution*, 228: 128–139
- Fenton H. J. H. 1894. Oxidation of tartaric acid in presence of iron. *Journal of the Chemical Society, Transactions*, 65: 899–910
- Fernando S., Gunasekara T., Holton, J. 2018. Antimicrobial Nanoparticles: applications and mechanisms of action. *Sri Lankan Journal of Infectious Diseases*, 8, 1: 2–11
- Ferrali M., Signorini C., Ciccoli L., Comporti, M. 1992. Iron release and membrane damage in erythrocytes exposed to oxidizing agents, phenylhydrazine, divicine and isouramil. *Biochemical Journal*, 285: 295–301
- Ferreira M. do A., Luersen M. A., Borges P. C. 2012. Nickel-titanium alloys: a systematic review. *Dental Press Journal of Orthodontics*, 17, 3: 71–82
- Finkel T. 2011. Signal transduction by reactive oxygen species. *The Journal of Cell Biology*, 194, 1: 7–15
- Fleming P. S., Dibiase A. T., Lee R. T. 2010. Randomized clinical trial of orthodontic treatment efficiency with self-ligating and conventional fixed orthodontic appliances. *American Journal of Orthodontics and Dentofacial Orthopedics*, 137: 738–742
- Fleury C., Petit A., Mwale F., Antoniou J., Zukor D. J., Tabrizian M., Huk O. L. 2006. Effect of cobalt and chromium ions on human MG-63 osteoblasts in vitro: Morphology, cytotoxicity, and oxidative stress. *Biomaterials*, 27, 18: 3351–3360
- Foster A. W., Osman D., Robinson N. J. 2014. Metal preferences and metallation. *The Journal of Biological Chemistry*, 289, 41: 28095–28103
- Fotakis G., Timbrell J. A. 2006. In vitro cytotoxicity assays: Comparison of LDH, neutral red, MTT and protein assay in hepatoma cell lines following exposure to cadmium chloride. *Toxicology Letters*, 160, 2: 171–177

- Fujishima A., Rao T. N., Tryk D. A. 2000. Titanium dioxide photocatalysis. *Journal of Photochemistry and Photobiology C: Photochemistry Reviews*, 1, 1: 1–21
- Fukai T., Ushio-Fukai M. 2011. Superoxide dismutases: role in redox signaling, vascular function, and diseases. *Antioxidants Redox Signaling*, 15, 6: 1583–1606
- Galaris D., Barbouti A., Pantopoulos K. 2019. Iron homeostasis and oxidative stress: An intimate relationship. *Biochimica et Biophysica Acta*, 1866, 12: 118535 doi: 10.1016/j.bbamcr.2019.118535: 38 p.
- Galaris D., Pantopoulos, K. 2008. Oxidative Stress and Iron Homeostasis: Mechanistic and Health Aspects. *Critical Reviews in Clinical Laboratory Sciences*, 45, 1: 1–23
- Galeotti A., Uomo R., Spagnuolo G., Paduano S., Cimino R., Valletta R., D'Antò V. 2013. Effect of pH on in vitro biocompatibility of orthodontic miniscrew implants. *Progress in Orthodontics*, 14, 1: 1–7
- Garcia-Contreras R., Sugimoto M., Umemura N., Kaneko M., Hatakeyama Y., Soga T., Tomita M., Scougall-Vilchis R. J., Contreras-Bulnes R., Nakajima H., Sakagami H. 2015. Alteration of metabolomic profiles by titanium dioxide nanoparticles in human gingivitis model. *Biomaterials*, 57: 33–40
- Gault N., Sandre C., Poncy J. L., Moulin C., Lefaix J. L., Bresson C. 2010. Cobalt toxicity: Chemical and radiological combined effects on HaCaT keratinocyte cell line. *Toxicology in Vitro*, 24, 1: 92–98
- Ghiciuc C. M., Ghiciuc O. N., Ochiuz L., Lupuşoru, C. E. 2017. Antibacterial effects of metal oxides-containing nanomaterials in dentistry. 2017 E-Health and Bioengineering Conference, EHB 2017, 365–368
- Gholinejad Z., Khadem Ansari M. H., Rasmi Y. 2019. Titanium dioxide nanoparticles induce endothelial cell apoptosis via cell membrane oxidative damage and p38, PI3K/Akt, NF- κ B signaling pathways modulation. *Journal of Trace Elements in Medicine and Biology*, 54: 27–35
- Gioka C., Bourauel C., Zinelis S., Eliades T., Silikas N., Eliades, G. 2004. Titanium orthodontic brackets: structure, composition, hardness and ionic release. *Dental Materials*, 20, 7: 693–700
- Giudice A. Lo, Nucera R., Matarese G., Portelli M., Cervino G., Giudice L., Militi A., Caccianiga G., Cicciu M., Cordasco G. 2016. Analysis of resistance to sliding expressed during first order correction with conventional and self-ligating brackets: an in-vitro study. *International Journal of Clinical and Experimental Medicine*, 9, 8: 15575–15581
- Glippa O., Engström-Öst J., Kanerva M., Rein A., Vuori K. 2018. Oxidative stress and antioxidant defense responses in *Acartia* copepods in relation to environmental factors. *PLOS ONE*, 13, 4: e0195981, doi:10.1371/JOURNAL.PONE.0195981: 15 p.
- Gonçalves T. S., Menezes L. M., Trindade C., Machado M. da S., Thomas P., Fenech M., Henriques J. A. P. 2014. Cytotoxicity and genotoxicity of orthodontic bands with or without silver soldered joints. *Mutation Research - Genetic Toxicology and Environmental Mutagenesis*, 762: 1–8

- Grilo L. F., Martins J. D., Cavallaro C. H., Nathanielsz P. W., Oliveira P. J., Pereira, S. P. 2020. Development of a 96-well based assay for kinetic determination of catalase enzymatic-activity in biological samples. *Toxicology in Vitro: An International Journal Published in Association with BIBRA*, 69, doi:10.1016/J.TIV.2020.104996: 10 p.
- Gromer S., Urig S., Becker K. 2004. The thioredoxin system-from science to clinic. *Medicinal Research Reviews*, 24, 1: 40–89
- Gstraunthaler G., Hartung T. 2002. Good cell culture practice: good laboratory practice in the cell culture laboratory for the standardization and quality assurance of in vitro studies. In: *Cell Culture Models of Biological Barriers: In vitro Test Systems for Drug Absorption and Delivery*. Taylor Francis: 112–120
- Haber F., Weiss J., Sesh J. O., Eiss W. 1934. The catalytic decomposition of hydrogen peroxide by iron salts. *Proceedings of the Royal Society of London. Series A - Mathematical and Physical Sciences*, 147, 861: 332–351
- Hafez H. S., Selim E. M. N., Kamel Eid F. H., Tawfik W. A., Al-Ashkar E. A., Mostafa Y. A. 2011. Cytotoxicity, genotoxicity, and metal release in patients with fixed orthodontic appliances: A longitudinal in-vivo study. *American Journal of Orthodontics and Dentofacial Orthopedics*, 140, 3: 298–308
- Hagens W. I., Oomen A. G., de Jong W. H., Cassee F. R., Sips A. J. A. M. 2007. What do we (need to) know about the kinetic properties of nanoparticles in the body? *Regulatory Toxicology and Pharmacology*, 49, 3: 217–229
- Hallab N. J., Anderson S., Caicedo M., Brasher A., Mikecz K., Jacobs J. J. 2005. Effects of soluble metals on human peri-implant cells. *Journal of Biomedical Materials Research - Part A*, 74, 1: 124–140
- Halliwell B. 1991. Reactive oxygen species in living systems: Source, biochemistry, and role in human disease. *The American Journal of Medicine*, 91, 3C: 14S-22S.
- Halliwell B., Chirico S., Crawford M. A., Bjerve K. S., Gey K. F. 1993. Lipid peroxidation: its mechanism, measurement, and significance. *The American Journal of Clinical Nutrition*, 57, 5 Suppl: 715S-724S
- Halliwell B., Gutteridge J. M. C. 2015. *Free Radicals in Biology and Medicine*. In *Free Radicals in Biology and Medicine*. 3rd ed. Oxford University Press
- Hamanaka R. B., Glasauer A., Hoover P., Yang S., Blatt H., Mullen A. R., Getsios S., Gottardi C. J., DeBerardinis R. J., Lavker R. M., Chandel N. S. 2013. Mitochondrial Reactive Oxygen Species Promote Epidermal Differentiation and Hair Follicle Development. *Science Signaling*, 6, 261: ra8, doi: 10.1126/scisignal.2003638: 25 p.
- Hamzeh M., Sunahara G. I. 2013. In vitro cytotoxicity and genotoxicity studies of titanium dioxide (TiO₂) nanoparticles in Chinese hamster lung fibroblast cells. *Toxicology in Vitro*, 27, 2: 864–873
- Hanawa T. 2004. Metal ion release from metal implants. *Materials Science and Engineering*, 24, 6–8: 745–752

- Happe A., Sielker S., Hanisch M., Jung S. 2019. The Biological Effect of Particulate Titanium Contaminants of Dental Implants on Human Osteoblasts and Gingival Fibroblasts. *The International Journal of Oral Maxillofacial Implants*, 34, 3: 673–680
- Harini R., Kannan M. S. 2020. Orthodontic Arch Wires-A Review. *European Journal of Molecular Clinical Medicine*, 7, 8: 1804–1810
- He L., He T., Farrar S., Ji L., Liu T., Ma X. 2017. Antioxidants Maintain Cellular Redox Homeostasis by Elimination of Reactive Oxygen Species. *Cellular Physiology and Biochemistry*, 44, 2: 532–553
- He W., Zhou Y. T., Wamer W. G., Boudreau M. D., Yin J. J. 2012. Mechanisms of the pH dependent generation of hydroxyl radicals and oxygen induced by Ag nanoparticles. *Biomaterials*, 33, 30: 7547–7555
- Herrero E., Ros J., Bellí G., Cabisco E. 2008. Redox control and oxidative stress in yeast cells. *Biochimica et Biophysica Acta (BBA) - General Subjects*, 1780, 11: 1217–1235
- House K., Sernetz F., Dymock D., Sandy J. R., Ireland A. J. 2008. Corrosion of orthodontic appliances—should we care? *American Journal of Orthodontics and Dentofacial Orthopedics*, 133, 4: 584–592
- Huang H.-H., Wang C.-C., Chiu S.-M., Wang J.-F., Liaw Y.-C., Lee T.-H., Chen, F.-L. 2005. Corrosion Behavior of titanium-containing Orthodontic Archwires in Artificial Saliva: Effects of Fluoride Ions and Plasma Immersion Ion Implantation Treatment. *Journal of Dental Sciences*, 24, 3: 134–140
- Huang M. L.-H., Chiang S., Kalinowsk D. S., Bae D.-H., Sahni S., Richardson D. R. 2019. The Role of the Antioxidant Response in Mitochondrial Dysfunction in Degenerative Diseases: Cross-Talk between Antioxidant Defense, Autophagy, and Apoptosis. *Oxidative Medicine and Cellular Longevity*, 6392763. doi: 10.1155/2019/6392763: 26 p.
- Hunt N. P., Cunningham S. J., Golden C. G., Sheriff M. 1999. An investigation into the effects of polishing on surface hardness and corrosion of orthodontic archwires. *The Angle Orthodontist*, 69, 5: 433–440
- Hunter P. 2008. The paradox of model organisms. The use of model organisms in research will continue despite their shortcomings. *EMBO Reports*, 9, 8: 717-720
- Ighodaro O. M., Akinloye O. A. 2018. First line defense antioxidants-superoxide dismutase (SOD), catalase (CAT) and glutathione peroxidase (GPX): Their fundamental role in the entire antioxidant defense grid. *Alexandria Journal of Medicine*, 54, 4: 287–293
- Inoue M., Sato, E. F., Nishikawa M., Park A.-M., Kira Y., Imada I., Utsumi K. 2003. Mitochondrial Generation of Reactive Oxygen Species and its Role in Aerobic Life. *Current Medicinal Chemistry*, 10, 2495–2505
- Institute of Medicine (US) Panel on Micronutrients. 2001. Dietary Reference Intakes for Vitamin A, Vitamin K, Arsenic, Boron, Chromium, Copper, Iodine, Iron, Manganese, Molybdenum, Nickel, Silicon, Vanadium, and Zinc. Washington DC: National Academies Press. doi:10.17226/10026

- Iorgulescu G. 2009. Saliva between normal and pathological. Important factors in determiningsystemic and oral health. *Journal of Medicine and Life*, 2, 3: 303-307
- Irani K. 2007. Reactive oxygen species. *Endothelial Biomedicine*, 33, 12: 375–383
- Issa Y., Brunton P., Waters C. M., Watts D. C. 2008. Cytotoxicity of metal ions to human oligodendroglial cells and human gingival fibroblasts assessed by mitochondrial dehydrogenase activity. *Dental Materials*, 24, 2: 281–287
- Jakubowski W., Bartosz, G. 1997. Estimation of oxidative stress in *Saccharomyces cerevisiae* with fluorescent probes. *The International Journal of Biochemistry Cell Biology*, 29,11: 1297–1301
- Jalili P., Gueniche N., Lancelleur R., Burel A., Lavault M. T., Sieg H., Böhmert L., Meyer T., Krause B. C., Lampen A., Estrela-Lopis I., Laux P., Luch A., Hogeveen K., Fessard V. 2018. Investigation of the in vitro genotoxicity of two rutile TiO₂ nanomaterials in human intestinal and hepatic cells and evaluation of their interference with toxicity assays. *NanoImpact*, 11: 69-81
- Jia P., Xu Y. J., Zhang Z. L., Li K., Li B., Zhang W., Yang, H. 2012. Ferric Ion Could Facilitate Osteoclast Differentiation and Bone Resorption through the Production of Reactive Oxygen Species. *Journal of Orthopaedic Research*, 30: 1843–1852
- Joly-Pottuz L., Dassenoy F., Belin M., Vacher B., Martin J. M., Fleischer, N. 2005. Ultralow-friction and wear properties of IF-WS₂ under boundary lubrication. *Tribology Letters*, 18, 4: 477–485
- Jomova K., Valko M. 2011. Advances in metal-induced oxidative stress and human disease. *Toxicology*, 283, 2–3: 65–87
- Joris F., Manshian B. B., Peynshaert K., De Smedt S. C., Braeckmans K., Soenen S. J. 2013. Assessing nanoparticle toxicity in cell-based assays: Influence of cell culture parameters and optimized models for bridging the in vitro-in vivo gap. *Chemical Society Reviews*, 42, 21: 8339–8359
- Jozefczak M., Remans T., Vangronsveld J., Cuypers A. 2012. Glutathione Is a Key Player in Metal-Induced Oxidative Stress Defenses. *International Journal of Molecular Sciences*, 13, 3: 3145–3175
- Kachoei M., Nourian A., Divband B., Kachoei Z., Shirazi S. 2016. Zinc-oxide nanocoating for improvement of the antibacterial and frictional behavior of nickel-titanium alloy. *Nanomedicine*, 11, 19: 2511–2527
- Kalaivani P., Saranya S., Poornima P., Prabhakaran R., Dallemer F., Vijaya Padma V., Natarajan K. 2014. Biological evaluation of new nickel(II) metallates: Synthesis, DNA/protein binding and mitochondrial mediated apoptosis in human lung cancer cells (A549) via ROS hypergeneration and depletion of cellular antioxidant pool. *European Journal of Medicinal Chemistry*, 82: 584–599
- Kameda T., Oda H., Ohkuma K., Sano N., Batbayar N., Terashima Y., Sato S., Terada K. 2014. Microbiologically influenced corrosion of orthodontic metallic appliances. *Dental Materials Journal*, 33, 2: 1–9

- Kamiloglu S., Sari G., Ozdal T., Capanoglu E. 2020. Guidelines for cell viability assays. *Food Frontiers*, 1, 3: 332–349
- Kao C. T., Ding S. J., Min Y., Hsu T. C., Cho, M. Y., Huang T. H. 2007. The cytotoxicity of orthodontic metal bracket immersion media. *European Journal of Orthodontics*, 29, 2: 198–203
- Karathia H., Vilaprinyo E., Sorribas A., Alves R. 2011. *Saccharomyces cerevisiae* as a Model Organism: A Comparative Study. *PLOS ONE*, 6, 2: e16015, doi:10.1371/JOURNAL.PONE.0016015: 10 p.
- Kasprzak K. S., Sunderman F. W., Salnikow K. 2003. Nickel carcinogenesis. *Mutation Research*, 533, 1–2: 67–97
- Keenan C. R., Goth-Goldstein R., Lucas D., Sedlak D. L. 2009. Oxidative stress induced by zero-valent iron nanoparticles and Fe(II) in human bronchial epithelial cells. *Environmental Science and Technology*, 43, 12: 4555–4560.
- Kehm R., Baldensperger T., Raupbach J., Höhn A. 2021. Protein oxidation - Formation mechanisms, detection and relevance as biomarkers in human diseases. *Redox Biology*, 42, 101901, doi:10.1016/J.REDOX.2021.101901: 23 p.
- Keinan D., Mass E., Zilberman U. 2010. Absorption of Nickel, Chromium, and Iron by the Root Surface of Primary Molars Covered with Stainless Steel Crowns. *International Journal of Dentistry*, 2010, 326124, doi:10.1155/2010/326124: 4 p.
- Kirkinezos I. G., Moraes C. T. 2001. Reactive oxygen species and mitochondrial diseases. *Seminars in Cell and Developmental Biology*, 12, 6: 449–457
- Kirkman H. N., Rolfo M., Ferraris A. M., Gaetani G. F. (1999). Mechanisms of Protection of Catalase by NADPH: kinetics and stoichiometry. *Journal of Biological Chemistry*, 274, 20: 13908–13914
- Koch A. L. (2014). Growth Measurement. *Methods for General and Molecular Microbiology*, 172–199
- Kohen R., Nyska A. 2002. Oxidation of Biological Systems: Oxidative Stress Phenomena, Antioxidants, Redox Reactions, and Methods for Their Quantification. *Toxicologic Pathology*, 30, 6: 620–650
- Konaka R., Kasahara E., Dunlap W. C., Yamamoto Y., Chien K. C., Inoue M. 2001. Ultraviolet irradiation of titanium dioxide in aqueous dispersion generates singlet oxygen. *Redox Report*, 6, 5: 319–325
- Kononenko V., Drobne D. 2019. In Vitro Cytotoxicity Evaluation of the Magnéli Phase Titanium Suboxides (Ti_xO_{2x-1}) on A549 Human Lung Cells. *International Journal of Molecular Sciences*, 20, 1: 196, <https://doi.org/10.3390/ijms20010196>: 15 p.
- Konseng S., Yoovathaworn K., Wongprasert K., Chunhabundit R., Sukwong P., Pissuwan D. 2016. Cytotoxic and inflammatory responses of TiO₂ nanoparticles on human peripheral blood mononuclear cells. *Journal of applied toxicology*, 36, 10: 1364-1373
- Kovač V., Bergant M., Ščančar J., Primožič J., Jamnik P., Poljšak B. (2021). Causation of Oxidative Stress and Defense Response of a Yeast Cell Model after Treatment with

- Orthodontic Alloys Consisting of Metal Ions. *Antioxidants*, 11, 1: 63, doi:10.3390/antiox11010063: 24 p.
- Kovac V., Poljsak B., Perinetti G., Primožic J., Reis F. S. 2019. Systemic Level of Oxidative Stress during Orthodontic Treatment with Fixed Appliances. *BioMed Research International*, 2019, doi:10.1155/2019/5063565: 6 p.
- Kovač V., Poljšak B., Primožič J., Jamnik P. 2020. Are metal ions that make up orthodontic alloys cytotoxic, and do they induce oxidative stress in a yeast cell model? *International Journal of Molecular Sciences*, 21, 21: 7993 doi:10.3390/ijms21217993:15 p.
- Krewski D., Acosta Jr D., Andersen M., Anderson H., Bailar III J. C., Boekelheide K., Brent R., Charnley G., Cheung V. G., Green Jr S., Kelsey K. T., Kerkvliet N. I., Li A. A., McCray L., Meyer O., Patterson R. D., Pennie W., Scala R. A., Solomon G. M., ... Zeise L. 2010. Toxicity Testing in the 21st Century: A Vision and a Strategy. *Journal of Toxicology and Environmental Health*, 13, 4: 51–138
- Kubrak O. I., Lushchak O. V., Lushchak J. V., Torous I. M., Storey J. M., Storey K. B., Lushchak V. I. 2010. Chromium effects on free radical processes in goldfish tissues: Comparison of Cr(III) and Cr(VI) exposures on oxidative stress markers, glutathione status and antioxidant enzymes. *Comparative Biochemistry and Physiology Part C: Toxicology Pharmacology*, 152, 3: 360–370
- Kuhta M., Pavlin D., Slaj M. M., Varga S., Lapter-Varga M., Slaj M. M. 2009. Type of archwire and level of acidity: Effects on the release of metal ions from orthodontic appliances. *Angle Orthodontist*, 79, 1: 102–110
- Kusy R. P. 2002. Orthodontic Biomaterials: From the Past to the Present. *Angle Orthodontist*, 72, 6: 501–512
- Lanone S., Boczkowski J. 2006. Biomedical applications and potential health risks of nanomaterials: molecular mechanisms. *Current Molecular Medicine*, 6, 6: 651–663
- Lazarova N., Krumova E., Stefanova T., Georgieva N., Angelova M. 2014. The oxidative stress response of the filamentous yeast *Trichosporon cutaneum* R57 to copper, cadmium and chromium exposure. *Biotechnology Biotechnological Equipment*, 28, 5: 855–862
- Lazić M. M., Majerič P., Lazić V., Milašin J., Jakšić M., Trišić D., Radović K. 2022. Experimental Investigation of the Biofunctional Properties of Nickel-Titanium Alloys Depending on the Type of Production. *Molecules*. 27, 6: 1960 doi: 10.3390/molecules27061960: 14 p.
- Lebeau P. F., Chen J., Byun J. H., Platko K., Austin R. C. 2019. The trypan blue cellular debris assay: a novel low-cost method for the rapid quantification of cell death. *MethodsX*, 6: 1174–1180
- Leonard S. S., Harris G. K., Shi X. 2004. Metal-induced oxidative stress and signal transduction. *Free Radical Biology and Medicine*, 37, 12: 1921–1942
- Levine R. L., Garland D., Oliver C. N., Amici A., Climent I., Lenz A. G., Ahn B. W., Shaltiel S., Stadtman E. R. 1990. Determination of carbonyl content in oxidatively modified proteins. *Methods in Enzymology*, 186: 464–478

- Li L., Sun W., Yu J., Lei W., Zeng H., Shi Bin. 2022. Effects of titanium dioxide microparticles and nanoparticles on cytoskeletal organization, cell adhesion, migration, and proliferation in human gingival fibroblasts in the presence of lipopolysaccharide. *Journal of Periodontal Research*, 57, 3: 644-659
- Li M., Zhu L., Lin D. 2011. Toxicity of ZnO nanoparticles to escherichia Coli: Mechanism and the influence of medium components. *Environmental Science and Technology*, 45, 5: 1977–1983
- Lim J., Yeap S. P., Che H. X., Low S. C. 2013. Characterization of magnetic nanoparticle by dynamic light scattering. *Nanoscale Research Letters*, 8, 1: 1–14
- Limberger K. M., Westphalen G. H., Menezes L. M., Medina-Silva R. 2011. Cytotoxicity of orthodontic materials assessed by survival tests in *Saccharomyces cerevisiae*. *Dental Materials*, 27, 5: e81–e86, doi:10.1016/j.dental.2011.01.001: 6 p.
- Liu S., Xu L., Zhang T., Ren G., Yang Z. 2010. Oxidative stress and apoptosis induced by nanosized titanium dioxide in PC12 cells. *Toxicology*, 267, 1–3: 172–177
- Liu X., Duan G., Li W., Zhou Z., Zhou R. 2017. Membrane destruction-mediated antibacterial activity of tungsten disulfide (WS₂). *RSC Advances*, 7: 37873-37880
- Longo V. D., Fabrizio P. 2012. Chronological aging in *Saccharomyces cerevisiae*. *Sub-Cellular Biochemistry*, 57: 101–121
- Longo V. D., Gralla E. B., Valentine J. S. 1996. Superoxide dismutase activity is essential for stationary phase survival in *Saccharomyces cerevisiae*. Mitochondrial production of toxic oxygen species in vivo. *The Journal of Biological Chemistry*, 271, 21: 12275–12280
- Lopert P., Day B. J., Patel M. 2012. Thioredoxin Reductase Deficiency Potentiates Oxidative Stress, Mitochondrial Dysfunction and Cell Death in Dopaminergic Cells. *PLOS ONE*, 7, 11: e50683, doi:10.1371/JOURNAL.PONE.0050683: 12 p.
- Lu J., Holmgren A. 2014. The thioredoxin antioxidant system. *Free Radical Biology and Medicine*, 66: 75–87
- Lundström F., Krasse B. 1987. Streptococcus mutans and lactobacilli frequency in orthodontic patients; the effect of chlorhexidine treatments. *European Journal of Orthodontics*, 9, 2: 109–116
- Lushchak V. I. 2011. Adaptive response to oxidative stress: Bacteria, fungi, plants and animals. *Comparative Biochemistry and Physiology Part C: Toxicology Pharmacology*, 153, 2: 175–190
- Mah W., Jiang G., Olver D., Cheung G., Kim B., Larjava H., Häkkinen L. 2014. Human Gingival Fibroblasts Display a Non-Fibrotic Phenotype Distinct from Skin Fibroblasts in Three-Dimensional Cultures. *PLoS ONE*, 9, 3: e90715, doi:10.1371/journal.pone.0090715: 20 p.
- Mahajan L., Verma P. K., Raina R., Pankaj N. K., Sood S., Singh M. 2018. Alteration in thiols homeostasis, protein and lipid peroxidation in renal tissue following subacute oral exposure of imidacloprid and arsenic in Wistar rats. *Toxicology Reports*, 5: 1114–1119

- Makihira S., Mine Y., Nikawa H., Shuto T., Iwata S., Hosokawa R., Kamoi K., Okazaki S., Yamaguchi Y. 2010. Titanium ion induces necrosis and sensitivity to lipopolysaccharide in gingival epithelial-like cells. *Toxicology in Vitro*, 24, 7: 1905–1910
- Malkiewicz K., Sztogryn M., Mikulewicz M., Wielgus A., Kamiński, J., Wierzchoń T. 2018. Comparative assessment of the corrosion process of orthodontic archwires made of stainless steel, titanium-molybdenum and nickel-titanium alloys. *Archives of Civil and Mechanical Engineering*, 18: 941–947
- Mamunya Y. P., Zois H., Apekis L., Lebedev E. V. 2004. Influence of pressure on the electrical conductivity of metal powders used as fillers in polymer composites. *Powder Technology*, 140, 1–2: 49–55
- Manta B., Hugo M., Ortiz C., Ferrer-Sueta G., Trujillo M., Denicola A. 2009. The peroxidase and peroxynitrite reductase activity of human erythrocyte peroxiredoxin 2. *Archives of Biochemistry and Biophysics*, 484, 2: 146–154
- Marambio-Jones C., Hoek E. M. V. 2010. A review of the antibacterial effects of silver nanomaterials and potential implications for human health and the environment. *Journal of Nanoparticle Research*, 12, 5: 1531–1551
- Marklund S., Marklund G. 1974. Involvement of the superoxide anion radical in the autoxidation of pyrogallol and a convenient assay for superoxide dismutase. *European Journal of Biochemistry*, 47, 3: 469–474
- Marques I. S. V., Araújo A. M., Gurgel J. A., Normandocorthoia, D. 2010. Debris, roughness and friction of stainless steel archwires following clinical use. *Angle Orthodontist*, 80, 3: 521–527
- Mathew M. T., Wimmer M. A. 2011. Tribocorrosion in artificial joints: In vitro testing and clinical implications. In: *Tribocorrosion of Passive Metals and Coatings*. Elsevier Ltd.
- Mavreas D., Athanasiou A. E. 2008. Factors affecting the duration of orthodontic treatment: a systematic review. *European Journal of Orthodontics*, 30, 4: 386–395
- McNaught A. D., Wilkinson A. 1997. *Compendium of Chemical Terminology: IUPAC Recommendations*. 2nd ed. Blackwell Science: 450 p.
- Mello D. F., Trevisan R., Rivera, N., Geitner N. K., Di Giulio R. T., Wiesner M. R., Hsu-Kim H., Meyer J. N. 2020. Caveats to the use of MTT, neutral red, Hoechst and Resazurin to measure silver nanoparticle cytotoxicity. *Chemico-Biological Interactions*, 315: 108868, doi:10.1016/J.CBI.2019.108868: 22 p.
- Mesa-Herrera F., Quinto-Aleman, D., Díaz M. 2019. A Sensitive, Accurate, and Versatile Method for the Quantification of Superoxide Dismutase Activities in Biological Preparations. *Reactive Oxygen Species*. 7, 19: 10–20
- Mesquita C. S., Oliveira R., Bento F., Geraldo D., Rodrigues J. V., Marcos J. C. 2014. Simplified 2,4-dinitrophenylhydrazine spectrophotometric assay for quantification of carbonyls in oxidized proteins. *Analytical Biochemistry*, 458: 69–71
- Messer R. L. W., Lucas L. C. 1999. Evaluations of metabolic activities as biocompatibility tools: a study of individual ions' effects on fibroblasts. *Dental Materials*, 15, 1: 1–6

- Messer R. L. W., Lucas L. C. 2000. Cytotoxicity of nickel–chromium alloys: bulk alloys compared to multiple ion salt solutions. *Dental Materials*, 16, 3: 207–212
- Metin-Gürsoy G., Taner L., Akca G. 2017. Nanosilver coated orthodontic brackets: in vivo antibacterial properties and ion release. *European Journal of Orthodontics*, 39, 1: 9–16
- Meyerstein D. 2021. Re-examining Fenton and Fenton-like reactions. *Nature Reviews Chemistry*, 5: 595–597
- Milheiro A., Nozaki K., Kleverlaan C. J., Muris J., Miura H., Feilzer A. J. 2016. In vitro cytotoxicity of metallic ions released from dental alloys. *Odontology*, 104, 2: 136–142
- Mikulewicz M., Chojnacka K. 2010. Trace Metal release from orthodontic appliances by in vivo studies: A systematic literature review. *Biological Trace Element Research*, 137, 2: 127–138
- Mitozo P. A., De Souza L. F., Loch-Neckel G., Flesch S., Maris A. F., Figueiredo C. P., Dos Santos A. R. S., Farina M., Dafre A. L. 2011. A study of the relative importance of the peroxiredoxin-, catalase-, and glutathione-dependent systems in neural peroxide metabolism. *Free Radical Biology and Medicine*, 51, 1: 69–77
- Močnik P., Kosec T., Kovač J., Bizjak M. 2017. The effect of pH, fluoride and tribocorrosion on the surface properties of dental archwires. *Materials Science and Engineering C*, 78: 682–689
- Morán-Martínez J., Beltrán Del Río-Parra R., Betancourt-Martínez N. D., García-Garza R., Jiménez-Villarreal J., Niño-Castañeda M. S., Nava-Rivera L. E., Facio Umaña J. A., Carranza-Rosale, P., Arellano Pérez-Vertti R. D. 2018. Evaluation of the Coating with TiO₂ Nanoparticles as an Option for the Improvement of the Characteristics of NiTi Archwires: Histopathological, Cytotoxic, and Genotoxic Evidence. *Journal of Nanomaterials*, 2585918, doi:10.1155/2018/2585918: 11 p.
- Moriwaki H., Osborne M. R., Phillips D. H. 2008. Effects of mixing metal ions on oxidative DNA damage mediated by a Fenton-type reduction. *Toxicology in Vitro*, 22, 1: 36–44
- Morones J., Elechiguerra J., Camacho A., Holt K., Kouri J., Ramirez J., Yacaman M. 2005. The bactericidal effect of silver nanoparticles. *Nanotechnology*, 16: 2346–2353
- Muguruma T., Iijima M., Brantley W. A., Nakagaki S., Endo K., Mizoguchi I. 2013. Frictional and mechanical properties of diamond-like carbon-coated orthodontic brackets. *European Journal of Orthodontics*, 35, 2: 216–222
- Murphy M. P. 2008. How mitochondria produce reactive oxygen species. *Biochemical Journal*, 417, 1: 1–13
- Nakagawa M., Matsuya S., Udoh K. 2002. Effects of fluoride and dissolved oxygen concentrations on the corrosion behavior of pure titanium and titanium alloys. *Dental Materials Journal*, 21, 2: 83–92
- Nakajima H., Okabe T. 1996. Titanium in dentistry: development and research in the U.S.A. *Dental Materials Journal*, 15, 2: 77–90
- Nanci A. 2016. Ten Cate's Oral histology: Development Development, Structure, and Function. Elsevier: 352 p.

- Nayak R. S., Khanna B., Pasha A., Vinay K., Narayan A., Chaitra K. 2015. Evaluation of Nickel and Chromium Ion Release During Fixed Orthodontic Treatment Using Inductively Coupled Plasma-Mass Spectrometer: An In Vivo Study. *Journal of International Oral Health*, 7, 8: 14–20
- Nemes Z., Dietz R., Liith J. B., Gomba S., Hackenthal E., Gross, F. 1979. The pharmacological relevance of vital staining with neutral red. *Experientia*, 35, 11: 1475–1476
- Ng C. T., Yong L. Q., Hande M. P., Ong C. N., Yu L. E., Bay B. H., Baeg G. H. 2017. Zinc oxide nanoparticles exhibit cytotoxicity and genotoxicity through oxidative stress responses in human lung fibroblasts and *Drosophila melanogaster*. *International Journal of Nanomedicine*, 12: 1621–1637
- Nguee A., Mae A. M., Ongkosuwito E. M., Jaddoe V. W. V., Wolvius E. B., Kragt, L. (2020). Impact of orthodontic treatment need and deviant occlusal traits on oral health-related quality of life in children: A cross-sectional study in the Generation R cohort. *American Journal of Orthodontics and Dentofacial Orthopedics*, 157, 6: 764-772
- Niki E. 2014. Antioxidants: basic principles, emerging concepts, and problems. *Biomedical Journal*, 37, 3: 106–111
- Noble J. E. 2014. Quantification of Protein Concentration Using UV Absorbance and Coomassie Dyes. In J. Lorsch (Ed.), *Methods in Enzymology*. Academic Press Inc, 536: 17–26
- Oh K.-T., Choo S.-U., Kim K.-M., Kim K.-N. 2005. A stainless steel bracket for orthodontic application. *European Journal of Orthodontics*, 27, 3: 237–244
- Oh K. T., Kim Y. S., Park Y. S., Kim K. N. 2004. Properties of super stainless steels for orthodontic applications. *Journal of Biomedical Materials Research Part B: Applied Biomaterials*, 69, 2: 183–194
- Ohkawa H., Ohishi N., Yagi K. 1979. Assay for lipid peroxides in animal tissues by thiobarbituric acid reaction. *Analytical Biochemistry*, 95, 2: 351–358
- Olteanu C., Muresan A., Daicovicu D., Tarmure V., Olteanu I., Irene K. M. L. W. 2009. Variations of some saliva markers of the oxidative stress in patients with orthodontic appliances. *Fiziologia – Physiology*, 19, 63: 27–29
- Orozco-Páez J., Méndez-Rodríguez M. A., Rodríguez-Cavallo E., Díaz-Caballero A., Méndez-Cuadro, D. 2021. Protein carbonylation associated with nickel liberation in orthodontic gingival overgrowth. *Archives of Oral Biology*, 125, 105103 doi:10.1016/J.ARCHORALBIO.2021.105103: 15 p.
- Ortiz A. J., Fernández E., Vicent, A., Calvo J. L., Ortiz C. 2011. Metallic ions released from stainless steel, nickel-free, and titanium orthodontic alloys: Toxicity and DNA damage. *American Journal of Orthodontics and Dentofacial Orthopedics*, 140, 3: 115–122
- Page B., Page M., Noel C. 1993. A new fluorometric assay for cytotoxicity measurements in vitro. *International Journal of Oncology*, 3, 3: 473–476
- Pallero M. A., Roden M. T., Chen Y.-F., Anderson P. G., Lemons J., Brott B. C., Murphy-Ullrich J. E. (2010). Stainless Steel Ions Stimulate Increased Thrombospondin-1-

- Dependent TGF-Beta Activation by Vascular Smooth Muscle Cells: Implications for In-Stent Restenosis. *Journal of Vascular Research*, 47, 4: 309–322
- Panjamurthy K., Manoharan S., Ramachandran C. R. 2005. Lipid peroxidation and antioxidant status in patients with periodontitis. *Cellular Molecular Biology Letters*, 10: 255–264
- Pardo M., Shuster-Meiseles T., Levin-Zaidman S., Rudich A., Rudich Y. 2014. Low cytotoxicity of inorganic nanotubes and fullerene-like nanostructures in human bronchial epithelial cells: Relation to inflammatory gene induction and antioxidant response. *Environmental Science and Technology*, 48, 6: 3457–3466
- Park J., Kim Y. 2000. *The Biomedical Engineering Handbook*. Bronzino J. (eds.). Taylor Francis Inc, 2, 1
- Park J., Lakes R. S. 2007. *Biomaterials: An Introduction*. Springer: 562 p.
- Patel E., Lynch C., Ruff V., Reynolds M. 2012. Co-exposure to nickel and cobalt chloride enhances cytotoxicity and oxidative stress in human lung epithelial cells. *Toxicology and Applied Pharmacology*, 258, 3: 367–375
- Patlevič P., Vaškova J., Švorc P., Vaško L., Švorc P. 2016. Reactive oxygen species and antioxidant defense in human gastrointestinal diseases. *Integrative Medicine Research*, 5, 4: 250–258
- Pavlatou M., Papastamataki M., Apostolakou F., Papassotiriou I., Tentolouris N. 2009. FORT and FORD: two simple and rapid assays in the evaluation of oxidative stress in patients with type 2 diabetes mellitus. *Metabolism*, 55, 11: 1657–1662
- Peiris M. K., Gunasekara C. P., Jayaweera P. M., Arachchi N. D. H., Fernando N. 2017. Biosynthesized silver nanoparticles: Are they effective antimicrobials? *Memorias Do Instituto Oswaldo Cruz*, 112, 8: 537–543
- Pérez-Navero J. L., Benítez-Sillero J. D., Gil-Campos M., Guillén-Del Castillo M., Tasset I., Túnez, I. 2009. Changes in oxidative stress biomarkers induced by puberty. *Anales de Pediatría*, 70, 5: 424–428
- Periasamy V. S., Athinarayanan J., Al-Hadi A. M., Juhaimi F. Al., Alshatwi A. A. 2015. Effects of Titanium Dioxide Nanoparticles Isolated from Confectionery Products on the Metabolic Stress Pathway in Human Lung Fibroblast Cells. *Archives of Environmental Contamination and Toxicology*, 68, 3: 521–533
- Perkhulyn N. V, Rovenko B. M., Lushchak O. V, Storey J. M., Storey K. B., Lushchak V. I. 2017. Exposure to sodium molybdate results in mild oxidative stress in *Drosophila melanogaster*. *Redox Report*, 22, 3: 137–146
- Pettersson M., Kelk P., Belibasakis G. N., Bylund D., Molin Thorén M., Johansson A. 2017. Titanium ions form particles that activate and execute interleukin-1 β release from lipopolysaccharide-primed macrophages. *Journal of Periodontal Research*, 52, 1: 21–32
- Pham-Huy L. A., He H., Pham-Huy C. 2008. Free radicals, antioxidants in disease and health. *International Journal of Biomedical Science*, 4, 2: 89–96

- Pisoschi A. M., Pop A. 2015. The role of antioxidants in the chemistry of oxidative stress: A review. *European Journal of Medicinal Chemistry*, 97: 55–74
- Poljak-Blazi M., Jaganjac M., Sabol I., Mihaljevic B., Matovina M., Grce M. 2011. Effect of ferric ions on reactive oxygen species formation, cervical cancer cell lines growth and E6/E7 oncogene expression. *Toxicology in Vitro*, 25, 1: 160–166
- Poljsak B., Jamnik P. 2010. Methodology for oxidative state detection in biological systems. In: *Handbook of Free Radicals: Formation, Types and Effects*. Kozyrev D., Slutsky V. (eds.). New York, USA, Nova Science Publishers: 421–448
- Pollard T. D., Cooper J. A. 2009. Actin, a central player in cell shape and movement. *Science*, 326, 5957: 1208–1212
- Portelli M., Miličič A., Cervino G., Lauritano F., Sambataro S., Mainardi A., Nucera R. 2017. Oxidative Stress Evaluation in Patients Treated with Orthodontic Self-ligating Multibracket Appliances: An Case-Control Study. *The Open Dentistry Journal*, 11, 1: 257–265
- Prabhu S., Poulouse E. K. 2012. Silver nanoparticles: mechanism of antimicrobial action, synthesis, medical applications, and toxicity effects. *International Nano Letters*, 2, 1: 1–10
- Prashant P. S., Nandan H., Gopalakrishnan M. 2015. Friction in orthodontics. *Journal of Pharmacy and Bioallied Sciences*, 7, 6: 334–338
- Proffit W. R., Fields H. W., Sarver D. M. 2007. Orthodontic Treatment Planning: Limitations, Controversies, and Special Problems. In: *Contemporary Orthodontics*. Elsevier: 284–286
- Putnam C. D., Arvai A. S., Bourne Y., Tainer J. A. 2000. Active and inhibited human catalase structures: ligand and NADPH binding and catalytic mechanism. *Journal of Molecular Biology*, 296, 1: 295–309
- Rabinow B. E. 2004. Nanosuspensions in drug delivery. *Nature Reviews. Drug Discovery*, 3, 9: 785–796
- Ramazan-zadeh B. A., Ahrari F., Sabzevari B., Habibi S. 2014. Original Articles Nickel Ion Release from Three Types of Nickel-titanium-based Orthodontic Archwires in the As-received State and After Oral Simulation. *Dental Clinics, Dental*, 8, 2: 71–76
- Rampersad S. N. 2012. Multiple Applications of Alamar Blue as an Indicator of Metabolic Function and Cellular Health in Cell Viability Bioassays. *Sensors*, 12, 9: 12347–12360
- Rana S., Kalaichelvan, P. T., Bondy, S. C., Brar, S. K., Rogers, J. V., Zhou, B. 2013. Ecotoxicity of Nanoparticles. *ISRN Toxicology*, 2013, 574648, doi:10.1155/2013/574648: 11 p.
- Rauscher H., Sokull-Klüttgen B., Stamm, H. 2013. The European Commission's recommendation on the definition of nanomaterial makes an impact. *Nanotoxicology*, 7, 7: 1195–1197
- Ray P. C., Yu H., Fu P. P. 2009. Toxicity and Environmental Risks of Nanomaterials: Challenges and Future Needs. *Journal of Environmental Science and Health. Part C, Environmental Carcinogenesis Ecotoxicology Reviews*, 27, 1: 1–35

- Reijnders C. M. A., Van Lier A., Roffel S., Kramer D., Scheper R. J., Gibbs S. (2015). Development of a Full-Thickness Human Skin Equivalent In Vitro Model Derived from TERT-Immortalized Keratinocytes and Fibroblasts. *Tissue Engineering. Part A*, 21, 17-18: 2448-2459
- Repetto G., del Peso A., Zurita J. L. 2008. Neutral red uptake assay for the estimation of cell viability/cytotoxicity. *Nature Protocols*, 3, 7: 1125–1131
- Repetto G., Sanz P. 1993. Neutral Red Uptake, Cellular Growth and Lysosomal Function: In Vitro Effects of 24 Metals. *Alternatives to Laboratory Animals*, 21, 4: 501–507
- Ricci J. E., Gottlieb R. A., Green D. R. 2003. Caspase-mediated loss of mitochondrial function and generation of reactive oxygen species during apoptosis. *The Journal of Cell Biology*, 160, 1: 65–75
- Rincic Mlinaric M., Durgo K., Katic V., Spalj S. 2019. Cytotoxicity and oxidative stress induced by nickel and titanium ions from dental alloys on cells of gastrointestinal tract. *Toxicology and Applied Pharmacology*, 383, 114784, doi:10.1016/j.taap.2019.114784: 25 p.
- Riss T. L., Moravec R. A., Niles A. L., Duellman S., Benink H. A., Worzella T. J., Minor L. 2016. Cell Viability Assays. In: *Assay Guidance Manual*. Markossian S, Grossman, A., Brimacombe, K. (eds). Bethesda (MD): Eli Lilly & Company and the National Center for Advancing Translational Sciences: 8 p.
- Rizzello L., Pompa P. P. 2014. Nanosilver-based antibacterial drugs and devices: Mechanisms, methodological drawbacks, and guidelines. *Chemical Society Reviews*, 43, 5: 1501–1518
- Rodríguez-Ruiz M., González-Gordo, S., Cañas A., Campos M. J., Paradelo A., Corpas F. J., Palma J. M. 2019. Sweet Pepper (*Capsicum annuum* L.) Fruits Contain an Atypical Peroxisomal Catalase That Is Modulated by Reactive Oxygen and Nitrogen Species. *Antioxidants*, 8, 9: 374, doi:10.3390/ANTIOX8090374: 18 p.
- Rodriguez R., Redma, R. 2005. Balancing the generation and elimination of reactive oxygen species. *Proceedings of the National Academy of Sciences of the United States of America*, 102, 9: 3175–3176
- Rogers L. K., Tamura T., Rogers B. J., Welty S. E., Hansen T. N., Smith C. V. 2004. Analyses of Glutathione Reductase Hypomorphic Mice Indicate a Genetic Knockout. *Toxicological Sciences*, 82, 2: 367–373
- Rohde M. M., Snyder C. M., Sloop J., Solst S. R., Donati G. L., Spitz D. R., Furdui C. M., Singh R. 2021. The mechanism of cell death induced by silver nanoparticles is distinct from silver cations. *Particle and Fibre Toxicology*, 18, 1: 1–24
- Rosenberg M., Azevedo N. F., Ivask A. 2019. Propidium iodide staining underestimates viability of adherent bacterial cells. *Scientific Reports*, 9, 1: 1–12
- Rossouw P., Kamelchuk L., Kusy R. 2003. A fundamental review of variables associated with low velocity frictional dynamics. *Seminars in Orthodontics*, 9, 4: 223–235

- Saafan A., Zaazou M. H., Sallam M. K., Mosallam O., El Danaf H. A. 2018. Assessment of Photodynamic Therapy and Nanoparticles Effects on Caries Models. *Open Access Macedonian Journal of Medical Sciences*, 6, 7: 1289–1295
- Sabella S., Carney R. P., Brunetti V., Malvindi M. A., Al-Juffali N., Vecchio G., Janes S. M., Bakr O. M., Cingolani R., Stellacci F., Pompa P. P. 2014. A general mechanism for intracellular toxicity of metal-containing nanoparticles. *Nanoscale*, 6, 12: 7052, doi:10.1039/C4NR01234H: 10 p.
- Saldaña L., Vilaboa N. 2010. Effects of micrometric titanium particles on osteoblast attachment and cytoskeleton architecture. *Acta Biomaterialia*, 6, 4: 1649–1660
- Saliani M., Jalal R., Goharshadi E. K. 2016. Mechanism of oxidative stress involved in the toxicity of ZnO nanoparticles against eukaryotic cells. *Nanomedicine Journal*, 3, 1: 1–14
- Salloum Z., Lehoux E. A., Harper M. E., Catelas I. 2018. Effects of cobalt and chromium ions on oxidative stress and energy metabolism in macrophages in vitro. *Journal of Orthopaedic Research*, 36, 12: 3178–3187
- Samorodnitzky-Naveh G. R., Redlich M., Rapoport L., Feldman Y., Tenne R. 2009. Inorganic fullerene-like tungsten disulfide nanocoating for friction reduction of nickel-titanium alloys. *Nanomedicine*, 4, 8: 943–950
- San Miguel S. M., Opperman L. A., Allen E. P., Zielinski J. E., Svoboda K. K. H. 2013. Antioxidant combinations protect oral fibroblasts against metal-induced toxicity. *Archives of Oral Biology*, 58, 3: 299–310
- Santos Genelhu M. C. L., Marigo M., Alves-Oliveira L. F., Cotta Malaquias L. C., Gomez R. S. 2005. Characterization of nickel-induced allergic contact stomatitis associated with fixed orthodontic appliances. *American Journal of Orthodontics and Dentofacial Orthopedics*, 128, 3: 378–381
- Sayes C. M., Wahi R., Kurian P. A., Liu Y., West J. L., Ausman K. D., Warheit D. B., Colvin V. L. 2006. Correlating Nanoscale Titania Structure with Toxicity: A Cytotoxicity and Inflammatory Response Study with Human Dermal Fibroblasts and Human Lung Epithelial Cells. *Toxicological Sciences*, 92, 1: 174–185
- Scharf B., Clement C. C., Zolla V., Perino G., Yan B., Elci S. G., Purdue E., Goldring S., MacAluso F., Cobelli N., Vachet R. W., Santambrogio L. 2014. Molecular analysis of chromium and cobalt-related toxicity. *Scientific reports*, 4: 5729, doi:10.1038/srep05729: 12 p.
- Schiff N., Grosogeat B., Lissac M., Dalard F. 2002. Influence of fluoride content and pH on the corrosion resistance of titanium and its alloys. *Biomaterials*, 23, 9: 1995–2002
- Schmalz G., Langer H., Schweikl H. 1998. Cytotoxicity of dental alloy extracts and corresponding metal salt solutions. *Journal of Dental Research*, 77, 10: 1772–1778
- Service R. F. 2003. Nanomaterials Show Signs of Toxicity. *Science*, 300, 5617: 243–243
- Sfondrini M. F., Cacciafesta V., Maffia E., Massironi S., Scribante A., Albert, G., Biesuz R., Klersy C. 2009. Chromium release from new stainless steel, recycled and nickel-free orthodontic brackets. *The Angle Orthodontist*, 79, 2: 361–367

- Shacter E. 2000. Quantification and Significance of Protein Oxidation in Biological Samples. *Drug Metabolism Reviews*, 32, 4: 307–326
- Shamaa M. S., Mansour M. M. 2019. Long-term assessment of the salivary oxidative stress status during orthodontic treatment with fixed appliances. *Egyptian Dental Journal*, 65, 4: 3151–3157
- Sharan J., Lale S. V, Koul V., Singh S., Mishr, M., Kharbanda O. P. 2017. Applications of Nanomaterials in Dental Science: A Review. Article in *Journal of Nanoscience and Nanotechnology*, 17, 4: 2235-2255
- Sharma V., Anderson D., Dhawan A. 2012. Zinc oxide nanoparticles induce oxidative DNA damage and ROS-triggered mitochondria mediated apoptosis in human liver cells (HepG2). *Apoptosis: An International Journal on Programmed Cell Death*, 17, 8: 852–870
- Shen C., James S. A., De jonge M. D., Turney T. W., Wright P. F. A., Feltis B. N. 2013. Relating Cytotoxicity, Zinc Ions, and Reactive Oxygen in ZnO Nanoparticle–Exposed Human Immune Cells. *Toxicological Sciences*, 136, 1: 120–130
- Shi X., Dalal N. S. 1990. On the hydroxyl radical formation in the reaction between hydrogen peroxide and biologically generated chromium(V) species. *Archives of Biochemistry and Biophysics*, 277, 2: 342–350
- Shojaei T. R., Soltani S., Derakhshani M. 2022. Synthesis, properties, and biomedical applications of inorganic bionanomaterials. In: *Fundamentals of Bionanomaterials*. Barhoum A., Jeevanandam J., Danquah M. K. (eds.). Elsevier: 139-174
- Shrivastava H. Y., Ravikumar T., Shanmugasundaram N., Babu M., Unni Nair B. 2005. Cytotoxicity studies of chromium(III) complexes on human dermal fibroblasts. *Free Radical Biology and Medicine*, 38, 1: 58–69
- Siddiqui M. A., Saquib Q., Ahamed M., Farshori N. N., Ahmad J., Wahab R., Khan S. T., Alhadlaq H. A., Musarrat J., Al-Khedhairi A. A., Pant A. B. 2015. Molybdenum nanoparticles-induced cytotoxicity, oxidative stress, G2/M arrest, and DNA damage in mouse skin fibroblast cells (L929). *Colloids and Surfaces B: Biointerfaces*, 125: 73–81
- Sies H. 2020. Oxidative Stress: Concept and Some Practical Aspects. *Antioxidants*, 9, 9: 852 doi:10.3390/ANTIOX9090852: 6 p.
- Singh S., Shi T., Duffin R., Albrecht C., van Berlo D., Höhr D., Fubini B., Martra G., Fenoglio I., Borm P. J. A., Schins R. P. F. 2007. Endocytosis, oxidative stress and IL-8 expression in human lung epithelial cells upon treatment with fine and ultrafine TiO₂: Role of the specific surface area and of surface methylation of the particles. *Toxicology and Applied Pharmacology*, 222, 2: 141–151
- Sitte N. 2003. Oxidative Damage to Proteins. In: *Aging at the Molecular Level. Biology of Aging and Its Modulation*, von Zglinicki T. (eds.). Springer: 27-45
- Smith A. D., Levander O. A. 2002. High-throughput 96-well microplate assays for determining specific activities of glutathione peroxidase and thioredoxin reductase. *Methods in Enzymology*, 347: 113–121

- Smith I. K., Vieweller T. L., Thorne C. A. 1988. Assay of Glutathione Reductase in Crude Tissue Homogenates Using 5,5'-Dithiobis(2-nitrobenzoic Acid)'. *Analytical biochemistry*, 175: 408–412
- Smith P. C., Martínez C., Martínez J., McCulloch C. A. 2019. Role of Fibroblast Populations in Periodontal Wound Healing and Tissue Remodeling. *Frontiers in Physiology*, 10, 270, doi: 10.3389/fphys.2019.00270: 11 p.
- Sohm B., Immel F., Bauda P., Pagnout C. 2015. Insight into the primary mode of action of TiO₂ nanoparticles on *Escherichia coli* in the dark. *Proteomics*, 15, 1: 98–113
- Spalj S., Mlacovic Zrinski M., Tudor Spalj V., Ivankovic Buljan Z. 2012. In-vitro assessment of oxidative stress generated by orthodontic archwires. *American Journal of Orthodontics and Dentofacial Orthopedics*, 141, 5: 583–589
- Spitz D. R., Oberley L. W. 2001. Measurement of MnSOD and CuZnSOD Activity in Mammalian Tissue Homogenates. *Current Protocols in Toxicology*, 8, 1: 7.5.1-7.5.11. doi:10.1002/0471140856.TX0705S08: 11 p.
- Staffolani N., Damiani F., Lilli C., Guerra M., Staffolani N. J., Beicastro S., Locci P. 1999. Ion release from orthodontic appliances. *Journal of Dentistry*, 27, 6: 449–454
- Strober W. 1997. Trypan Blue Exclusion Test of Cell Viability. *Current Protocols in Immunology*, 21(1), A.3B.1-A.3B.2, doi:10.1002/0471142735.IMA03BS21: 2 p.
- Strober W. 2001. Trypan Blue Exclusion Test of Cell Viability. *Current Protocols in Immunology*, 11: A.3B.1-A.3B.2., doi:10.1002/0471142735.IMA03BS111: 3 p.
- Su L. J., Zhang J. H., Gomez H., Murugan R., Hong X., Xu D., Jiang F., Peng Z. Y. 2019. Reactive Oxygen Species-Induced Lipid Peroxidation in Apoptosis, Autophagy, and Ferroptosis. *Oxidative Medicine and Cellular Longevity*, 2019: 5080843, doi: 10.1155/2019/5080843: 14 p.
- Suárez-López del Amo F., Garaicoa-Pazmiño C., Fretwurst T., Castilho R. M., Squarize C. H. 2018. Dental implants-associated release of titanium particles: A systematic review. *Clinical Oral Implants Research*, 29, 11: 1085–1100
- Suarez C., Vilar T., Sevilla P., Gil F. J. 2011. In vitro corrosion behaviour of lingual orthodontic archwires. *International Journal of Corrosion*, 132: 1–9
- Sudjalim T., Woods M., Manton D. 2006. Prevention of white spot lesions in orthodontic practice: a contemporary review. *Australian Dental Journal*, 51, 4: 284–289
- Sumimoto H. 2008. Structure, regulation and evolution of Nox-family NADPH oxidases that produce reactive oxygen species. *The FEBS Journal*, 275, 13: 3249–3277
- Sutow E. J., Maillet W. A., Taylor J. C., Hall, G. C. 2004. In vivo galvanic currents of intermittently contacting dental amalgam and other metallic restorations. *Dental Materials*, 20, 9: 823–831
- Suzuki Y. J., Carini M., Butterfield D. A. 2010. Protein Carbonylation. *Antioxidants Redox Signaling*, 12, 3: 323-325
- Takano Y., Taguchi T., Suzuki I., Balis J. U., Yuri K. 2002. Cytotoxicity of Heavy Metals on Primary Cultured Alveolar Type II Cells. *Environmental Research*, 89, 2: 138–145

- Talic N. F. 2011. Adverse effects of orthodontic treatment: A clinical perspective. *Saudi Dental Journal*, 23, 2: 55–59
- Tanaka K., Shimakawa G., Nakanishi S. 2020. Time-of-day-dependent responses of cyanobacterial cellular viability against oxidative stress. *Scientific Reports*, 10, 1: 1–10
- Tandoğan B., Ulusu N. N. 2008. The inhibition kinetics of yeast glutathione reductase by some metal ions. *Journal of Enzyme Inhibition and Medicinal Chemistry*, 22, 4: 489–495
- Tenne R., Margulis L., Genut M., Hodes G. 1992. Polyhedral and cylindrical structures of tungsten disulphide. *Nature*, 360, 6403: 444–446
- Teo W. Z., Chng E. L. K., Sofer Z., Pumera M., 2014. Cytotoxicity of exfoliated transition-metal dichalcogenides (MoS₂, WS₂, and WSe₂) is lower than that of graphene and its analogues. *Chemistry - An European Journal*, 20, 31: 9627-9632
- Terpilowska S., Siwicka-Gieroba D., Krzysztof Siwicki A. 2018. Cell Viability in Normal Fibroblasts and Liver Cancer Cells After Treatment with Iron (III), Nickel (II), and their Mixture. *Journal of Veterinary Research*, 62, 4: 535-542
- Terpilowska S., Siwicki A. K. 2018. Interactions between chromium(III) and iron(III), molybdenum(III) or nickel(II): Cytotoxicity, genotoxicity and mutagenicity studies. *Chemosphere*, 201: 780–789
- Terpilowska S., Siwicki A. K. 2019. Pro- and antioxidant activity of chromium(III), iron(III), molybdenum(III) or nickel(II) and their mixtures. *Chemico-Biological Interactions*, 298: 43–51
- Tetz L. M., Kamau P. W., Cheng A. A., Meeker J. D., Loch-Carus R. 2013. Troubleshooting the dichlorofluorescein assay to avoid artifacts in measurement of toxicant-stimulated cellular production of reactive oxidant species. *Journal of Pharmacological and Toxicological Methods*, 67, 2: 56–60
- Thievensen I., Thompson P. M., Berlemont S., Plevoc, K. M., Plotnikov S. V., Zemljic-Harpf A., Ross R. S., Davidson M. W., Danuse, G., Campbell S. L., Waterman C. M. 2013. Vinculin-actin interaction couples actin retrograde flow to focal adhesions, but is dispensable for focal adhesion growth. *The Journal of Cell Biology*, 202, 1: 163–177
- Thorstenson G. A., Kusy R. P. 2002. Comparison of resistance to sliding between different self-ligating brackets with second-order angulation in the dry and saliva states. *American Journal of Orthodontics and Dentofacial Orthopedics*, 121, 5: 472–482
- Tian K. V., Festa G., Szentmiklósi L., Maróti B., Arcidiacono L., Laganà G., Andreani C., Licoccia S., Senesi R., Cozza P. 2017. Compositional studies of functional orthodontic archwires using prompt-gamma activation analysis at a pulsed neutron source. *Journal of Analytical Atomic Spectrometry*, 32, 7: 1420–1427
- Townsend D. M., Tew K. D., Tapiero H. 2003. The importance of glutathione in human disease. *Biomedicine Pharmacotherapy*, 57, 3–4: 145–155
- Tripathi V. K., Subramaniyan S. A., Hwang I. 2019. Molecular and Cellular Response of Co-cultured Cells toward Cobalt Chloride (CoCl₂)-Induced Hypoxia. *ACS Omega*, 4, 20882–20893

- Tsang H. 2016. EU Harmonises Test Methods for Nickel Release under REACH. SGS Group Management SA.
<https://www.sgs.com/en/news/2016/01/safeguards-02216-eu-harmonises-test-methods-for-nickel-release-under-reach> (18.5.2020)
- Tu B. P., Weissman J. S. 2004. Oxidative protein folding in eukaryotes: mechanisms and consequences. *The Journal of Cell Biology*, 164, 3: 341–346
- Turkez H., Sonmez E., Turkez O., Mokhtar Y. I., Stefano A. D., Turgut G. 2014. The Risk Evaluation of Tungsten Oxide Nanoparticles in Cultured Rat Liver Cells for Its Safe Applications in Nanotechnology. *Brazilian Archives Of Biology And Technology*, 57, 4: 532-541
- Turrens J. F. 2003. Mitochondrial formation of reactive oxygen species. *Journal of Physiology*, 552, 2: 335–344
- Upadhyay D., Panchal M. A., Dubey R. S., Srivastava V. K. 2006. Corrosion of alloys used in dentistry: A review. *Materials Science and Engineering: A*, 432, 1–2: 1–11
- Urban R., Jacobs J., Gilbert J., Galante J. 1994. Migration of corrosion products from modular hip prostheses. Particle microanalysis and histopathological findings. *The Journal of Bone and Joint Surgery. American Volume*, 76, 9: 1345–1359
- Uriu-Adams J. Y., Keen C. L. 2005. Copper, oxidative stress, and human health. *Molecular Aspects of Medicine*, 26, 4–5: 268–298
- Uzunboy S., Demirci Çekiç S., Apak R. 2019. Determination of Cobalt(II)-Hydrogen Peroxide-Induced DNA Oxidative Damage and Preventive Antioxidant Activity by CUPRAC Colorimetry. *Analytical Letters*, 52, 17: 2663–2676
- Valiakhmetov A. Y., Kuchin A. V., Suzina N. E., Zvonarev A. N., Shepelyakovskaya A. O. 2019. Glucose causes primary necrosis in exponentially grown yeast *Saccharomyces cerevisiae*. *FEMS Yeast Research*, 19, 3: 19 doi:10.1093/femsyr/foz019: 19 p.
- Valko M., Morris H., Cronin M. 2005. Metals, Toxicity and Oxidative Stress. *Current Medicinal Chemistry*, 12, 10: 1161–1208
- Valko M., Rhodes C. J., Moncol J., Izakovic M., Mazur M. 2006. Free radicals, metals and antioxidants in oxidative stress-induced cancer. *Chemico-Biological Interactions*, 160, 1: 1–40
- Van Breusegem F., Vranová E., Dat J. F., Inzé D. 2001. The role of active oxygen species in plant signal transduction. *Plant Science*, 161, 3: 405–414
- Vázquez J., González B., Sempere V., Mas A., Torija M. J., Beltran G. 2017. Melatonin reduces oxidative stress damage induced by hydrogen peroxide in *Saccharomyces cerevisiae*. *Frontiers in Microbiology*, 8: 1066, doi:10.3389/fmicb.2017.01066: 14 p.
- Velasco-Ibáñez R., Lara-Carrillo E., Morales-Luckie R. A., Romero-Guzmán E. T., Toral-Rizo V. H., Ramírez-Cardona M., García-Hernández V., Medina-Solís C. E. 2020. Evaluation of the release of nickel and titanium under orthodontic treatment. *Scientific Reports*, 10, 1: 1-10
- Velasco-Ortega E., Jos A., Cameá, A. M., Pato-Mourelo J., Segura-Egea J. J. 2010. In vitro evaluation of cytotoxicity and genotoxicity of a commercial titanium alloy for dental

- implantology. *Mutation Research - Genetic Toxicology and Environmental Mutagenesis*, 702, 1: 17–23
- Verma S., Dhiman S. 2015. Metal Hypersensitivity in Orthodontic Patients. *Journal of Dental Materials and Techniques*, 4, 2: 111-114
- von Fraunhofer J. A. 1997. Corrosion of orthodontic devices. *Seminars in Orthodontics*, 3, 3: 198–205
- Wang X., Roper M. G. 2014. Measurement of DCF fluorescence as a measure of reactive oxygen species in murine islets of Langerhans. *Analytical Methods*, 6, 9: 3019–3024
- Wang Y., Ding L., Yao C., Li C., Xing X., Huang Y., Gu T., Wu M. 2017. Toxic effects of metal oxide nanoparticles and their underlying mechanisms. *Science China Materials*, 60, 2: 93–108
- Wang Y., Su H., Gu Y., Song X., Zhao J. 2017. Carcinogenicity of chromium and chemoprevention: a brief update. *OncoTargets and Therapy*, 10: 4065–4079
- Wang Y., Yao C., Li C., Ding L., Liu J., Dong P., Fang H., Lei Z., Shi G., Wu M. 2015. Excess titanium dioxide nanoparticles on the cell surface induce cytotoxicity by hindering ion exchange and disrupting exocytosis processes. *Nanoscale*, 7, 30: 13105–13115
- Wang Z. L. 2008. Splendid One-Dimensional Nanostructures of Zinc Oxide: A New Nanomaterial Family for Nanotechnology. *ACS Nano*, 2, 10: 1987–1992
- Wataha J. C., Craig R. G., Hanks C. T. 1991. The Release of Elements of Dental Casting Alloys into Cell-culture Medium. *Journal of Dental Research*, 70, 6: 1014–1018
- Wei S., Shao T., Ding P. 2011. Improvement of orthodontic friction by coating archwire with carbon nitride film. *Applied Surface Science*, 257, 24: 10333–10337
- Wendl B., Wiltsche H., Lankmayr E., Winsauer H., Walter A., Muchitsch A., Jakse N., Wendl M., Wendl T. 2017. Metal release profiles of orthodontic bands, brackets, and wires: an in vitro study. *Journal of orofacial orthopedics = Fortschritte der Kieferorthopädie : Organ/official journal Deutsche Gesellschaft für Kieferorthopädie*, 78, 6: 494–503
- Wepner L., Färber H. A., Jaensch A., Weber A., Heuser F., Keilig L., Singer L., Bourauel C. P. 2021. In Vitro Ion Release of Wires in Removable Orthodontic Appliances. *Materials*, 14, 12: 3402, doi:10.3390/ma14123402: 17 p.
- Weydert C. J., Cullen J. J. 2010. Measurement of superoxide dismutase, catalase and glutathione peroxidase in cultured cells and tissue. *Nature Protocols*, 5, 1: 51–66
- Whitesides G. M. 2003. The “right” size in nanobiotechnology. *Nature Biotechnology*, 21, 10: 1161–1165
- WHO (2001). Declaration of Helsinki Ethical Principles for Medical Research Involving Human Subjects. *Bulletin of the World Health Organization*, 79, 4: 373–374
- Widu F., Drescher D., Junker R., Bourauel C. 1999. Corrosion and biocompatibility of orthodontic wires. *Journal of Materials Science: Materials in Medicine*. 10, 5: 275-281
- Wu L., Zhang J., Watanabe W. 2011. Physical and chemical stability of drug nanoparticles. *Advanced Drug Delivery Reviews*, 63, 6: 456–469

- Xue Y., Zhang T., Zhang B., Gong F., Huang Y., Tang M. 2016. Cytotoxicity and apoptosis induced by silver nanoparticles in human liver HepG2 cells in different dispersion media. *Journal of Applied Toxicology*, 36, 3: 352–360
- Yakubov G. E., Macakova L., Wilson S., Windust J. H. C., Stokes J. R. 2015. Aqueous lubrication by fractionated salivary proteins: Synergistic interaction of mucin polymer brush with low molecular weight macromolecules. *Tribology International*, 89: 34-45
- Yamyar S., Daokar S. 2019. Oxidative Stress Levels in Orthodontic Patients and Efficacy of Antioxidant Supplements in Combating Its Effects- A Randomized Clinical Study. *Orthodontic Journal of Nepal*, 9, 2: 29–34
- Yang X., Li J., Liang T., M, C., Zhang Y., Chen H., Hanagata N., Su H., Xu M. 2014. Antibacterial activity of two-dimensional MoS₂ sheets. *Nanoscale*, 6, 17: 10126–10133
- Yin H., Casey P. S., McCall M. J., Fenech M. 2010. Effects of surface chemistry on cytotoxicity, genotoxicity, and the generation of reactive oxygen species induced by ZnO nanoparticles. *Langmuir*, 26, 19: 15399–15408
- Yin J. J., Liu J., Ehrenshaft M., Roberts J. E., Fu P. P., Maso R. P., Zhao B. 2012. Phototoxicity of nano titanium dioxides in HaCaT keratinocytes—Generation of reactive oxygen species and cell damage. *Toxicology and Applied Pharmacology*, 263, 1: 81–88
- Yu K. N., Yoon T. J., Minai-Tehrani A., Kim J. E., Park S. J., Jeong M. S., Ha S. W., Lee J. K., Kim J. S., Cho M. H. 2013. Zinc oxide nanoparticle induced autophagic cell death and mitochondrial damage via reactive oxygen species generation. *Toxicology in Vitro*, 27, 4: 1187–1195
- Yuan P., Zhou Q., Hu X. 2018. The Phases of WS₂ Nanosheets Influence Uptake, Oxidative Stress, Lipid Peroxidation, Membrane Damage, and Metabolism in Algae. *Environmental Science and Technology*, 52, 22: 13543–13552
- Zakrzewski W., Dobrzynski M., Dobrzynski W., Zawadzka-Knefel A., Janecki M., Kurek K., Lubojanski A., Szymonowicz M., Rybak Z., Wiglusz R. J. 2021. Nanomaterials Application in Orthodontics. *Nanomaterials*, 11, 2: 1–19
- Zhang J., Song W., Guo J., Zhang J., Sun Z., Li L., Ding F., Gao M. 2013. Cytotoxicity of different sized TiO₂ nanoparticles in mouse macrophages. *Toxicology and Industrial Health*, 29, 6: 523-533
- Zhang L., Haddouti E. M., Welle K., Burger C., Wirtz D. C., Schildberg F. A., Kabir K. 2020. The Effects of Biomaterial Implant Wear Debris on Osteoblasts. *Frontiers in Cell and Developmental Biology*, 8: 352, doi: 10.3389/fcell.2020.00352: 17 p.
- Zhao Z. 2019. Iron and oxidizing species in oxidative stress and Alzheimer’s disease. *Aging medicine*, 2, 2: 82–87
- Zheng J., Zhou Z. R. 2007. Friction and wear behavior of human teeth under various wear conditions. *Tribology International*, 40, 2: 278–284

ACKNOWLEDGEMENTS

Looking back, I realize that I did a lot of work that took many days that stretched into the evenings, many nights that were far too short, and many weekends without the »weekend part«. But all this outweighs the satisfaction of what I have achieved and the thought that all this time I had people by my side who helped me and supported me.

My deepest gratitude to my mentor, assoc. prof. dr. Borut Poljšak, cannot be put into words. Thank you, Borut! You provided me with mentorship in the truest sense of the word. Your advice, encouragement, conversations, opportunities, time, and moral support have given a young PhD student more than he could have hoped for. While I still adhered to the original dissertation plan, you gave me the freedom and opportunity to independently research scientific topics and implement them in my work. You recognized my aversion to certain expensive research methods and supported my curiosity with your own resources, for which I am very grateful. One can only wish to be mentored by such a person as you, Borut.

The other important person during my research, to whom I am also very grateful, was prof. dr. Polona Jamnik. You put me in charge of the proteomics lab and allowed me to expand my knowledge and learn and develop a wide range of lab techniques. The thought that I could just knock on your office door and ask for help or advice was very welcome. I am very grateful for the many hours you have invested in me and my research.

I would also like to thank all of the researchers I have had the opportunity to work with:

- Assoc. prof. dr. Jasmina Primožič for the help and support during the clinical research study and for the financial support from the J3-2520 project.
- Prof. dr. Radmila Milačič and prof. dr. Jamez Ščančar for the ICP-MS analysis.
- Prof. dr. Darko Makovec and assoc. prof. dr. Slavko Kralj for the characterization of NP.
- Prof. dr. Sue Gibbs for the HGF donation and research collaboration.
- Prof. dr. Mojca Narat for enabling research in her laboratory.

A special thank you goes to Laura for making my 4 year journey so much easier. I would like to take this opportunity to apologize for the late hours, evening meetings, and my mood swings that you had to deal with. Thank you for being there for me. You are simply the best!

Thank you mom and dad for supporting me and believing in me.

Without the other members of "The Submarine" there would be no happy times during my doctoral studies. The morning coffee, lunch, afternoon drinks, and conversations during the day kept me going when things were difficult for me. I would especially like to mention the help of Matej Šergan, who always had a solution to my problem, for which I am very grateful.

ANNEXES

ANNEX A

Ethical approval (0120-523/2018/8)



REPUBLIKA SLOVENIJA
MINISTRSTVO ZA ZDRAVJE

Komisija Republike Slovenije za medicinsko etiko

Vito Kovač, mag. biotehnol.

Zdravstvena fakulteta
Zdravstvena pot 5
1000 Ljubljana

vito.kovac@zf.uni-lj.si

Številka: 0120-523/2018/8

Datum: 24. januar 2019

Zadeva: Ocena etičnosti predložene raziskave

Spoštovani gospod Vito Kovač, mag. biotehnol.

Komisija Republike Slovenije za medicinsko etiko (KME) je dne 8. 11. 2018 (datirano z datumom 12. 11. 2018) od vas prejela vlogo za oceno etičnosti raziskave z naslovom "Oksidativni stres kot posledica ortodontskega zdravljenja z nesnemnimi ortodontskimi aparati".

Raziskava bo potekala v okviru vašega doktorskega študija Bioznanosti iz znanstvenega področja Biotehnologija pod mentorstvom izr. prof. dr. Boruta Poljšaka, dipl. san. inž. in somentorstvom izr. prof. dr. Jasmine Primožič, dr. dent. med.

KME je na seji 11. decembra 2018¹ ugotovila, da je vloga popolna ter raziskava etično sprejemljiva. S tem vam za izvedbo raziskave izdaja svoje soglasje.

P.S.: Pri morebitnih nadaljnjih dopisih v zvezi z raziskavo se obvezno sklicujte na številko tega dopisa.

S spoštovanjem,

Pripravila:
Maja Žejn

dr. Božidar Voljč, dr. med.,
predsednik KME

¹ Seznam članov KME, ki so odločali o vlogi, in izjava, da KME deluje v skladu z zadevnimi zakoni in priporočili, sta na voljo na spletni strani KME (zavihek "Meni", rubrika "Seje").

ANNEX B

Patients consent

Izjava/soglasje

Spoštovani!

Vabimo Vas, da se vključite v pilotno študijo, s katero želimo preučiti oksidativni stres kot posledico zdravljenja z nesnemnimi ortodontskimi aparati. Uporaba ortodontskega aparata (kolikor časa je pač potrebno za zdravljenje z ortodontskim aparatom) lahko zaradi izluževanja kovinskih ionov iz aparata poveča delež prostih radikalov v krvi.

Kratek opis poteka raziskave:

Pred onamestitvijo nesemnega ortodontskega aparata se iz prsta sodelujočega v raziskavi odvzame kapljica kapilarne krvi (50 µL), v kateri se opravi FORT in FORD analiza (določi se celokupen antioksidativen potencial izražen v koncentraciji Troloxa in delež prostih radikalov izražen kot koncentracija H₂O₂) in 1 mL slina, katera se uporabi za AES analizo (določi se koncentracija kovinskih ionov). Nato udeležencu ortodont namesti nesnemni zobni aparat in po 24, 48, 72 urah ter po 7 dneh se vrne kapilarna kri (FORT in FORD) in slina (AES). Tako vzorčenje se ponovi vsak mesec in po treh mesecih se vzorčenje zaključí. Ortodontski aparat se sname po uspešnem zdravljenju. Vsak sodelujoči je zaprosen, da izpolni še anonimni vprašalnik o življenjskih navadah, ki vplivajo na stanje oksidativnega stresa.

Sodelovanje v raziskavi je anonimno. V izogib upravljanju z osebnimi podatki, bo posameznik sodelujoč v raziskavi ustrezno kodiran, prav tako tudi osebni podatki posameznika.

Rezultati bodo obdelani in predstavljeni izključno v sumarni obliki. Rezultatov posameznega udeleženca tako ne bo mogoče pridobiti.

Sodelovanje posameznika je prostovoljno in lahko od nje kadarkoli, brez kakršnih koli posledic odstopi.

S spodnjim podpisom izkažete strinjanje, da ste pripravljeni sodelovati v predstavljeni raziskavi.

S spoštovanjem,

Ime in priimek:

Podpis

Datum:

ANNEX C

Questionnaire

Vprašalnik za ugotavljanje oksidativnega stresa

I. Splošni podatki o udeležencu (-ki) preizkusa:

Šifra udeleženca (-ke) /izpolni vodja testiranja/:

1. Starost: _____ let
2. Spol: M - moški, Ž – ženski

II. Splošno počutje in zadovoljstvo

1. Kako ocenjujete svoje splošno počutje oz. zdravstveno stanje?
 - a) sem popolnoma zdrav in sem v dobri kondiciji
 - b) počutim se dobro
 - c) ne počutim se preveč dobro (brez energije...)
 - d) počutim se bolnega
2. Kako ste zadovoljni s svojim življenjem?
 - a) večinoma sem zelo zadovoljen
 - b) zadovoljen sem
 - c) nisem prav zadovoljen, a tudi ne nezadovoljen
 - d) nezadovoljen sem
 - e) večinoma sem zelo nezadovoljen
3. Svoje delo (poklicne, študijske ali druge delovne obveznosti) občutim kot:
 - a) zelo stresno
 - b) stresno
 - c) malo stresno
 - d) nestresno

III. Funkcionalno zdravje

Prosimo, odgovorite na vprašanja, tako da obkrožite črke a, b ali c pred odgovorom, ki vam najbolj ustreza.

Prebava

1. Imate slabo prebavo? A) pogosto B) včasih C) redko ali nikoli
2. Vas napenja in imate vetrove? A) pogosto B) včasih C) redko ali nikoli
3. Ste po zaužitem obroku zaspani? A) pogosto B) včasih C) redko ali nikoli
4. Imate sindrom
razdražljivega črevesja (diareja)?..... A) pogosto B) včasih C) redko ali nikoli

Srce in obtočila

5. Kakšen je vaš
krvni pritisk? A) 140/90 ali višji B) med 125/85 in 140/90 C)
nižji kot 125/80
6. Se hitro zadihate? A) pogosto B) včasih C) redko ali nikoli
7. So vaše roke in noge mrzle? A) pogosto B) včasih C) redko ali nikoli
8. Je zdravnik ugotovil,
da imate slabo prekrvavitev?..... A) pogosto B) včasih C) redko ali nikoli
9. Koliko članov vaše družine (starši, stari starši, tete, strici)
je umrlo zaradi bolezni srca in ožilja? A) trije ali več B) dva C) eden ali nobeden

Imunski sistem

10. Kolikokrat na leto ste prehlajeni? A) trikrat ali večkrat B) dvakrat C) enkrat ali nikoli
11. Koliko dni navadno trajajo izraziti simptomi prehlada? A) tri dni ali dlje B) dva dneva C) en dan ali nič
12. Povprečno kolikokrat na leto jemljete antibiotike? A) dvakrat ali večkrat B) enkrat C) nikoli
13. Imate pogosta vnetja, ki jih spremljajo bolečine in pordelost? A) da C) ne
14. Imate pogoste alergijske reakcije? A) da B) občasno C) ne

Duševno zdravje

15. Se težje zberete, kot ste se nekoč? A) pogosto B) včasih C) redko ali nikoli
16. Si težje zapomnite stvari kot pred časom? ... A) pogosto B) včasih C) redko ali nikoli
17. Ste kdaj depresivni? A) pogosto B) včasih C) redko ali nikoli
18. Se vas kdaj polaščajo občutki strahu in tesnobe? A) pogosto B) včasih C) redko ali nikoli

Hormonski sistem

19. Imate pogosto močno željo po sladkih prigrizkih ali poživilih? A) pogosto B) včasih C) redko ali nikoli
20. Bi svoj način življenja označili kot stresen? A) pogosto B) včasih C) redko ali nikoli
21. Morate nov dan začeti s poživilom ali sladkim prigrizkom? A) pogosto B) včasih C) redko ali nikoli

Koža, nohti in lasje

22. Imate suho kožo? A) pogosto B) včasih C) redko ali nikoli
23. Imate akne? A) pogosto B) včasih C) redko ali nikoli
24. Imate izpuščaje, luskavico ali dermatitis? .. A) pogosto B) včasih C) redko ali nikoli
25. So vaši nohti krhki in razpokani? A) pogosto B) včasih C) redko ali nikoli
26. Imate mastne oziroma suhe in krhke lase? . A) pogosto B) včasih C) redko ali nikoli

Telesna kondicija

27. Povprečno kolikokrat na teden ste telesno dejavni? A) redko ali nikoli B) enkrat C) dvakrat ali večkrat
28. Kolikokrat si med telesnimi napori pretegnete mišice? A) pogosto B) včasih C) redko ali nikoli
29. Ali ponoči spite manj kot 6 ur in pol? A) pogosto B) včasih C) redko ali nikoli
30. Kako pogosto ste utrujeni? A) pogosto B) včasih C) redko ali nikoli
31. Ali sami menite, da imate dobro telesno kondicijo? A) redko ali nikoli B) včasih C) pogosto

Splošna zdravstvena slika

32. Kolikokrat na leto obiščete zdravnika? A) dvakrat ali pogosteje B) enkrat C) nobenkrat

33. Povprečno kolikokrat na leto jemljete zdravila,
predpisana z receptom? A) dvakrat ali pogosteje B) enkrat C)
nobenkrat
34. Ali...? A) ste debeli B) imate prekomerno telesno težo C) imate
idealno telesno težo
35. Ste bili kot otrok pogosto bolni? A) pogosto B) včasih C) redko ali nikoli
36. Imate kake kronične zdravstvene težave?.... A) da C) ne

Točkovalnik ankete o funkcionalnem zdravju

Najvišje število možnih točk je 72. Odgovor na vsako vprašanje v anketnem vprašalniku se vrednoti z vrednostmi od 0 do 2 in sicer:

- odgovor »pogosto« 2 točki,
- odgovor »včasih« 1 točko in
- odgovor »redko ali nikoli« 0 točk.

Od 0 do 15 točk:

Ste funkcionalno zdravi in imate dovolj rezerve za prilagajanje stresnim dogajanjem v življenju. Bodite pozorni na odgovore, pri katerih ste zbrali veliko število točk.

Od 16 do 30 točk:

Vaše zdravje je nekoliko boljše od povprečnega, a še vedno ni optimalno. Čas je, da naredite korak naprej ter izboljšate način življenja in prehrane.

Od 31 do 50 točk:

Vaše zdravje je povprečno slabo. Če ne boste nemudoma ukrepali, ga boste spodkopali še bolj in lahko računate na težave, ki se bodo pokazale pozneje v življenju. Obiščite strokovnjaka za prehrano in pazite, kaj pojedete in popijete.

Od 51 do 72 točk:

Ste »vertikalni bolnik« in kmalu boste postali »horizontalni«, če ne boste v svoj način življenja in prehrane uvedli nekaj sprememb. Posvetujte se s strokovnjakom za prehrano, ta vam bo svetoval, s katero hrano in prehranskimi dodatki boste spet vzpostavili dobro zdravje.¹

Doseženo število točk:

¹ Holford, P.: 100 % Zdravi (Prevod dela: 100 % Health).- Ljubljana: MLadinska knjiga, 2000, str. 21

IV. Test kazalcev toksemije

Prosimo, odgovorite še na naslednja vprašanja. Nekatera so podobna tistim, na katera ste odgovorili v predhodnem testu. Naj vas to ne moti. Ta test je osredotočen na stanje v mesecu tik pred začetkom poizkusa, predhodni pa je zajemal splošno stanje funkcionalnega zdravja udeleženca (-ke).

Obkrožite ustrezne odgovore

	Znaki toksemije (zastajanja strupov v telesu)	Intenzivnost pojava		
		* enkrat tedensko ali pogosteje	** 1-2 krat mesečno	***manj kot 1 krat mesečno
1.	“Nejasna” glava	a) pogosto*	b) včasih**	c) redko/nikoli** *
2.	Nezmožnost zbrati se	a) pogosto	b) včasih	c) redko/nikoli
3.	Vzkipljivost	a) pogosto	b) včasih	c) redko/nikoli
4.	Vznemirjen želodec	a) pogosto	b) včasih	c) redko/nikoli
5.	Kronično zaprtje ali pogoste driske	a) pogosto	b) včasih	c) redko/nikoli
6.	Otrdelost v predelu ramen (lopatice)	a) pogosto	b) včasih	c) redko/nikoli
7.	Črno (temno) blato	a) pogosto	b) včasih	c) redko/nikoli
8.	Smrdeče blato	a) pogosto	b) včasih	c) redko/nikoli
9.	Neprijeten telesni vonj	a) pogosto	b) včasih	c) redko/nikoli
10.	Kronična utrujenost	a) pogosto	b) včasih	c) redko/nikoli
11.	Občutek staranja	a) pogosto	b) včasih	c) redko/nikoli
12.	Potreba po veliko spanja	a) pogosto	b) včasih	c) redko/nikoli
13.	Nespečnost	a) pogosto	b) včasih	c) redko/nikoli
14.	Uvela, postarana koža	a) precej	b) nekoliko	c) malo/nič
15.	Gube na obrazu	a) precej	b) nekoliko	c) malo/nič
16.	Zasvojenost s sladkarijami, kavo, cigareti, škrobnimi živili...	a) precej	b) nekoliko	c) malo/nič
17.	Prenajedanje	a) pogosto	b) včasih	c) redko/nikoli
18.	Pomanjkanje teka	a) pogosto	b) včasih	c) redko/nikoli
19.	Hranjenje iz navade ali “za moč”	a) pogosto	b) včasih	c) redko/nikoli
20.	Glavobol pri zburanju	a) pogosto	b) včasih	c) redko/nikoli

21.	Glavobol, ki nastane, ko smo izpustili obrok, in mine, ko se najemo	a) pogosto	b) včasih	c) redko/nikoli
22.	Zamašen nos ob zbujanju	a) pogosto	b) včasih	c) redko/nikoli
23.	Katar v grlu ob zbujanju	a) pogosto	b) včasih	c) redko/nikoli
24.	Kisel, grenak ali slan okus v ustih ob zbujanju	a) pogosto	b) včasih	c) redko/nikoli
25.	Krmežljave oči ob zbujanju	a) pogosto	b) včasih	c) redko/nikoli
26.	Zamašena ušesa ob zbujanju	a) pogosto	b) včasih	c) redko/nikoli
27.	Zadah iz ust (ko se zbudimo ali pozneje)	a) pogosto	b) včasih	c) redko/nikoli
28.	Obložen jezik	a) pogosto	b) včasih	c) redko/nikoli
29.	Motne, krvave oči	a) pogosto	b) včasih	c) redko/nikoli
30.	Vrtoglavost, omotičnost	a) pogosto	b) včasih	c) redko/nikoli

Točkovanje:

“pogosto” = 2 točki,

“včasih” = 1 točka,

“redko/nikoli” = 0 točk.

Skupno točk: _____

V. Fizični dejavniki zdravja

1. Koliko **vode** in svežih sokov popijete dnevno (ne čajev ali drugih napitkov):

- nič (največ 1 dcl)
- več kot 0,1 do 0,5 litra
- več kot 0,5 do 1,0 litra
- več kot 1,0 do 1,5 litra
- več kot 1,5 do 2,0 litra

f) več kot 2 litra (navedite koliko): _____ l

2. Koliko časa dnevno porabite za naslednje aktivnosti v običajnem (delovnem) dnevu:

	manj kot 15 min	0,5 ure	1 uro	1,5 ure	2 uri	2,5 ure ali več
--	-----------------	---------	-------	---------	-------	-----------------

Vrednotenje rezultatov testa kazalcev toksemije

Čim višji je rezultat, tem višja je raven toksemije – zastajanja strupov v organizmu.

Dr. Ostan priporoča naslednjo kategorizacijo rezultatov:

- 0 točk ali 1 točka: brez znakov toksemije,
- od 2 do 10 točk: nizka toksemija
- od 11 do 24 točk: srednja toksemija
- od 25 do 42 točk: visoka toksemija
- od 43 do 60 točk: zelo visoka toksemija

Zaradi zastajanja strupov v telesu nastajajo mnoge bolezni. Zato je se z višanjem ravni toksemije povečuje možnost obolenj.

Za telesno gibanje (intenzivna hoja, tek, delo na vrtu...)	x	x	x	x	x	x
Bivanje na zraku	x	x	x	x	x	x
Bivanje na sončni svetlobi (ne v avtu ipd)	x	x	x	x	x	x

3. Sredi dneva si privoščim počitek oz. sprostitvev:

- a) vsak dan /pogosto b) včasih c) redko/nikoli

6. Običajno (če nimam nočne izmene...) grem spat

- a) pred 22. uro
b) med 22. in 23. uro
c) med 23. in 24. uro
d) med polnočjo in eno uro
e) po eni uri zjutraj

7. Običajno spim _____ ur dnevno.

8. Moje spanje je praviloma:

- a) dobro (spim globoko in se zbudim spočit-a)
b) slabo

9. Ali ste se zadnja 2 dneva ukvarjali s športom. Navedite s katerim, kako intenzivno in koliko časa: _____

10. Ali kadite? Da, ne

Koliko cigaret na dan? _____

VI. Prehrana

1. Koliko obrokov hrane užijete dnevno:

- a) en b) dva c) tri d) štiri e) pet f) šest ali več

2. Moj glavni (največji) obrok je:

- a) zajtrk
b) kosilo
c) večerja
d) kosilo in večerja združena v enem obroku
e) drugo : _____

3. Spat grem s polnim želodcem:

- a) vsak dan /pogosto b) včasih c) redko d) nikoli

4. Moja prehrana je:

- a) mešana
b) vegetarijanska

- c) veganska (samo hrana rastlinskega izvora)
- d) presna (samo hrana, ki ni toplotno obdelana)
- e) drugo (navedite) _____

5. **Meso** (vključno mesnini izdelki in ribami) jem:

- a) vsak dan v več obrokih
- b) vsak dan v enem od obrokov
- c) večkrat na teden
- d) redko (enkrat na teden ali redkeje)
- e) nikoli.

6. **Surovo sadje in zelenjavo** uživam:

- a) 5 krat na dan ali več
- b) 2 - 4 krat na dan
- c) enkrat dnevno
- d) nekajkrat na teden
- e) redko/ ne uživam

7. **Surova hrana** (sadje, zelenjava, jedrca...) predstavlja v moji prehrani:

- a) veliko večino ali celoto
- b) večino
- c) polovico
- d) manjši del
- e) zelo majhen del ali nič

8. **Sveže** stisnjene sadne ali zelenjavne **sokove** uživam:

- a) vsak dan
- b) nekajkrat tedensko
- e) včasih
- f) nikoli (zelo redko)

9. Moja prehrana je:

- a) pestra,
- b) enolična/ pomanjkljiva.

10. Običajno jem:

- a) preveč,
- b) ravno pravo količino,
- c) premalo.

11. Sladkarije (npr. čokolado, kekse, slaščice...) uživam:

- a) vsak dan
- b) večkrat na teden
- c) enkrat na teden
- d) včasih/ redko
- e) nikoli

12. Kako pogosto se odločate za čistilne prehranske dneve oz. shujševalne kure?

	Vrsta prehranskega režima	Za to vrsto omejevalne prehrane se odločam:		
1.	Shujševalni dnevi (tudi s kuhano hrano)	a) pogosto (enkrat mesečno ali pogosteje)	b) včasih	c) redko/nikoli

2.	Čistilni dnevi s surovim sadjem in zelenjavo	a) pogosto	b) včasih	c) redko/nikoli
3.	Post ob svežih sokovih ali vodi	a) pogosto	b) včasih	c) redko/nikoli

13. Prehranske dodatke (npr. vitamine, minerale) uživam:

a) vsak dan b) vsak teden (enkrat ali nekajkrat) c) včasih/redko d) ne uživam jih.

Navedite katere: _____

VII. Drugi dejavniki zdravja

1. Kako pogosto užijete naslednje snovi?

Vrsta snovi	Pogostnost			
Kava	a) vsak dan _____ skodelic	b) vsak teden (vsaj enkrat)	c) včasih/redko	d) nikoli
Črni ali zeleni čaj	a) vsak dan _____ skodelic	b) vsak teden (vsaj enkrat)	c) včasih/redko	d) nikoli
Alkoholne pijače	a) vsak dan _____ enot*	b) vsak teden	c) včasih/redko	d) nikoli
Kajenje	a) vsak dan _____ cigaret	b) vsak teden	c) včasih/redko	d) nikoli
Zadrževanje v zakajenem prostoru	a) vsak dan _____ ur	b) vsak teden	c) včasih/redko	d) nikoli
Zdravila	a) vsak dan _____ tablet	b) vsak teden	c) včasih/redko	d) nikoli
Dodatki k prehrani	a) vsak dan _____ tablet	b) vsak teden	c) včasih/redko	d) nikoli
Kontracepcijske tablete	DA/NE			

Opomba: * ena enota alkohola=1dcl vina=0,3 dcl žgane pijače= 3 dcl piva

Telesna višina: _____ cm Telesna teža : _____ BMI (teža v kg / (višina v m)²) _____
 (od 18,5 do 24,9 = normalno; 30 in več = debelost)

Ali imate trenutno menstruacijo DA...NE..

Datum: _____

2 .Morebitni predlogi, pripombe, komentarji:

Zahvaljujemo se vam, da ste sodelovali v preizkusu. Prosimo, oddajte vprašalnik enemu od nosilcev študije. Včasih se po preizkusu pojavi potreba, da udeležencu postavimo še kakšno vprašanje. Če nimate nič proti, vas zato prosimo, da napišete svoje ime in priimek ter naslov. Ti podatki bodo na voljo le nosilcem raziskave, rezultati testiranja pa bodo uporabljeni le v študijske namene.

Ime in priimek: _____

Naslov:

e-naslov: _____

tel.

Datum: _____

ANNEX D

ICP-MS operating parameters

Parameter	Type/Value
<i>Sample introduction</i>	
Nebuliser	Miramist
Spray chamber	Scott
Skimmer and sampler	Ni
<i>Plasma conditions</i>	
Forward power	1550 W
Plasma gas flow (Ar)	15.0 L/min
Carrier gas flow (Ar)	1.05 L/min
Dilution gas flow (Ar)	0.10 L/min
Collision gas flow (He)	4.5 mL/min
Oct bias	-100 V
Cell entrance	-100 V
Cell exit	-150 V
Deflect	-75 V
Plate bias	-150 V
Sample uptake rate	0.3 mL/min
<i>Data acquisition parameters</i>	
Isotopes monitored	^{47}Ti , ^{52}Cr , ^{56}Fe , ^{59}Co , ^{60}Ni , ^{95}Mo
Isotopes of internal standards	^{72}Ge , ^{103}Rh

ANNEX E

Release of metal ions from SS, Ni-Ti, β -Ti and Co-Cr alloys

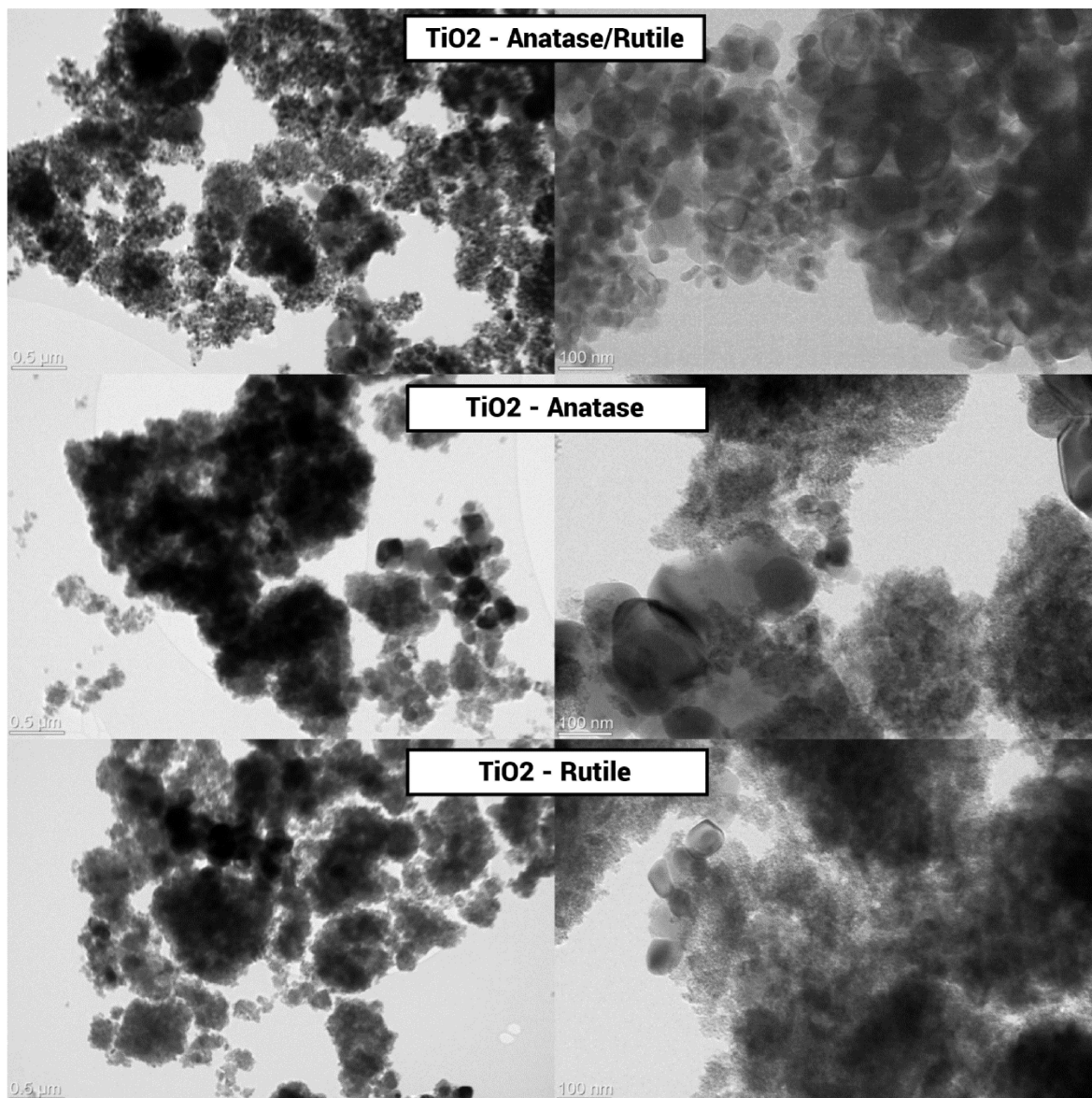
Stainless steel archwire (Damon - Ormco, USA)	Ti (ng/mL)	Cr (ng/mL)	Fe (ng/mL)	Co (ng/mL)	Ni (ng/mL)	Mo (ng/mL)
12 h	<0.1	0.36	3.59	<0.01	0.50	<0.05
24 h	<0.1	<0.05	2.28	<0.01	<0.05	<0.05
48 h	<0.1	0.23	3.00	<0.01	0.36	<0.05
7 days	<0.1	0.22	6.14	<0.01	0.21	<0.05
30 days	<0.1	0.25	6.36	<0.01	0.23	<0.05
60 days	<0.1	0.17	7.41	<0.01	<0.05	<0.05
90 days	<0.1	0.58	13.36	<0.01	2.11	<0.05
Ni-Ti archwire (rematitan® super elastic - Dentaurum, Germany)	Ti (ng/mL)	Cr (ng/mL)	Fe (ng/mL)	Co (ng/mL)	Ni (ng/mL)	Mo (ng/mL)
12 h	0.73	<0.05	<0.1	<0.01	0.73	<0.05
24 h	0.50	<0.05	<0.1	<0.01	1.43	<0.05
48 h	1.87	<0.05	<0.1	<0.01	2.22	<0.05
7 days	1.30	<0.05	<0.1	<0.01	3.01	<0.05
30 days	/	/	/	/	/	/
60 days	2.74	<0.05	<0.1	<0.01	6.10	<0.05
90 days	9.59	<0.05	<0.1	<0.01	12.97	<0.05
Ni-Ti archwire (Biostarter® - Forestadent, Germany)	Ti (ng/mL)	Cr (ng/mL)	Fe (ng/mL)	Co (ng/mL)	Ni (ng/mL)	Mo (ng/mL)
12 h	0.52	<0.05	<0.1	<0.01	24.59	<0.05
24 h	0.50	<0.05	<0.1	<0.01	41.81	<0.05
48 h	2.28	<0.05	<0.1	<0.01	60.62	<0.05
7 days	<0.1	<0.05	<0.1	<0.01	44.23	<0.05
30 days	5.27	<0.05	<0.1	<0.01	94.03	<0.05
60 days	10.07	<0.05	<0.1	<0.01	131.93	<0.05
90 days	9.53	<0.05	<0.1	<0.01	116.66	<0.05

Ti-Mo archwire (rematitan® SPECIAL - Dentaurum, Germany)		Ti (ng/mL)	Cr (ng/mL)	Fe (ng/mL)	Co (ng/mL)	Ni (ng/mL)	Mo (ng/mL)
12 h		<0.1	<0.05	<0.1	<0.01	<0.05	<0.05
24 h		1.04	<0.05	<0.1	<0.01	<0.05	<0.05
48 h		1.64	<0.05	<0.1	<0.01	<0.05	<0.05
7 days		0.76	<0.05	<0.1	<0.01	<0.05	<0.05
30 days		2.39	<0.05	<0.1	<0.01	<0.05	<0.05
60 days		1.12	<0.05	<0.1	<0.01	<0.05	<0.05
90 days		8.26	<0.05	<0.1	<0.01	<0.05	0.45
Co-Cr-Ni archwire (Elgiloy® - Rocky Mountain Orthodontics, USA)		Ti (ng/mL)	Cr (ng/mL)	Fe (ng/mL)	Co (ng/mL)	Ni (ng/mL)	Mo (ng/mL)
12 h		<0.1	0.16	1.27	6.21	0.90	0.27
24 h		<0.1	0.42	4.59	9.43	2.02	0.78
48 h		<0.1	0.85	8.29	14.49	3.79	1.28
7 days		<0.1	0.52	4.08	13.54	3.37	1.02
30 days		<0.1	1.23	11.68	24.74	6.80	1.95
60 days		<0.1	1.58	13.84	30.46	8.29	2.47
90 days		<0.1	1.66	13.77	31.45	8.55	2.54
Co-Cr-Ni archwire (Remaloy® - Dentaurum, Germany)		Ti (ng/mL)	Cr (ng/mL)	Fe (ng/mL)	Co (ng/mL)	Ni (ng/mL)	Mo (ng/mL)
12 h		<0.1	<0.05	<0.1	8.96	1.86	<0.05
24 h		<0.1	0.34	1.42	13.27	3.77	<0.05
48 h		<0.1	0.92	6.67	13.38	3.94	<0.05
7 days		<0.1	0.42	1.62	17.02	5.06	<0.05
30 days		<0.1	1.22	4.74	28.68	10.14	<0.05
60 days		<0.1	1.40	6.80	31.56	11.07	<0.05
90 days		<0.1	1.15	4.66	28.98	9.09	<0.05

Stainless steel brackets (Discovery® Dentaurum, Germany)		Ti (ng/mL)	Cr (ng/mL)	Fe (ng/mL)	Co (ng/mL)	Ni (ng/mL)	Mo (ng/mL)
	-	<0.1	0.82	8.27	<0.01	1.10	<0.05
12 h		<0.1	0.82	8.27	<0.01	1.10	<0.05
24 h		<0.1	1.05	13.96	<0.01	1.72	0.15
48 h		<0.1	2.64	39.45	<0.01	4.19	0.70
7 days		<0.1	1.99	70.07	<0.01	3.89	0.47
30 days		<0.1	4.50	126.48	<0.01	10.07	1.25
60 days		<0.1	6.36	178.31	<0.01	22.29	1.66
90 days		<0.1	6.92	200.25	<0.01	37.03	1.83
Stainless steel molar bands (W-Fit Forestadent, Germany)		Ti (ng/mL)	Cr (ng/mL)	Fe (ng/mL)	Co (ng/mL)	Ni (ng/mL)	Mo (ng/mL)
	Form	<0.1	1.01	23.02	<0.01	1.85	<0.05
12 h		<0.1	1.01	23.02	<0.01	1.85	<0.05
24 h		<0.1	3.73	36.85	<0.01	4.01	<0.05
48 h		<0.1	1.52	45.30	<0.01	3.45	<0.05
7 days		<0.1	7.01	67.99	<0.01	7.67	<0.05
30 days		<0.1	2.72	70.64	<0.01	6.59	<0.05
60 days		<0.1	3.13	70.84	<0.01	7.73	<0.05
90 days		<0.1	7.44	113.98	<0.01	11.31	<0.05

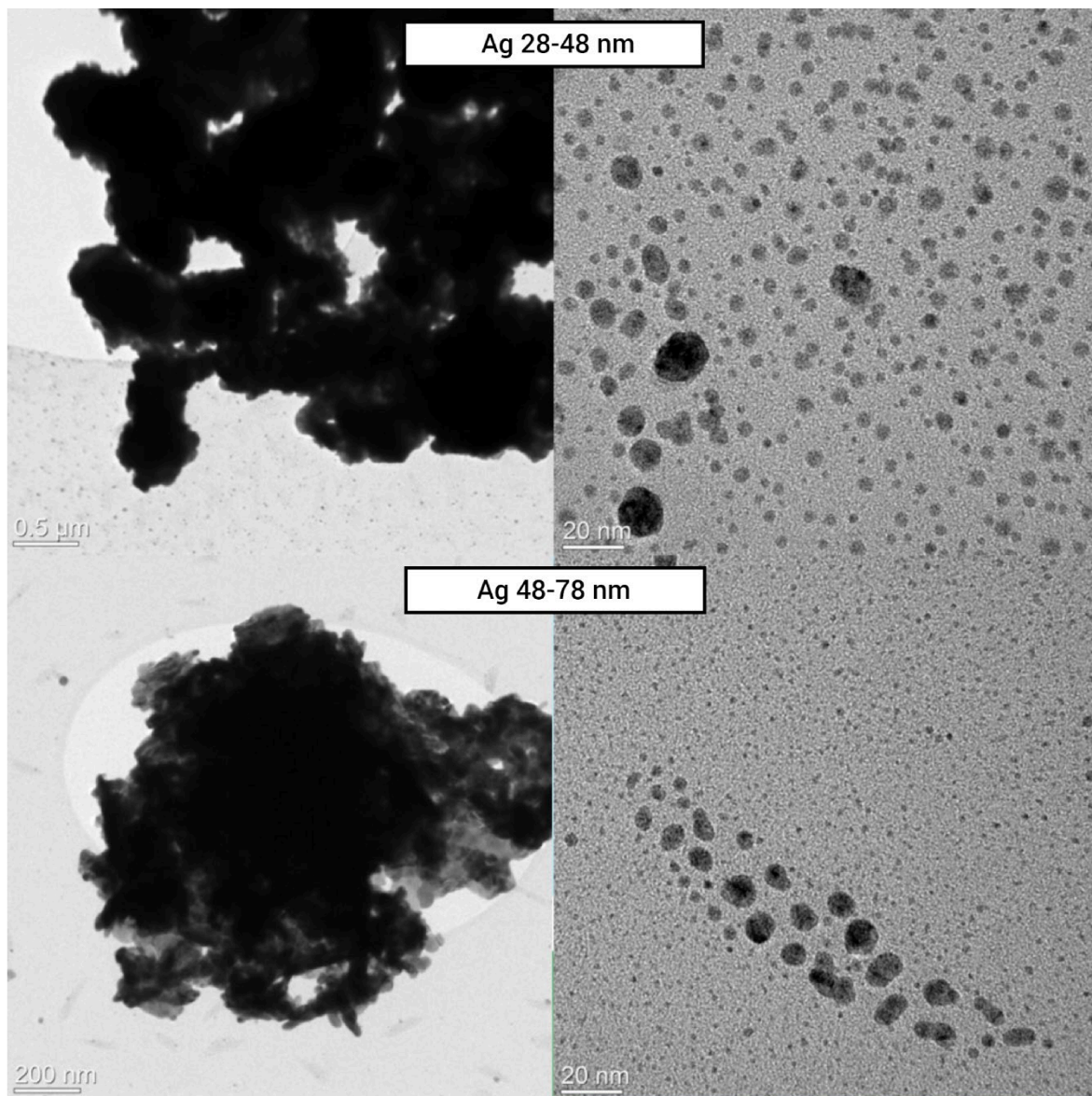
ANNEX F

TEM pictures of TiO₂ NP



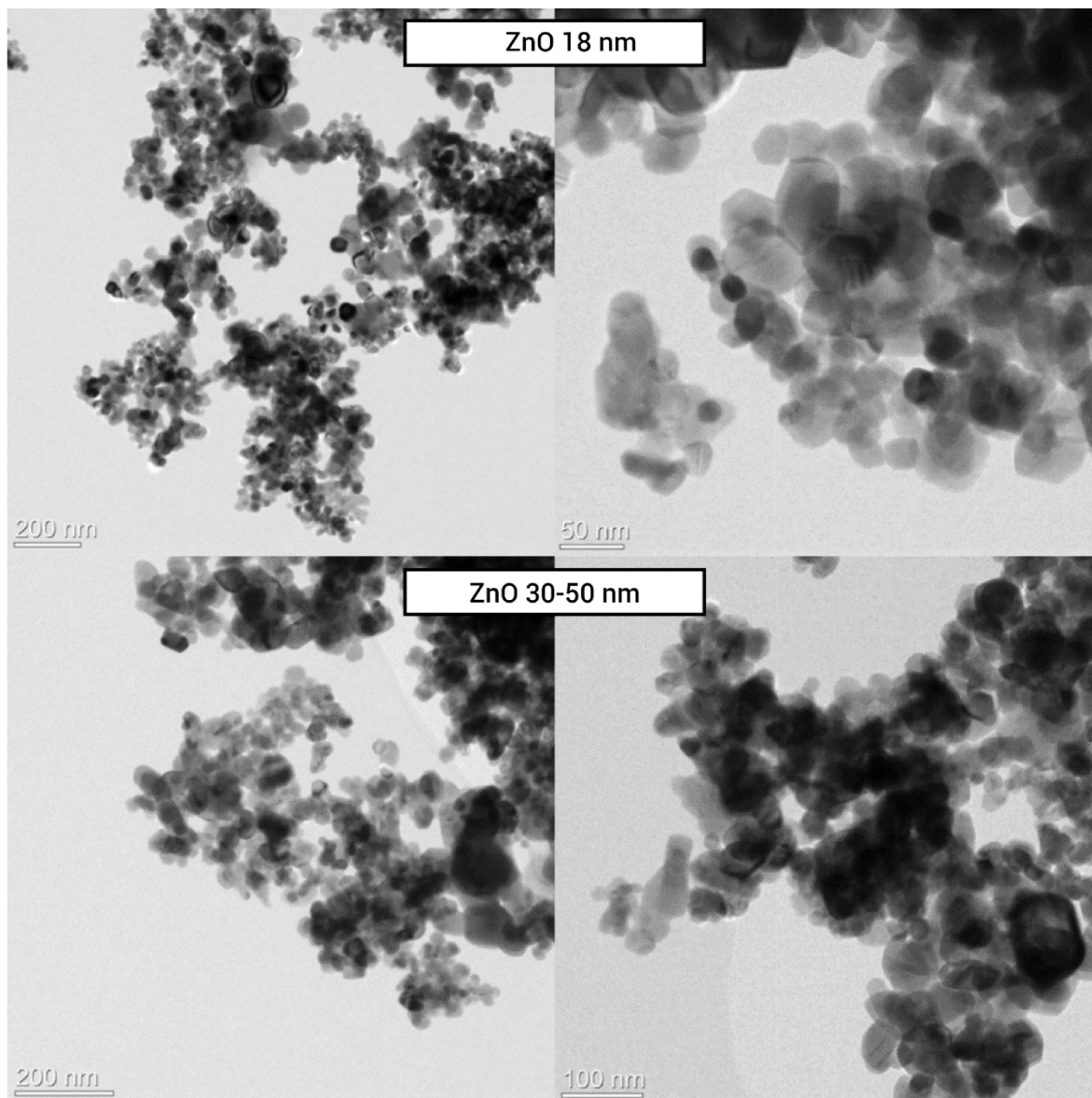
ANNEX G

TEM pictures of Ag-NP



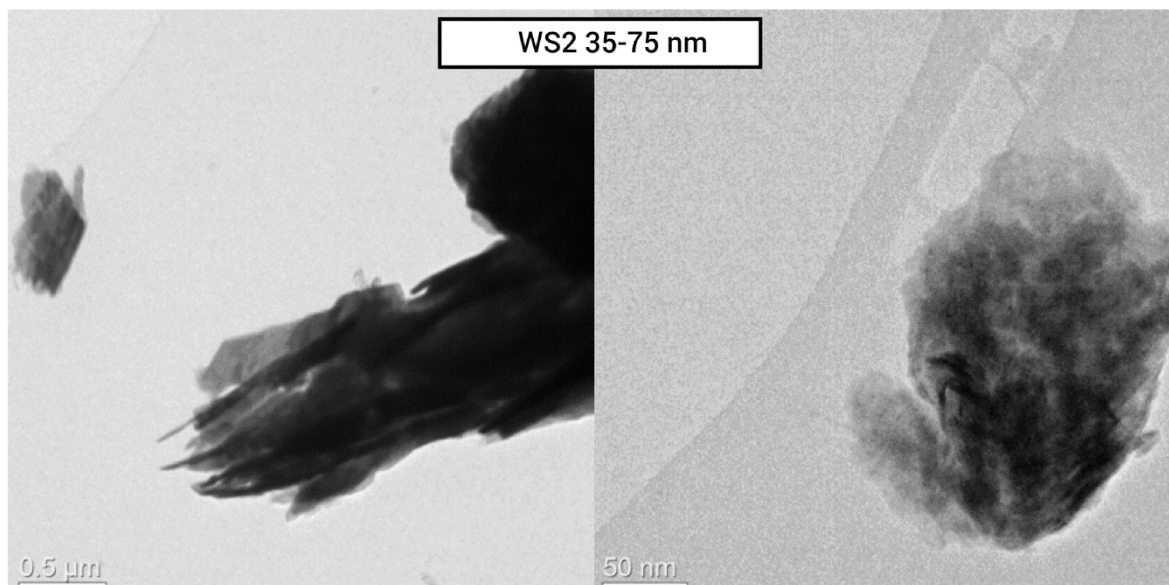
ANNEX H

TEM pictures of ZnO-NPs



ANNEX I

TEM pictures of WS₂-NPs



ANNEX J

Consent from publisher Hindawi for the re-publication of article in the print and electronic versions of the doctoral dissertation

Dear Dr Kovač,

Thank you for your query.

All our journals are open access (<http://about.hindawi.com/authors/open-access/>), including *BioMed Research International*. All articles are published under the Creative Commons Attribution License (<https://creativecommons.org/licenses/by/4.0/>), which permits unrestricted use, distribution, and reproduction in any medium, provided the original work is properly cited.

You are free to reuse this article with proper citation and attribution of the Hindawi article, making it clear that the original publication is free to access under the CC-BY 4.0 licence. If a figure is indicated to be from previous copyrighted work, you should seek permission from the copyright holder of the original publication that included the figure.

You can see how to cite the article at: <https://www.hindawi.com/journals/bmri/2019/5063565/>

Please let me know if you have any further questions.

Best regards,
Ramya

Ramya Kabali

Research Integrity Team Leader

e. ramya.kabali@hindawi.com



Hindawi

Hindawi.com | [Twitter](#) | [Facebook](#) | [LinkedIn](#) | [YouTube](#)

ANNEX K

Published article Kovač et al., 2019

Hindawi
BioMed Research International
Volume 2019, Article ID 5063565, 6 pages
<https://doi.org/10.1155/2019/5063565>



Research Article

Systemic Level of Oxidative Stress during Orthodontic Treatment with Fixed Appliances

Vito Kovac,¹ Borut Poljsak,¹ Giuseppe Perinetti ,² and Jasmina Primozic ³

¹Faculty of Health Sciences, University of Ljubljana, Slovenia

²Private Practice, Nocciano (PE), Italy

³Medical Faculty, University of Ljubljana, Slovenia

Correspondence should be addressed to Jasmina Primozic; jasminaprimozic@gmail.com

Received 1 March 2019; Revised 8 April 2019; Accepted 24 April 2019; Published 23 May 2019

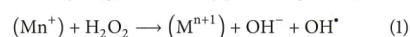
Guest Editor: Filipa S. Reis

Copyright © 2019 Vito Kovac et al. This is an open access article distributed under the Creative Commons Attribution License, which permits unrestricted use, distribution, and reproduction in any medium, provided the original work is properly cited.

The aim of the study was to assess the level of selected systemic oxidative stress parameters during the first week of orthodontic treatment with fixed appliances. Fifty-four males with malocclusion and having a similar lifestyle were randomized using a computer based procedure and allocated to either the treatment group (TG; n=27; 24.6 ± 1.7 years) or control group (CG; n=27; 24.7 ± 1.7 years). Capillary blood was collected at baseline and 6 hours, 24 hours, and 7 days after archwire insertion. At the same time points, capillary blood was retrieved in the CG. In order to determine the oxidative stress, both the reactive oxygen species (ROS) formation and the antioxidative defense (AD) potential were measured using the ROS testing and oxygen free radicals defense (equivalent to antioxidant defense) testing, respectively, by a blinded operator. The ratio between ROS and AD (ROS/AD) was calculated and data were analyzed using nonparametric tests. No drop-outs or harms were detected. At baseline, neither ROS [1.54 [1.22; 2.12] and 1.74 [1.40; 2.01] for the TG and CG, respectively), AD [1.19 [0.66; 1.50] and 1.19 [0.57; 1.42] for the TG and CG, respectively), nor ROS/AD levels were significantly different (p>0.05). After 24 hours, the ROS level significantly increased in the TG (2.05 [1.71; 2.26]) and was higher compared to the CG ROS level (1.67 [1.29; 1.95]; p=0.025), while for the AD level, no marked between and within group differences were detected. A notable change of ROS/AD ratio was observed over time only within the TG (p=0.026). Moreover, a significantly higher ROS/AD ratio was detected 24 hours after archwire insertion in the TG compared to the CG (2.69 [1.44; 3.89] and 1.79 [1.45; 2.35], respectively), followed by a decrease. Orthodontic treatment with fixed appliances might induce systemic oxidative stress in the short-term, since ROS levels and ROS/AD levels are normalized within 7 days after archwire insertion.

1. Introduction

The oral cavity is subjected to various external factors, including dental materials that have substantial oxidizing potential and have the ability to generate reactive oxygen species (ROS) [1]. Increased reactive oxygen species (ROS) cause oxidative stress, which is defined as the imbalance between ROS and antioxidant defense (AD) in favor of the former. During orthodontic treatment with fixed appliances, the subjects are exposed to heavy metals released from corroded appliances, which might increase the levels of ROS through metal-catalyzed free radical reactions (Fenton and Fenton-like reactions). Many metal ions such as chromium undergo redox cycling, thus directly producing ROS [2]:



Moreover, during orthodontic treatment various inflammatory mediators (i.e., cytokines) causing aseptic inflammation in the periodontal ligament are being released after mechanical force application to the teeth inducing a cascade of reactions in the periodontal tissue, which leads to tissue remodeling and tooth movement. Since there is sound evidence indicating that periodontal inflammation is one of the main sources of ROS in the mouth [3], it is plausible that also aseptic inflammation might be associated with oxidative stress induced damage.

Several in vitro studies showed that both orthodontic brackets [4] and archwires [2] induce oxidative stress, associated with heavy metals release. In vivo studies that aimed to assess either salivary biomarkers [5, 6] of oxidative stress or biomarkers in the gingival crevicular fluid [7], reported

different results. On the one hand Olteanu et al. [6] and Buczko et al. [5] reported that orthodontic treatment modifies the oxidative-antioxidative balance in the patients' saliva. In particular, Olteanu et al. [6] demonstrated that markers of oxidative stress (ceruloplasmin and malondialdehyde) increased to their highest levels 24 hours after orthodontic appliance insertion and decreased back to their initial levels 7 days after insertion. Similarly, Buczko et al. [5] evidenced a marked increase in salivary oxidative stress biomarkers one week after orthodontic appliance insertion and a decrease to normal values at the 24-week follow-up. On the other hand Atung Ozcan et al. [7] concluded that the levels of examined oxidative stress biomarkers did not change after one and six months of orthodontic treatment.

The varying results might be due to the different methodologies used and due to the different materials of orthodontic appliances to which the subjects were exposed. Moreover, the use of single biomarkers for estimating the oxidative stress is limiting, since oxidative stress is a result of an imbalance between ROS and AD in favor of the former [8, 9]. Therefore, the ratio between ROS and AD appears to be a more accurate indicator of oxidative stress [10]. To establish the complex relationship between ROS and AD direct and indirect methods can be used [11]. Direct methods relate to ROS measurements of superoxide, H_2O_2 , OH^\cdot . These species are very reactive and their quantitation can be assessed only with electron paramagnetic resonance. Therefore, indirect methods are usually used, which include measurement of the balance between ROS and AD and measurements of each antioxidant separately (i.e., catalase, superoxide dismutase, vitamin C, reduced glutathione, vitamin E, etc.). The main limitation of the latter is that it does not assess the synergistic effect between different antioxidants [11].

Apart from the above-mentioned *in vitro* and *in vivo* studies of oxidative stress biomarkers changes in the local environment due to exposure to orthodontic fixed appliances, there is still paucity of data regarding oxidative stress induction at the systemic level during orthodontic treatment. Therefore, the aim of the present study was to assess the systemic level of oxidative stress during orthodontic treatment with fixed appliances, determined from capillary blood samples. The hypothesis tested was that selected oxidative stress parameters in capillary blood do change during the first week of orthodontic treatment with fixed appliances.

2. Material and Methods

2.1. Subjects and Study Design. Ethical approval for this study was gained (No. 0120-523/2018/8) from the National Medical Ethics Committee and informed consent was obtained from all subjects before inclusion. The study protocol was designed and performed following the Declaration of Helsinki for medical research involving human subjects. The data used to support the findings of this study are available from the corresponding author upon request.

A group of 54 male subjects aged between 19.7 and 28.2 years who were seeking orthodontic treatment at the Department of Orthodontics of the University Medical Centre of Ljubljana, Slovenia, due to mild crowding and teeth

malalignment were recruited based on a preliminary questionnaire regarding their lifestyle habits. Subjects with oral pathology (including periodontal disease), poor oral hygiene, and known allergies as well as smoking subjects or subjects undergoing any pharmaceutical therapy, including food additives with antioxidant properties intake, were excluded. Females were not included due to possible false results as a consequence of hormonal fluctuation. Randomization was performed according to a computer based procedure having groups of equal numerosity. Twenty-seven subjects were allocated to the treatment group (TG, aged 24.6 ± 1.7 years), while the control group (CG, aged 24.7 ± 1.7 years) consisted of 27 age-matched subjects. No subject left the study.

During the study, the subjects of both groups were asked to follow a similar diet regimen (3 portions [400 g] of fruit and vegetable/day, avoidance of antioxidant supplements, and no alcohol intake) and to perform very similar activities (avoidance of extreme sport activities and sun exposure; avoidance of nocturnal life).

The fixed orthodontic appliance used in the TG was composed by stainless steel brackets (Gemini brackets, 3M Unitek; USA) attached to the upper and lower teeth and two Nickel-Titanium archwires (3M Unitek; USA) inserted in the bracket's slots.

For the evaluation of oxidative stress the balance between ROS and AD was assessed from capillary blood. The FORT (free oxygen radicals testing) and FORD (free oxygen radicals defense) assays were performed as previously described [12], using a dedicated spectrophotometer Free Oxygen Radical Monitor (FORM[®], CR 3000, Callegari, Parma, Italy). Blood samples of 50 μ l for FORD and 20 μ l for FORT were collected in a sterile regimen from the tip of the subject's finger into a heparinized tube, mixed with provided reagents, centrifuged, and analyzed in the spectrophotometer by measuring light absorption at a wavelength of 505 nm. FORT and FORD values were measured immediately after blood collection. The FORT test results are given as FORT units (0,26 mg/l H_2O_2), while the results of the FORD test are expressed as mmol/l of Trolox (6-hydroxy-2,5,7,8-tetramethylchroman-2-carboxylic acid; a water-soluble analog of vitamin E). Principles of the determination of oxidative stress in human blood using FORD and FORT tests were previously described [13–15]. FORT and FORD analyses were performed by a blinded operator.

Capillary blood was collected before the insertion of the fixed orthodontic appliance and at 6 hours, 24 hours, and 7 days' time point. At the same time points, blood was collected and analyzed also from the matched controls. To exclude any possible influence of periodontal inflammation on the measurements of oxidative stress parameters, two weeks before the beginning of the study, all the participants were instructed regarding oral hygiene activities. At baseline, the periodontal status was assessed by measuring probing depth at six sites around every erupted tooth of each subject. Furthermore, the bleeding on probing index was used at each time point to determine the presence of inflammation.

2.2. Sample Size Calculation. Sample size of at least 26 subjects for each group was needed to detect an effect size

coefficient of 0.8 (which is regarded as “large effect” [16]) for the measured parameters in any comparison between the groups, with an alpha set at 0.05 and a power of 0.80.

2.3. Statistical Analysis. The Statistical Package for Social Sciences Software release 20.0 (SPSS Inc., Chicago, Illinois, USA) was used for data analysis. The balancing of experimental groups by age was tested with a Mann-Whitney U-test. After testing the normality of the data with the Shapiro-Wilk test and Q-Q normality plots and the equality of variance among the datasets using a Levene test, nonparametric methods were used for data analysis.

A Friedman test was used to assess the significance of the differences in every parameter (FORT, FORD, and FORT/FORD ratio) over the time points within each group. When significant interactions were seen, a Bonferroni-corrected Wilcoxon test was used for pairwise comparisons. A Mann-Whitney U-test was used to assess the significance of the differences in every parameter between the two groups within each time point.

The results were considered to be significant at p-values below 0.05.

The intra-assay and inter-assay coefficients of variation were reported to be 3.7% and 6.2%, respectively, for the FORT and 4.2% and 6.6%, respectively, for the FORD [12].

3. Results

The results of the FORT and FORD assays for the TG and CG group at different time points are reported in Table I. At baseline, no significant differences were detected between the TG and CG, neither for FORT ($p > 0.05$) nor FORD ($p > 0.05$) levels.

The FORT level in the TG increased to significantly higher values than those in the CG ($p = 0.025$) at the 24 hours' time point, and decreased to normal values similar to those seen in the CG at the 7 days' time point. Although a decrease of the FORD level was detected in the TG at the 24 hours' time point, this was not statistically significantly different from the CG.

A significant change of the FORT level over time was seen within the TG ($p = 0.026$), while no notable changes were detected for the FORD level ($p > 0.05$). In the CG, neither FORT nor FORD levels changed markedly over time ($P > 0.05$).

The FORT/FORD ratio, expressing the balance between ROS and AD is represented in Figure 1. At baseline and 6 hours, no significant differences regarding the FORT/FORD ratio were observed between the TG and CG ($p = 0.897$ and $p = 0.528$, respectively). At 24 hours, the FORT/FORD ratio increased significantly in the TG as compared to the CG ($p = 0.044$). Finally, at the 7 days' time point, no significant differences regarding the FORT/FORD ratio were measured between the two groups ($p = 0.299$). None of the subjects had signs of periodontal disease/inflammation over the observational period.

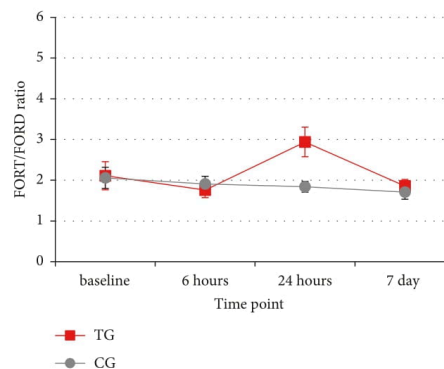


FIGURE 1: Mean values and standard errors of the longitudinal changes of the FORT/FORD ratio in the treated (TG) and control (CG) groups.

4. Discussion

It has been postulated, that orthodontic treatment with fixed appliances might play an important role in inducing oxidative stress and related damage [1]. Until recently, only local environment levels of ROS and/or antioxidant defense were assessed during orthodontic treatment, by examining either saliva [5–7, 17] or the gingival crevicular fluid [7]. To our best knowledge, the present study is the first attempt to determine the oxidative stress induced at the systemic level by orthodontic treatment. Both, the ROS formation as well as the AD potential were measured in blood/serum, and the ratio between them was calculated [12] in subjects undergoing orthodontic treatment and in a control group.

The results evidenced a marked short-term systemic increase of ROS as well as an increase in the ratio between ROS and AD, among subjects undergoing orthodontic treatment. In accordance with the study of Olteanu et al. [6] that revealed maximum levels of salivary oxidative stress biomarkers 24 hours after the start of orthodontic treatment, the present study also denoted a significant increase of the systemic (blood/serum) ROS/AD ratio 24 hours after the start of treatment. Similarly to the previous report [6], after 7 days of treatment, a decrease of the ROS/AD ratio to normal values as those measured in the CG was observed also in the present study. A recent study by Buczko et al. [5] evidenced significant changes of the total oxidative status index (ratio between the total oxidative status and total antioxidative status) in unstimulated and stimulated saliva during orthodontic treatment. The authors [5] revealed an increase of the total oxidative status in saliva at 1 week and a significant decrease of it at 24 weeks follow-up, which is in contrast with the results of the present study, as the systemic ROS/AD ratio normalized after 7 days.

It could be hypothesized that oxidative stress during orthodontic treatment might be induced by different factors: local and systemic exposure to heavy metals, inflammation of

TABLE 1: The FORT and FORD levels among the treated and control groups over the observational period.

Parameter	Group	Baseline	6 hours	24 hours	7 days	Diff.
FORT	TG	1.54 (1.22;2.12)	1.78 (1.22;2.15)	2.05 (1.71;2.26), <i>a</i>	1.64 (1.22;2.08), <i>b</i>	0.026; S
	CG	1.74 (1.40;2.01)	1.71 (1.22;2.01)	1.67 (1.29;1.95)	1.64 (1.29;1.92)	0.100; NS
	Diff.	0.602; NS	0.376; NS	0.025; S	0.910; NS	
FORD	TG	1.19 (0.66;1.50)	1.23 (0.89;1.45)	1.04 (0.51;1.45)	0.96 (0.66;1.49)	0.33; NS
	CG	1.19 (0.57;1.42)	1.07 (0.66;1.44)	0.91 (0.66;1.41)	1.20 (0.72;1.57)	0.887; NS
	Diff.	0.775; NS	0.276; NS	0.43; NS	0.307; NS	

Data is presented as median (25th; 75th percentile). TG, treated group, n=27; CG, control group, n=27; Diff., p-values; significance of the difference between the groups within each time point or over time within either group. Results of the pairwise comparisons between time points: *a*, significantly different from the baseline; *b*, significantly different from 24 hours. NS, not statistically significant; S, statistically significant.

the periodontal tissues due to poor oral hygiene, and aseptic inflammation in the periodontal ligament due to mechanical force application.

In vitro studies [2, 4] have shown that metal ions such as nickel, cobalt, and chromium, released either from corroded orthodontic brackets and archwires, induce oxidative stress. Despite the smaller corrosion susceptibility of titanium alloys, due to the protective titanium oxide layer, mechanical friction in the contact between bracket and archwire during orthodontic treatment leads to the disruption of the protective titanium oxide layer [18, 19], causing corrosion and release of titanium ions, which might increase ROS production [1]. Likewise, the in vivo study by Buczko et al. [5] explained the increase of ROS/AD ratio in saliva after one week as an effect of heavy metal exposure during orthodontic treatment, since the highest concentration of nickel ions was measured simultaneously.

Also in the present study, patients could have been exposed to nickel, cobalt, chromium, and titanium released from the parts of the orthodontic appliance used, all of which might have induced the systemic elevation of the ROS/AD ratio after 24 hours of orthodontic treatment. However, at the 7 days' time point, contrasting the results of salivary oxidative stress biomarkers [5], the ROS/AD ratio normalized, most probably due to adaptive stress responses and induction of antioxidative endogenous defense. This is in accordance with two other in vivo studies [7, 17] that reported no marked changes of the salivary [7, 17] and gingival crevicular fluid [7] oxidative stress biomarkers after 4-5 weeks and six months of orthodontic treatment. Of note, the contrasting results could also be due to the great variability in the timing of nickel ions increase in saliva, which ranges from 10 minutes to four weeks after orthodontic appliance insertion [20, 21].

A second cause of the significant systemic elevation of ROS and ROS/AD ratio could be the periodontal inflammation induced by increased plaque apposition due to the orthodontic appliance. Although periodontal inflammation has been associated with ROS formation [3], Portelli et al. [17] reported no notable correlation between oxidative stress biomarkers and oral hygiene in patients undergoing orthodontic treatment. Similarly, periodontal inflammation as a cause of oxidative stress could be excluded in the present study, as all the subjects had excellent oral hygiene without any signs of periodontal inflammation at each time point.

A final explanation for the increase in ROS and ROS/AD ratio detected in the present study 24 hours after the start of orthodontic treatment could be a result of the expression of proinflammatory mediators in the periodontal ligament induced by mechanical force application on the tooth. In fact, the mechanism of orthodontic tooth movement with fixed appliances is characterized by a cascade of events, triggered by the strain of the periodontal ligament fibers, leading to an inflammatory process that allows appropriate tissue remodeling. It has been shown that this inflammation might occur only at a subclinical (i.e., molecular level) and might be limited to the alveolar bone, with no systemic consequences in terms of elevation of C-Reactive Protein [22]. However, this does not exclude, that the short-term elevation of systemic ROS and ROS/AD ratio seen in the

present study is a consequence of the aseptic inflammation in the periodontal ligament due to force application induced by the orthodontic appliance.

Limitations of the Study. It is generally accepted that two or more assays should be utilized to assess oxidative stress status, whenever possible to enhance validity, since each technique measures something different and has its own inherent limitations and no method by itself can be said to be a completely accurate measure of antioxidant status and ROS formation [11]. In the present study ROS and different antioxidants present in the blood as well as their interactions were assessed with FORT and FORD. Although changes in the ROS/AD ratio were observed over time, their main cause(s) could not be determined. In fact, the observed ROS/AD ratio changes can be related to many factors (i.e., endogenous antioxidants activation, inflammation, and blood metal ions), the assessment of which was beyond the scope of the present study. On the other hand, the possible influence of periodontal inflammation on the measured systemic oxidative stress parameters could be excluded, since no signs of inflammation were detected in any of the subjects over the observed period of time, the influence of sterile periodontal inflammation due to force application and blood metal ions content could not be excluded as the cause of increased ROS observed in the TG. In fact, due to ethical reasons it was not feasible to retrieve consecutive larger venous blood samples four times over a period of one week for assessing any possible changes of inflammation mediators as well as heavy metals in venous blood. Moreover, previous studies [23] reported that heavy metal ions (i.e., nickel) are detectable in blood only after long-term exposure.

Given that the results presented here are descriptive and future research is needed for a better understanding of which factors (presence of heavy metals and/or inflammation) have a direct causative impact on increased parameters of ROS and ROS/AD ratio observed in the blood of the treated group. Nevertheless, due to the short-term elevation of oxidative stress parameters during the first week of orthodontic treatment, increased intake of natural antioxidants would be recommended. However, a study on the efficacy of antioxidant treatment during orthodontic therapy should be performed to determine the rational and dosage of their use. In fact, an excess use of antioxidants might also induce harmful health effects [24, 25].

5. Conclusions

Orthodontic treatment with fixed appliances might induce systemic oxidative stress, but only in the short-term. In particular, the elevation of ROS and ROS/AD levels is seen only 24 hours after the start of orthodontic treatment, while normalization of the levels occurs within 7 days after archwire insertion most probably due to adaptive endogenous antioxidative response. However, intermittent changes of the ROS and AD levels during orthodontic treatment (i.e., at each archwire reactivation) could not be excluded. Future studies should be performed to confirm the activation of endogenous antioxidant defense (superoxide dismutase,

catalase, and glutathione peroxidase activity) as well as the main cause of increased oxidative stress (heavy metal release and/or inflammation) during orthodontic treatment with fixed appliances.

Data Availability

The data used to support the findings of this study are available from the corresponding author upon request.

Conflicts of Interest

The authors declare no conflicts of interest.

Acknowledgments

The study was funded by the Slovenian Research Agency and Croatian Science Foundation (P3-0388; J3-8199/2014-09-7500).

References

- [1] P. Żukowski, M. Maciejczyk, and D. Waszkiel, "Sources of free radicals and oxidative stress in the oral cavity," *Archives of Oral Biology*, vol. 92, pp. 8–17, 2018.
- [2] S. Spalj, M. Mlacovic Zrinski, V. Tudor Spalj, and Z. Ivankovic Buljan, "In-vitro assessment of oxidative stress generated by orthodontic archwires," *American Journal of Orthodontics and Dentofacial Orthopedics*, vol. 141, no. 5, pp. 583–589, 2012.
- [3] L. Tóthová and P. Celec, "Oxidative stress and antioxidants in the diagnosis and therapy of periodontitis," *Frontiers in Physiology*, vol. 8, article 1055, 2017.
- [4] Z. I. Buljan, S. P. Ribaric, M. Abram, A. Ivankovic, and S. Spalj, "In vitro oxidative stress induced by conventional and self-ligating brackets," *The Angle Orthodontist*, vol. 82, no. 2, pp. 340–345, 2012.
- [5] P. Buczko, M. Knaš, M. Grycz, I. Szarmach, and A. Zalewska, "Orthodontic treatment modifies the oxidant–antioxidant balance in saliva of clinically healthy subjects," *Advances in Medical Sciences*, vol. 62, no. 1, pp. 129–135, 2017.
- [6] C. Olteanu, A. Muresan, D. Daicovicin et al., "Variations of some saliva markers of the oxidative stress in patients with orthodontic appliances," *Physiology*, vol. 19, pp. 26–29, 2009.
- [7] S. S. Atug Ozcan, I. Ceylan, E. Ozcan, N. Kurt, I. M. Dagsuyu, and C. F. Canakci, "Evaluation of oxidative stress biomarkers in patients with fixed orthodontic appliances," *Dis Markers*, vol. 2014, Article ID 597892, p. 10, 2014.
- [8] L. Deguillaume, M. Leriche, and N. Chaumerliac, "Impact of radical versus non-radical pathway in the Fenton chemistry on the iron redox cycle in clouds," *Chemosphere*, vol. 60, no. 5, pp. 718–724, 2005.
- [9] P. A. Riley, "Free radicals in biology: oxidative stress and the effects of ionizing radiation," *International Journal of Radiation Biology*, vol. 65, no. 1, pp. 27–33, 1994.
- [10] J. Wang, H. M. Schipper, A. M. Velly, S. Mohit, and M. Gornitsky, "Salivary biomarkers of oxidative stress: a critical review," *Free Radical Biology & Medicine*, vol. 85, pp. 95–104, 2015.
- [11] B. Poljsak and P. Jamnik, "Methodology for oxidative state detection in biological systems," in *Handbook of Free Radicals: Formation, Types and Effects*, D. Kozyrev and V. Slutsky, Eds., pp. 421–448, Nova Science Publishers, New York, NY, USA, 2010.
- [12] M. G. Pavlatou, M. Papastamatiki, F. Apostolou, I. Papsotiriou, and N. Tentolouris, "FORT and FORD: two simple and rapid assays in the evaluation of oxidative stress in patients with type 2 diabetes mellitus," *Metabolism*, vol. 58, no. 11, pp. 1657–1662, 2009.
- [13] B. Palmieri and V. Sblendorio, "Oxidative stress tests: overview on reliability and use. Part II," *European Review for Medical and Pharmacological Sciences*, vol. 11, pp. 383–399, 2007.
- [14] B. Palmieri and V. Sblendorio, "Current status of measuring oxidative stress," *Methods in Molecular Biology*, vol. 594, pp. 3–17, 2010.
- [15] J. Ogrin Papić and B. Poljšak, "Antioxidant potential of selected supplements in vitro and the problem of its extrapolation for in vivo," *Journal of Health Sciences*, vol. 2, no. 1, pp. 5–12, 2012.
- [16] J. Cohen, "A power primer," *Psychological Bulletin*, vol. 112, no. 1, pp. 155–159, 1992.
- [17] M. Portelli, A. Militi, G. Cervino et al., "Oxidative stress evaluation in patients treated with orthodontic self-ligating multibracket appliances: an in vivo case-control study," *The Open Dentistry Journal*, vol. 11, no. 1, pp. 257–265, 2017.
- [18] M. Abedini, H. M. Ghasemi, and M. Nili Ahmadabadi, "Tribochemical behavior of NiTi alloy in martensitic and austenitic states," *Materials and Corrosion*, vol. 30, no. 10, pp. 4493–4497, 2009.
- [19] P. Močnik, T. Kosec, J. Kovač, and M. Bizjak, "The effect of pH, fluoride and tribocorrosion on the surface properties of dental archwires," *Materials Science and Engineering C: Materials for Biological Applications*, vol. 78, pp. 682–689, 2017.
- [20] R. M. De Souza and L. M. De Menezes, "Nickel, chromium and iron levels in the saliva of patients with simulated fixed orthodontic appliances," *The Angle Orthodontist*, vol. 78, no. 2, pp. 345–350, 2008.
- [21] M. Natarajan, S. Padmanabhan, A. Chitharanjan, and M. Narasimhan, "Evaluation of the genotoxic effects of fixed appliances on oral mucosal cells and the relationship to nickel and chromium concentrations: an in-vivo study," *American Journal of Orthodontics and Dentofacial Orthopedics*, vol. 140, no. 3, pp. 383–388, 2011.
- [22] J. K. MacLaine, A. B. Rabie, and R. Wong, "Does orthodontic tooth movement cause an elevation in systemic inflammatory markers?" *European Journal of Orthodontics*, vol. 32, no. 4, pp. 435–440, 2010.
- [23] M. Mikulewicz and K. Chojnacka, "Trace Metal release from orthodontic appliances by in vivo studies: A systematic literature review," *Biological Trace Element Research*, vol. 137, no. 2, pp. 127–138, 2010.
- [24] B. Poljsak and I. Milisav, "The neglected significance of "antioxidative stress"," *Oxidative Medicine and Cellular Longevity*, vol. 2012, Article ID 480895, 12 pages, 2012.
- [25] B. Poljsak, D. Šuput, and I. Milisav, "Achieving the balance between ros and antioxidants: when to use the synthetic antioxidants," *Oxidative Medicine and Cellular Longevity*, vol. 2013, Article ID 956792, 11 pages, 2013.

ANNEX L

Consent from publisher MDPI for the re-publication of article in the print and electronic versions of the doctoral dissertation

8 MDPI Open Access Information and Policy

All articles published by MDPI are made immediately available worldwide under an open access license. This means:

- everyone has free and unlimited access to the full-text of *all* articles published in MDPI journals;
- everyone is free to re-use the published material if proper accreditation/citation of the original publication is given;
- open access publication is supported by the authors' institutes or research funding agencies by payment of a comparatively low **Article Processing Charge (APC)** for accepted articles.

8.1 Permissions

No special permission is required to reuse all or part of article published by MDPI, including figures and tables. For articles published under an open access Creative Common CC BY license, any part of the article may be reused without permission provided that the original article is clearly cited. Reuse of an article does not imply endorsement by the authors or MDPI.

ANNEX M

Published article Kovač et al., 2020



Article

Are Metal Ions That Make up Orthodontic Alloys Cytotoxic, and Do They Induce Oxidative Stress in a Yeast Cell Model?

Vito Kovač¹, Borut Poljšak¹, Jasmina Primožič² and Polona Jamnik^{3,*}

¹ Faculty of Health Sciences, University of Ljubljana, Zdravstvena pot 5, 1000 Ljubljana, Slovenia; vito.kovac@zf.uni-lj.si (V.K.); borut.poljsak@zf.uni-lj.si (B.P.)

² Medical Faculty, University of Ljubljana, Vrazov trg 2, 1000 Ljubljana, Slovenia; jasminaprimozic@gmail.com

³ Biotechnical Faculty, University of Ljubljana, Jamnikarjeva ulica 101, 1000 Ljubljana, Slovenia

* Correspondence: polona.jamnik@bf.uni-lj.si; Tel.: +386-1-3203-729

Received: 4 October 2020; Accepted: 26 October 2020; Published: 27 October 2020



Abstract: Compositions of stainless steel, nickel-titanium, cobalt-chromium and β -titanium orthodontic alloys were simulated with mixtures of Fe, Ni, Cr, Co, Ti and Mo metal ions as potential oxidative stress-triggering agents. Wild-type yeast *Saccharomyces cerevisiae* and two mutants Δ Sod1 and Δ Ctt1 were used as model organisms to assess the cytotoxicity and oxidative stress occurrence. Metal mixtures at concentrations of 1, 10, 100 and 1000 μ M were prepared out of metal chlorides and used to treat yeast cells for 24 h. Every simulated orthodontic alloy at 1000 μ M was cytotoxic, and, in the case of cobalt-chromium alloy, even 100 μ M was cytotoxic. Reactive oxygen species and oxidative damage were detected for stainless steel and both cobalt-chromium alloys at 1000 μ M in wild-type yeast and 100 μ M in the Δ Sod1 and Δ Ctt1 mutants. Simulated nickel-titanium and β -titanium alloy did not induce oxidative stress in any of the tested strains.

Keywords: metal ion; orthodontic appliances; yeast; cytotoxicity; oxidative stress; lipid oxidation

1. Introduction

Each part of an orthodontic appliance, whether an archwire, bracket or band, may differ from other parts by their composition and characteristics [1]. To make a fixed orthodontic appliance, some parts have to be joined together, whether that be by brazing, soldering or welding [2]. Many metallic alloys, ranging from different series of stainless steel, to nickel-titanium, pure titanium, and cobalt-chromium, are being used for manufacturing orthodontic devices, and all of them possess unique physical and mechanical properties [3]. Most of the orthodontic alloys form a so-called oxide layer, which makes them corrosion resistant. However, over time with exposure to the harsh, constantly changing oral environment, those biocompatible metal materials tend to locally corrode and biodegrade, thus releasing metal ions into the oral cavity [4,5]. In addition, galvanic corrosion might occur, when wire and brackets made out of two different alloys are soldered together, accelerating the release of metal ions [6].

The biocompatibility of orthodontic appliances has been extensively studied in the literature. In most cases, the release of metal ions from such appliances into artificial saliva either at low [5] or neutral pH [7–9] was analyzed, focusing on Ni, Cr, Fe and Co ions [10]. Although highly variable values of metal ion release were reported and the values did not exceed the recommended daily dietary intake [11], their toxic potential should not be neglected, especially on the local level within the oral cavity.

The ability of metal ions to generate reactive oxygen species (ROS) could contribute to the overall toxicity of fixed orthodontic appliances [12]. Iron, chromium, cobalt, nickel, titanium, and molybdenum

are all classified as transition metals, which can undergo redox cycling reactions, thus forming ROS [13]. If the ever-increasing ROS molecules are not maintained at physiological levels, an overly large amount of generated ROS can lead to oxidative stress, which disrupts cellular redox homeostasis and consequently damages biomolecules (lipids, protein, and DNA). To counter these harmful effects and to scavenge overproduced ROS, a defense system comprising enzymatic and nonenzymatic systems is possessed by each cell. Superoxide dismutase (SOD), catalase (CAT) and glutathione peroxidase (GPx) are examples of some of the enzymes responsible for the maintenance of intracellular redox status [14].

Currently, in vitro cell lines are mostly being used to evaluate the cytotoxicity of orthodontic materials. To assess the agents' ability to have toxic consequences on living cells [15], a yeast model organism *Saccharomyces cerevisiae* could also be used. Namely, its genome is well described [16], and the use of yeast as a model organism is relevant for human disease studies due to yeast proteins being homologous to human proteins [17]. In addition, features such as genetic tracing, ability to scale-up and the short generation time enable yeast to perform as an effective research model [18]. The similarity between *S. cerevisiae* and other eukaryotes in biochemical and molecular biological levels [19] appears to be useful when studying oxidative stress damage because of the potential mitochondrial respiration and oxidative damage accumulation in yeast [20].

To our knowledge, simulating orthodontic alloys with metal ions on this scale has not been previously performed. This study aimed to evaluate whether the metal ions that form selected orthodontic alloys are cytotoxic and capable of inducing oxidative stress in the yeast model organism *Saccharomyces cerevisiae*. Moreover, wild-type *S. cerevisiae* and two mutants lacking either SOD or CAT enabled a comparison to reveal whether superoxide anion and H₂O₂ lacking defense system contributes to metal-ion-induced toxicity.

2. Results

2.1. Cell Culturability

The toxic assessment of the treatment of each yeast strain (Wt, Δ Sod1, Δ Ctt1) with distinct metal ions combinations at different concentrations is presented in Figure 1 as CFU/mL cell counts (Figure 1A1–E1) and as percentages of cell culturability (Figure 1A2–E2). A lower cell culturability can be seen between the wild type and the other two mutants. All strains had a significantly lower cell culturability ($p < 0.05$) when treated with any of the metal ions at a 1000 μ M concentration except for Δ Ctt1 treated with Ni-Ti. Treatment with stainless steel (SS) (Figure 1A1,A2) at concentrations lower than 1000 μ M had almost no effect on the cell culturability, while a significantly decreased percentage ($p < 0.05$) of cell culturability was detected when treating wild-type and Δ Sod1 strains with concentrations of 1000 μ M. The yeast strains treated with Elgiloy (ELG) (Figure 1B1) already had a significantly lower ($p < 0.05$) cell culturability at 10 μ M concentrations for the wild-type and Δ Ctt1 strains and 1000 μ M concentration for the Δ Sod1 strain compared with the untreated corresponding control strains. The mean culturability values for the cells treated with ELG (Figure 1B2) were significantly lower ($p < 0.05$) than those for the untreated corresponding controls for concentrations equal to or above 100 μ M for wild type and Δ Sod1; meanwhile, for Δ Ctt1, a decrease in the cell survival rate was already detected, but not statistically significant, for the treatment with the 1 μ M ELG concentration. Similarly, treatment with Remaloy (REM) at the 100 μ M concentration and higher concentrations caused a statistically significant decrease ($p < 0.05$) in cell culturability of the wild-type and Δ Sod1 strains; meanwhile, for the Δ Ctt1 strains, REM concentrations of 10 μ M significantly ($p < 0.05$) influenced cell culturability. A statistically significant decrease ($p < 0.05$) in cell culturability was detected for wild-type strains treated with 10 μ M or higher concentrations of nickel-titanium (NiTi), whereas almost no effect on the culturability of Δ Sod1 and Δ Ctt1 was seen when treated with concentrations lower than 1000 μ M. With the increasing concentration of β -titanium (TiMo), a decrease in culturability of every yeast strain was noticed and as in almost all other cases, the 1000 μ M metal concentration had a statistically significant impact ($p < 0.05$) on the cell culturability.

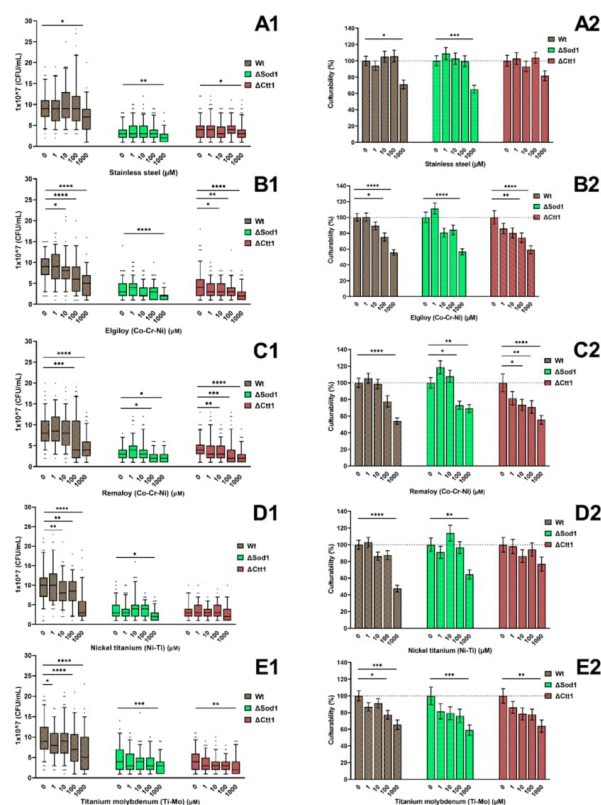


Figure 1. Cell culturability, expressed as CFU/mL, of yeast cells treated with different compositions and concentrations of metal ions. Wild-type yeast and two yeast mutants Δ Sod1 and Δ Ctt1 were subjected to metal ions simulating (A) stainless steel, (B,C) cobalt-chromium Elgiloy and Remaloy, (D) nickel-titanium, and (E) β -titanium alloys. The box-plots (A1–E1) show an absolute values of CFU/mL, while the grouped columns (A2–E2) present relative values according to the untreated control group. The untreated control group is set at 100%, and the dotted line represents 100% culturability. Significant differences ($p < 0.05$ are indicated with * ($p < 0.05$, ** $p < 0.01$, *** $p < 0.001$, and **** $p < 0.0001$).

2.2. Cell Metabolic Activity

The metabolic activities of different yeast strains according to distinct metal ions combinations at different concentrations are presented in Figure 2. No statistically significant difference was seen when comparing the metabolic activity values for each treated sample with the corresponding untreated control. For SS, REM and NiTi, an increase in metabolic activity was concomitant with the increase in the concentrations used but only in the wild-type yeast strain. Treating wild-type yeast with ELG did not affect metabolic activity. On the other hand, treating wild-type yeast with TiMo had a minor decreasing effect of metabolic activity, and its effect gradually increased with the increasing concentrations of TiMo metal ion mixture. Mutant strains with different metal treatments displayed a decreasing trend in their metabolic activity with the increase in SS, ELG, REM and NiTi concentrations. For mutants treated with TiMo, only the highest concentration decreased their metabolic activity. A comparison

between the untreated yeast strains showed a much greater metabolic activity of mutant yeast cells compared with wild-type yeast (Figure 2F).

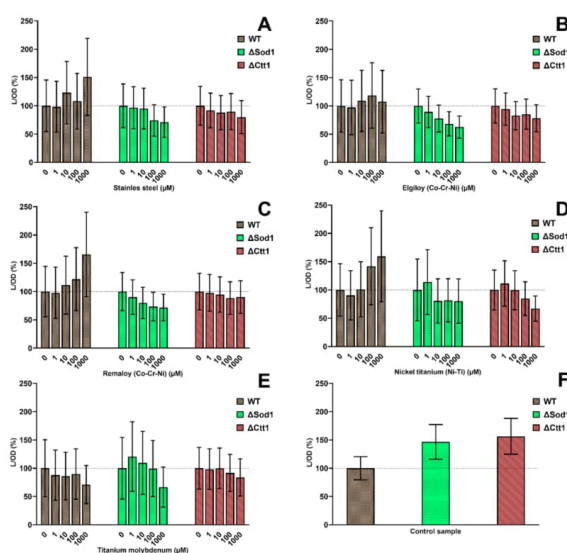


Figure 2. Metabolic activity of wild-type yeast and two yeast mutants Δ Sod1 and Δ Ctt1 treated with different combinations of metal ions: stainless steel (A), cobalt-chromium Elgiloy (B), Remaloy (C), nickel-titanium (D), and β -titanium (E). For each yeast strain, the untreated control group represents 100% (dotted line). A comparison among untreated control groups of each yeast strain is shown in the graph (F).

2.3. Intracellular Oxidation

The ROS levels for the wild-type, Δ Sod1, and Δ Ctt1 yeast strains are shown in Figure 3 as F/OD (Figure 3A1–E1) and F/OD percentages (Figure 3A2–E2). Different ROS level measurements were obtained when the assessment was performed by adding fluorescent dye immediately after metal ion treatment (protocol I) or by adding it after 24 h (protocol II). Regardless of the metal ion combination and concentration, the values were twice as high for the wild-type strains, five-fold higher for Δ Sod1 and three-fold higher for the Δ Ctt1 strains when measured according to protocol II. According to the results obtained with protocol I, adding the fluorescent dye immediately after the 1000 μ M metal ion treatment with SS, ELG and REM yielded significantly ($p < 0.05$) higher ROS values than the untreated control group in all yeast strains, but treating with the same and lower concentrations of TiMo had no significant effect on the ROS level. NiTi metal ion mixture at the 1000 μ M concentration had the opposite effect on the Δ Sod1 and Δ Ctt1 mutant yeast cells. When detecting ROS levels, a significant decrease ($p < 0.05$) was measured for the Δ Sod1 mutant, and a considerable decrease was measured for the Δ Ctt1 mutant yeast.

According to the results obtained with protocol II, the addition of fluorescent dye after the 24 h metal ion treatment in many cases indicated a decrease in ROS levels, compared to the results from protocol I, with the exclusion of Δ Sod1 mutant where stagnating values at SS, REM and TiMo metal treatment were observed. The wild-type strain exhibited a decrease in ROS level when increasing all metal ion mixtures, although not statistically proven. The NiTi and TiMo treatments had a similar effect on the yeast strains as SS, ELG and REM.

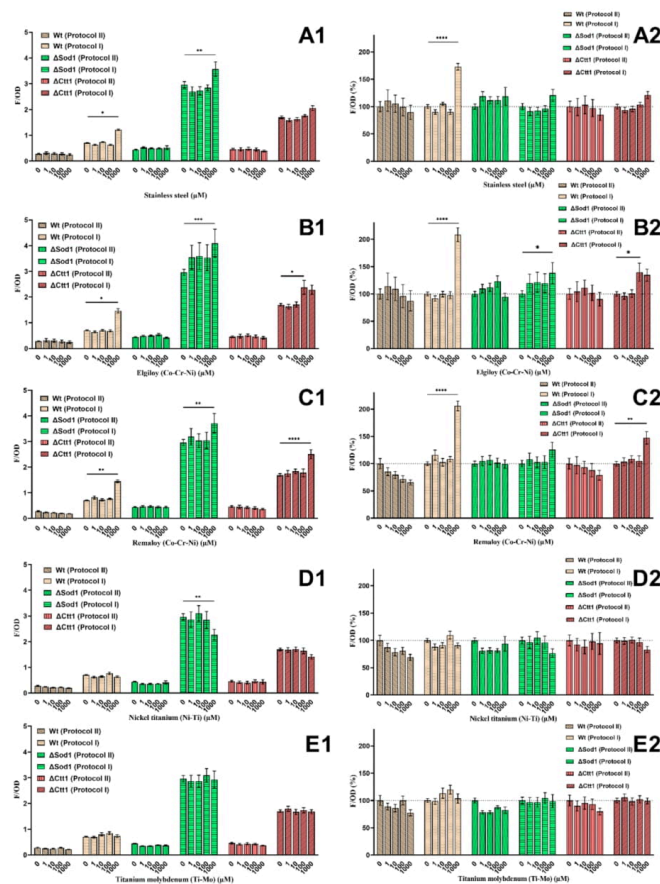


Figure 3. Intracellular oxidation performed with two different methods for wild-type yeast and two yeast mutants Δ Sod1 and Δ Ctt1, and metal treatment: stainless steel (A), cobalt-chromium Elgiloy (B) and Remaloy (C), nickel-titanium (D) and β -titanium (E). Grouped columns represent either absolute values (A1–E1) or relative values according to the untreated control group (A2–E2). For each yeast strain, the untreated control group represents 100% (dotted line). Significant differences ($p < 0.05$) are indicated with * ($p < 0.05$), ** ($p < 0.01$), *** ($p < 0.001$), and **** ($p < 0.0001$).

2.4. Oxidative Lipid Damage

In Figure 4, a series of results are shown to evaluate whether the metal treatment caused lipid oxidative damage. SS, ELG, and REM showed a statistically significant increase ($p < 0.05$) in lipid oxidation in all yeast strains at the 1000 μ M concentration compared with the untreated control, and for Δ Sod1 and Δ Ctt1 increased lipid oxidation occurred even at 100 μ M. Treating wild-type yeast with NiTi and TiMo metal ions had no significant effect. Treating Δ Sod1 with the same two metal ion mixtures had no proven effect, but a decrease in lipid oxidation in Δ Ctt1 mutant can be seen at the 1000 μ M concentration. The untreated mutant yeast cell lines Δ Sod1 and Δ Ctt had nearly two-fold higher levels of lipid oxidation compared with the untreated wild-type yeast (Figure 4F).

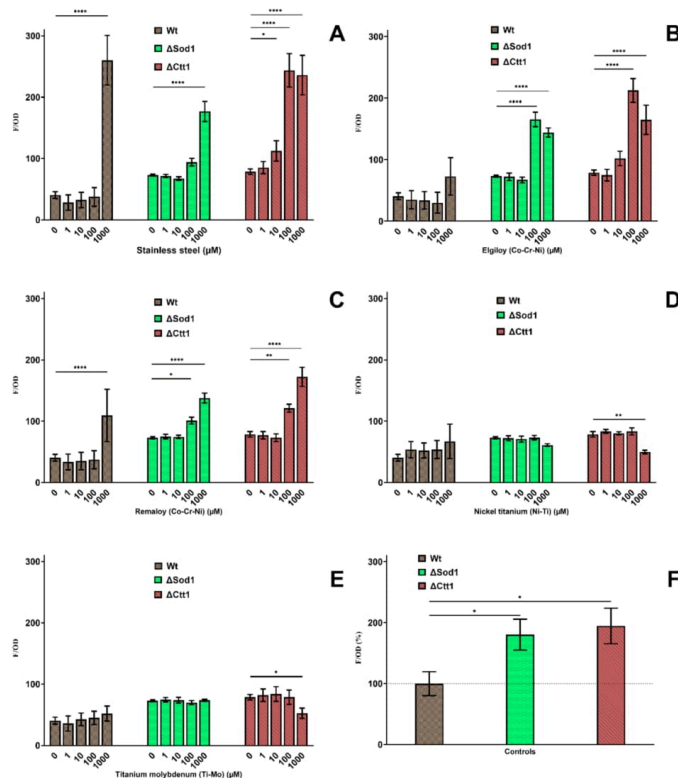


Figure 4. Influence of 24-h metal treatment on the formation of oxidative lipid damage. Wild-type, Δ Sod1, and Δ Ctt1 yeast strains were treated with different concentrations of stainless steel (A), cobalt-chromium Elgiloy (B) and Remaloy (C), nickel-titanium (D), and β -titanium (E). Graph (F) compares untreated control groups of different yeast strains relative to the wild type. Significant differences ($p < 0.05$) are indicated with * ($p < 0.05$, ** $p < 0.01$ and **** $p < 0.0001$).

3. Discussion

Although several studies are available in the literature regarding the biocompatibility and potential cytotoxic impact of the metal ions released from implants [21–23], restorations [24–26] and orthodontic appliances such as Fe, Ni, Cr, Co, Ti, and Mo [27–29], no previous report has simulated orthodontic alloys with metal ion mixtures to evaluate their potential. Cultured animal or human cell lines such as fibroblasts [28] and osteoblasts [30] have been mainly used to evaluate the cytotoxic effect of orthodontic appliances, and currently, only a few studies [31,32] have included yeast for these type of studies. Limberger et al. [31] compared the results on *S. cerevisiae* with other cell lines and concluded that microorganisms are a reliable model for cytotoxic testing of orthodontic materials. Therefore, in the present study, *S. cerevisiae* was used as a model organism as it can provide a large number of results in a short time period due to its quick growth and easy handling. Simple and genetically well-annotated, yeast *S. cerevisiae* is the most well-understood eukaryotic organism and is often used to elaborate fundamental insights into mammalian cell biology. The major advantage of yeast-based studies lies in the high throughput that provides invaluable information about medical disorders related to metals.

Possessing the same antioxidant defensive pathways as mammalian cells, yeast presents an appropriate model organism to investigate oxidative stress and related intracellular oxidative damage. Furthermore, the effect of combining some of the metal ions in the right ratios was evaluated to better simulate the composition of orthodontic alloys. Choosing to simulate stainless steel, nickel-titanium, β titanium, and two cobalt-chromium alloys with metal ions seemed to be appropriate as those five alloys are currently the most used, and their chemical compositions were previously reported by Arndt et al. [33] and Kusky [34].

Although parts of orthodontic appliances of different composition of metal alloys are available, it is the responsibility of the practitioner to ensure that the right kind of material is being used for the best possible patient treatment and safety. Being familiar with orthodontic alloys and their biocompatibility is an additional issue that should be considered when fulfilling patients' needs or addressing patients' problems. For instance, gingival hyperplasia, glossitis, erythema multiforme and labial desquamation might occur from metal ions that are released from orthodontic appliances [35]. Therefore, for a clinical procedure to be successful and safe, the biocompatibility of metal alloys, which combines fields of biology and engineering as well as patient risk factors and clinical experience, should concomitantly be considered [36]. Such improvement in clinical knowledge can be seen in the gradual abandonment of conventional brazing in favor of laser welding [37]. Not only are laser welded joints more durable than brazed joints, EDAX analysis clearly shows material corrosion of brazed joints, whereas laser welded joints had little to no corrosion [5]. That is why the biocompatibility of brazed joints is questionable, especially as the brazing solder used to combine alloys constitutes potentially dangerous metal ions such as zinc, copper and silver [38].

Almost all fixed orthodontic appliances are made out of metal alloys. Amongst them, stainless steel, nickel-titanium, β -titanium and cobalt-chromium alloys are the most commonly used orthodontic materials. Previous studies have shown that orthodontic appliances made out of the previously mentioned materials release metal ions over time [39]. The amount of released metal ions is largely dependent on the type of alloy, surrounding environment and the exposure time. While metal ions being non-biodegradable, they could accumulate in tissues and have toxic local and systemic effects [40,41]. The study was set to evaluate potential cytotoxic effects that fixed metal orthodontic appliances might have through the excretion of metal ions. One approach would be submerging orthodontic materials in medium, enabling a direct contact with the cells. Another approach includes the orthodontic material being incubated in some sort of medium (e.g., artificial saliva) for a long period of time and the emerged metal ion eluate is being used to treat the cells. But by using constituent elements, like metal chlorides, a controlled environment can be simulated, where all the metal ions that compromise an orthodontic alloy are released in the same manner, thus enabling the necessary information about the potential cytotoxic damage, that might occur during the orthodontic treatment. The different methodological approaches used in both in vitro and in vivo studies of metal ion release and inconsistent results [42] made it difficult to select correct metal ion concentrations. In some in vitro experiments, cumulated concentrations of metal release over 30 days of some orthodontics alloys could not be detected or could be as much 7000 ng/mL [43]. Metal ion concentrations of in vivo experiments involving patients' saliva had a much lower release, between 4 and 30 ng/mL [10]. Locally in vivo, near to the orthodontic alloy, metal ion concentration could be much higher than in the saliva. To investigate possible adverse effects and mechanism of action as well as to find the lowest observed adverse effect level [44] of selected cytotoxic or oxidative stress parameters, the metal concentration interval between 1 and 1000 μ M was used in the presented study.

It was shown that metal ions might impact cell culturability. One of the reasons is the causation of oxidative stress. All metal ions used in the study are transition metals, which can catalyze Fenton and Haber–Weiss reactions, resulting in ROS formation, such as superoxide anions ($\bullet\text{O}_2^-$), hydrogen peroxide (H_2O_2), and hydroxyl radicals ($\bullet\text{OH}$) [45]. Each organism (cell) contains various antioxidant defense systems, including SOD and CAT, which are two enzymes that provide a defense grid for removing ROS [46]. The yeast mutants lacking defensive enzymes, ΔSod1 and ΔCtt1 , exhibited higher

ROS formation and consequently more oxidative damage. A superoxide anion ($\bullet\text{O}^-_2$) is formed in the respiratory chain of every mitochondria-containing cell; although less reactive than other ROS, it represents a precursor for most of them [47]. Cytosolic SOD (Sod1) scavenges for $\bullet\text{O}^-_2$ and converts it to H_2O_2 , which is further degraded to H_2O and O_2 by cytosolic catalase (Ctt1) [48]. In our study, yeast mutants lacking the Sod1 gene have higher ROS levels than the Ctt1-lacking mutants despite the same amount of lipid oxidation. Meanwhile, SOD is the only antioxidant enzyme capable of converting $\bullet\text{O}^-_2$, and H_2O_2 can be reduced by both catalases and glutathione peroxidases. Importantly, there were more isozymes of both SOD and catalase enzyme in the cell [46]. That is why the mutants in our study, lacking one form of the enzyme, can survive and adapt to the oxidative environment. Limberger et al. [31] used multiple yeast mutants with either antioxidant defense or DNA repair deficiency to assess the cytotoxicity of orthodontic materials but did not demonstrate any oxidative stress-related ROS formation or oxidative damage. Nevertheless, yeast has proven to be a suitable model organism, as we were able to detect oxidative stress and an impact on viability at 10× lower concentrations when oxidative defense-deprived strains were used. Using a wild-type strain as well as the ΔSod1 and ΔCtt1 mutants, we could compare the occurrence of oxidative stress among them.

A major difference among yeast strains can be seen in the cell culturability values. Untreated mutated yeast cells had at least two-fold lower cell culturability than untreated wild-type yeast. This may be because mutants lacking genes for antioxidant defense tend to adapt slowly to new metal-induced stress environments. When comparing metal-ion treated cells with the untreated control, the treated mutants had lower cell culturability values than the untreated control. Any metal ion concentration of 1000 μM had a significant negative effect on yeast survival. Even the 100 μM concentration of all metal ion combinations, except stainless steel, showed a negative effect. Meldawar et al. [49] observed that at approximately 425 μM of pure Ni ions in human epithelial embryonic cell lines (L132) resulted in 50% viability, but Ti ions and the combination of the two had no impact on the cell lines even at 3750 μM concentrations. The results cannot be compared with our study because an LC50 was obtained at the 1000 μM NiTi concentration, and TiMo alloy comprising almost strictly Ti ions showed a dose-dependent decrease in cellular viability. Issa et al. [50] used metal chlorides to assess the survivability of human gingival fibroblast (HGF) and oligodendrocytes (MO3.13). The cobalt concentrations were the first to cause 50% survivability, followed by the nickel and then chromium concentrations. The LC50 for HGF was Co = 705 μM , Ni = 828 μM and Cr = 1971 μM ; and for MO3.13, it was Co = 215 μM , Ni = 817 μM and Cr = 2084 μM . Although they did not test combinations of different metal ions, the obtained information is valuable as it seems that choosing the right model organism to evaluate cytotoxicity is as important as the metal ion composition of the alloy. Namely, Terpilowska et al. [51] showed that a combination of metal ions can have a synergistic or even antagonistic effect that cannot be observed when treating cells with a single metal.

Assessing the metabolic activity of cells yielded very disparate results. Specifically, the assay quantifies the ATP present in cells, which is proportional to the number of viable, metabolically active cells in the medium. This might not be the case with wild-type yeast strain because its cell culturability and metabolic activity do not share the same outcome when treated with some of the metal ions. In stress situations, ATP depletion is the step before viability loss [52], because the membrane and electron transport chain are first affected by toxic metals [53]. Under mild stress conditions, cells might use ATP to activate defense systems. On the other hand, under increased oxidative stress, which results in intracellular oxidative damage, ATP is decreased due to the damage to mitochondria [54]. Akhova et al. [55] explained that ATP increase could occur due to oxidative stress response, such as antioxidant genes being transcribed [56]. Meanwhile, unnecessary energy-consuming processes are canceled. Because the mutants in our study lack one of the most important genes for oxidative stress defense, they cannot cope as well with oxidative stress as the wild-type strain. Notably, the untreated mutant strains had higher metabolic activity compared with the untreated wild-type strain; hence, activation of the antioxidant defense system was already established.

The intracellular oxidation assay provided information on whether the cytotoxicity of metal ions is due to ROS formation. The measured values after 24 h of incubation of yeast cells with metal ions showed that only the 1000 μM concentrations of SS, ELG, and REM metal ion increased ROS levels but only when administering the fluorescent dye as soon as the metal treatment starts. The results can be deceiving for two reasons. First, if the obtained fluorescence is plotted against the number of culturable cells, the values are much higher compared with the untreated control sample, especially for mutant strains, as their viability decreased in a dose-dependent manner. $\text{H}_2\text{DCF-DA}$ dye can cross the cell membrane, where it is cleaved by intracellular esterase and further oxidized by ROS to exhibit high fluorescence [57]. This process can be conducted only in live cells. A problem of dye leakage could occur [58], but it was excluded by cell washing before measurement. Second, the fluorescent values for untreated yeast mutants were higher than for untreated wild-type yeast. Thus, the mutants already had to cope with the emerging ROS from the start and for 24 h until the analysis was performed. That is, they had ample time to adapt and overcome the stress or succumb to it. That could explain why no increase in ROS was observed when intracellular oxidation after 24 h of treatment was measured.

To further investigate oxidative stress, malondialdehyde (MDA), a product of lipid oxidation, was analyzed. As in ROS detection, the lipid oxidation in mutants was almost two times higher when compared with the wild type. An identical series of values were obtained when comparing the amount of MDA to the amount of ROS, which corresponds to our findings. The MDA levels for the wild type were significantly different for SS, ELG, and REM at 1000 μM and for both mutants even at 100 μM . Indeed, neither NiTi nor TiMo induced ROS formation or lipid oxidation, despite previous studies showing that Ni [59], Ti [60], and Mo [61] ions have that ability. A small increase in lipid oxidation could be seen in the wild type, but it was not significant.

The metal concentrations of Cr, Fe, Mo and Ni ions at 1000 μM and higher have been proven to decrease cell viability and the occurrence of apoptosis [62]. Caicedo et al. [63] tested the harmful effects of metal ions from medical devices on Jurkat cells and provided a scale for them, and the negative effects were as follows: Ni > Co > Mo > Cr \geq Fe. Interestingly, the two regarded as most harmful, Ni and Co, had different modes of action. Lower concentrations of Ni were needed to induce oxidative stress-related DNA damage and apoptosis (50 and 100 μM , respectively) compared with Co, but the Co concentration could decrease viability and inhibit proliferation at 500 and 100 μM , respectively.

4. Materials and Methods

4.1. Preparation of Yeast Cultures

Stock culture of wild type *S. cerevisiae* ATCC 204508 (American Type Culture Collection, Manassas, WV, USA), ΔSod1 *S. cerevisiae* Y06913 (EUROSCARE, Oberursel, Germany) and ΔCtt1 *S. cerevisiae* Y04718 (EUROSCARE, Oberursel, Germany) were grown in yeast extract-peptone-dextrose broth (Merck, Darmstadt, Germany) and incubated in an incubator shaker (InforsHT, Bottmingen, Switzerland) at 28 °C and 220 RPM. The genotypes of each yeast strains are listed in Table 1. The early stationary phase of *S. cerevisiae* yeast strains was adjusted to approximately 1×10^7 cell/mL. The yeast strains were then kept in PBS medium (Merck, Darmstadt, Germany) in the desired stationary phase until metal ion treatment.

Table 1. *Saccharomyces cerevisiae* strains used in the study.

Strain	Genotype	Source
ATCC 204508 (Wt)	MATa; SUC2; mal; mel; gal2; CUP1; flo1; flo8-1; hap1	American Type Culture Collection, Manassas, Virginia, United States
Y06913 (ΔSod1)	BY4741; MATa; ura3 Δ 0; leu2 Δ 0; his3 Δ 1; met15 Δ 0; YJR104c::kanMX4	EUROSCARE, Oberursel, Germany
Y04718 (ΔCtt1)	BY4741; MATa; ura3 Δ 0; leu2 Δ 0; his3 Δ 1; met15 Δ 0; YGR088w::kanMX4	EUROSCARE, Oberursel, Germany

4.2. Preparation of Metal Ion Solutions

As described in Table 2, 0.2 M metal ion stock solutions of 5 orthodontic alloy types were prepared. High-purity salts of $\text{FeCl}_3 \times 6\text{H}_2\text{O}$, $\text{CrCl}_3 \times 6\text{H}_2\text{O}$, $\text{NiCl}_2 \times 6\text{H}_2\text{O}$ and $\text{CoCl}_2 \times 6\text{H}_2\text{O}$ (all bought from Merck, Darmstadt, Germany) as well as TraceCERT® titanium and molybdenum standards (Merck, Darmstadt, Germany) were dissolved with sterile ddH₂O and had their pH adjusted to 7. Before treatment, metal stock solutions were briefly sonicated in an ultrasound bath (Sonis 3 GT, Iskra Pio, Šentjernej, Slovenia).

Table 2. Metal ion ratios for orthodontic alloys adapted from the manufacturer's (Dentaurum, Ispringen, Germany) material safety data sheet [64].

Orthodontic Alloy	Metal Composition (w/v)					
	Fe	Ni	Cr	Co	Ti	Mo
Stainless steel (SS)	72%	10%	18%			
Cobalt-chromium (Elgiloy—ELG)	18%	15%	20%	40%		7%
Cobalt-chromium (Remaloy—REM)	5%	21%	20%	50%		4%
Nickel-titanium (NiTi)		55%			45%	
β-titanium (TiMo)					78%	12%

4.3. Metal Treatment of Yeast Strains

Five metal ion mixtures with final concentrations of 1, 10, 100 and 1000 μM were used to treat yeast strains with a final volume of 10 mL. One sample of each yeast strain was not treated with metal mixtures as it served as a control. The incubation period of 24 h followed in an incubator shaker (InforsHT, Bottmingen, Switzerland) at 28 °C and 220 RPM.

4.4. Cell Culturability

After 24 h, metal-treated cells and the control sample of untreated cells were diluted with PBS medium in the range from 10^{-2} to 10^{-5} . Ten microliters of the metal-treated yeast solution was spotted on a solid YPD-agar plates (Merck, Darmstadt, Germany) and incubated for 48 h at 28 °C. After the incubation, formed colonies were counted and the culturability results were expressed as 1×10^7 colony-forming units per milliliter (CFU/mL).

4.5. Cell Metabolic Activity

For the assessment of cell metabolic activity, BacTiter-Glo™ Microbial Cell Viability Assay (Promega, San Luis Obispo, CA, USA) was used and performed according to the manufacturer's instructions. In brief, a volume of the provided reagent was mixed with the same amount of cell suspension in a 96-well plate; after 5 min of incubation, the formed luminescence and optical density at 650 nm (OD₆₅₀) were recorded using a Tecan microplate reader (Männedorf, Switzerland). The results were expressed as a ratio of luminescence/optical density (L/OD) relative to the untreated control.

4.6. Intracellular Oxidation

Fluorescent dye 2',7'-dichlorofluorescein diacetate (H₂DCF-DA) [65,66] with two slightly different approaches was used to detect intracellular reactive oxygen species (ROS). In the first approach (protocol I), immediately after the addition of metal ion mixtures to the yeast suspension, H₂DCF-DA (Merck, Darmstadt, Germany) was added to a final concentration of 10 μM. After 24 h of incubation, the cells were washed once with PBS medium, and fluorescence (excitation/emission = 488/520 nm) and OD (650 nm) were measured using a Varioskan™ LUX (ThermoFisher, Waltham, MA, USA) microplate reader. In the second approach (protocol II), 24 h metal-treated and untreated cells were first washed

once with PBS medium, and then the dye was added in a final concentration of 10 μM . After 30 min of incubation in the dark, the cells were washed again with PBS medium, and then fluorescence and OD with the same parameters were measured using Varioskan™ LUX (ThermoFisher, Waltham, MA, USA). In both cases, the results were expressed as F/OD relative to the untreated control.

4.7. Oxidative Lipid Damage

For the analysis of oxidative lipid damage [67], the thiobarbituric acid reactive substances (TBARS) assay was employed. It is based on the detection of malondialdehyde (MDA), a marker for oxidative stress damage, which emits fluorescent light at 555 nm. Treated and untreated cells were washed once with PBS medium after 24 h metal ion mixtures treatment. A reagent containing 91.8 mM trichloroacetic acid (Merck, Darmstadt, Germany), 2.5 mM thiobarbituric acid (Merck, Darmstadt, Germany), 45.4 μM butylhydroxytoluene (Merck, Darmstadt, Germany) and 25 mM HCl (Merck, Darmstadt, Germany) was added to the pellet, which was thoroughly resuspended and homogenized twice (Bullet Blender Storm 24, Next Advance, Troy, New York, NY, USA) with 5 min of incubation on ice in between. The homogenate was incubated at 90 °C (Thermomixer R, Eppendorf, Hamburg, Germany) for 30 min followed by 10 min of incubation on ice. Butanol (Merck, Darmstadt, Germany) was added to the homogenate and centrifuged at 10,000 \times g for 10 min. Fluorescence (excitation/emission = 515/555 nm) and OD (650 nm) were measured on a Varioskan™ LUX (ThermoFisher, Waltham, MA, USA) microplate reader. The results were expressed as F/OD relative to the untreated control.

4.8. Statistical Analysis

For CFU/mL counts, ten technical repetitions were performed for each of the seven biological repetitions. When testing the cell metabolic activity, five biological repetitions with two technical repetitions were used for analysis. H₂DCF-DA was applied immediately after the metal treatment on six biological replicates with two technical replicates each. To measure the intracellular oxidation after 24 h, at least three biological replicates with two technical replicates were used. The assessment of the lipid oxidation occurrence was performed with five biological replicates and two technical replicates. For the analysis, the untreated control sample of every yeast strain was set at 100%, and the treated samples were plotted against it. Visual presentation and statistical analysis were performed with GraphPad Prism (version 8.02 for Windows, GraphPad Software, La Jolla, CA, USA, www.graphpad.com). Shapiro–Wilk and D’Agostino and Pearson tests were used to analyze the normal distribution of the acquired data. Normally distributed data were analyzed with one-way ANOVA followed by Dunnett’s post hoc test for multiple comparisons and non-normally distributed data were analyzed with Kruskal–Wallis test followed by Dunn’s post hoc test. Cutoff for the statistical significance of data was considered when $p < 0.05$.

5. Conclusions

The metal ion concentrations of 1000 μM were proven to be cytotoxic to *S. cerevisiae*, even the 100 μM concentrations in the case of simulated cobalt-chromium treatment. The same concentrations of simulated stainless steel and cobalt-chromium alloys exhibited ROS formation, which was observed in yeast mutants ΔSod1 and ΔCt1 already at 100 μM . Untreated yeast mutants had higher ROS and MDA basal levels than the untreated wild-type strain, indicating that even under untreated conditions, both mutants had increased intracellular ROS levels due to incomplete defense. When evaluating titanium-containing nickel-titanium and β -titanium ion mixtures, there was no evidence of oxidative stress formation, indicating that a different kind of cytotoxic mechanism must exist when yeast cells are exposed to these two simulated alloys.

According to the presented results, the metal ions released from fixed orthodontic appliances into the oral cavity due to corrosion and biodegradation possess a low-risk profile for users, as only extremely high metal concentrations induced cytotoxicity and oxidative stress, as presented in our in vitro study on the *S. cerevisiae* model organism; however, increased ROS might occur on the local level

in the oral cavity, especially in patients with a deficiency in antioxidant defense systems, which should be further investigated.

Author Contributions: V.K., B.P., J.P. and P.J. conceptualized the study. V.K. carried out and analyzed experiments. V.K. wrote the original draft, V.K., B.P., J.P. and P.J. reviewed and edited the manuscript. All authors have read and agreed to the published version of the manuscript.

Funding: This work was supported by the Slovenian Research Agency (grant numbers P3-0388 and J3-2523).

Conflicts of Interest: The authors declare no conflict of interest.

Abbreviations

ROS	Reactive oxygen species
SOD	Superoxide dismutase
CAT	Catalase
GPx	Glutathione peroxidase
L	Luminescence
OD	Optical density
H ₂ DCF-DA	2',7'-dichlorofluorescein diacetate
MDA	Malondialdehyde
CFU	Colony forming units
PBS	Phosphate-Buffered Saline
Wt	Wild type
SS	Stainless steel
ELG	Elgiloy
REM	Remaloy
NiTi	Nickel-titanium
TiMo	B-titanium
EDAX	Energy-dispersive X-ray spectroscopy

References

1. Wendl, B.; Wiltsche, H.; Lankmayr, E.; Winsauer, H.; Walter, A.; Muchitsch, A.; Jakse, N.; Wendl, M.; Wendl, T. Schwermetallfreisetzungprofile aus kieferorthopädischen Bändern Brackets und Drähten: Eine in-vitro-Untersuchung. *J. Orofac. Orthop.* **2017**, *78*, 494–503. [[CrossRef](#)]
2. Nascimento, G.; Santos, R.L.D.; Pithon, M.M.; De Souza Araújo, M.T.; Nojima, M.G.; Nojima, L.I. The effect of electric spot-welding on the mechanical properties of different orthodontic wire alloys leonard euler andrade. *Mater. Res.* **2012**, *15*, 409–414. [[CrossRef](#)]
3. Abdallah, M.-N.; Lou, T.; Retrouvey, J.-M.; Suri, S. Biomaterials used in orthodontics: Brackets, archwires, and clear aligners. In *Advanced Dental Biomaterials*; Elsevier: Amsterdam, The Netherlands, 2019; pp. 541–579.
4. Sifakakis, I.; Eliades, T. Adverse reactions to orthodontic materials. *Aust. Dent. J.* **2017**, *62*, 20–28. [[CrossRef](#)] [[PubMed](#)]
5. Lucchese, A.; Carinci, F.; Brunelli, G.; Monguzzi, R. An in vitro study of resistance to corrosion in brazed and laser-welded orthodontic appliances. *Eur. J. Inflamm.* **2011**, *9*, 67–72.
6. Muguruma, T.; Iijima, M.; Mizoguchi, I. Corrosion of laser-welded stainless steel orthodontic wires. *Orthod. Waves* **2018**, *77*, 18–23. [[CrossRef](#)]
7. Mikulewicz, M.; Chojnacka, K.; Wołowicz, P. Release of metal ions from fixed orthodontic appliance An in vitro study in continuous flow system. *Angle Orthod.* **2014**, *84*, 140–148. [[CrossRef](#)] [[PubMed](#)]
8. Tahmasbi, S.; Ghorbani, M.; Sheikh, T.; Yaghoubnejad, Y. Galvanic Corrosion and Ion Release from Different Orthodontic Brackets and Wires in Acidic Artificial Saliva. *J. Dent. Sch. Shahid Beheshti Univ. Med. Sci.* **2019**, *32*, 37–44. [[CrossRef](#)]
9. Reimann, S.; Rewari, A.; Keilig, L.; Widu, F.; Jäger, A.; Bourauel, C. Materialtechnische Untersuchungen kieferorthopädischer Brackets nach Wiederaufbereitung. *J. Orofac. Orthop.* **2012**, *73*, 454–466. [[CrossRef](#)]
10. Mikulewicz, M.; Chojnacka, K. Trace Metal release from orthodontic appliances by in vivo studies: A systematic literature review. *Biol. Trace Elem. Res.* **2010**, *137*, 127–138. [[CrossRef](#)]

11. Mikulewicz, M.; Chojnacka, K. Release of metal ions from orthodontic appliances by in vitro studies: A systematic literature review. *Biol. Trace Elem. Res.* **2011**, *139*, 241–256. [[CrossRef](#)]
12. Bandeira, A.M.; Ferreira Martinez, E.; Ana Dias Demasi, P. Evaluation of toxicity and response to oxidative stress generated by orthodontic bands in human gingival fibroblasts. *Angle Orthod.* **2020**, *90*, 285–290. [[CrossRef](#)] [[PubMed](#)]
13. Kanti Das, T.; Wati, M.R.; Fatima-Shad, K. Oxidative Stress Gated by Fenton and Haber Weiss Reactions and Its Association with Alzheimer's Disease. *Arch. Neurosci.* **2014**, *2*, e20078. [[CrossRef](#)]
14. Nuran Ercal, B.S.P.; Hande Gurer-Orhan, B.S.P.; Nukhet Aykin-Burns, B.S.P.; Ercal, N.; Gurer-Orhan, H.; Aykin-Burns, N. Toxic metals and oxidative stress. Part I: Mechanisms involved in metal induced oxidative damage. *Curr. Top. Med. Chem.* **2001**, *1*, 529–539. [[CrossRef](#)]
15. Toy, E.; Yuksel, S.; Ozturk, F.; Karatas, O.H.; Yalcin, M. Evaluation of the genotoxicity and cytotoxicity in the buccal epithelial cells of patients undergoing orthodontic treatment with three light-cured bonding composites by using micronucleus testing. *Korean J. Orthod.* **2014**, *44*, 128–135. [[CrossRef](#)] [[PubMed](#)]
16. Galagan, J.E.; Henn, M.R.; Ma, L.J.; Cuomo, C.A.; Birren, B. Genomics of the fungal kingdom: Insights into eukaryotic biology. *Genome Res.* **2005**, *15*, 1620–1631. [[CrossRef](#)] [[PubMed](#)]
17. Costa, V.; Moradas-Ferreira, P. Oxidative stress and signal transduction in *Saccharomyces cerevisiae*: Insights into ageing, apoptosis and diseases. *Mol. Aspects Med.* **2001**, *22*, 217–246. [[CrossRef](#)]
18. Khurana, V.; Lindquist, S. Modelling neurodegeneration in *Saccharomyces cerevisiae*: Why cook with baker's yeast? *Nat. Rev. Neurosci.* **2010**, *11*, 436–449. [[CrossRef](#)]
19. Sigler, K.; Chaloupka, J.; Brozmanová, J.; Stadler, N.; Höfer, M. Oxidative stress in microorganisms—I. Microbial vs. higher cells—Damage and defenses in relation to cell aging and death. *Folia Microbiol. Praha* **1999**, *44*, 587–624. [[CrossRef](#)]
20. Moradas-Ferreira, P.; Costa, V.; Piper, P.; Mager, W. The molecular defences against reactive oxygen species in yeast. *Mol. Microbiol.* **1996**, *19*, 651–658. [[CrossRef](#)]
21. Traini, T.; Danza, M.; Zollino, I.; Altavilla, R.; Lucchese, A.; Sollazzo, V.; Trapella, G.; Brunelli, G.; Carinci, F. Histomorphometric evaluation of an immediately loaded implant retrieved from human mandible after 2 years. *Int. J. Immunopathol. Pharmacol.* **2011**, *24*, 31–36. [[CrossRef](#)]
22. Cal, E.; Cetintas, V.; Boyacioglu, H.; Güneri, P. Cytotoxicity of Dental Implants: The Effects of Ultrastructural Elements. *Int. J. Oral Maxillofac. Implants* **2017**, *32*, 1281–1287. [[CrossRef](#)] [[PubMed](#)]
23. Chandar, S.; Kotian, R.; Madhyastha, P.; Kabekkodu, S.; Rao, P. In vitro evaluation of cytotoxicity and corrosion behavior of commercially pure titanium and Ti-6Al-4V alloy for dental implants. *J. Indian Prosthodont. Soc.* **2017**, *17*, 35–40. [[CrossRef](#)] [[PubMed](#)]
24. Cîndea Ciurea, A.; Şurlin, P.; Stratul, Ş.I.; Soancă, A.; Roman, A.; Moldovan, M.; Tudoran, B.L.; Pall, E. Evaluation of the biocompatibility of resin composite-based dental materials with gingival mesenchymal stromal cells. *Microsc. Res. Tech.* **2019**, *82*, 1768–1778. [[CrossRef](#)]
25. Jiang, R.D.; Lin, H.; Zheng, G.; Zhang, X.M.; Du, Q.; Yang, M. In vitro dentin barrier cytotoxicity testing of some dental restorative materials. *J. Dent.* **2017**, *58*, 28–33. [[CrossRef](#)]
26. Caldas, I.P.; Alves, G.G.; Barbosa, I.B.; Scelza, P.; De Noronha, F.; Scelza, M.Z. In vitro cytotoxicity of dental adhesives: A systematic review. *Dent. Mater.* **2019**, *35*, 195–205. [[CrossRef](#)] [[PubMed](#)]
27. Hafez, H.S.; Selim, E.M.N.; Kamel Eid, F.H.; Tawfik, W.A.; Al-Ashkar, E.A.; Mostafa, Y.A. Cytotoxicity, genotoxicity, and metal release in patients with fixed orthodontic appliances: A longitudinal in-vivo study. *Am. J. Orthod. Dentofac. Orthop.* **2011**, *140*, 298–308. [[CrossRef](#)]
28. Ortiz, A.J.; Fernández, E.; Vicente, A.; Calvo, J.L.; Ortiz, C. Metallic ions released from stainless steel, nickel-free, and titanium orthodontic alloys: Toxicity and DNA damage. *Am. J. Orthod. Dentofac. Orthop.* **2011**, *140*, 115–122. [[CrossRef](#)] [[PubMed](#)]
29. Velasco-Ortega, E.; Jos, A.; Cameán, A.M.; Pato-Mourello, J.; Segura-Egea, J.J. In vitro evaluation of cytotoxicity and genotoxicity of a commercial titanium alloy for dental implantology. *Mutat. Res. Genet. Toxicol. Environ. Mutagen.* **2010**, *702*, 17–23. [[CrossRef](#)]
30. Bueno, R.C.; Basting, R.T. In vitro study of human osteoblast proliferation and morphology on orthodontic mini-implants. *Angle Orthod.* **2015**, *85*, 920–926. [[CrossRef](#)]
31. Limberger, K.M.; Westphalen, G.H.; Menezes, L.M.; Medina-Silva, R. Cytotoxicity of orthodontic materials assessed by survival tests in *Saccharomyces cerevisiae*. *Dent. Mater.* **2011**, *27*, e81–e86. [[CrossRef](#)]

32. Gonçalves, T.S.; De Menezes, L.M.; Trindade, C.; Machado, M.D.S.; Thomas, P.; Fenech, M.; Henriques, J.A.P. Cytotoxicity and genotoxicity of orthodontic bands with or without silver soldered joints. *Mutat. Res. Genet. Toxicol. Environ. Mutagen.* **2014**, *762*, 1–8. [[CrossRef](#)] [[PubMed](#)]
33. Arndt, M.; Brück, A.; Scully, T.; Jäger, A.; Bourauel, C. Nickel ion release from orthodontic NiTi wires under simulation of realistic in-situ conditions. *J. Mater. Sci.* **2005**, *40*, 3659–3667. [[CrossRef](#)]
34. Kusy, R.P. Orthodontic Biomaterials: From the Past to the Present. *Angle Orthod.* **2002**, *72*, 501–512. [[CrossRef](#)]
35. Nayak, R.S.; Khanna, B.; Pasha, A.; Vinay, K.; Narayan, A.; Chaitra, K. Evaluation of Nickel and Chromium Ion Release During Fixed Orthodontic Treatment Using Inductively Coupled Plasma-Mass Spectrometer: An In Vivo Study. *J. Int. oral Heal. JIOH* **2015**, *7*, 14–20.
36. Chaturvedi, T.; Upadhyay, S. An overview of orthodontic material degradation in oral cavity. *Indian J. Dent. Res.* **2010**, *21*, 275. [[CrossRef](#)] [[PubMed](#)]
37. Hurt, A.J. Digital technology in the orthodontic laboratory. *Am. J. Orthod. Dentofac. Orthop.* **2012**, *141*, 245–247. [[CrossRef](#)]
38. Freitas, M.P.M.; Oshima, H.M.S.; Menezes, L.M. Release of toxic ions from silver solder used in orthodontics: An in-situ evaluation. *Am. J. Orthod. Dentofac. Orthop.* **2011**, *140*, 177–181. [[CrossRef](#)]
39. Quadras, D.; Nayak, U.; Kumari, N.; Priyadarshini, H.; Gowda, S.; Fernandes, B. In vivo study on the release of nickel, chromium, and zinc in saliva and serum from patients treated with fixed orthodontic appliances. *Dent. Res. J. Isfahan.* **2019**, *16*, 209–215. [[CrossRef](#)]
40. Amini, F.; Jafari, A.; Amini, P.; Sepasi, S. Metal ion release from fixed orthodontic appliances—An in vivo study. *Eur. J. Orthod.* **2012**, *34*, 126–130. [[CrossRef](#)]
41. Kovac, V.; Poljsak, B.; Perinetti, G.; Primožic, J.; Reis, F.S. Systemic Level of Oxidative Stress during Orthodontic Treatment with Fixed Appliances. *Biomed Res. Int.* **2019**, *2019*. [[CrossRef](#)]
42. Martín-Cameán, A.; Jos, Á.; Mellado-García, P.; Iglesias-Linares, A.; Solano, E.; Cameán, A.M. In vitro and in vivo evidence of the cytotoxic and genotoxic effects of metal ions released by orthodontic appliances: A review. *Environ. Toxicol. Pharmacol.* **2015**, *40*, 86–113. [[CrossRef](#)] [[PubMed](#)]
43. Bhaskar, V.; Subba Reddy, V. Biodegradation of nickel and chromium from space maintainers: An in vitro study. *J. Indian Soc. Pedod. Prev. Dent.* **2010**, *28*, 6. [[CrossRef](#)] [[PubMed](#)]
44. National Research Council. *Applications of Toxicogenomic Technologies to Predictive Toxicology and Risk Assessment*; National Academies Press: Washington, DC, USA, 2007.
45. Zhao, Z. Iron and oxidizing species in oxidative stress and Alzheimer's disease. *AGING Med.* **2019**, *2*, 82–87. [[CrossRef](#)] [[PubMed](#)]
46. Ighodaro, O.M.; Akinloye, O.A. First line defence antioxidants-superoxide dismutase (SOD), catalase (CAT) and glutathione peroxidase (GPX): Their fundamental role in the entire antioxidant defence grid. *Alex. J. Med.* **2018**, *54*, 287–293. [[CrossRef](#)]
47. Turrens, J.F. Mitochondrial formation of reactive oxygen species. *J. Physiol.* **2003**, *552*, 335–344. [[CrossRef](#)]
48. Farrugia, G.; Balzan, R.; Madeo, F.; Breitenbach, M. Oxidative stress and programmed cell death in yeast. *Front. Oncol.* **2012**, *2*, 64. [[CrossRef](#)]
49. El Medawar, L.; Rocher, P.; Hornez, J.C.; Traisnel, M.; Breme, J.; Hildebrand, H.F. Electrochemical and cytocompatibility assessment of NiTiNOL memory shape alloy for orthodontic use. In *Proceedings of the Biomolecular Engineering*; Elsevier: Amsterdam, The Netherlands, 2002; Volume 19, pp. 153–160.
50. Issa, Y.; Brunton, P.; Waters, C.M.; Watts, D.C. Cytotoxicity of metal ions to human oligodendroglial cells and human gingival fibroblasts assessed by mitochondrial dehydrogenase activity. *Dent. Mater.* **2008**, *24*, 281–287. [[CrossRef](#)]
51. Terpilowska, S.; Siwicki, A.K. Interactions between chromium(III) and iron(III), molybdenum(III) or nickel(II): Cytotoxicity, genotoxicity and mutagenicity studies. *Chemosphere* **2018**, *201*, 780–789. [[CrossRef](#)]
52. Orrenius, S. Mechanisms of Oxidative Cell Damage. In *Free Radicals: From Basic Science to Medicine*; Birkhäuser Basel: Basel, Switzerland, 1993; pp. 47–64.
53. Chen, A.; Zeng, G.; Chen, G.; Liu, L.; Shang, C.; Hu, X.; Lu, L.; Chen, M.; Zhou, Y.; Zhang, Q. Plasma membrane behavior, oxidative damage, and defense mechanism in *Phanerochaete chrysosporium* under cadmium stress. *Process. Biochem.* **2014**, *49*, 589–598. [[CrossRef](#)]
54. Huang, M.L.-H.; Chiang, S.; Kalinowski, D.S.; Bae, D.-H.; Sahni, S.; Richardson, D.R. The Role of the Antioxidant Response in Mitochondrial Dysfunction in Degenerative Diseases: Cross-Talk between Antioxidant Defense, Autophagy, and Apoptosis. *Oxid. Med. Cell. Longev.* **2019**, *2019*, 6392763. [[CrossRef](#)] [[PubMed](#)]

55. Akhova, A.V.; Tkachenko, A.G. ATP/ADP alteration as a sign of the oxidative stress development in *Escherichia coli* cells under antibiotic treatment. *FEMS Microbiol. Lett.* **2014**, *353*, 69–76. [[CrossRef](#)] [[PubMed](#)]
56. Cruz, C.M.; Rinna, A.; Forman, H.J.; Ventura, A.L.M.; Persechini, P.M.; Ojcius, D.M. ATP activates a reactive oxygen species-dependent oxidative stress response and secretion of proinflammatory cytokines in macrophages. *J. Biol. Chem.* **2007**, *282*, 2871–2879. [[CrossRef](#)] [[PubMed](#)]
57. Wang, X.; Roper, M.G. Measurement of DCF fluorescence as a measure of reactive oxygen species in murine islets of Langerhans. *Anal. Methods* **2014**, *6*, 3019–3024. [[CrossRef](#)]
58. Diaz, G.; Liu, S.; Isola, R.; Diana, A.; Falchi, A.M. Mitochondrial localization of reactive oxygen species by dihydrofluorescein probes. *Histochem. Cell Biol.* **2003**, *120*, 319–325. [[CrossRef](#)] [[PubMed](#)]
59. Chen, C.Y.; Wang, Y.F.; Lin, Y.H.; Yen, S.F. Nickel-induced oxidative stress and effect of antioxidants in human lymphocytes. *Arch. Toxicol.* **2003**, *77*, 123–130. [[CrossRef](#)] [[PubMed](#)]
60. Gholinejad, Z.; Khadem Ansari, M.H.; Rasmi, Y. Titanium dioxide nanoparticles induce endothelial cell apoptosis via cell membrane oxidative damage and p38, PI3K/Akt, NF- κ B signaling pathways modulation. *J. Trace Elem. Med. Biol.* **2019**, *54*, 27–35. [[CrossRef](#)] [[PubMed](#)]
61. Siddiqui, M.A.; Saquib, Q.; Ahamed, M.; Farshori, N.N.; Ahmad, J.; Wahab, R.; Khan, S.T.; Alhadlaq, H.A.; Musarrat, J.; Al-Khedhairi, A.A.; et al. Molybdenum nanoparticles-induced cytotoxicity, oxidative stress, G2/M arrest, and DNA damage in mouse skin fibroblast cells (L929). *Colloids Surf. B Biointerfaces* **2015**, *125*, 73–81. [[CrossRef](#)]
62. Terpilowska, S.; Siwicki, A.K. Pro- and antioxidant activity of chromium(III), iron(III), molybdenum(III) or nickel(II) and their mixtures. *Chem. Biol. Interact.* **2019**, *298*, 43–51. [[CrossRef](#)]
63. Caicedo, M.; Jacobs, J.J.; Reddy, A.; Hallab, N.J. Analysis of metal ion-induced DNA damage, apoptosis, and necrosis in human (Jurkat) T-cells demonstrates Ni²⁺ and V³⁺ are more toxic than other metals: Al³⁺, Be²⁺, Co²⁺, Cr³⁺, Cu. *J. Biomed. Mater. Res. Part A* **2008**, *86A*, 905–913. [[CrossRef](#)]
64. Dentaurum Materials for Orthodontic Products. Available online: <https://www.dentaurum.de/files/KFO-Werkstoffliste-20.pdf> (accessed on 27 August 2020).
65. Jakubowski, W.; Bartosz, G. Estimation of oxidative stress in *Saccharomyces cerevisiae* with fluorescent probes. *Int. J. Biochem. Cell Biol.* **1997**, *29*, 1297–1301. [[CrossRef](#)]
66. Tetz, L.M.; Kamau, P.W.; Cheng, A.A.; Meeker, J.D.; Loch-Carusio, R. Troubleshooting the dichlorofluorescein assay to avoid artifacts in measurement of toxicant-stimulated cellular production of reactive oxidant species. *J. Pharmacol. Toxicol. Methods* **2013**, *67*, 56–60. [[CrossRef](#)]
67. Ohkawa, H.; Ohishi, N.; Yagi, K. Assay for lipid peroxides in animal tissues by thiobarbituric acid reaction. *Anal. Biochem.* **1979**, *95*, 351–358. [[CrossRef](#)]

Publisher's Note: MDPI stays neutral with regard to jurisdictional claims in published maps and institutional affiliations.



© 2020 by the authors. Licensee MDPI, Basel, Switzerland. This article is an open access article distributed under the terms and conditions of the Creative Commons Attribution (CC BY) license (<http://creativecommons.org/licenses/by/4.0/>).

ANNEX N

Published article Kovač et al., 2021



Article

Causation of Oxidative Stress and Defense Response of a Yeast Cell Model after Treatment with Orthodontic Alloys Consisting of Metal Ions

Vito Kovač ¹, Matic Bergant ², Janez Ščančar ² , Jasmina Primožič ³ , Polona Jamnik ⁴ and Borut Poljšak ^{1,*}

¹ Faculty of Health Sciences, University of Ljubljana, Zdravstvena pot 5, 1000 Ljubljana, Slovenia; kovacv@zf.uni-lj.si

² Department of Environmental Sciences, Jozef Stefan Institute, Jamova 39, 1000 Ljubljana, Slovenia; matic.bergant@ijs.si (M.B.); janez.scancar@ijs.si (J.Š.)

³ Department of Dental and Jaw Orthopedics, Medical Faculty, University of Ljubljana, Hrvatski trg 6, 1000 Ljubljana, Slovenia; jasminaprimozic@gmail.com

⁴ Biotechnical Faculty, University of Ljubljana, Jamnikarjeva ulica 101, 1000 Ljubljana, Slovenia; polona.jamnik@bf.uni-lj.si

* Correspondence: poljsakb@zf.uni-lj.si

Abstract: Misaligned teeth have a tremendous impact on oral and dental health, and the most efficient method of correcting the problem is orthodontic treatment with orthodontic appliances. The study was conducted to investigate the metal composition of selected orthodontic alloys, the release of metal ions, and the oxidative consequences that the metal ions may cause in the cell. Different sets of archwires, stainless steel brackets, and molar bands were incubated in artificial saliva for 90 days. The composition of each orthodontic material and quantification of the concentration of metal ions released were evaluated. Metal ion mixtures were prepared to determine the occurrence of oxidative stress, antioxidant enzyme defense system, and oxidative damage to proteins. The beta titanium alloy released the fewest metal ions and did not cause oxidative stress or protein damage. The metal ions from stainless steel and the cobalt-chromium alloy can cause oxidative stress and protein damage only at high concentrations. All metal ions from orthodontic alloys alter the activity of antioxidant enzymes in some way. The determined amounts of metal ions released from orthodontic appliances in a simulated oral environment are still below the maximum tolerated dose, and the concentrations of released metal ions are not capable of inducing oxidative stress, although some changes in antioxidant enzyme activity were observed at these concentrations.

Keywords: orthodontic appliance; metal ion release; oxidative stress; ROS; antioxidative defense



Citation: Kovač, V.; Bergant, M.; Ščančar, J.; Primožič, J.; Jamnik, P.; Poljšak, B. Causation of Oxidative Stress and Defense Response of a Yeast Cell Model after Treatment with Orthodontic Alloys Consisting of Metal Ions. *Antioxidants* **2022**, *11*, 63. <https://doi.org/10.3390/antiox11010063>

Academic Editor: Gustavo Rafael Mazzaron Barcelos

Received: 22 November 2021

Accepted: 23 December 2021

Published: 28 December 2021

Publisher's Note: MDPI stays neutral with regard to jurisdictional claims in published maps and institutional affiliations.



Copyright: © 2021 by the authors. Licensee MDPI, Basel, Switzerland. This article is an open access article distributed under the terms and conditions of the Creative Commons Attribution (CC BY) license (<https://creativecommons.org/licenses/by/4.0/>).

1. Introduction

The number of patients seeking orthodontic treatment for malocclusions is constantly increasing. Depending on the type and severity of malocclusion, various treatment options are available, including fixed orthodontic appliances. The parts of fixed orthodontic appliances, including brackets, archwires, and bands, are made of various alloys that are meant to be durable, strong, resistant, and most importantly, biocompatible. However, the oral environment, with its constantly changing pH, temperatures, and biological and enzymatic compositions, is a stressful environment for any orthodontic appliance [1]. According to the American Board of Orthodontics, treatment with fixed appliances lasts approximately 24 months [2]; this raises the question of the safe use of such appliances. It is reported that glossitis, gingivitis, contact stomatitis, multifiform erythema, and gingival hypertrophy may occur during orthodontic treatment, which could be related to the toxic effects of metal ions released by fixed orthodontic appliances [3].

Stainless steel, nickel-titanium (Ni-Ti), cobalt-chromium-nickel (Co-Cr-Ni), and β -titanium (β -Ti) are the most commonly used alloys for fixed orthodontic appliances. Nickel

(Ni) has been described as the most allergic compound among orthodontic alloys [4], closely followed by Cr [5]. Titanium (Ti) is also widely used, not only in dentistry but also in other medical fields and also cosmetics. In addition, the most common metals in orthodontic alloys (Ni, Cr, Co, Fe, Ti) have been shown to cause toxic or biological side effects [6,7]. Although biocompatibility concerns arose over the years due to intraoral corrosion and tribocorrosion of various alloys, such as stainless steel, cobalt-chromium, and nickel-titanium, resulting in the increased release of ions with potentially toxic consequences, no consistent results were obtained to date. When evaluating scientific data, the oral environment, especially saliva, also has an impact on metallic materials as it is itself an electrolyte [8]. In vitro evaluation of the release of metal ions from orthodontic alloys is usually performed in artificial saliva, with an emphasis on mimicking in vivo conditions in terms of pH, temperature, and saliva composition [9].

Electrochemical corrosion reactions at the surface of biomaterials are redox reactions in which surface metals are oxidized to metal cations and metal oxides, which in turn can be released into the biological system [10]. Overproduction of reactive oxygen species (ROS), either endogenous or from exogenous sources, alters the redox balance between ROS and the cellular antioxidant system. This results in oxidative stress, which damages DNA, proteins, and lipids and has serious consequences. The best-known mechanism for the generation of ROS by metal ions is the Fenton reaction, in which transition metal ions react with hydrogen peroxide (H_2O_2) to produce a very reactive hydroxyl radical ($\bullet OH$). Another metal ion ROS generating reaction is the Haber–Weiss reaction, in which a reduction of a metal ion occurs, and molecules of superoxide radical ($O_2^{\bullet -}$) and H_2O_2 form $\bullet OH$ [11]. Some metal ions have the redox capacity to generate oxidative stress via the Fenton or Haber–Weiss reaction, but they indirectly enhance the production of radicals by oxidizing glutathione, inducing NADPH oxidases, and affecting enzyme binding sites. Fe, Cr, Cu, Co, Ni belong to the transition metals [12] and are considered redox-active metals, i.e., they can transfer electrons between substrates, generating free radicals from the Fenton and Haber–Weiss reactions [13]. Iron can exist in ferrous (+II) and ferric (+III) forms, where ferrous ions react with oxygen to form superoxide radicals [14] or generate hydroxyl radicals via the Fenton reaction [15]. Nevertheless, iron is also an essential cofactor for many enzymes of the electron transport chain as well as a cofactor for many catalases and peroxidases of the antioxidant defense [16]. Cr, Co, Ni, and certain metal ions can also participate in the Fenton-like reaction instead of iron [17]. Chromium occurs biologically in trivalent (Cr[III]) and hexavalent (Cr[VI]) forms, with the hexavalent form considered toxic but efficiently reduced to lower oxidation states and detoxified by chelators in vivo [18]. The reduction of hexavalent Cr produces reactive oxygen species such as superoxide and hydroxyl radicals, further unbalancing the redox scale [19]. Cobalt is another metal that uses the Fenton reaction to form reactive oxygen species [20]. Unlike other transition metals, nickel produces little ROS, but the mechanism of the Fenton reaction is the same [21]. The oxidation of Ni(II) to Ni(III) could be the cause of ROS formation. Molybdenum is an essential element in many functional enzymes of respiratory pathways and oxidative stress defense [22,23].

Under oxidative stress conditions, DNA, protein, and lipid damage occurs [24]. Xia et al. [25] suggest that increased oxidant levels in the cells initially trigger an antioxidant defense response, followed by inflammation and consequently cytotoxicity if the stress signal is strong enough. Thus, the first cellular response to increased oxidant concentrations is the induction of the cellular antioxidant defense system. To maintain redox balance, a complex endogenous antioxidant defense system is established in cells consisting of enzymatic antioxidants such as superoxide dismutase (SOD), catalase (CAT), peroxiredoxin (PRDX), glutathione peroxidase (GPx), glutathione reductase (GR), and thioredoxin reductase (TrxR) and endogenous non-enzymatic antioxidants such as glutathione (GSH) as well as exogenous vitamin C, carotenoids, and flavonoids [26]. The progression of oral diseases such as periodontitis, an inflammation of the gingival tissues, is closely associated with oxidative stress [27]. Markers of oxidative stress are also demonstrated in other periodontal diseases [28].

In this study, two topics were investigated: first, the release of metal ions from orthodontic appliances and the metal composition of orthodontic alloys, and second, the activation of the enzymatic antioxidant defense system and oxidative damage to proteins as a result of cell treatment with metal ions. Parts of orthodontic appliances (wires, brackets, and molar bands) made of different alloys (stainless steel, Ni-Ti, β -Ti, and Co-Cr) were incubated in a simulated oral environment for 90 days, and the amount of metal ions released was recorded over the period. The metal composition of each orthodontic alloy was also determined, and the data obtained were used to prepare metal ion mixtures further. In our previous study [7], we investigated the possible adverse effects that metal ion mixtures of different orthodontic alloys may have on a yeast cell model, highlighting the aspect of cytotoxicity and the formation of ROS. It was found that certain metal ion mixtures can cause cytotoxic effects and oxidative stress at certain concentrations. Since oxidative stress defense mechanisms are activated before the stress occurs, the focus here was on observing the activity of cellular enzymatic antioxidants deployed at metal ion concentrations ranging from 1 μ M to 1000 μ M. To assess oxidative damage to proteins, the carbonyl content of proteins was used as a marker.

2. Materials and Methods

2.1. Orthodontic Material Preparation

In the study, eight different types of samples were analyzed. Among them, six samples were different types of wires: stainless steel (Damon 0.016 \times 0.25, Ormco, Brea, CA, USA), nickel-titanium (BioStarter 0.016", Forestadent, Pforzheim, Germany and rematitan super elastic 0.016" Dentaaurum, Ispringen, Germany), titanium-molybdenum (rematitan SPECIAL, Dentaaurum, Ispringen, Germany), chromium-cobalt (Elgiloy 0.036" Rocky Mountain Orthodontics, Denver, CO, USA and remaloy 0.036" Dentaaurum, Germany), and the remaining two were stainless steel brackets (Discovery Dentaaurum, Ispringen, Germany) and stainless steel bands (W-Fit Form Forestadent, Pforzheim, Germany). A detailed description of all the samples is provided in Table 1. Both the upper and lower sections of each type of archwire were analyzed. In addition, a set of 24 brackets and 4 molar bands were tested. Each part of an apparatus (wire, bracket, and band) had the surface measured using a digital caliper. All materials were sterile before the beginning of the study.

To simulate oral conditions, artificial saliva was prepared using an aqueous solution of NaCl, KCl, $\text{CaCl}_2 \cdot 2\text{H}_2\text{O}$, $\text{NaH}_2\text{PO}_4 \cdot 2\text{H}_2\text{O}$, $\text{Na}_2\text{S} \cdot 9\text{H}_2\text{O}$, and urea in concentrations of 400 mg/mL, 400 mg/mL, 960 mg/L, 690 mg/L, 5 mg/L, and 1000 mg/L, respectively. All reagents were of high purity and purchased from Merck (Darmstadt, Germany). Ultrapure water (Milli-Q, 18.2 M Ω cm) obtained from a Direct-Q 5 Ultrapure water system (Millipore, Watertown, MA, USA) was used for the solution preparation. The medium was then adjusted to a pH of 6.7–6.8, resembling neutral pH in the oral cavity. A WTW 330 pH (Weilheim, Germany) meter was employed to determine the pH.

Teflon beakers were used to minimize blanks and to prevent the absorption of metals on the walls of the containers during the experiment. To each beaker, 250 mL of artificial saliva were added along with the sample of parts of fixed orthodontic appliances (either two sets of wires, 24 brackets, or 4 molar bands). To control the blanks arising from the chemicals and the potential leaching of metal ions from the beakers used, 250 mL of artificial saliva were added into the Teflon beaker and analyzed along with the samples throughout the experiment. Blank values were subtracted from the determined concentrations of elements released from orthodontic appliances into the artificial saliva. All the experiments were prepared in duplicate. Samples were incubated in a dust-free incubator at 37 °C for 90 days. They were gently shaken to distribute the released metal ions into the leaching solution evenly. Sampling was carried out at seven different time points ($t_1 = 12$ h, $t_2 = 24$ h, $t_3 = 48$ h, $t_4 = 7$ days, $t_5 = 30$ days, $t_6 = 60$ days, and $t_7 = 90$ days). Before the sampling procedure, each Teflon beaker was gently turned upside down two times to ensure the even distribution of elements in the sample volume. From each beaker, 3 mL of sample were taken, acidified with 6 μ L of supra pure nitric acid, and stored at -20 °C until the analysis.

Table 1. Orthodontic materials used in the study with their corresponding metal composition in weight percentages (%).

Component	Type	Specification	Parts in the Sample	Combined Surface (cm ²)	Fe (%)	Ni (%)	Cr (%)	Co (%)	Mo (%)	Ti (%)
Archwire	Stainless steel	Damon 0.016 × 0.25 Ormco, Brea, CA, USA	2	5.104	58.3	14.6	27.1	<0.1	<0.1	<0.1
	Ni-Ti	Biostarter 0.016" Forestadent, Pforzheim, Germany	2	4.172	<0.1	73.8	<0.1	<0.1	<0.1	26.2
	Ni-Ti	rematitan super elastic 0.016" Dentaurum, Ispringen, Germany	2	4.149	<0.1	73.2	<0.1	<0.1	<0.1	26.8
	Ti-Mo	rematitan SPECIAL 0.032" Dentaurum, Ispringen, Germany	2	6.846	<0.1	<0.1	<0.1	<0.1	8.18	91.8
	Co-Cr-Ni	Elgiloy 0.036" Rocky Mountain Orthodontics, Denver, CO, USA	2	9.476	6.12	19.9	21.6	49.7	2.65	<0.1
	Co-Cr-Ni	remaloy.036" Dentaurum, Ispringen, Germany	2	9.217	1.42	26.1	19.4	53.2	<0.1	<0.1
Brackets	Stainless steel	Discovery Dentaurum, Ispringen, Germany	24	14.478	55.4	17.8	24.9	<0.1	1.95	<0.1
Molar bands	Stainless steel	W-Fit Form Forestadent, Pforzheim, Germany	4	9.881	57	18.2	24.9	<0.1	<0.1	<0.1

Metal Release and Alloy Constitution Analysis

To determine the metal composition of samples, approximately 10 mg of each sample were completely digested in 5 mL of appropriate acid by heating the solution at 90 °C. Stainless steel samples were digested in aqua regia, all titanium-based alloys in a mixture of HNO₃, HF, and HCl (4:2:1 volume ratio), and Elgiloy and remaloy alloys in pure hydrochloric acid. Total metal ion concentrations in the digested samples and concentrations of metal ions released in the artificial saliva were determined by inductively coupled plasma mass spectrometry (ICP-MS) on an Agilent 7700x ICP-MS instrument (Tokyo, Japan), using matrix-matched standards for calibration. ICP-MS measurement parameters are presented in Table S1 of the supplementary material. Measurement uncertainty for all elements analyzed was better than ±3%.

Since there are no certified reference materials available for the determination of trace elements in orthodontic appliances, the accuracy of the determination of metal ions in the analyzed samples was assessed by the spike recovery test. For this purpose, bracket samples were spiked with known amounts of the elements analyzed before the digestion process, and the analytical procedure was applied. For checking the accuracy of the determination of the concentrations of metal ions released into artificial saliva, the samples collected 90 days after incubation were spiked with known amounts of metals and concentrations determined by ICP-MS. Good agreement between the theoretically calculated and measured concentrations (differences did not exceed ±5%) was obtained, confirming the accurate determination of total metal concentrations and the concentrations released into artificial saliva by ICP-MS. Blank samples of artificial saliva were analyzed along with the samples investigated throughout the experiment.

2.2. Orthodontic Metal Ion Solutions and Yeast Metal Treatment

To simulate orthodontic alloys, high-purity salts of FeCl₃·6H₂O, CrCl₃·6H₂O, NiCl₂·6H₂O, and CoCl₂·6H₂O, as well as titanium and molybdenum standards for AAS (TraceCERT, Merck, Darmstadt, Germany), were used. Final concentrations of 0.2 M stock solutions of metal mixtures were prepared with sterile ddH₂O and had their pH adjusted to 7. Mixtures were also sonicated in an ultrasound bath to ensure sterile conditions. A detailed description of each metal ion concentration is represented in Table 1.

2.3. Preparation of Yeast Culture and Metal Treatment

S. cerevisiae wild type yeast strain BY4742 (EUROSCARF, Oberursel, Germany) was grown until the early stationary phase in a liquid yeast extract-peptone-glucose medium ((2% (w/v) glucose, 2% (w/v) peptone, and 1% (w/v) yeast extract (Merck, Darmstadt, Germany)) at 28 °C with 220 RPM constant shaking. After reaching the desired density, the yeast culture was transferred into PBS buffer (Merck, Darmstadt, Germany).

Yeast cultures were exposed to metal ion mixtures in concentrations of 1 μM, 10 μM, 100 μM, and 1000 μM. The untreated yeast culture served as a control sample. Treatment lasted 24 h in an incubator shaker at 28 °C and 220 RPM.

2.4. Reactive Oxygen Species (ROS) Level Determination

Detection of intracellular ROS level was performed using the fluorescent dye 2',7'-dichlorofluorescein diacetate (H₂DCF-DA). After the metal treatment, cells were washed twice with 50 mM potassium phosphate buffer, and the dye was added in a final concentration of 10 μM. An incubation time of 30 min in the dark and another washing step were employed before the dye fluorescence (ex/em = 488/520 nm) was measured with a Varioskan LUX microplate reader (ThermoFisher, Waltham, MA, USA). To determine cell viability, cell suspensions were properly diluted with PBS to a dilution of 10⁻⁶ and plated on solid YPD plates. After 48 h incubation at 28 °C, yeast colonies formed on the solid YPD plates and were counted. The number of formed yeast colonies was expressed as colony forming units (CFU). The results were expressed as the fluorescence divided with values for the cell viability to obtain more accurate results.

2.5. Enzymatic Antioxidants Activity Determination

2.5.1. Cell Lysate Preparation

Yeast cell samples were collected after 24 h metal treatment, centrifuged for 5 min at 4000 RPM and 4 °C, and washed twice with PBS. The cell pellet was resuspended in lysis buffer (0.05 M Tris-HCl pH 8 with protease inhibitor (Roche, Basel, Switzerland)) followed by glass bead homogenization. Cell lysates were centrifuged at 20,000 × *g* and 4 °C for 20 min. The protein concentration of the obtained supernatant was determined using the Bradford assay [29].

2.5.2. Superoxide Dismutase (Sod) Activity

Determination of SOD activity is based on the autoxidative ability of pyrogallol at alkaline pH [30]. When pyrogallol oxidates, a yellow product (purpurogallin) is formed, and the color change can be spectrophotometrically monitored at 420 nm absorbance, but in the presence of SOD, the rate of color change is depleted. The assay measures activities of all SOD types (Cu-Zn-SOD, Mn-SOD, and EC-SOD). When the final concentration of 0.3 mM pyrogallol is added to the wells with 50 mM cacodylic acid, 1 mM DTPA, and the enzyme sample, the color change rate at 420 nm is observed every 15 s for 5 min. More SOD is present in the sample, when the lesser the color change was observed. Results are expressed as the percentage activity of the SOD enzyme after treatment, compared to the enzyme activity of the untreated control sample.

2.5.3. Catalase (CAT) Activity

CAT activity was determined by the rate of hydrogen peroxide removal, which can be observed as a decrease in absorbance at 240 nm. Lysate samples were diluted at 1:50 with 50 mM phosphate buffer. In a well, phosphate buffer, the diluted sample and 10 mM H₂O₂ were combined. The decrease in absorbance at 240 nm was monitored every 20 s for 5 min. Results are expressed as the percentage activity of the CAT enzyme after treatment, compared to the enzyme activity of the untreated control sample.

2.5.4. Glutathione Peroxidase (GPx) Activity

GPx activity was determined with an adapted method from Smith and Levander [31]. Samples were mixed with a stock solution of 6.5 mM EDTA-Na₂, 1.3 mM NaN₃, 0.5 mM NADPH, 2.5 mM GSH, and 1.7 U/mL GR in 65 mM PBS. For the reaction to begin, 250 μM H₂O₂ were added. Absorbance change was measured every 15 s at 340 nm. Results are expressed as the percentage activity of the GPx enzyme after treatment, compared to the enzyme activity of the untreated control sample.

2.5.5. Glutathione Reductase (GR) Activity

Measurement of GR activity was adapted from Glippa et al. [32] with small adaptations. The assay was based on the GR's ability to convert oxidized glutathione (GSSG) to reduced glutathione (GSH) by using NADPH as a substrate. Formed GSH reacts with the 5,5'-dithiobis (2-nitrobenzoic acid) (DTNB) to generate a yellow-colored product. The change in the absorbance was measured after 3–6 min at 412 nm. Results are expressed as the percentage activity of the GR enzyme after treatment, compared to the enzyme activity of the untreated control sample.

2.5.6. Thioredoxin Reductase (TrxR) Activity

The method from Smith and Levander [31] was slightly modified for TrxR activity evaluation. First, the reagent composing of 10 mM EDTA-Na₂, 5 mM DTBN, 240 μM NADPH, and 0.2 mg/mL bovine serum albumin in 100 mM PBS was prepared. Then, lysate samples were separated into two groups: the first group was treated with 5% ethanol; the second group was treated with 5% ethanol containing 1.47 mM inhibitor auranofin. By adding the mixed reagent to samples, changes in absorbance at 412 nm were observed

every 15 s for 5 min. Results are expressed as the percentage activity of the TrxR enzyme after treatment, compared to the enzyme activity of the untreated control sample.

2.5.7. Peroxiredoxin (PRDX) Activity

PRDX activity was determined according to the method proposed by Ali and Hadwan [33]. Lysate samples were mixed with 2.1 mM 1,4-dithio-DL-threitol, 10 mM NaN₃, 50 mM phosphate buffer, and 2.1 mM H₂O₂. After 3 min, the reaction was stopped by adding the titanium reagent (0.1% TiCl₄ in 20% H₂SO₄). Due to residual H₂O₂, the concentration of newly formed peritanic acid could be assessed spectrometrically at 405 nm. Results are expressed as the percentage activity of the PRDX enzyme after treatment, compared to the enzyme activity of the untreated control sample.

2.5.8. In-Gel Enzyme Activity

Zymograms of SOD and CAT were performed according to Weydert and Cullen [34]. The SOD gel assay was conducted on 12% non-denaturing polyacrylamide gel with a 5% stacking gel. At least 150 µg of the protein sample were used for each sample and loaded onto the gel. Samples were subjected to electrophoresis conditions for 3 h at 40 mA and 4 °C. Gels were stained for 20 min with SOD stain (2.43 mM NBT, 28 mM TEMED, and 0.14 M riboflavin 5'-phosphate in 50 mM PBS) and then washed twice with dH₂O. Washed gels were placed in fresh dH₂O and left under fluorescent light for at least 30 min or until distinctive bands appeared. Gels were washed three more times and were imaged. The same electrophoresis procedure was applied for CAT, but CAT and GPx gel assays were performed on 7.5% gels. Before staining, CAT gels were incubated in 0.003% H₂O₂ for 10 min, then washed twice with dH₂O. The 2% ferric chloride and 2% potassium ferricyanide were prepared separately and used to stain the CAT gels. As soon as the bands appeared, the gel was washed extensively, and an image of the gel was taken. The band intensity of each gel image was determined by ImageJ, image-analysis software (Java-based image processing software, National Institutes of Health, Bethesda, MD, USA), and the activity of the treated samples was compared to the untreated control.

2.6. Oxidative Protein Damages

The reaction between 2,4-dinitrophenylhydrazine (DNPH) and protein carbonyl groups was employed to assess oxidative damage on proteins. Following the proposed method of Mesquita et al. [35], we combined our lysate sample with 10 mM DNPH and after a 10 min incubation, 6 M NaOH were added. Absorbance at 450 nm was obtained after 10 min and was compared between the sample containing protein and the sample where the lysate was substituted with buffer solution. Results are expressed as a percentage of protein oxidative damage after certain metal treatment, compared to the untreated control sample.

2.7. Statistical Analysis

A graphical presentation and statistical analysis were performed with GraphPad Prism (version 8.02 for Windows, GraphPad Software, La Jolla, CA, USA). A single-factor analysis of variance (One-way ANOVA) and Dunnett's post hoc test were used to determine the differences between results. Results are expressed as means with 95% confidential intervals. Statistical significance was set at $p < 0.05$.

3. Results

3.1. Metal Ion Release

The metal compositions (Fe, Ni, Cr, Co, Ti, and Mo) of each part of the orthodontic appliances are presented in Table 1. Damon stainless steel archwires (Ormco, Brea, CA, USA), Discovery stainless steel brackets (Dentaurum, Ispringen, Germany), and W-Fit Form stainless steel bands (Forestadent, Pforzheim, Germany) had roughly the same composition of Fe, Ni, and Cr. Among them, only Discovery stainless steel brackets contained Mo (Mo = 1.95%). Both Ni-Ti archwires, rematitan super elastic (Dentaurum,

Ispringen, Germany), and Biostarter (Forestadent, Pforzheim, Germany), included in the present study, had a very similar metal composition, Ni \approx 73%, and Ti \approx 26%. The two Co-Cr-Ni archwires, Elgiloy (Rocky Mountain Orthodontics, Denver, CO, USA), and remaloy (Dentaurum, Ispringen, Germany) differ from each other in every measured metal ion content, and only Elgiloy contained Mo (Mo = 2.65%). The rematitan SPECIAL Ti-Mo archwire (Dentaurum, Ispringen, Germany) was composed of Ti = 91.81% and Mo = 8.18%.

The release of metal ions from orthodontic appliances into artificial saliva (expressed in ng/mL) during the 90-day monitoring period is shown in Figure 1, while the corresponding metal ion concentrations are given in the supplementary material (Table S2).

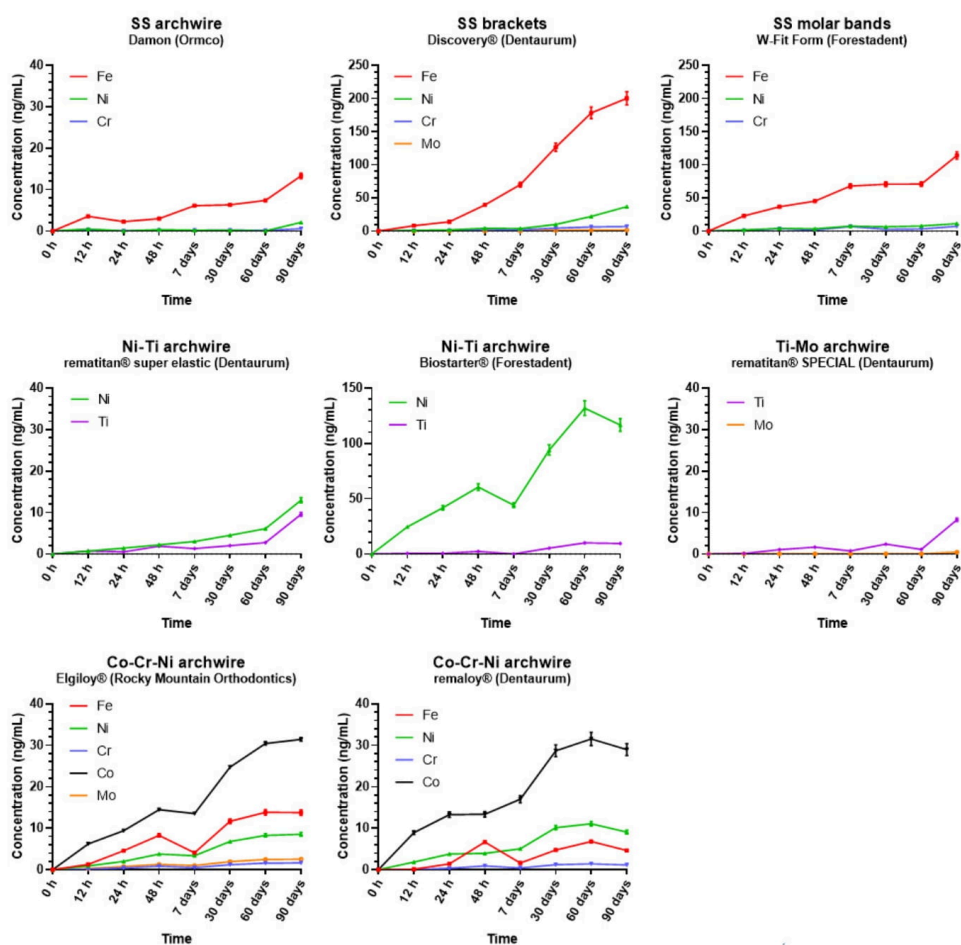


Figure 1. The release of metal ions from different parts of fixed orthodontic appliances into artificial saliva at different time points during the 90-day observational period. The results represent the average concentration of two parallel samples with standard deviations.

As evident from Figure 1, in both stainless steel brackets and molar bands, Fe release was dominant over the other metals with a concentration of \approx 200 ng/mL in the case of

brackets and ≈ 114 ng/mL for molar bands at t_7 . Similarly, the amount of Fe released from stainless steel archwire steadily increased until the end of the study (Fe ≈ 13.3 ng/mL), while Ni and Cr concentrations released from them were near zero at all time points except at t_7 , when an increase in their concentrations was observed (≈ 2.1 ng/mL and ≈ 0.6 ng/mL, for Ni and Cr, respectively).

Regarding the Ni-Ti archwires, the same amount of Ti was released from both Ni-Ti archwires examined (Ti ≈ 9.5 ng/mL), while higher amounts of Ni were released (≈ 13 ng/mL and ≈ 116 ng/mL for Ni Dentaurum and Ni Forestadent, respectively). In the case of Ti-Mo archwires, Mo was below the limit of detection, except at t_7 , when its concentration was 0.45 ng/mL. Ti released from Ti-Mo archwires remained constant, approximately 1.5 ng/mL, during the entire observational period with a small peak, detected at the last time point (Ti ≈ 8.3 ng/mL). Metal release from both Cr-Co-Ni archwires increased gradually during the observational period. The concentrations of Cr, Co, and Ni detected were similar for both Elgiloy and remaloy archwires. Of note, a different concentration of Fe release (FeRemaloy ≈ 4.6 ng/mL, FeElgiloy ≈ 13.7 ng/mL) and the absence of Mo in the Remaloy archwire were detected. At t_7 , both Cr-Co-Ni archwires experienced stagnation in metal ions' release with concentrations of ≈ 1.5 ng/mL, ≈ 30 ng/mL, and ≈ 9 ng/mL for Cr, Co, and Ni, respectively.

3.2. Intracellular Oxidation Level

The ROS marker used to assess the intracellular oxidation level, H_2DCFDA , is hydrolyzed intracellularly and converted to fluorescent DFC in the presence of ROS [36]. There is a correlation between the CFU count and the fluorescence intensity of the dye, since only metabolically active cells can hydrolyze the dye into a fluorescent product [37,38]. Valiakhmetov et al. [39] showed that under stress conditions, the population of viable ROS generating cells responds proportionally with the death of the cell population, implying that fluorescence intensity alone is not sufficient as an indicator of ROS generation and must be coupled with an assay for cell viability [40]. Figure 2 shows the relationship between the intensity of the fluorescent signal and the yeast cell CFU count. A significant increase in the ROS generation, as well as the cytotoxicity, was observed when treating yeast cells with a 1000 μM concentration of SS and 100 μM and 1000 μM Co-Cr concentration. When treating yeast cells with any other metal mixture or concentration, there was no observed difference between the treated and the untreated control cells.

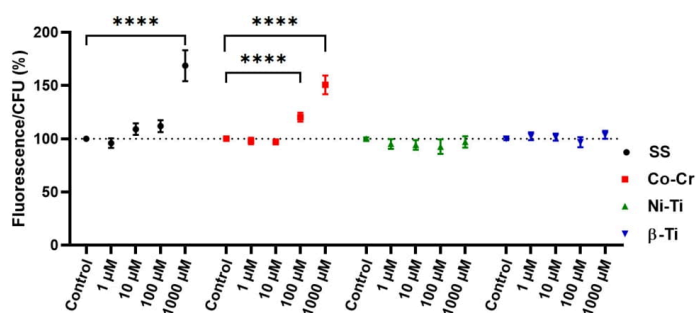


Figure 2. Ratio between the intensity of the fluorescence signal and CFU after treatment of yeast cells with different metal ion mixtures and concentrations. The percentage ratio of fluorescent dye intensity and the yeast CFU value were used to compare the intracellular oxidation of the treated viable cells to the untreated control sample, which was set at 100%. Means with the 95% confidence interval are shown, and the statistically different measurements are labeled with * ($p < 0.05$), ** ($p < 0.01$), *** ($p < 0.001$), and **** ($p < 0.0001$).

3.3. Enzymatic Antioxidative Defense

The ability of enzymatic antioxidant defenses to remove excess oxygen radicals and their products prevents the development of oxidative damage of molecules. For this reason, the enzymatic antioxidative defense system was assessed by measuring the activity of superoxide dismutase, catalase, glutathione peroxidase, glutathione reductase, peroxiredoxin, thioredoxin reductase. As an increase in protein or mRNA expression of antioxidant enzymes does not necessarily mean an increase in activity, both spectrophotometric enzymatic assays and native gel electrophoresis methods were used to assess enzymatic antioxidative defenses.

In-gel antioxidant activity of SOD enzyme (Figure 3) did not show any statistically significant differences between metal treated and untreated control samples, even though some differences in the mean values could be observed. When treating yeast cells with any 1000 μM metal ion concentrations, a shift in the CAT band position was observed, while a statistically significant decrease in CAT activity was observed only in 1000 μM SS treated cells.

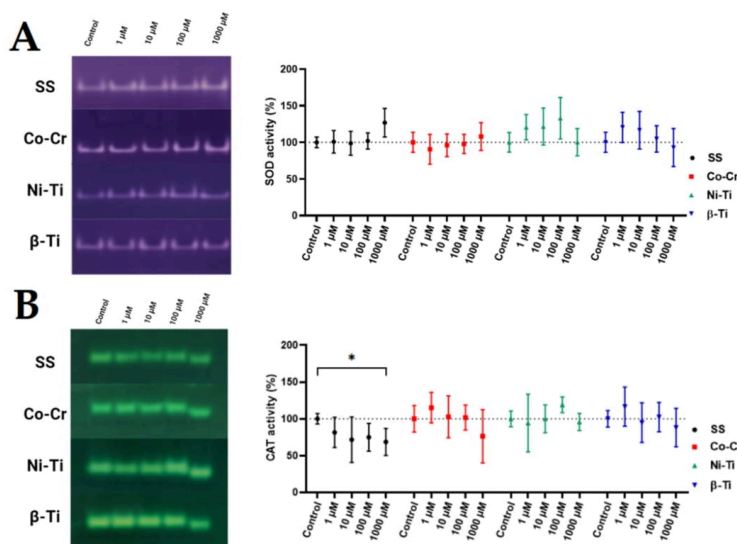


Figure 3. In-gel antioxidative activity of SOD (A) and CAT (B) enzyme after metal ion mixture treatment. The most representative images are shown ($n = 5$). Statistically different results in the graph are labeled with * ($p < 0.05$).

Figure 4 shows the activity of the following enzymes: SOD, CAT, GPx, GR, PRDX, and TrxR, measured spectrophotometrically. The activity of the enzyme SOD increased only when the cells were treated with a concentration of 1000 μM SS. On the other hand, treatment of the cells with different concentrations and metal mixtures did not result in any changes in SOD activity. The CAT activity assay gave more variable results, as the CAT activity decreased noticeably with an increasing metal concentration, with the activity decreasing significantly only when treated with a 1000 μM SS and 1000 μM Ni-Ti concentration. GPx activity was not affected by metal treatment, except that a significant increase in GPx activity was detected when cells were treated with 1000 μM Ni-Ti and 1000 μM β -Ti concentrations. Cell lysates from 1000 μM SS treatment had a decreasing effect on the GR activity, whereas 1000 μM Co-Cr and 10, 100, and 1000 μM β -Ti treatment significantly increased the GR activity. Again, there was a decrease in the activity of

1000 μ M SS cell lysate in the case of TrxR activity, but in all other lysates of cells treated with 100 μ M and 1000 μ M concentrations, TrxR activity was statistically increased. In the case of PRDX activity, only a decrease in activity was observed in the cell lysate from treatment with 1000 μ M SS.

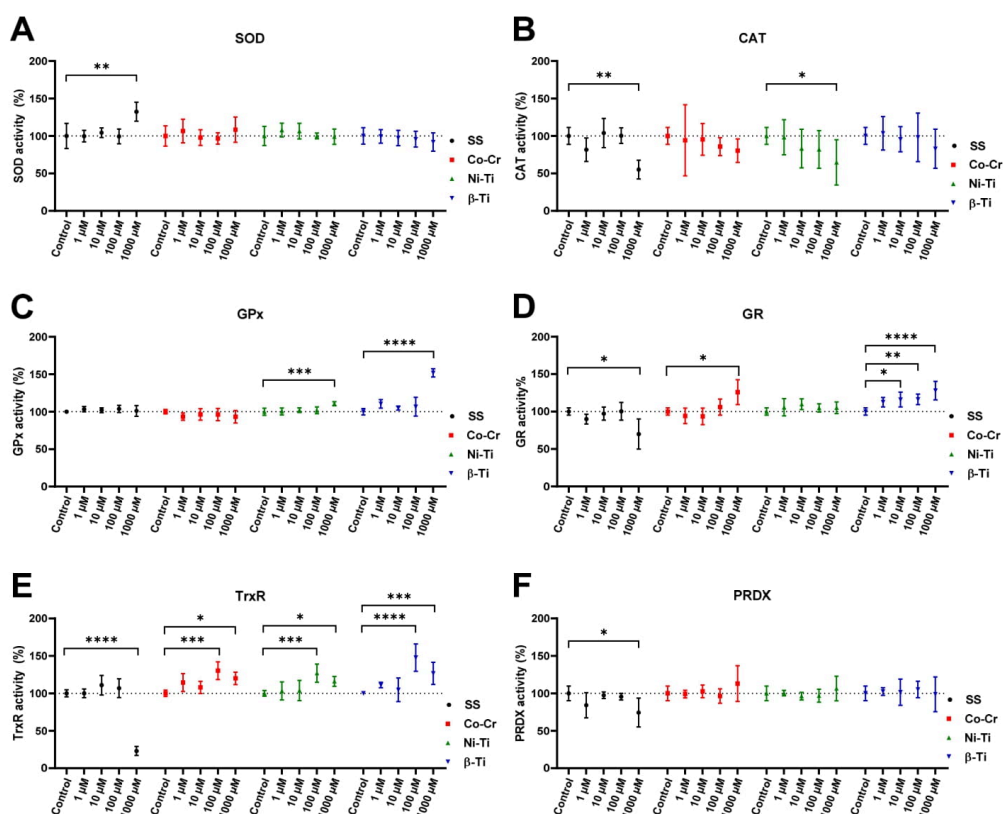


Figure 4. Change in antioxidant enzyme activities when yeast cells are treated with increasing concentrations of different metal ion mixtures, compared to the untreated control. Graph (A) shows SOD, (B) shows CAT, (C) shows GPx, (D) shows GR, (E) shows TrxR, and (F) shows PRDX activity. The untreated sample was set at 100%, and the means with 95% confident interval are shown. Statistically different results are labeled with * ($p < 0.05$), ** ($p < 0.01$), *** ($p < 0.001$), and **** ($p < 0.0001$).

3.4. Protein Oxidative Damage

When proteins are oxidized, stable carbonyl groups are produced on the amino acid side chains, thus making them an ideal marker for determining the oxidative damage to proteins (Figure 5). A statistical difference in protein oxidative damage between the untreated control and the one treated with metal mixtures was observed in the case of 1000 μ M SS, 100 μ M, and 1000 μ M Co-Cr concentrations. Cell lysates from NiTi and β -Ti treatment did not show any changes in protein carbonyl content, compared to the untreated control sample.

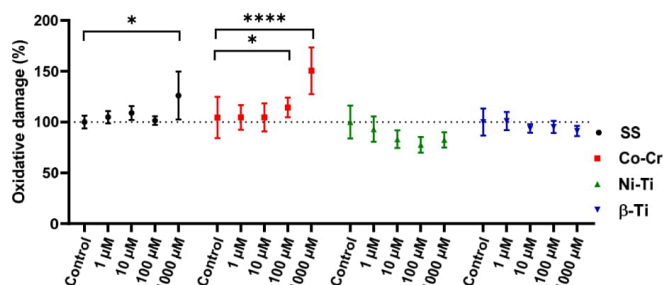


Figure 5. Protein carbonyl content as a result of oxidative protein damage as a result of cell treatment with various metal ions. The control sample was set at 100%, and the means with 95% confident interval are shown. Statistically different results are labeled with * ($p < 0.05$), ** ($p < 0.01$), *** ($p < 0.001$), and **** ($p < 0.0001$).

4. Discussion

4.1. Topic: Metal Ion Release in a Simulated Environment

The present study evidenced an increase in metal ions' concentrations released from different parts of fixed orthodontic appliances over 90 days of exposure to artificial saliva. Although an increase in the measured cumulative concentrations was detected over the observational period, all the measured ions' concentrations were still far below the recommended dietary intake levels. This sense of safety may be underestimated due to non-toxic concentrations of metals inducing biological effects in oral cells [41]. Hypersensitivity to metals, such as nickel, must also be a prime concern when treating orthodontic patients [42]. Overall, the quantity of leached ions increased during the study with minor fluctuations, probably due to minor sampling or measuring errors. Of note, we aimed to assess the concentrations of the five most common metal ions present in alloys of orthodontic appliances. Therefore, it cannot be excluded that other metal ions were also released from the samples. By using pH-neutral artificial saliva, we evaded the possible pH fluctuation that occurs in the oral cavity due to food and biofilm decomposition [43]. This indicates that higher ion release values could be obtained in vivo. Metallic alloys are in use in many medicinal applications, ranging from cardiovascular orthopedic, craniofacial, otorhinology, and dentistry fields [44]. Their biocompatibility makes them inert and allows them to perform the intended requirements while not causing any adverse effects to the host [45]. These ideal properties are endangered by the occurrence of tibocorrosion [46] by which released particles and metal cations from alloys could provoke adverse local tissue reactions [47,48]. According to Brantley and Eliades [49], there are mainly four types of orthodontic alloys in common orthodontic use with the following compositions: stainless steel (Cr = 17–20%, Ni = 8–12%, Fe to balance), cobalt-chromium (Co = 40%, Cr = 20%, Ni = 15%, Mo = 7%, Fe = 16%, other metals = 2%), nickel-titanium (Ni = 55%, Ti = 45%), and β-titanium (Ti = 77.8%, Mo = 11.3%, other metals = 10%) [50,51]. The composition of our orthodontic alloys is slightly different from the presented ones, but there are a lot of different alloy types currently on the market, each having changes in its composition [52].

Ni-Ti archwires were obtained from two manufacturers, and different metal ions releases were detected, despite the same metal composition. Ti concentrations in both archwires were nearly equal after 90 days of exposure but increased steadily throughout the study. While titanium should form an oxide layer to protect against corrosion [53], its increase in the medium is a sign of the deterioration of this protective surface. When observing rematitan super elastic Ni-Ti archwire (Dentaurum) ion release patterns, the concentration of Ni and Ti ions increased in the same manner; the Biostarter Ni-Ti archwire (Forestadent) had ten times more metal ions released than the other Ni-Ti wire. Even though the composition of alloys is the same among different manufacturers, they are

not necessarily of the same quality. In addition, surface topography, processing, and finishing techniques in archwire production play a major part in corrosion resistance since surface roughness and surface defects are the major corrosion sites [54]. According to The European Committee for Standardization devised via EN 1811:2011, nickel released from products must not exceed $0.5 \mu\text{g}/\text{cm}^2/\text{week}$ [55]. After just 7 days, Ni-Ti_{Biostarter} released $2568 \mu\text{g}/\text{cm}^2/\text{week}$ nickel, and after 13 weeks (90 days), we obtained $0.501 \mu\text{g}/\text{cm}^2/\text{week}$ ion release which is the same as the prescribed nickel limit. Because metal release rates were nonlinear for 90 days, a much higher release was obtained in the first week of exposure compared to the last week of exposure, emphasizing the meaning of the performed longitudinal study. Of all orthodontic alloys used in the study, only Co-Cr-Ni alloy metal release seemed to plateau, but since it happened at the end of the study, we cannot conclude that it happened because of metal saturation.

Ni was released in six times higher concentrations from Ni-Ti archwires than the stainless steel archwire, an effect also observed by Charles et al. [56] and Hussain et al. [57], where the nickel release of Ni-Ti-archwire was $4.85 \text{ ng}/\text{mL}$ compared to the stainless steel archwire $0.41 \text{ ng}/\text{mL}$ ion release. This was expected, as the nickel amounts to more than 55% of the Ni-Ti orthodontic alloy, compared to 15% in the SS alloy. Contrary to our findings, Suárez et al. [58] compared corrosion resistance of stainless steel, Ni-Ti, and titanium archwire. They found out that the stainless steel alloy was the least corrosive resistant, meaning that the protective role of Cr_2O_3 oxide film in stainless steel is lesser than TiO_2 from the titanium-containing alloy.

The smallest cumulative amounts of metal ions released were from β -Ti archwires, since this type of archwire has more titanium content to form the protective oxide layer and also a fair share of Mo to form the MoO_3 oxide layer [59]. The Ti-Mo archwire released almost two times fewer Ti metal ions compared to both Ni-Ti archwires, whereas the Mo ion release was negligible until the last sampling time point.

According to the reported upper intake limits (UL), the highest levels of dietary intake that impose no threat to the general population for the examined metal ions are $\text{UL}_{\text{Ni}} = 1 \text{ mg}/\text{d}$, $\text{UL}_{\text{Fe}} = 45 \text{ mg}/\text{d}$, $\text{UL}_{\text{Mo}} = 2 \text{ mg}/\text{d}$, and $\text{UL}_{\text{Ti}} = 1.1 \text{ mg}/\text{d}$ [60]. For Cr, an upper intake limit has not yet been established, but its recommended daily intake is $200 \mu\text{g}/\text{d}$ [60]. Comparing our findings with the UL, even when considering the cumulative concentrations, none of the examined released metal ions exceeded the prescribed daily intake concentrations. Interestingly, after comparing released ion concentrations for each orthodontic material with the alloys' metal composition, it appears that there is no correlation. Stainless steel brackets, for example, contain 56% of Fe, but the relative percentage of the released Fe metal ions was much higher than that at 80%. A similarity to our findings was previously reported by Hwang et al. [61]. In their study, Hussain et al. [62] concluded that the ion release is not dependent on the alloy ion amount but rather on the nature of the alloy and its manufacturing process.

Several previous *in vitro* studies aimed to assess the release of metal ions from orthodontic appliances leading to contradicting results. Straightforward comparisons are not possible due to the different study designs, in terms of the material analyzed, immersion media, and analytical equipment. Mikulewicz et al. [63] reported that an orthodontic appliance made of stainless steel after a period of 30 days of immersion in artificial saliva leached $2382 \text{ ng}/\text{mL}$ Fe, $573 \text{ ng}/\text{mL}$ Ni, and $101 \text{ ng}/\text{mL}$ Cr. Even after adding up the concentrations of metal ions released from stainless steel brackets, molar bands, and archwires after 90 days of exposure, the results, although similar in the ratios between specific metal ions concentrations, were significantly smaller ($304.01 \text{ ng}/\text{mL}$ Fe, $46.83 \text{ ng}/\text{mL}$ Ni and $13.87 \text{ ng}/\text{mL}$ Cr) in comparison with that reported previously by Mikulewicz et al. [63]. The higher values evidenced by Mikulewicz et al. could be due to their specific study design that included constant shaking of the samples at 120 rpm over a period of 30 days whereas in our study samples were slightly shaken only before sampling. By this, we were able to measure the concentrations of leached metal ions only due to the pure diffusion of ions with no additional mechanical forces to enhance the ion release. Even higher values of

Fe and Cr ions released from stainless steel orthodontic appliances were shown by Hwang et al. [61], while similar results were reported regarding the concentrations of Ni ions released from Ni-Ti archwires. Kuhta et al. [64] compared the Ni-Ti wire with stainless steel wire and gained similar results to this study for Ti. They also showed how acidic pH values impacted more ions being released. Ortiz et al. [3] also compared the metal release of titanium and stainless steel, but in the combination of brackets and bands, and also found that the titanium-containing alloy is more biocompatible than others.

The above-mentioned studies all used some sort of a combination of wire, brackets, and bands to determine metal ion release. In the present study, metal ion release from brackets, molar bands, and archwires were measured separately and in the case of archwires, also according to their material alloys composition. This could be regarded as a limitation of the study since it excluded the possible corrosive effect and related ions released due to different materials' interactions. The additional mechanical aspect of bracket, band, and archwire friction should not be neglected because they can additionally contribute to the metal ions' release [65]. Performing multi-element analysis with the ICP-MS, we were able to determine exactly which part of the orthodontic appliance accounted for the greatest ions release compared to the others and its release profile characteristic during the 90-day study. The number of separate parts tested would appropriately simulate the usual amount of which orthodontic appliances are composed in everyday clinical practice. When submerging orthodontic materials, previously mentioned studies did not account for the adsorption of positively charged ions to the negatively charged surface. To prevent this occurrence, the submersion medium should be acidified to provide an excess of H⁺ ions. In our study, to obtain a steady pH level of seven for 90 days, acidifying was inadequate. To our knowledge, this was the first study to use Teflon beakers as vessels for orthodontic material submersion, thus preventing any possible metal ion adsorption to the beaker surface and maintaining a constant pH level throughout the study.

Recently, Wendl et al. [66] tested ion release from several types of brackets, bands, and archwires, but only for Ni, Cr, Mn, and Co. This study does not directly apply to *in vivo* conditions but provides an important insight into how each orthodontic alloy reacts differently in a simulated environment. Although a 90-day study is quite representative of the use of archwires, it does not represent the simulation for the use of brackets and molar bands, which are subjected to the oral cavity for approximately two to three years.

Moreover, *in vitro* experiments are not able to simulate an actual *in vivo* environment fully. For example, corrosion is the main reason for ion release, and the scale of it depends on the formation of passive oxide layers on the surfaces of orthodontic materials. These oxide layers, Cr oxide or Ti oxide, effectively prevent corrosion [67] but are highly influenced by the changes in the oral environment, such as pH and temperature levels. In our study, a constant pH and temperature were retained to avoid a potential increase in ion release [64].

Obtained results of metal ion release enabled us to estimate the metal ion combinations and concentrations for further studies of oxidative stress causation and consequently involvement of the enzymatic antioxidative stress defense. Namely, such defense represents the first cellular response to increased oxidant levels [25].

4.2. Topic: Metal Ion Exposure, Oxidative Stress, and the Enzymatic Antioxidant Defense System Induction

There are not many studies dealing with ROS caused by dental or orthodontic alloys. In our study, we found an increased formation of ROS in Figure 2 only in two types of metal ion mixtures: stainless steel and cobalt-chromium. The simulation of nickel-titanium and β -titanium alloys, in the form of metal cations, did not lead to the formation of ROS. Similar results were obtained in a previous study [7]. Interestingly, the study by Spalj et al. [68] showed that Ni-Ti wire produced the highest amount of ROS while SS and β -titanium wire did not. In their further study, they showed that only high concentrations of Ni and TiO₂ salt-induced the formation of ROS in gastrointestinal tract cell lines [69]. As in our study, Pallero et al. [70] also used a mixture of ions to simulate the alloy SS and evaluate

the formation of ROS. They also confirmed that the metal mixture SS increases the levels of ROS in vascular smooth muscle cells, for which Fe, Cr, Ni, and Mo ions seem to be responsible. As for Co-Cr alloy, Salloum et al. [71] used Co and Cr ions separately to observe ROS production in macrophages. Only Co(II) ions induced oxidative stress in macrophages, while Cr(III) ions did not. On the other hand, previous studies show that Cr(II) also induces oxidative stress, but to a lesser extent than Co(II) [72,73]. The combined effect of using a Co-Cr metal ion mixture resulted in an increase in ROS in yeast cells at 100 μM and 1000 μM concentrations [72]. The addition of Cr(III), Fe(III), Mo(III), or Ni(II) ions to mouse embryo fibroblasts and liver HepG2 cells increased the formation of ROS in a dose-dependent manner, which was first observed at concentrations as low as 100 μM [74].

Each organism has an appropriate antioxidant defense system to cope with the overproduction of ROS and maintain redox homeostasis. Figure 4 shows the cell enzymatic antioxidants such as superoxide dismutase (SOD), catalase (CAT), glutathione peroxidase (GPx), glutathione reductase (GR), peroxiredoxinreductase (PRDX), and thioredoxins (Trx) used to suppress ROS overproduction. Non-enzymatic molecules such as glutathione also play a key role in antioxidant defense [75] but were not the subject of our study. The activity of the above enzymes is used to assess the occurrence of increased ROS levels because the cell's enzymatic antioxidant defense system responds earlier to an elevated level of ROS as it can be detected as a result of oxidative damage. The most important *in vivo* defense enzyme is considered to be SOD, which converts $\text{O}_2^{\bullet-}$ to H_2O_2 , which is then further converted to H_2O by CAT. The reduction in H_2O_2 is also mediated by the glutathione peroxidase (GPx) protein family, which uses low molecular weight thiols such as glutathione (GHS) as a catalyst for the conversion of H_2O_2 to H_2O [76]. Because SOD, CAT, and GPx are metalloenzymes, metal ions are implemented as cofactors and as such are a necessity for the enzyme activity. Copper, zinc, and manganese are essential for SOD, iron for CAT, and selenium for GPx activity [77]. Several thiol-containing enzymes, thioredoxin reductase (TrxR) and peroxiredoxin (PRDX), are also involved in the removal of H_2O_2 [78], but require a reducing agent in the form of NADPH. Thus, NADPH and its oxidized form NADP^+ are essential cofactors of the enzymes TrxR and GR (Figure 6).

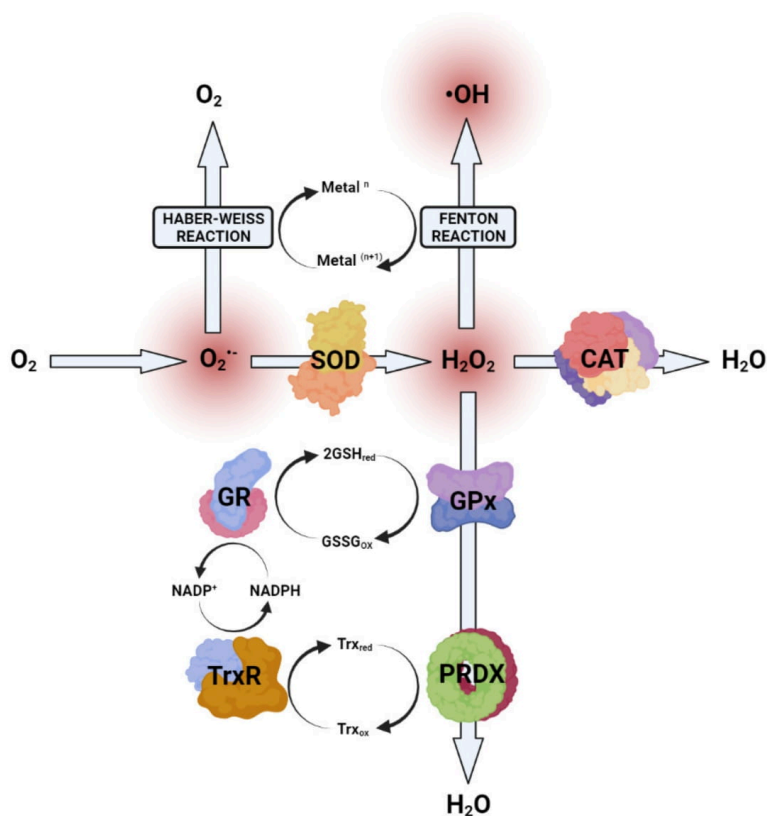


Figure 6. Generation of ROS and the involvement of the enzymatic antioxidative defense system. $O_2^{\bullet -}$ superoxide anion; $\bullet OH$ hydroxyl radical; SOD superoxide dismutase; CAT catalase; GPx glutathione peroxidase; GR glutathione reductase; PRDX peroxiredoxin; TrxR thioredoxin reductase.

Because of its easy accessibility, rapid growth, and genetic relevance to human disease, *Saccharomyces cerevisiae* is a suitable model organism for oxidative stress studies [79]. Through evolution, all eukaryotic organisms, from yeast to vertebrates, possess the same antioxidant enzymes [80], making the yeast *S. cerevisiae* particularly important for simulating the eukaryotic cellular processing of ROS. *S. cerevisiae* in the stationary phase strongly resemble multicellular organisms because the yeast cells in the stationary phase transit from the fermentative to mitochondrial respiratory metabolism for energy and growth. Second, the cells in the stationary phase are in a quiescent state in which they are neither dividing nor preparing to divide. The last reason is that any damage that has occurred is accumulated and must be prevented or repaired, as the potential masking or mitigation of damage by new divisions or synthesis is diminished [81]. The transition to respiration naturally increases the production of ROS and evokes modulation of the antioxidant system, making stationary cells more susceptible to oxidative stressors [82]. Stationary yeast cells are permanently exposed to endogenously produced ROS, which attacks the same cell all the time, and oxidative damages are accumulated. If we were to use yeast cells in the exponential phase, the main source of energy would come from glycolysis, and the cells would be exposed to the stressor only for a short time before starting to divide

again, leading to potentially false results [83]. Furthermore, the budding of cells forming new daughter cells also prevents the possible accumulation of damaged molecules in the mother cells [84]. Such exponentially growing cells rarely occur in the natural environment or human body; thus, extrapolation of obtained results from exponential phase cells to multicellular organisms would be misleading. When oxidative stress occurs, antioxidant defense mechanisms are theoretically activated to prevent potential oxidative damage. Since an increase in protein or mRNA expression of antioxidant enzymes does not necessarily mean an increase in activity, we used both spectrophotometric enzymatic assays and native gel electrophoresis to assess enzymatic defense. Treatment of yeast cells with Fe, Cr, and Ni ions, in the case of 1000 μM SS, increased the activity of SOD. This could be due to either excessive leakage of the SOD substrate, superoxide, from the electron transport chain due to mitochondrial damage or increased function of NADPH oxidase (NOX). The product of superoxide reduction by SOD should be the generation of H_2O_2 , which should also trigger the increase of CAT, GPx, or PRDX, which was not confirmed in our study. Indeed, a decrease in the activity of CAT and PRDX was observed, whereas the activity of GPx did not change. One possible explanation is that H_2O_2 , when generated, immediately enters the Fenton reaction with metal cations, especially Fe cations, forming a hydroxyl radical. This is evident to some degree when cells are treated with 1000 μM Fe, Ni, and Cr combinations, with the increase in ROS level, decreased cell viability, and increased protein carbonyl content. Further evidence is the absolute annihilation of TrxR activity [85], which converts NADP^+ to NADPH, a general mediator of the detoxifying and antioxidant defense system [86]. When cells were treated with Co-Cr metal ion mixtures, no statistically significant difference in enzyme activity was observed, although a slight increase in SOD and PRDX was noticed. Again, CAT activity appears to decrease in a dose-dependent manner when yeast cells are treated with all-metal ion mixtures, even statistically significant in the case of SS and Ni-Ti. Atli et al. [87] observed that the inhibition of CAT is due to the binding of the metal ion to the enzyme—SH groups. Lower CAT activity in yeast cells was also observed by Bayliak et al. [88] and was due to inhibition by high substrate concentrations, as CAT activity is not linear with H_2O_2 concentration. The authors suggested that a critical oxidant concentration in the cells might be the cause for the observed results. When evaluating the CAT in-gel activity, conclusions could be drawn about the CAT inhibition at high concentrations of metal treatments. The higher electrophoretic mobility of the CAT enzyme (band) when exposed to 1000 μM metal concentrations could be a consequence of the potential oxidation of the catalase. This argument could be supported by the study of Rodríguez-Ruiz et al. [89], in which they found the same increase in band mobility due to increasing H_2O_2 treatment and potential oxidative damage.

It is emphasized that the concentrations of reduced, oxidized, and total glutathione are markers of the oxidative stress response [90]. Since the GPx enzyme uses GSH as a substrate, its activity should be closely related to the GSH/GSSG ratio. Metal ion mixtures of SS and Co-Cr did not affect GPx activity, but the Ni-Ti and β -Ti mixture increased the activity at 1000 μM concentrations. As for the activity of GR, which regenerates GSSG to GSH used for GPx activity, no link between these two enzymes could be established. According to Tandoğan and Uluşu [91], Ni^{2+} ions coexist with GSSG for binding the active site of the GR enzyme, inhibiting its activity. SS, Co-Cr, and Ni-Ti metal alloy mixtures contain different amounts of Ni^{2+} ions, but the Ni-Ti mixture did not change the activity of GR, while the Co-Cr mixture increased the activity, and the SS mixture decreased it. Compared to GPx, PRDX enzymes can reduce organic and inorganic H_2O_2 without using metal ions as cofactors [92] and often compete with GPx for H_2O_2 dissociation [93]. This was not observed in the presented study, as the activity of PRDX enzyme did not change, except when yeast cells were treated with a concentration of 1000 μM , where the activity was significantly inhibited. The inhibition of PRDX is supported by the fact that the TrxR enzyme is also inhibited at this specific concentration of the SS ion mixture, which means that the electron donor, thioredoxin (Trx), is absent for the reaction to occur.

Lazarova et al. [94] found an increase in SOD and CAT activity after 6 h of treatment with Cr ions. Feng et al. [95] also observed an increase in SOD and CAT activity, but only when cells were treated with low Cr concentrations and for a short time. Longer exposures and higher chromium concentrations inhibited enzyme activities, implying that antioxidant enzymes can only protect cells to a certain extent before the organism succumbs to the fate of oxidative stress. When macrophage cells are treated with Cr(III) ions for 12 h, there is a dose-dependent inhibition of CAT activity, apparently due to Cr ions replacing Fe in the active sites of the CAT enzyme [72].

A similar study was performed by Terpilowska et al. [74] by treating BAKB/3T3 and HepG2 cells with chromium, iron, nickel, and molybdenum. An increase in the intracellular ROS level and MDA concentrations were observed. The authors observed how each individual metal affected oxidative stress markers, but concluded that a mixture of two metals (e.g., chromium and iron) had an additive effect on oxidative stress generation. When the SOD, CAT, and GPx activity were evaluated, an increase in activity was observed at 100 μM and 200 μM ion concentrations, but a statistically significant decrease was observed only with increasing metal concentrations above 400 μM . The same effect was observed by Kalaivani et al. [96] for nickel and by Siddiqui et al. [97] for molybdenum. In a cell-free study, treatment of the CAT enzyme with concentrations of 0–50 μM Cr(III) ions increased the activity of the CAT enzyme, but when the 50 μM concentration is exceeded, the enzyme activity decreases, probably due to interactions between the active site of CAT and the excess of chromium ions [98].

The release of Co and Cr ions from alloys is already documented in many studies on hip replacement implants [99–101], but also to a lesser extent on orthodontic alloys. When macrophages were treated with Co(II), Cr(VI), and Cr(III) ions for 24, 48, and 72 h, Cr(VI) ions induced the expression of SOD, CAT, and GPx proteins, whereas Cr(III) and Co(II) had no effect. A negligible effect of Cr(III) and Co(II) on the enzyme CAT was also found by Fleury et al. [102]. Both Co(II) and Cr(III) appeared to be cytotoxic to macrophages at concentrations of 24 ppm and 250 ppm, but only Co(II) was able to induce the production of ROS and protein carbonylation [71]. The difference between the toxicity of the two Cr ions might lie in the accessibility of the ions to enter the cell. While Cr(VI) can easily pass through the anion channels, Cr(III) can only be taken up into the cell via phagocytosis [103]. On the other hand, Magone et al. [104] suggested the possibility of Cr(III) oxidation to Cr(IV) to ensure cell membrane passage. In the present study, Co(II) chlorides and Cr(III) chlorides were used to simulate Co-Cr alloys because Co(III) and Cr(VI) are rapidly reduced to lower oxidation states under physiological conditions [105].

Studies on the effects of orthodontic alloys on antioxidant enzyme activity are perplexing. After 1 and 24 weeks of orthodontic treatment, the activity of SOD, CAT, and PRDX were not observed in unstimulated total saliva, but a decrease in the activity of SOD and CAT was observed in stimulated total saliva [106]. A research study by Bandeira et al. [107] showed that stainless steel bands induced the expression of *SOD1* and *PRDX1* genes but not the *GPX1* gene.

The determination of carbonylated proteins can be used as a biomarker for metal-induced oxidative stress since the reaction is irreversible [94]. As expected, oxidative damage to proteins occurs only when excessive amounts of ROS are produced, so the graphs from Figures 2 and 5 look similar. The same effect was observed in other studies [71,72]. The protein oxidation of 100 μM and 1000 μM concentrations for Co(II) and Cr(III) in the study [72] agreed with our result when the Co-Cr mixture was treated with the same concentrations. Lazarova et al. [94] treated yeast cells with 1000 μM concentrations of Cr ions for 6 h and observed an increase in ROS production and consequently an increase in protein carbonyl content. When yeast cells were treated with NiTi and β -Ti in the presented study, no oxidative stress was observed.

An interesting observation was made by Scarcello et al. [108] when they used Fe particles instead of solid materials. Immediately after Fe particles were synthesized, they formed a protective oxide layer on their surface [109]. The generation of ROS occurred

even in the presence of the oxide layer for Fe particles, but SS powder did not generate ROS. This study is also in agreement with Fagali et al. [110]. They both emphasize that direct contact with the material (surface chemistry) and not indirect contact (degradation products—Fe³⁺ ions) causes ROS generation. In contrast to Fe-containing alloys, Co-Cr alloys have a direct and indirect effect on ROS values [111], mainly due to the immediate Co dissolution in body fluids, thus changing the protective oxide layer to chromium and molybdenum oxide [9].

In general, Co-Cr alloys are the toughest, stiffest, and more wear-resistant compared to Fe-based (stainless steel) and Ti-based alloys [112], but the alloy SS offers the best price-performance ratio, and the Ti-based alloys have their specific strength and are also considered to be the best biocompatible as well as the most corrosion-resistant [113,114]. As evidenced in this study, the β -Ti alloy wire arch released the least metal ions during the 90-day incubation, followed by the SS, Ni-Ti, and Co-Cr alloy. As expected, the SS brackets and molar bands used in this study released more metal ions due to their larger combined surface area. To hypothesize the amount of metal ions that could be released from an entire orthodontic appliance consisting of 2 archwires, 24 brackets, and 4 bands, the concentration after 90 days gives a total of 400 ng/mL when only the SS alloy is used. These results reflect only passive ion diffusion from orthodontic alloys and do not take into account possible physiological or biological changes that could increase the release of metal ions. Regarding the composition of the orthodontic alloy, the combined release of metal ions was comparable to the 10 μ M metal ion mixtures used to treat yeast cells. Concentrations of 100 μ M and 1000 μ M were also used to evaluate possible effects that a higher metal ion release could have. When yeast cells were treated with either 1000 μ M SS or 100 μ M and 1000 μ M Co-Cr mixtures, we observed a positive correlation between the occurrence of oxidative stress and oxidative protein damage. No unilateral interpretation could be made when assessing the overall enzymatic antioxidant defense system.

When the increased activity of the SOD enzyme was observed, it was expected that the activity of the CAT or GPx enzyme would also increase due to H₂O₂ production in the dismutase reaction, but this increase was not observed. The mechanism of enzyme activation is very complex, and only the evaluation of multiple antioxidant enzyme activities can provide an estimate of the extent of oxidative stress occurrence in cells. Since we used metal ion mixtures in the present study, we were not able to identify a specific metal responsible for inducing oxidative stress or affecting the activity of antioxidant enzymes. It is worth noting that the changes in enzyme activity are transient and time-dependent, as the defense response is very dynamic, but the damages caused are the final products that accumulate in the cell.

5. Conclusions

Orthodontic appliances should be biocompatible for short- and long-term use to ensure safety and so as not to harm the patient during orthodontic treatment. The release of metal ions from different orthodontic alloys during a 90-day exposure to artificial saliva did not exceed the recommended upper limits for daily metal intake. The β -Ti alloy was considered the most biocompatible alloy, as its metal release was the lowest among the other orthodontic alloys tested. Depending on the composition of the metal alloy, metal ion mixtures were prepared for the treatment of yeast cells. The metal ion mixtures of stainless steel and cobalt-chromium induced oxidative stress at high (non-physiological) concentrations as well as the oxidation of proteins in the form of carbonylation. A diverse antioxidant enzyme defense system was also induced when cells were treated with metal ions at higher concentrations. Although metal ions can cause oxidative stress and oxidative damage, as well as induce enzymatic antioxidant defenses, the risk of adverse effects on patient health from treatment with fixed orthodontic appliances is considered low because we have shown that concentrations of released metal ions from selected orthodontic materials do not exceed the concentration required to induce oxidative stress and cause cellular protein damage. It is possible that locally high metal concentrations may be present

due to corrosion or metal degradation. Therefore, it is important that the antioxidant defense system is activated and effectively protects against possible increased ROS and oxidative stress-induced damage.

Supplementary Materials: The following are available online at <https://www.mdpi.com/article/10.3390/antiox11010063/s1>, Table S1: ICP-MS operating parameters for determination of element concentrations, Table S2: Release of metal ions from stainless steel, Co-Cr-Ni, Ni-Ti, β -Ti archwire, stainless steel brackets, and molar bands.

Author Contributions: All authors discussed and agreed upon the idea, and made scientific contributions: writing—original draft preparation, V.K.; experiment designing, V.K. and B.P.; experiment performing, V.K. and M.B.; data analysis, V.K., M.B. and J.Š.; writing—review and editing, V.K., B.P., J.Š., P.J. and J.P.; supervision, B.P., P.J. and J.P. All authors have read and agreed to the published version of the manuscript.

Funding: This work was supported by the Slovenian Research Agency (grant numbers P3-0388, P1-0143, and J3-2520).

Institutional Review Board Statement: Not applicable.

Informed Consent Statement: Not applicable.

Data Availability Statement: Data is contained within the article and supplementary materials.

Acknowledgments: We would like to acknowledge Radmila Milačič for organizing this collaboration.

Conflicts of Interest: The authors declare no conflict of interest.

References

1. Barrett, R.D.; Bishara, S.E.; Quinn, J.K. Biodegradation of orthodontic appliances. Part I. Biodegradation of nickel and chromium in vitro. *Am. J. Orthod. Dentofac. Orthop.* **1993**, *103*, 8–14. [[CrossRef](#)]
2. Moresca, R. Orthodontic treatment time: Can it be shortened? *Dent. Press J. Orthod.* **2018**, *23*, 90–105. [[CrossRef](#)]
3. Ortiz, A.J.; Fernández, E.; Vicente, A.; Calvo, J.L.; Ortiz, C. Metallic ions released from stainless steel, nickel-free, and titanium orthodontic alloys: Toxicity and DNA damage. *Am. J. Orthod. Dentofac. Orthop.* **2011**, *140*, 115–122. [[CrossRef](#)]
4. Keinan, D.; Mass, E.; Zilberman, U. Absorption of Nickel, Chromium, and Iron by the Root Surface of Primary Molars Covered with Stainless Steel Crowns. *Int. J. Dent.* **2010**, *2010*, 326124. [[CrossRef](#)]
5. Maheshwari, M.; Verma, S.K.; Dhiman, S.K. Metal Hypersensitivity in Orthodontic Patient. *J. Dent. Mater. Tech.* **2015**, *4*, 111–115.
6. Sifakakis, I.; Eliades, T. Adverse reactions to orthodontic materials. *Aust. Dent. J.* **2017**, *62*, 20–28. [[CrossRef](#)]
7. Kovač, V.; Poljšak, B.; Primožič, J.; Jamnik, P. Are Metal Ions That Make up Orthodontic Alloys Cytotoxic, and Do They Induce Oxidative Stress in a Yeast Cell Model? *Int. J. Mol. Sci.* **2020**, *21*, 7993. [[CrossRef](#)]
8. Arregui, M.; Latour, F.; Gil, F.J.; Pérez, R.A.; Giner-Tarrida, L.; Delgado, L.M. Ion Release from Dental Implants, Prosthetic Abutments and Crowns under Physiological and Acidic Conditions. *Coatings* **2021**, *11*, 98. [[CrossRef](#)]
9. Hanawa, T. Metal ion release from metal implants. *Mater. Sci. Eng. C* **2004**, *24*, 745–752. [[CrossRef](#)]
10. House, K.; Sernetz, F.; Dymock, D.; Sandy, J.R.; Ireland, A.J. Corrosion of orthodontic appliances—Should we care? *Am. J. Orthod. Dentofac. Orthop.* **2008**, *133*, 584–592. [[CrossRef](#)]
11. Shi, X.; Dalal, N.S. Vanadate-Mediated Hydroxyl Radical Generation from Superoxide Radical in the Presence of NADH: Haber-Weiss vs Fenton Mechanism. *Arch. Biochem. Biophys.* **1993**, *307*, 336–341. [[CrossRef](#)]
12. Desurmont, M. Carcinogenic effect of metals. *Sem. Hop.* **1983**, *59*, 2097–2099.
13. Rahman, K. Studies on free radicals, antioxidants, and co-factors. *Clin. Interv. Aging* **2007**, *2*, 219.
14. Park, H.S.; Kim, S.R.; Lee, Y.C. Impact of oxidative stress on lung diseases. *Respirology* **2009**, *14*, 27–38. [[CrossRef](#)]
15. Prousek, J. Preparation and utilization of nano ZVI in Fenton-like reactions View project Fenton chemistry in biology and medicine*. *Pure Appl. Chem* **2007**, *79*, 2325–2338. [[CrossRef](#)]
16. Alfonso-Prieto, M.; Vidossich, P.; Rovira, C. The reaction mechanisms of heme catalases: An atomistic view by ab initio molecular dynamics. *Arch. Biochem. Biophys.* **2012**, *525*, 121–130. [[CrossRef](#)]
17. Lloyd, R.V.; Hanna, P.M.; Mason, R.P. The Origin of the Hydroxyl Radical Oxygen in the Fenton Reaction. *Free Radic. Biol. Med.* **1997**, *22*, 885–888. [[CrossRef](#)]
18. De Flora, S. Threshold mechanisms and site specificity in chromium(VI) carcinogenesis. *Carcinogenesis* **2000**, *21*, 533–541. [[CrossRef](#)]
19. Shi, X.; Dalal, N.S.; Kasprzak, K.S. Generation of Free Radicals from Hydrogen Peroxide and Lipid Hydroperoxides in the Presence of Cr(III). *Arch. Biochem. Biophys.* **1993**, *302*, 294–299. [[CrossRef](#)]
20. Leonard, S.; Gannett, P.M.; Rojanasakul, Y.; Schwegler-Berry, D.; Castranova, V.; Vallyathan, V.; Shi, X. Cobalt-mediated generation of reactive oxygen species and its possible mechanism. *J. Inorg. Biochem.* **1998**, *70*, 239–244. [[CrossRef](#)]

21. Lu, H.; Shi, X.; Costa, M.; Huang, C. Carcinogenic effect of nickel compounds. *Mol. Cell. Biochem.* **2005**, *279*, 45–67. [[CrossRef](#)]
22. Mendel, R.R.; Bittner, F. Cell biology of molybdenum. *Biochim. Biophys. Acta—Mol. Cell Res.* **2006**, *1763*, 621–635. [[CrossRef](#)]
23. Zhuang, Y.; Liu, P.; Wang, L.; Luo, J.; Zhang, C.; Guo, X.; Hu, G.; Cao, H. Mitochondrial oxidative stress-induced hepatocyte apoptosis reflects increased molybdenum intake in caprine. *Biol. Trace Elem. Res.* **2016**, *170*, 106–114. [[CrossRef](#)] [[PubMed](#)]
24. Fagali, N.S.; Grillo, C.A.; Puntarulo, S.; Fernández, M.; De Mele, L. Biodegradation of metallic biomaterials: Its relation with the generation of reactive oxygen species Impact on rural population of agrochemicals used in transgenic crops in Argentina View project Eradication of burst release of copper ions from copper-bea. In *Reactive Oxygen Species, Lipid Peroxidation and Protein Oxidation*; Catalá, A., Ed.; Nova Science Publishers: Hauppauge, NY, USA, 2015; ISBN 9781633218864.
25. Xia, T.; Kovochich, M.; Liong, M.; Mädler, L.; Gilbert, B.; Shi, H.; Yeh, J.; Zink, J.; Nel, A. Comparison of the mechanism of toxicity of zinc oxide and cerium oxide nanoparticles based on dissolution and oxidative stress properties. *ACS Nano* **2008**, *2*, 2121–2134. [[CrossRef](#)]
26. Mironczuk-Chodakowska, I.; Witkowska, A.M.; Zujko, M.E. Endogenous non-enzymatic antioxidants in the human body. *Adv. Med. Sci.* **2018**, *63*, 68–78. [[CrossRef](#)]
27. Tóthová, L.; Celec, P. Oxidative stress and antioxidants in the diagnosis and therapy of periodontitis. *Front. Physiol.* **2017**, *8*, 1–14. [[CrossRef](#)]
28. Tóthová, L.; Kamodyová, N.; Červenka, T.; Celec, P. Salivary markers of oxidative stress in oral diseases. *Front. Cell. Infect. Microbiol.* **2015**, *5*, 73. [[CrossRef](#)] [[PubMed](#)]
29. Bradford, M. A Rapid and Sensitive Method for the Quantitation of Microgram Quantities of Protein Utilizing the Principle of Protein-Dye Binding. *Anal. Biochem.* **1976**, *72*, 248–254. [[CrossRef](#)]
30. Mesa-Herrera, F.; Quinto-Aleman, D.; Díaz, M. A Sensitive, Accurate, and Versatile Method for the Quantification of Superoxide Dismutase Activities in Biological Preparations. *React. Oxyg. Species* **2019**, *7*, 10–20. [[CrossRef](#)]
31. Smith, A.D.; Levander, O.A. High-throughput 96-well microplate assays for determining specific activities of glutathione peroxidase and thioredoxin reductase. In *Methods in Enzymology*; Academic Press Inc.: Cambridge, MA, USA, 2002; Volume 347, pp. 113–121.
32. Glippa, O.; Engström-Öst, J.; Kanerva, M.; Rein, A.; Vuori, K. Oxidative stress and antioxidant defense responses in *Acartia* copepods in relation to environmental factors. *PLoS ONE* **2018**, *13*, e0195981. [[CrossRef](#)]
33. Ali, S.K.; Hadwan, M.H. Precise Spectrophotometric Method for measurement of Peroxiredoxin activity in Biological Samples. *Res. J. Pharm. Technol.* **2019**, *12*, 2254. [[CrossRef](#)]
34. Weydert, C.J.; Cullen, J.J. Measurement of superoxide dismutase, catalase and glutathione peroxidase in cultured cells and tissue. *Nat. Protoc.* **2010**, *5*, 51–66. [[CrossRef](#)]
35. Mesquita, C.S.; Oliveira, R.; Bento, F.; Geraldo, D.; Rodrigues, J.V.; Marcos, J.C. Simplified 2,4-dinitrophenylhydrazine spectrophotometric assay for quantification of carbonyls in oxidized proteins. *Anal. Biochem.* **2014**, *458*, 69–71. [[CrossRef](#)] [[PubMed](#)]
36. Keston, A.S.; Brandt, R. The fluorometric analysis of ultramicro quantities of hydrogen peroxide. *Anal. Biochem.* **1965**, *11*, 1–5. [[CrossRef](#)]
37. Sousa, C.A.; Soares, H.M.V.M.; Soares, E.V. Nickel Oxide (NiO) Nanoparticles Induce Loss of Cell Viability in Yeast Mediated by Oxidative Stress. *Chem. Res. Toxicol.* **2018**, *31*, 658–665. [[CrossRef](#)]
38. Breuer, P.; Drocourt, J.L.; Bunschoten, N.; Zwietering, M.H.; Rombouts, F.M.; Abee, T. Characterization of uptake and hydrolysis of fluorescein diacetate and carboxyfluorescein diacetate by intracellular esterases in *Saccharomyces cerevisiae*, which result in accumulation of fluorescent product. *Appl. Environ. Microbiol.* **1995**, *61*, 1614. [[CrossRef](#)]
39. Valiakhmetov, A.Y.; Kuchin, A.V.; Suzina, N.E.; Zvonarev, A.N.; Shepelyakovskaya, A.O. Glucose causes primary necrosis in exponentially grown yeast *Saccharomyces cerevisiae*. *FEMS Yeast Res.* **2019**, *19*, 19. [[CrossRef](#)]
40. Tanaka, K.; Shimakawa, G.; Nakanishi, S. Time-of-day-dependent responses of cyanobacterial cellular viability against oxidative stress. *Sci. Rep.* **2020**, *10*, 20029. [[CrossRef](#)]
41. Faccioni, F.; Franceschetti, P.; Cerpelloni, M.; Fracasso, M.E. In vivo study on metal release from fixed orthodontic appliances and DNA damage in oral mucosa cells. *Am. J. Orthod. Dentofac. Orthop.* **2003**, *124*, 687–693. [[CrossRef](#)]
42. Santos Genelhu, M.C.L.; Marigo, M.; Alves-Oliveira, L.F.; Cotta Malaquias, L.C.; Gomez, R.S. Characterization of nickel-induced allergic contact stomatitis associated with fixed orthodontic appliances. *Am. J. Orthod. Dentofac. Orthop.* **2005**, *128*, 378–381. [[CrossRef](#)]
43. Galeotti, A.; Uomo, R.; Spagnuolo, G.; Paduano, S.; Cimino, R.; Valletta, R.; D'Antò, V. Effect of pH on in vitro biocompatibility of orthodontic miniscrew implants. *Prog. Orthod.* **2013**, *14*, 1–7. [[CrossRef](#)] [[PubMed](#)]
44. Ratner, B.D.; Hoffman, A.S.; Schoen, F.J.; Lemons, J.E. *Biomaterials Science: An Introduction to Materials*, 3rd ed.; Academic Press Inc.: Cambridge, MA, USA, 2013; pp. 1–1555.
45. Williams, D.F. On the mechanisms of biocompatibility. *Biomaterials* **2008**, *29*, 2941–2953. [[CrossRef](#)] [[PubMed](#)]
46. Eliaz, N. Corrosion of Metallic Biomaterials: A Review. *Materials* **2019**, *12*, 407. [[CrossRef](#)] [[PubMed](#)]
47. Anderson, J.; Rodriguez, A.; Chang, D. Foreign body reaction to biomaterials. *Semin. Immunol.* **2008**, *20*, 86–100. [[CrossRef](#)]
48. Urban, R.; Jacobs, J.; Gilbert, J.; Galante, J. Migration of corrosion products from modular hip prostheses. Particle microanalysis and histopathological findings. *J. Bone Jt. Surg. Am.* **1994**, *76*, 1345–1359. [[CrossRef](#)]
49. Brantley, W.A.; Eliades, T. *Orthodontic Materials: Scientific and Clinical Aspects*; Thieme: Stuttgart, Germany, 2001; ISBN 9780865779297.

50. Eliades, T. Orthodontic materials research and applications: Part 2. Current status and projected future developments in materials and biocompatibility. *Am. J. Orthod. Dentofac. Orthop.* **2007**, *131*, 253–262. [[CrossRef](#)] [[PubMed](#)]
51. David, A.; Lobner, D. In vitro cytotoxicity of orthodontic archwires in cortical cell cultures. *Eur. J. Orthod.* **2004**, *26*, 421–426. [[CrossRef](#)]
52. Dentaureum Materials for Orthodontic Products. Available online: <https://www.dentaureum.de/files/KFO-Werkstoffliste-20.pdf> (accessed on 27 August 2020).
53. Ramazan-zadeh, B.A.; Ahrari, F.; Sabzevari, B.; Habibi, S. Original Articles Nickel Ion Release from Three Types of Nickel-titanium-based Orthodontic Archwires in the As-received State and After Oral Simulation. *Dent. Clin. Dent. Prospect. J. Dent. Res. Dent. Clin. Dent. Prospect* **2014**, *8*, 71–76. [[CrossRef](#)]
54. Hunt, N.P.; Cunningham, S.J.; Golden, C.G.; Sheriff, M. An investigation into the effects of polishing on surface hardness and corrosion of orthodontic archwires. *Angle Orthod.* **1999**, *69*, 433–440. [[CrossRef](#)]
55. Tsang, H. EU Harmonises Test Methods for Nickel Release under REACH. Available online: <https://www.sgs.com/en/news/2016/01/safeguards-02216-eu-harmonises-test-methods-for-nickel-release-under-reach> (accessed on 20 April 2020).
56. Charles, A.; Gangurde, P.; Jacob, S.; Jatol-Tekade, S.; Senkutvan, R.; Vadgaonkar, V. Evaluation of nickel ion release from various orthodontic arch wires: An in vitro study. *J. Int. Soc. Prev. Community Dent.* **2014**, *4*, 12. [[CrossRef](#)]
57. Hussain, H.D.; Ajith, S.D.; Goel, P. Nickel release from stainless steel and nickel titanium archwires—An in vitro study. *J. Oral Biol. Craniofacial Res.* **2016**, *6*, 213–218. [[CrossRef](#)] [[PubMed](#)]
58. Suárez, C.; Vilar, T.; Sevilla, P.; Gil, J. In vitro corrosion behaviour of lingual orthodontic archwires. *Int. J. Corros.* **2011**, *2011*, 482485. [[CrossRef](#)]
59. Huang, H.-H.; Wang, C.-C.; Chiu, S.-M.; Wang, J.-F.; Liaw, Y.-C.; Lee, T.-H.; Chen, F.-L. Corrosion Behavior of titanium-containing Orthodontic Archwires in Artificial Saliva: Effects of Fluoride Ions and Plasma Immersion Ion Implantation Treatment. *J. Dent. Sci.* **2005**, *24*, 134–140. [[CrossRef](#)]
60. Institute of Medicine (US) Panel on Micronutrients. *Dietary Reference Intakes for Vitamin A, Vitamin K, Arsenic, Boron, Chromium, Copper, Iodine, Iron, Manganese, Molybdenum, Nickel, Silicon, Vanadium, and Zinc*; National Academies Press: Washington, DC, USA, 2001.
61. Hwang, C.J.; Shin, J.S.; Cha, J.Y. Metal release from simulated fixed orthodontic appliances. *Am. J. Orthod. Dentofac. Orthop.* **2001**, *120*, 383–391. [[CrossRef](#)]
62. Hussain, S.; Asshaari, A.; Osman, B.; AL-Bayaty, F. In Vitro-Evaluation of Biodegradation of Different Metallic Orthodontic Brackets. *J. Int. Dent. Med. Res.* **2017**, *7*, 76–83.
63. Mikulewicz, M.; Chojnacka, K.; Woźniak, B.; Downarowicz, P. Release of metal ions from orthodontic appliances: An in vitro study. *Biol. Trace Elem. Res.* **2012**, *146*, 272–280. [[CrossRef](#)]
64. Kuhta, M.; Pavlin, D.; Slaj, M.M.; Varga, S.; Lapter-Varga, M.; Slaj, M.M. Type of archwire and level of acidity: Effects on the release of metal ions from orthodontic appliances. *Angle Orthod.* **2009**, *79*, 102–110. [[CrossRef](#)] [[PubMed](#)]
65. Staffolani, N.; Damiani, F.; Lilli, C.; Guerra, M.; Staffolani, N.J.; Beicastro, S.; Locci, P. Ion release from orthodontic appliances. *J. Dent.* **1999**, *27*, 449–454. [[CrossRef](#)]
66. Wendl, B.; Wiltche, H.; Lankmayr, E.; Winsauer, H.; Walter, A.; Muchitsch, A.; Jakse, N.; Wendl, M.; Wendl, T. Metal release profiles of orthodontic bands, brackets, and wires: An in vitro study. *J. Orofac. Orthop. Fortsch. Kieferorthopädie* **2017**, *78*, 494–503. [[CrossRef](#)] [[PubMed](#)]
67. Eliades, T.; Pratsinis, H.; Kletsas, D.; Eliades, G.; Makou, M. Characterization and cytotoxicity of ions released from stainless steel and nickel-titanium orthodontic alloys. *Am. J. Orthod. Dentofac. Orthop.* **2004**, *125*, 24–29. [[CrossRef](#)] [[PubMed](#)]
68. Spalj, S.; Mlacovic Zrinski, M.; Tudor Spalj, V.; Ivankovic Buljan, Z. In-vitro assessment of oxidative stress generated by orthodontic archwires. *Am. J. Orthod. Dentofac. Orthop.* **2012**, *141*, 583–589. [[CrossRef](#)] [[PubMed](#)]
69. Rincic Mlinaric, M.; Durgo, K.; Katic, V.; Spalj, S. Cytotoxicity and oxidative stress induced by nickel and titanium ions from dental alloys on cells of gastrointestinal tract. *Toxicol. Appl. Pharmacol.* **2019**, *383*, 114784. [[CrossRef](#)]
70. Pallero, M.A.; Roden, M.T.; Chen, Y.-F.; Anderson, P.G.; Lemons, J.; Brott, B.C.; Murphy-Ullrich, J.E. Stainless Steel Ions Stimulate Increased Thrombospondin-1-Dependent TGF-Beta Activation by Vascular Smooth Muscle Cells: Implications for In-Stent Restenosis. *J. Vasc. Res.* **2010**, *47*, 309–322. [[CrossRef](#)]
71. Salloum, Z.; Lehoux, E.A.; Harper, M.E.; Catelas, I. Effects of cobalt and chromium ions on oxidative stress and energy metabolism in macrophages in vitro. *J. Orthop. Res.* **2018**, *36*, 3178–3187. [[CrossRef](#)]
72. Scharf, B.; Clement, C.; Zolla, V.; Perino, G.; Yan, B.; Elci, S.; Purdue, E.; Goldring, S.; Macaluso, F.; Cobelli, N.; et al. Molecular analysis of chromium and cobalt-related toxicity. *Sci. Rep.* **2014**, *4*, 5729. [[CrossRef](#)]
73. Petit, A.; Mwale, F.; Tkaczyk, C.; Antoniou, J.; Zukor, D.; Huk, O. Induction of protein oxidation by cobalt and chromium ions in human U937 macrophages. *Biomaterials* **2005**, *26*, 4416–4422. [[CrossRef](#)] [[PubMed](#)]
74. Terpilowska, S.; Siwicki, A.K. Pro- and antioxidant activity of chromium(III), iron(III), molybdenum(III) or nickel(II) and their mixtures. *Chem. Biol. Interact.* **2019**, *298*, 43–51. [[CrossRef](#)] [[PubMed](#)]
75. Sevcikova, M.; Modra, H.; Slaninova, A.; Svobodova, Z. Metals as a cause of oxidative stress in fish: A review. *Vet. Med.* **2011**, *56*, 537–546. [[CrossRef](#)]
76. Arthur, J. The glutathione peroxidases. *Cell. Mol. Life Sci.* **2000**, *57*, 1825–1835. [[CrossRef](#)]

77. Nenkova, G.; Petrov, L.; Alexandrova, A. Role of Trace Elements for Oxidative Status and Quality of Human Sperm. *Balk. Med. J.* **2017**, *34*, 343. [[CrossRef](#)]
78. Gromer, S.; Urig, S.; Becker, K. The thioredoxin system—From science to clinic. *Med. Res. Rev.* **2004**, *24*, 40–89. [[CrossRef](#)]
79. Lushchak, V.I. Adaptive response to oxidative stress: Bacteria, fungi, plants and animals. *Comp. Biochem. Physiol. Part C Toxicol. Pharmacol.* **2011**, *153*, 175–190. [[CrossRef](#)] [[PubMed](#)]
80. Ferro, D.; Franchi, N.; Bakiu, R.; Ballarin, L.; Santovito, G. Molecular characterization and metal induced gene expression of the novel glutathione peroxidase 7 from the chordate invertebrate *Ciona robusta*. *Comp. Biochem. Physiol. Part C Toxicol. Pharmacol.* **2018**, *205*, 1–7. [[CrossRef](#)]
81. Longo, V.D.; Gralla, E.B.; Valentine, J.S. Superoxide dismutase activity is essential for stationary phase survival in *Saccharomyces cerevisiae*. Mitochondrial production of toxic oxygen species in vivo. *J. Biol. Chem.* **1996**, *271*, 12275–12280. [[CrossRef](#)] [[PubMed](#)]
82. Vázquez, J.; González, B.; Sempere, V.; Mas, A.; Torija, M.J.; Beltran, G. Melatonin reduces oxidative stress damage induced by hydrogen peroxide in *Saccharomyces cerevisiae*. *Front. Microbiol.* **2017**, *8*, 1066. [[CrossRef](#)] [[PubMed](#)]
83. Longo, V.D.; Fabrizio, P. Chronological aging in *Saccharomyces cerevisiae*. *Subcell. Biochem.* **2012**, *57*, 101–121. [[CrossRef](#)] [[PubMed](#)]
84. Sigler, K.; Chaloupka, J.; Brozmanová, J.; Stadler, N.; Höfer, M. Oxidative stress in microorganisms—I. Microbial vs. higher cells—damage and defenses in relation to cell aging and death. *Folia Microbiol.* **1999**, *44*, 587–624. [[CrossRef](#)] [[PubMed](#)]
85. Lopert, P.; Day, B.J.; Patel, M. Thioredoxin Reductase Deficiency Potentiates Oxidative Stress, Mitochondrial Dysfunction and Cell Death in Dopaminergic Cells. *PLoS ONE* **2012**, *7*, e50683. [[CrossRef](#)]
86. Agledal, L.; Niere, M.; Ziegler, M. The phosphate makes a difference: Cellular functions of NADP. *Redox Rep.* **2010**, *15*. [[CrossRef](#)] [[PubMed](#)]
87. Atli, G.; Canli, M. Response of antioxidant system of freshwater fish *Oreochromis niloticus* to acute and chronic metal (Cd, Cu, Cr, Zn, Fe) exposures. *Ecotoxicol. Environ. Saf.* **2010**, *73*, 1884–1889. [[CrossRef](#)]
88. Bayliak, M.; Semchyshyn, H.; Lushchak, V. Effect of hydrogen peroxide on antioxidant enzyme activities in *Saccharomyces cerevisiae* is strain-specific. *Biochem.* **2006**, *71*, 1013–1020. [[CrossRef](#)] [[PubMed](#)]
89. Rodríguez-Ruiz, M.; González-Gordo, S.; Cañas, A.; Campos, M.J.; Paradelo, A.; Corpas, F.J.; Palma, J.M. Sweet Pepper (*Capsicum annuum* L.) Fruits Contain an Atypical Peroxisomal Catalase That Is Modulated by Reactive Oxygen and Nitrogen Species. *Antioxidants* **2019**, *8*, 374. [[CrossRef](#)]
90. Kubrak, O.I.; Lushchak, O.V.; Lushchak, J.V.; Torous, I.M.; Storey, J.M.; Storey, K.B.; Lushchak, V.I. Chromium effects on free radical processes in goldfish tissues: Comparison of Cr(III) and Cr(VI) exposures on oxidative stress markers, glutathione status and antioxidant enzymes. *Comp. Biochem. Physiol. Part C Toxicol. Pharmacol.* **2010**, *152*, 360–370. [[CrossRef](#)] [[PubMed](#)]
91. Tandoğan, B.; Uluşu, N.N. The inhibition kinetics of yeast glutathione reductase by some metal ions. *J. Enzym. Inhib. Med. Chem.* **2008**, *22*, 489–495. [[CrossRef](#)] [[PubMed](#)]
92. Khalifaa, H.H.; Hadwana, M.H. Simple Method for the Assessment of Peroxiredoxin Activity in Biological Sample. *Chem. Data Collect.* **2020**, *27*, 100376. [[CrossRef](#)]
93. Mitozo, P.A.; De Souza, L.F.; Loch-Neckel, G.; Flesch, S.; Maris, A.F.; Figueiredo, C.P.; Dos Santos, A.R.S.; Farina, M.; Dafre, A.L. A study of the relative importance of the peroxiredoxin-, catalase-, and glutathione-dependent systems in neural peroxide metabolism. *Free Radic. Biol. Med.* **2011**, *51*, 69–77. [[CrossRef](#)] [[PubMed](#)]
94. Lazarova, N.; Krumova, E.; Stefanova, T.; Georgieva, N.; Angelova, M. The oxidative stress response of the filamentous yeast *Trichosporon cutaneum* R57 to copper, cadmium and chromium exposure. *Biotechnol. Biotechnol. Equip.* **2014**, *28*, 855–862. [[CrossRef](#)]
95. Feng, M.; Yin, H.; Peng, H.; Liu, Z.; Lu, G.; Dang, Z. Hexavalent chromium induced oxidative stress and apoptosis in *Pycnoporus sanguineus*. *Environ. Pollut.* **2017**, *228*, 128–139. [[CrossRef](#)] [[PubMed](#)]
96. Kalaivani, P.; Saranya, S.; Poornima, P.; Prabhakaran, R.; Dallemer, F.; Vijaya Padma, V.; Natarajan, K. Biological evaluation of new nickel(II) metallates: Synthesis, DNA/protein binding and mitochondrial mediated apoptosis in human lung cancer cells (A549) via ROS hypergeneration and depletion of cellular antioxidant pool. *Eur. J. Med. Chem.* **2014**, *82*, 584–599. [[CrossRef](#)] [[PubMed](#)]
97. Siddiqui, M.A.; Saquib, Q.; Ahamed, M.; Farshori, N.N.; Ahmad, J.; Wahab, R.; Khan, S.T.; Alhadlaq, H.A.; Musarrat, J.; Al-Khedhairi, A.A.; et al. Molybdenum nanoparticles-induced cytotoxicity, oxidative stress, G2/M arrest, and DNA damage in mouse skin fibroblast cells (L929). *Colloids Surfaces B Biointerfaces* **2015**, *125*, 73–81. [[CrossRef](#)]
98. Chen, L.; Zhang, J.; Zhu, Y.; Zhang, Y. Interaction of chromium(III) or chromium(VI) with catalase and its effect on the structure and function of catalase: An in vitro study. *Food Chem.* **2018**, *244*, 378–385. [[CrossRef](#)]
99. Back, D.; Young, D.; Shimmin, A. How do serum cobalt and chromium levels change after metal-on-metal hip resurfacing? *Clin. Orthop. Relat. Res.* **2005**, *438*, 177–181. [[CrossRef](#)] [[PubMed](#)]
100. Allan, D.G.; Parsley, B.; Dyrstad, B.; Trammell, R.; Milbrandt, J.C. Elevation of Serum Cobalt and Chromium Levels in Patients With Metal-On-Metal Resurfacing Hip Prostheses: A 3-Year Follow-up. *J. Arthroplasty* **2007**, *22*, 311. [[CrossRef](#)]
101. Antoniou, J.; Zukor, D.; Mwale, F.; Minarik, W.; Petit, A.; Huk, O. Metal ion levels in the blood of patients after hip resurfacing: A comparison between twenty-eight and thirty-six-millimeter-head metal-on-metal prostheses. *J. Bone Jt. Surg. Am.* **2008**, *90* (Suppl. 3), 142–148. [[CrossRef](#)]
102. Fleury, C.; Petit, A.; Mwale, F.; Antoniou, J.; Zukor, D.J.; Tabrizian, M.; Huk, O.L. Effect of cobalt and chromium ions on human MG-63 osteoblasts in vitro: Morphology, cytotoxicity, and oxidative stress. *Biomaterials* **2006**, *27*, 3351–3360. [[CrossRef](#)]

103. Wang, Y.; Su, H.; Gu, Y.; Song, X.; Zhao, J. Carcinogenicity of chromium and chemoprevention: A brief update. *Onco Targets Ther.* **2017**, *10*, 4065–4079. [[CrossRef](#)] [[PubMed](#)]
104. Magone, K.; Luckenbill, D.; Goswami, T. Metal ions as inflammatory initiators of osteolysis. *Arch. Orthop. Trauma Surg.* **2015**, *135*, 683–695. [[CrossRef](#)]
105. Baskey, S.; Lehoux, E.; Catelas, I. Effects of cobalt and chromium ions on lymphocyte migration. *J. Orthop. Res.* **2017**, *35*, 916–924. [[CrossRef](#)]
106. Buczko, P.; Knaš, M.; Grycz, M.; Szarmach, I.; Zalewska, A. Orthodontic treatment modifies the oxidant–antioxidant balance in saliva of clinically healthy subjects. *Adv. Med. Sci.* **2017**, *62*, 129–135. [[CrossRef](#)] [[PubMed](#)]
107. Bandeira, A.M.; Martinez, E.F.; Demasi, A.P.D. Evaluation of toxicity and response to oxidative stress generated by orthodontic bands in human gingival fibroblasts. *Angle Orthod.* **2020**, *90*, 285–290. [[CrossRef](#)]
108. Scarcello, E.; Herpain, A.; Tomatis, M.; Turci, F.; Jacques, P.J.; Lison, D. Hydroxyl radicals and oxidative stress: The dark side of Fe corrosion. *Colloids Surfaces B Biointerfaces* **2020**, *185*, 110542. [[CrossRef](#)]
109. Crane, R.A.; Scott, T.B. Nanoscale zero-valent iron: Future prospects for an emerging water treatment technology. *J. Hazard. Mater.* **2012**, *211–212*, 112–125. [[CrossRef](#)] [[PubMed](#)]
110. Fagali, N.S.; Grillo, C.A.; Puntarulo, S.; Fernández Lorenzo de Mele, M.A. Is there any difference in the biological impact of soluble and insoluble degradation products of iron-containing biomaterials? *Colloids Surfaces B Biointerfaces* **2017**, *160*, 238–246. [[CrossRef](#)] [[PubMed](#)]
111. Kim, E.C.; Kim, M.K.; Leesungbok, R.; Lee, S.W.; Ahn, S.J. Co–Cr dental alloys induces cytotoxicity and inflammatory responses via activation of Nrf2/antioxidant signaling pathways in human gingival fibroblasts and osteoblasts. *Dent. Mater.* **2016**, *32*, 1394–1405. [[CrossRef](#)]
112. Marti, A. Cobalt-base alloys used in bone surgery. *Injury* **2000**, *31*, D18–D21. [[CrossRef](#)]
113. Bazaka, O.; Bazaka, K.; Kingshott, P.; Crawford, R.J.; Ivanova, E.P. Chapter 1 Metallic Implants for Biomedical Applications. *Chem. Inorg. Biomater.* **2021**, *8*, 1–98. [[CrossRef](#)]
114. Pohler, O.E.M. Unalloyed titanium for implants in bone surgery. *Injury* **2000**, *31*, D7–D13. [[CrossRef](#)]